EXPERIMENTAL STUDY ON FOUNDATION ISOLATION USING GEOSYNTHETICS

by

Murat Çalıkoğlu

B.Sc., Civil Engineering, Yeditepe University, 2014

Submitted to the Institute for Graduate Studies in
Kandilli Observatory and Earthquake Research in partial fulfillment of
the requirements for the degree of
Master of Science

Graduate Program in Earthquake Engineering

Bogazici University

2017

ACKNOWLEDGEMENT

First of all, I would like to express my gratefulness to my supervisor Prof. Dr. Ayşe Edinçliler for her trust, patience, worthless support as well as guidance and all kind of advices during my graduation and thesis period.

I would like to thank my committee members Prof. Dr. Erdal Şafak and Prof. Dr. Erol Güler for their contributions.

I would like to express my sincere thanks to my friend Hüseyin Metin Doğan for his help during the preparation of the experimental setup.

I am very thankful to Oktay Çırağ, Emre Özdemir and Ekrem Ulusoy for their sincere supports, cooperation and friendly approaches during the experiments.

Most of all, I would like to express my deep sense of gratitute to my family for their endless supports, patiences, self-sacrifices and encouragements.

ABSTRACT

EXPERIMENTAL STUDY ON FOUNDATION ISOLATION USING GEOSYNTHETICS

In the last decades, alternative low cost seismic isolation techniques which are commonly known as Geotechnical Seismic Isolation (GSI) systems were developed to mitigate earthquake hazards. These are known as Rubber Soil Mixtures (RSM) and Geosynthetics. Soil isolation and foundation isolation are the types of GSI with geosynthetics which can easily be applicable for low-to-mid rise buildings. The aim of this study is to determine the effects of foundation isolation with geosynthetics on seismic performance of low-to-mid rise buildings by using shaking table experiments. The proposed GSI system is comprised of a geotextile overlying geomembrane placed underneath the foundation with three different configurations. More importantly, this study is the first study on foundation isolation with geosynthetics considering different configurations by using shaking table under seismic loadings. Two different shaking table models representing the fixed based and isolated based buildings were designed as a 1:10 scaled building models. The effects of foundation isolation in terms of the number of the story of the building, type of geosynthetic couples, GSI configuration and dynamic motion characteristics on the seismic performance of the model buildings were evaluated. The comparative results of the fixed based and isolated based building models revealed that the proposed GSI systems can substantially reduce the horizontal accelerations, horizontal story drifts, Arias intensity, base shear, and base moment of the buildings under different seismic motions. The proposed method in this study can be a good alternative method to mitigate earthquake hazards for developing countries.

ÖZET

GEOSENTETİK KULLANILARAK TEMEL İZOLASYONU ÜZERİNE DENEYSEL ÇALIŞMA

Son yıllarda, binalarda deprem hasarlarını önleyebilmek için Geoteknik Sismik İzolasyon (GSI) sistemleri olarak bilinen düşük bütçeli alternatif sismik izolasyon sistemleri üzerine çalışmalar yapılmıştır. Bu sistemler, atık lastik-kum karışımı ve geosentetikler olarak bilinmektedirler. GSI sistemi, zemin izolasyonu ve temel izolasyonu olarak ikiye ayrılmaktadır. Bu çalışmanın amacı, geosentetiklerle temel izolasyonunun az ve orta katlı yapıların sismik performansına etkisinin sarsma masası deneyleriyle belirlenmesidir. Önerilen GSI sistemi, bina temeli altına yerleştirilmiş geomembran ve üzerine yerleştirilmiş geotekstil çiftinden oluşmaktadır. Daha da önemlisi bu çalışma, sismik yükler altında geosentetiklerin temel izolasyon malzemesi olarak kullanılarak farklı konfigürasyonlarda sarsma masasında incelenmesi açısından literatürde bir ilktir. İki farklı sarsma masası modeli, temel izolasyonsuz ve temel izolasyonlu, 1/10 ölçekli bina modeli olarak oluşturulmuştur. Bina kat sayısı, GSI tipleri, GSI konfigürasyonları ve deprem hareketi karakteristikleri açısından temel izolasyonunun bina modelinin sismik performansına etkileri değerlendirilmiştir. Temel izolasyonsuz ve izolasyonlu bina modelleri arasındaki kıyaslamanın sonuçlarına göre, önerilen GSI sistemi yatay ivme, yatay kat öteleme, Arias şiddeti, taban kesmesi ve taban momenti üzerinde farklı sismik yükler altında önemli ölçüde azalım sağlamıştır. Bu çalışmada önerilen GSI sistemi, gelişmekte olan ülkeler için deprem hasarlarını azaltmada alternatif sismik izolasyon sistemi olabilir.

TABLE OF CONTENTS

LIST OF FIGURES

LIST OF TABLES

LIST OF SYMBOLS

a’	Acceeleration of the soil without the influence of the container
a	Measured acceleration
a_b	Block acceleration at the first observation of sliding
A	Accelerometer
A_b	Residual acceleration
A_t	Measured peak table acceleration
B	Width of the foundation
D	Depth of penetration of synthetic liner
D_s	Block slip displacement
F_d	Dynamic force
H	Horizontal length of isolated soil mass
Hz	Hertz
L	Optical displacement sensor
m_1	Weight of soil in the container
m_2	Weight of total laminates
g	Gravitational acceleration
ϕ	Internal friction angle
ϕ_d	Dynamic friction angles at the first observation of sliding

LIST OF ACRONYMS/ABBREVIATIONS

ASTM	American Standard Test Method
CL	Curve Shaped Liner
CL1	Curve Shaped Liner with a Length of 105 cm
CL2	Curve Shaped Liner with a Length of 70 cm
CM-5	Control Model of 5-Story Building Model
CM-3	Control Model of 3-Story Building Model
ESB	Equivalent Shear Beam
FAS	Fourier Amplitude Spectrum
FPS	Friction Pendulum System
GSI	Geotechnical Seismic Isolation
GG	Geotextile-Geomembrane
HDPE	High-Density Polyethylene
KOERI	Kandilli Observatory and Earthquake Research Institute
LRB	Lead Rubber Bearing
ODS	Optical Distance Sensors
PEER	Pasific Earthquake Engineering Research Center
PGA	Peak Ground Acceleration
PGD	Peak Ground Displacement
PGV	Peak Ground Velocity
PTFE	Polytetrafluoroethylene
RMS	Root Mean Square
RSM	Rubber-Soil Mixture
SI	Seismic Isolation
SL	Straight Liner
SP	Poorly Graded Sand
SSB	Spherical Sliding Bearings
SSI	Soil-Structure Interaction
USCS	Unified Soil Classification System

1. INTRODUCTION

1.1. General Information

Many different techniques have been proposed to mitigate severe damages on low-to-midrise buildings from destructive earthquakes. Formerly, such techniques used to minimise earthquake damages on structures could be summarized as shear walls, braced frames, moment resisting frames, high ductility reinforcement and use of damping devices. Nowadays, most commonly used seismic isolation devices are known as Lead-Rubber-Bearing, High-Damping-Rubber-Bearing and Friction Pendulum System. The basis of the seismic isolation system is reduction of seismic forces acting on the structure caused by seismicity with an interaction between foundation and structure considering less rigidity. The period of the isolated structure will be higher than period of a fixed-based building (Kelly, 2001; Hussain, 2014). Major advantages of the seismic isolation is to reduce the natural frequency that diminishes the acceleration on the structure, and to provide less damage to structural members (Bozorgnia and Bertero, 2004). However, the utilization of the conventional seismic isolation system has some drawbacks. Conventional seismic base isolation can be quite expensive to implement and maintain. Mechanical maintenance, high cost of the operating system and obstacles in accessibility are the main disadvantages of these systems. Thus, there is a new kind of SI system which is cost-effective, easily applicable and accessable way to mitigate earthquake hazard, which is called as Geotechnical Seismic Isolation (GSI) systems (Tsang, 2008).

The fundamental purpose of GSI system is to allow the building to behave with lower level of seismic excitation and to shift the period of the structure by cutting off the transmission path. However, some interaction between foundation and building is inevitable. GSI system can be defined as a seismic isolation system that involves direct interaction with natural earth materials or manmade materials in contrast to the commonly used structural seismic isolation system in which the flexible or sliding interface is positioned between a structure and its foundation. An interesting property of the GSI systems is similarity to the

conventional seismic isolation systems that involve Lead Rubber Bearing (LRB) and Spherical Sliding Bearings (SSB). Both systems are identical in terms of decoupling of the structure from the ground. Geotechnical seismic isolation systems provide reduction of the acceleration and increase of the period of wave motion. GSI systems are divided into two different types that are Rubber Soil Mixtures (RSM) and geosynthetics. Rubber Soil Mixtures can also be recommended around the foundation of the structures as seismic isolation method. RSM is able to dissipate the high frequency components of seismic energy. Use of RSM provides alternative solution to the consumption of the scrap tires from all over the world. For the GSI with geosynthetics, smooth synthetic liners can be placed underneath the foundation of structures or between soil layers for the dissipation of the seismic energy via sliding. GSI with gesoynthetics are manmade materials that are combination of a geotextile and a high-density polyethylene geomembrane, which are called as geotextile-geomembrane (GG) couple. Geosynthetic liners placed under foundations can absorb seismic energy and transmit smaller ground motions to an overlying structure by limitting the transfer of shear force across the isolation interface. Geosynthetics are costly efficient and accessable so that easy to apply. However, they require to resist long-term creep effects, chemical and biological distortion. Thus, these phenomena may be handicap for the use of geosynthetics and should be taken into consideration (Tsang, 2008; Yegian and Catan, 2004; Yegian *et al.,* 1995).

Two alternative approaches, soil and foundation isolation, can be adopted for the implementation of this concept. The system on which geosynthetic liner is placed within the soil profile at some depth underneath the foundation of the structure is known as soil isolation. In this system, soil is able to slide on synthetic liner and soil layer above the liner is isolated from soil deposit below the foundation. Synthetic liner placed inside the soil deposit can provide dissipation of seismic energy via slip deformation. If soil isolation is used, permanent deformations related to slip deformations must be in the acceptable limit range. Curved shaped liners is recommended to restore gravitational force so that isolated soil will be in its original horizontal pozition (Georgarakos *et al.,* 2005). However, the system is able to slide to impose cut off at the acceleration transmitted through the overlying structure. This may cause excessive slip displacement at the synthetic liner. Therefore, the effects of slip deformations near the edges of isolated regions have to be considered in the design of the structure. On the other hand, foundation isolation, which is the subject of this

study, is the placement of the geotextile-geomembrane couple immediately underneath the foundation of the structure with different configurations. Use of horizontally placed smooth geosynthethic liner underneath the foundation provides absorption and dissipation of the seismic energy via sliding along the interface of the geosynthetics. Thus, smaller accelerations can be transmitted to the above structure. Concepts of foundation isolation and conventional base isolation are similar. However, entire building is completely isolated from the ground by the means of geosynthetic liner in foundation isolation (Tsang, 2008; Yegian and Catan, 2004; Yegian and Kadakal, 2004; Yegian *et al.*, 1995).

1.2. Problem Statement

Seismically resistant structures are needed in the case of destructive earthquake events. Thus, base isolation or seismic isolation comes into sight. In general, foundation stands on the soil firmly during an seismic action, and seismic waves are fully transmitted to the overlying structure. Therefore, mechanical devices have been developed in order to limit and mitigate seismic energy transmission through superstructure. These devices are referred as base isolators or more commonly as seismic isolators. Typically, a base isolator provides additional damping to absorb the wave energy. In seismic isolation, natural period of the building is shifted away from that of the earthquake natural period. However, installation cost and maintenance cost of the conventional isolator devices are quite high for operational area. On the other hand, geotechnical seismic isolation systems are easily applicable, accessible and inexpensive way of reducing transmitted accelerations through overlying structures expecially, low-to-mid rise buildings. In the previous studies, it was proposed that GSI system is cost-effective and easily applicable alternative to mitigate earthquake effects for developing countries.

1.3. Objective of the Thesis

Aim of this study is to investigate the effectiveness of geosynthetic liners as geotechnical seismic isolation system on earthquake hazard mitigation of low-to-midrise structures under different earthquake motions by using shaking table facility. In this study, focussed topic is foundation isolation with geosynthetic couples that are placed underneath the foundation to provide damage mitigation against earthquake motions by absorbing the seismic energy through sliding. Two different configuration types were considered on 1:10 scaled three and five story model buildings. Effects of configuration on the seismic performance were evaluated by adopting cylindrical shaped liner and straight liner as foundation isolation system. This thesis is the first experimental study in literature in terms of different configuration type under different earthquakes on low-to-mid rise buildings. Additionally, seismic behavior of soil-foundation-structure system under different excitations was determined in this study. Effects of the GSI couples, configuration types of proposed GSI system, earthquake motion characteristics and number of stories were evaluated in this study.

This thesis can be divided into three main parts. First, theoretical and experimental background of the proposed GSI system were given. Then, experimental studies including material and methods and shaking table tests for different cases were introduced. Finally, the results of the shaking table experiments, discussion of the test results, and summary and conclusions are presented.

1.4. Organization of the Thesis

This thesis is organized as follows. In the first two chapters, brief introduction and literature review about conventional and geotechnical seismic isolation are presented. Also, previous studies about shaking table experiments are mentioned in Chapter 2. Then, Chapter 3 is composed of experimental study including materials and methods, input ground motion selection, instrumentation and shaking table test setup. Experimental results are mentioned

in Chapter 4. Parametric study is given in the Chapter 5. Summary and conclusion are introduced in Chapter 6.

2. LITERATURE REVIEW

2.1. Seismic Isolation

Numerios techniques were invented over the past century in order to mitigate earthquake hazards on the structure decoupling from the ground. The common proposal for many researchers that supported the use of rollers, sand layers or similar materials was to provide sliding of the buildings. For example, specially designed sand layer between foundation and superstructure so that the building has been prevented from destructive seismic events by sliding was used in China. The use of rollers under the structure as early examples of seismic protection technique were pioneered in Sevastapool, Crimea and Mexico City (Kelly, 2004).

From now on, many techniques such as use of shear-wall, braced frame, moment resistant frame and damping device, were used to minimise the earthquake effects on structures (Hussain, 2014). However, robust structures are exposed to relatively high floor accelerations. On the other hand, large inter-story drifts may occur in the presence of flexible structures. Due to the large drifts and high accelerations, considerable damages are able to occur and this may cause costly and valuable consequences which are not tolerable for worthy structures. As a results of these considerations, concept of base isolation was adopted in order to diminishing inter-story drifts as well as reducing floor accelerations (Yang *et al.*, 2003).

In 6th century BC, the first region at which the concept of base isolation was used, was discovered in Pasargadac, Iran as seen in Figure 2.1. Namely *'tomb of cyrus'* has huge stones and mortar foundation which was smoothed at top. Smoothed stones were connected to each other in order to prepare sliding area in the presence of earthquake event. Moreover, timber materials was used to provide base isolation between foundation and building with rolling movement under bearing walls as seen in Figure 2.2. In 1980's, the first pattent was declared for mechanical isolators (Hussain, 2014). Recently, Armenia, Chile, China, Indonesia, Italy,

Japan, New Zealand, USA and Uzbekistan have adopted the concept of base isolation and used them for protection of structures (Kelly,2004).

Figure 2.1. Tomb of Cyrus: The First Evidence of Base Isolation (Hussain, 2014).

Figure 2.2. Use of Timber as Base Isolator (Hussain, 2014).

In 1986, the first base-isolated building was constructed in Japan by applying isolation methods. Structural engineers considered the concept of base isolation in the application. Base isolation or seismic isolation was firstly used in bridges that are more prone to be affected by an earthquake in 1970's (Kelly, 2001). The first implementation of the seismic isolation was observed in 1985 by using elastomeric bearings in United States. This structure is the first in using isolation bearings as base isolation (Kelly, 2004).

The term “base isolation” or more commonly as “seismic isolation” means the separation of a superstructure from its foundation. However, some isolation techniques are not used at the base level so that base isolation term is replaced with seismic isolation, nowadays (Hussain, 2014). Base isolation or seismic isolation is a technique that mitigate damaging effects of an earthquake by decoupling the building from its foundation. On the other hand, reduced interaction between structure and ground provides mitigation from damage to buildings during an earthquake (Barole, 2016).

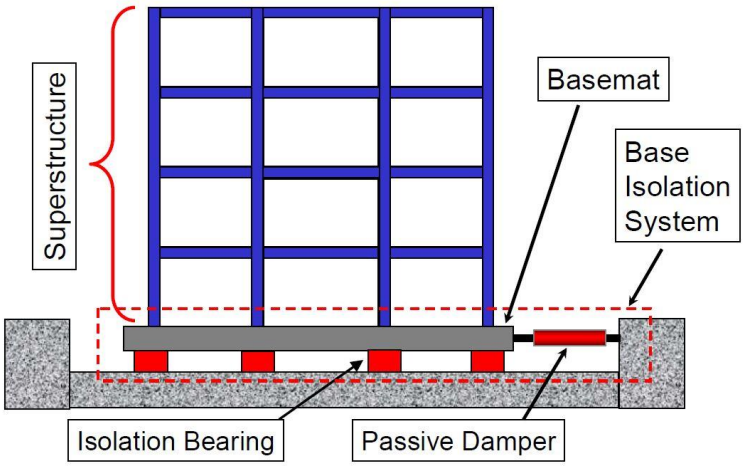

Figure 2.3. Configuration of Seismic Isolation (Barole, 2016).

Fundamental purpose of the system is to minimize transmitted seismic forces to the buildings and provide flexibility to the structure during an earthquake event (Barole, 2016). Ductility concept comes into prominence. However, ductiliy allows structure to maintain deformability after elastic limit and this causes irreversable deformations that results in structural damages such as cracking and spelling of concrete as seen in Figure 2.4 (Hussain, 2014; Symans, 2013). Base isolation attempts to diminish the demand instead of increasing the capacity of structure so that capacity will exceed the demand (Kelly, 2001). Seismic isolation controls the transmission of horizontal accelerations to the buildings by reducing the earthquake forces. Period shifting and cutting off transmission path are constitute the main strategies to succeed base isolation. Use of isolator increases the fundamental period of the structure and provides safety against predominant frequecies of earthquakes as seen in Figure 2.5 (Symans, 2013).

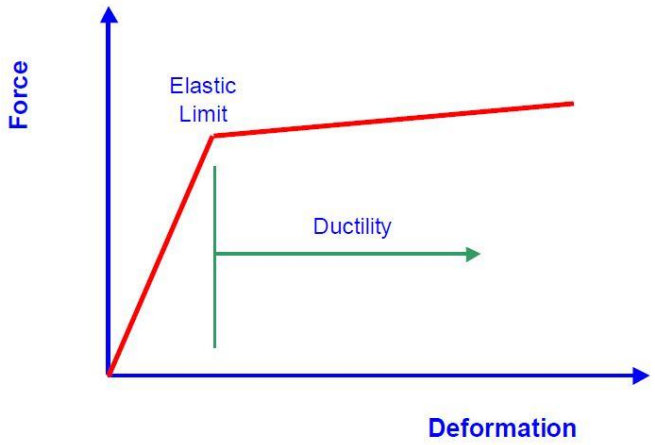

Figure 2.4. Ductility Concept of Design (Hussain, 2014; Symans, 2013).

Objectives of the seismic isolation system can be listed as below (Symans, 2013):

- Maintaining the use of a facility,
- Minimizing the damaging effects of the earthquakes,
- Reducing the transmitted accelerations to protect buildings from damage,
- Reducing earthquake forces by providing flexibility to increase period,
- Dissipating the seismic energy to manage the displacement of isolation system, and
- Providing rigidity under wind and minor earthquakes.

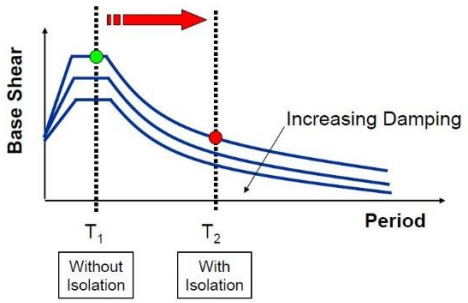

Figure 2.5. Shift of Period in Base Isolated Structures (Symans, 2013).

Underground soil effects are important for the applicability of the seismic base isolation. If a structure is low-rise building on stiff soil, system will be the most effective under earthquake. However, if the high-rise building is lying on the soft soil and has a high fundamental period, isolation system will be the least effective in the presence of earthquake

event as seen in Figure 2.6. (Symans, 2013). Softer soils have more tendency to produce ground motion at lower frequencies and thus, seismic isolation systems are not suitable for soft soil conditions (Tüzün, 2015).

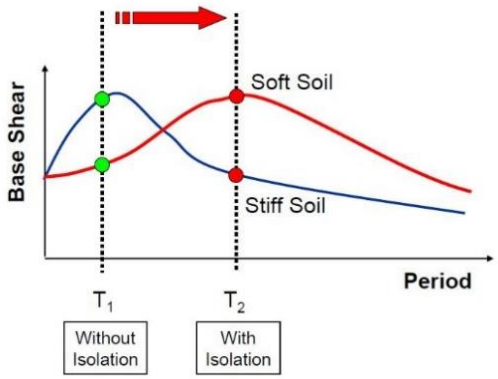

Figure 2.6. Shift of Period in Base Isolated Structures (Symans, 2013).

If a structure is perfectly rigid, then acceleration exerted on the structure due to the seismic event will be equal to the acceleration of the ground. It means displacement difference between structure and ground will be zero due to the zero period of building. On the other hand, if a structure is perfectly flexible, then acceleration exerted on the structure will be equal to zero.

While ground is sliding towards the direction of seismic action, building will not move. Therefore, ground displacement will be the relative displacement between the building and the ground due to the infinite period for perfectly flexible buildings as shown in Figure 2.7 and Figure 2.8 (Kelly, 2001).

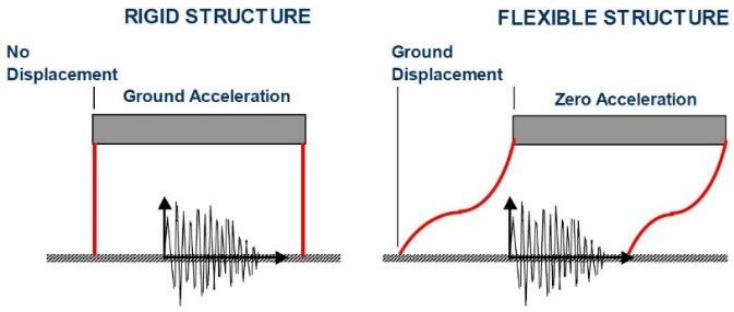

Figure 2.7. Transmission of Ground Motions (Kelly, 2001).

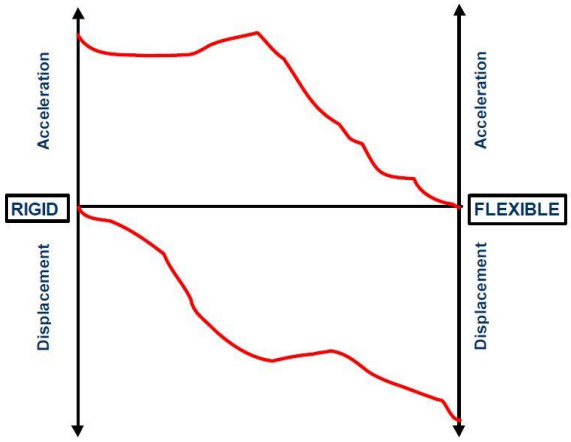

Figure 2.8. Acceleraton and Displacement Responses for Structures (Kelly, 2001).

Conventional structures experience inter-story drifts and amplified accelerations at upper floor levels. On the contrary, accelerations are relatively uniform throughout the height of the structure and deformations occured at the isolation layers of the structure in seismically isolated structures as seen in Figure 2.9.

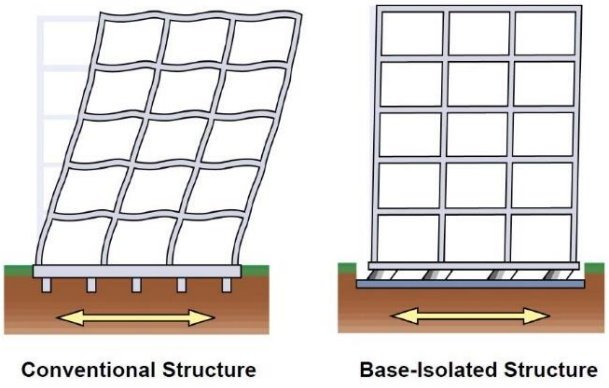

Figure 2.9. Behavior of the Structure Under Seismic Excitation (Symans, 2013).

Provided that decoupling the building and the underlying supporting foundation in order to isolate structure from the ground, some specific devices are installed between the building and foundation so as to attain the effectiveness of the seismic isolation. There are two main different approaches to apply base isolation (Yang *et al.*, 2003). To achieve the first approach of the base isolation, installation of some devices which have low horizontal stiffness and high vertical stiffness between the foundation and the superstructure are

required. By this devices, predominant period of the structure is able to be shifted away from the high frequency range of the earthquakes. These devices are known as elastomeric bearings that are commonly considered as laminated rubber bearings (LRB) composed of several layers of steel and stiff rubber shown in Figure 2.10. Major objective of this type of isolation that provides additional stiffness against minor earthquakes and wind forces is to reduce transmitted shear forces by increasing the period of system (Yang *et al.*, 2003).

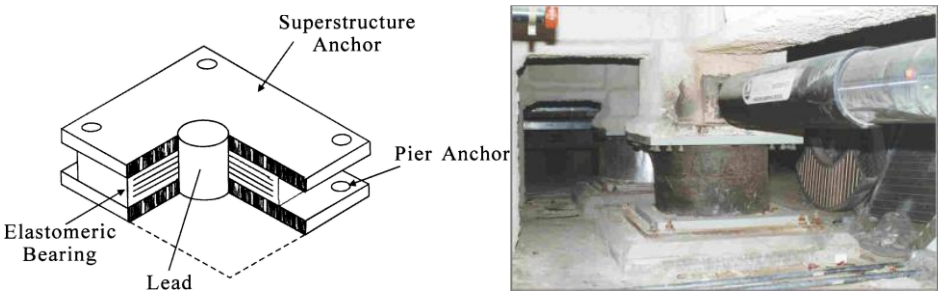

Figure 2.10. Laminated Elastomeric Bearing with Lead Core (Yang *et al.*, 2003).

The second approach is to increase flexibility so as to provide a sliding or friction surface between the foundation and the base of the structure. Friction coefficient is kept as low in order not to restrain sliding of the system. On the other hand, it must be sufficient to provide stiffness against wind forces and minor earthquakes. The most common type of sliding isolator is friction pendulum system (FPS) that is made up of steel ball and spherical concave surface as seen in Figure 2.11. FPS can return its original position so, it does not require restoring force. However, an additional system is needed for actuation of the elastomeric bearing system (Yang *et al.*, 2003).

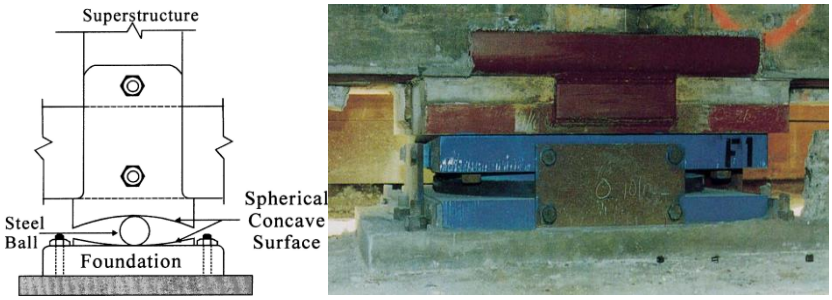

Figure 2.11. Friction Pendulum System (Yang *et al.*, 2003).

Other conventional seismic isolation techniques are listed in Figure 2.12.

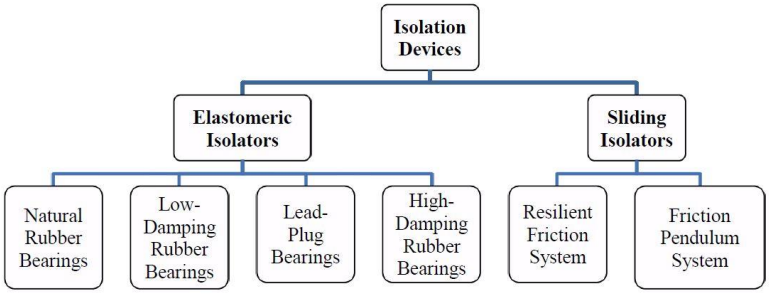

Figure 2.12. Types of Isolation Techniques (Hussain, 2014).

A seismic isolation system should meet the following requirements (Yang *et al.*, 2003):

- Flexibility to shift predominant period of the structure,
- Flexibility to increase demand,
- Adequate stiffness so as to resist service loads,
- Sufficient capacity to mitigate large displacement to a tolerable level, and
- Satisfactory rigidity to make no discrepancies between non-isolated and isolated buildings under service loads.

Besides above mention points, a complete design of the base isolation should ensure the following criteria (Yang *et al.*, 2003) :

- Minimum size and location of the isolators required under maximum service loading,
- Dimensions of the isolator to provide period shifting,
- Damping ratio to control displacement of the structure within design limit, and
- Performance checks under possible loading conditions.

The main advantage of the seismic isolation is to provide an economical solution rather than increasing strength of the buildings. When the control of the movement of the building is taken over, destructive shakings caused by earthquakes are mitigated (Barole, 2016). Reductions in floor acceleration, inter-story drifts and damage to structural members are another advantages of the system (Hussain, 2014). Base isolation provides ability to improve

seismic performance of the existing structures by retrofitting. It also provides an economical and reliable solution to design new earthquake resistant structures. Moreover, seismic isolation provides ability to function operational after a major earthquake. During the retrofitting of a structure, isolators are able to be installed while the structure is being used. The primary cost of the system may be expensive but, reparing after a major earthquake will be more costly. Thus, primary cost of the system is minimal when compared to future possibilities (Mayes *et al.,* 2012).

Use of seismic isolation and energy dissipation devices brings about several benefits. Simpler and less sensitive structures are provided by the system. In fact, isolation system does not absorb the seismic energy. It deflects the energy through the dynamics of the system. Damage is concentrated on the isolation system and more reliable than conventional structural components due to the predictable performance of the isolation system. On the other hand, technical benefits of using seismic isolation system should also be taken into consideration. A fixed based system experiences 2.5-4 times greater ground acceleration at the top of the structure. In the isolated buildings, elastic base shear is reduced by a factor of 3 to 7 based on the earthquake characteristics and period of the structure. Also, reduction in inter-story drift by a factor of 4 to 8 is observable. Furthermore, cost of the base isolation system is 2-5% of the total cost of the structure. Thus, when compared to the conventional design, benefits of the seismic isolation system outweights its handicaps.

However, when it comes to the drawbacks of the system. One drawback with active seismic isolation techniques is the relatively high cost of maintenance for the control system and actuators that provide continuity in functionality of the system at all the time. In elastomeric bearings, substantial damping has to be implemented into the system so that large displacement problems can be overcome. Rupture and erosion effects can be seen in this type of seismic isolation. Yielding of metallic dampers results in interruption in response of the structure against an earthquake. Another possible problem is for friction pendulum system. If the sliding surface of the system is not made concave, restoring force and sliding movement are not provided in FPS. Moreover, concavity is needed to overcome the friction force to start sliding movement. Also, costs of routine mechanical maintenance and control of the LRB and FPS systems are relatively high (Yang *et al.,* 2003). Base isolation is not applicable for high-rise buildings and structures built on soft soils (Srivastav, 2015). Due to

the mentioned drawbacks of the isolation systems, researchers are in needs for a new kind of an isolation technique that is more applicable and cost-effective aspect of implementation process. In the following parts, a new and cost-effective system was introduced.

2.2. Geotechnical Seismic Isolation

Due to the high installation and maintenance costs of conventional seismic isolation methods, a new kind of isolation technique that is cost-effective and accessable are proposed to mitigate damaging effects during earthquakes. To be accepted by the countries that use conventional seismic isolation systems, technical efficency and feasability are important tasks. Recently, two distinctive and reliable methods in proposed isolation system that aim to provide flexibility and sliding interface in contact with geological segments and geotechnical isolation mechanism (Tsang, 2008). One of them is smooth synthetic liners lying underneath the foundation of structures or between soil layers so as to dissipate earthquake energy via sliding (Yegian and Kadakal, 2004; Yegian and Catan, 2004). Another method is set around the foundation of structures to absorb energy and behave similar to cushion, which is commonly known as Rubber-Soil Mixtures (RSM). In developing countries, low cost of mentioned methods for seismic isolation provides benefits in the lack of resources and not adequate techniques. The aforementioned seismic isolation method by using geotechnics is described as Geotechnical Seismic Isolation (GSI). Typical demonstration of the GSI systems is shown in Figure 2.13 (Xiong *et al.,* 2011). GSI systems are composed of man-made materials in contrast to conventional seismic isolation systems that use laminated rubber bearing and spherical sliding bearings as seen in Figure 2.14 (Tsang *et al.,* 2012). Comparatively, GSI system provide more benefits than conventional seismic isolation techniques. GSI systems are environmentally friendly, economical and strong when compared to structural seismic isolation systems. For the evaluation of the performance of GSI systems, a series of shaking table tests were conducted by Xiong *et al.* (2011). As a results of the test showed that GSI systems reduced the acceleration response of the superstructure and performance of the system is based on rubber content, thickness of layer and characteristics of seismic ground motion (Xiong *et al.,* 2011).

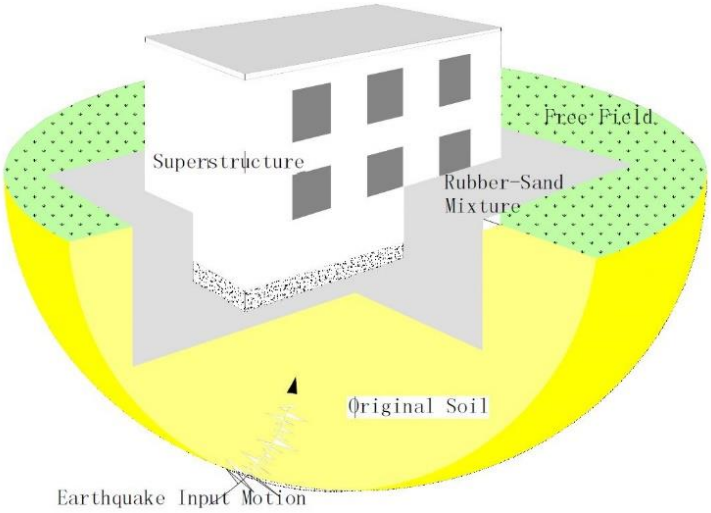

Figure 2.13. Schematic View of GSI System (Xiong *et al.*, 2011).

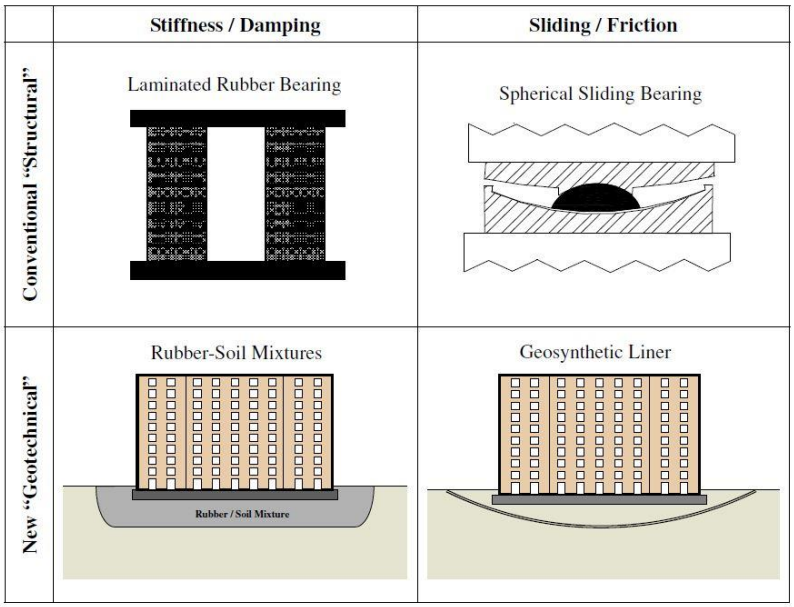

Figure 2.14. Proposed classification of seismic isolation systems (Tsang *et al.*, 2012).

Detailed information about the types of GSI system as Rubber-Soil Mixtures and Geosynthetics was given in the following parts.

2.2.1. Rubber-Soil Mixture

It is an inevitable fact that manufacture and use of the vehicles are dramatically increasing. This means, huge amount of scrap tires are disposed every year. As a shape and size of scrap tires, researchers did not attempt to use them entirely. Thus, instead of using as a whole, they decided to disintegrate scrap tires into small pieces which was commonly known as tire chips as seen in Figure 2.15. High porosity and high rubber content of the tire chips provide great compressibility under loading (Edil and Bosscher, 1994). Use of tire chips is proposed in the waterfront retaining structures by (Hazarika *et al.* 2008).

Figure 2.15. Tire Chips.

Rubber is exceedingly capable of absorbing the seismic wave energy that is the preliminary consideration of the mechanism resulting in the decrease in grond motion effects. Firstly, it was used in the 1960's in the mitigation of the earthquake hazards on structures. However, possibility of swing and bounce effects obstracted the use of rubbers as seismic isolator in case of an earthquake. Therefore, use of rubber-soil mixture, except pure rubber, took place in geotechnical seismic isolation systems (Tsang, 2009).

Another way of using rubber is scrap-tires that are obtained by the recycling of the rubbers. The reason for selection of rubber as seismic isolator is durability and fireproof properties of rubbers. According to the Rubber Manifacturers Association, 300 million

scrap-tires were disposed in 2005. Moreover, they are expecting a 2% increase in generation of scrap-tires (Tsang, 2009). Furthermore, internal heating concept of scrap tires is a great concept helded by civil engineers. Guidelines for mitigation of internal heating are firstly developed in 1995 (Humprey, 2005). In the alleviation of the potential obstacles with concept, Standard Practice for Civil Engineering Applications of Scrap Tires (ASTM D6270-98) is published in consequence (Tsang *et al.,* 2010). Numerical and experimental studies are given in the following parts.

2.2.1.1. Numerical Study. Mashiri *et al.* (2010) proposed the use of soil-scrap tire mixture around the foundation as a low cost seismic isolation method. Numerical studies including rubber-soil mixture were conducted by Tsang *et al.* (2012) as base isolation. Representative demonstration of seismic isolation by the rubber-soil mixture is shown in Figure 2.16 (Tsang, 2008; Tsang *et al.,* 2012).

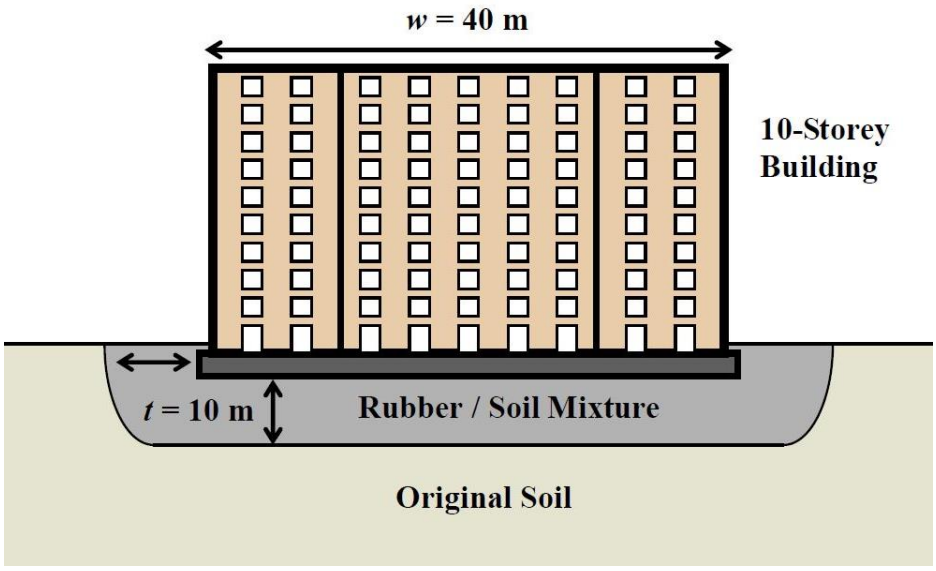

Figure 2.16. Seismic Isolation by A Rubber-Soil Mixture (RSM) (Tsang, 2008).

RSM can dissipate the high-frequency content of the earthquake energy. RSM layers concentrates the deformation demand caused by seismic excitation (Tsang *et al.,* 2012). Seismic effects in vertical direction are reduced in the RSM systems that are capable of carrying gravity loads (Boominathan *et al.*, 2015). Moreover, The use of RSM provide reduction in stockpile volume of tires. In the numerical analysis conducted by Tsang (2008),

different scenarios were considered as effectiveness of peak and root-mean-square ground acceleration in vertical and horizontal directions as seen in Figure 2.17. As it can be seen from figure, substantial decrease in acceleration results was observed in the presence of RSM. Also, frequency was shifted when compared to pure sand. It means, period of the system was increased.

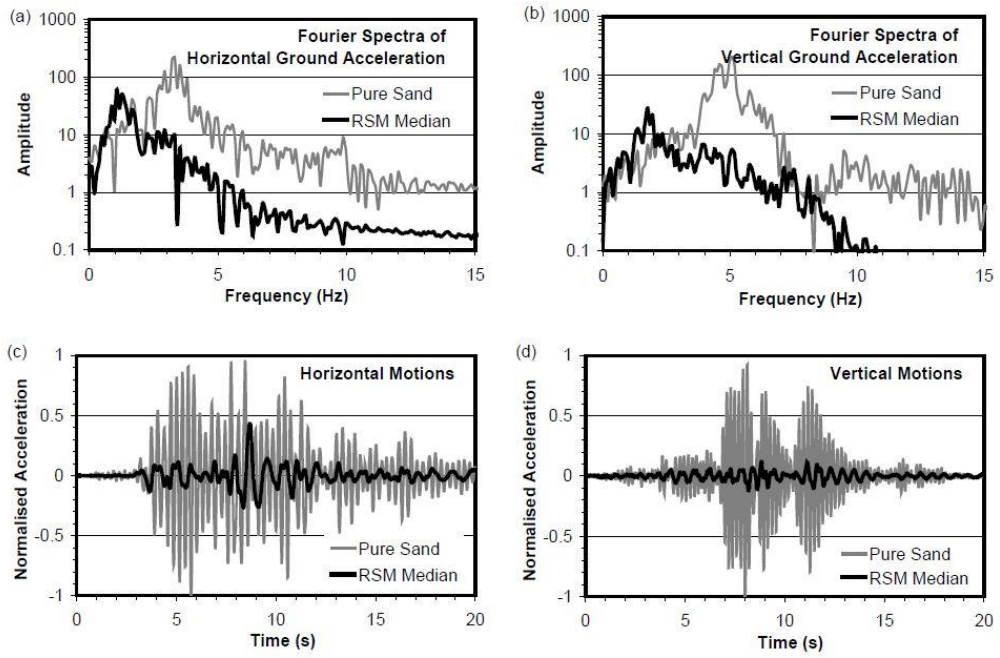

Figure 2.17. Numerical Analysis Results Considering Pure Sand and RSM (a) Fourier Amplitude Spectra of Horizontal Ground Motion, (b) Fourier Amplitude Spectra of Vertical Ground Motion, (c) Horizontal Ground Motion Time History, (d) Vertical Ground Motion Time History (Tsang, 2008).

Vertical ground motions are considered in rubber-soil mixtures instead of conventional structural isolation systems. Papazoglous and Elnashai (1996) studied the destructive effects of vertical seismic waves. According to the results of their studies, vertical ground motions dramatically affects the axial forces, moments and shear forces exerted on the columns by increasing them. Furthermore, according to Bozorgnia and Niazi (1993), near-field earthquakes affects the structures in short periods in vertical direction.

Idris (1990) stated that nonlinear seismic response occurs when the underlying soil demonstrates nonlinearity between medium and high level of ground motion levels.

Hauksson and Gross (1991) claimed that near-field ground conditions causes severe damages in structures so that RSM is not advantageous in providing safety against level of shaking. However, soil behaves as passive isolator for high frequency content near-field earthquakes. Thus, excellent capability of energy absorption in rubber makes RSM systems more flexible and reliable system in terms of nonlinear site response.

Another benefit of using RSM can be defined as soil resonance that occurs when high energy seismic wave complies with natural frequency of the soil deposit. If the thickness of RSM layer is specified properly, then harmful effects of ground motion level are able to be minimized (Tsang *et al., 2008).*

In addition to above mentioned benefits of using RSM, effects under the liquefaction phenomenon have to be taken into consideration. Liquefaction occurs in case of reduction in the shear strength of soil and effective shear strength. Viscousity and density of soil and ground motion level constitute the formation of liquefaction phenomena. Preliminary studies conducted by Promputthangkoon and Hyde (2007) demonstrated the reduction in shear strength of RSM in the presence of additional quantity of tire chips. Mixing the rubber with soil helps to improve the soil performance and provides attenuation in peak and RMS ground acceleration so that liquefaction is mitigated (Tsang *et al.,* 2007; Tsang, 2008).

RSM and tire shreds are very prone to settlement under loading due to the their high compressibility. However, Edil and Bosscher (1994) stated that compressibility of rubbers can be reduced depending on the application of loads. That means, preloading is able to minimize plastic compression against ground settlement (Tsang *et al.,* 2007; Tsang, 2008; Tsang *et al.,* 2010).

Besides all above mentioned points, environmental effects of rubber material is also considered in literature due to the long term effects in terms of using rubber. Liu (2000) conducted several studies on this debate about metallic and organic properties. According to the regulatory limits determined by Toxicity Characteristics Leaching Procedure Regulatory Limits and Extraction Procedure Toxicity indicated that rubbers are innoxious recycled materials in using RSM as earthquake hazard mitigation (Tsang *et al.,* 2007; Tsang, 2008; Tsang *et al.,* 2008; Tsang *et al.,* 2010).

Another numerical study was conducted by Adir (2013). 14 numerical analyses were performed for eight different scenarios with QUAD4M software for dynamic and time domain analysis in 2D under three different earthquake motions as shown in Figure 2.18. Low-to-mid rise structures were considered in numerical study. Tire Crumb Sand (TCS) mixtures were used as a geotechnical seismic isolation material. Three performance indicator parameters which are horizontal acceleration, story drift and period lengthening ratio were determined with their peak and RMS values. Tire crumbs were used as 10%, 20% and 30% in terms of containing rubber material. According to this study, substantial reductions were observed in these three performance indicator parameters. Results of numerical study on TCS30 as GSI material underneath 18 story model building with pile were shown in Figure 2.19 as a demonstration of the effectiveness of this study (Adir, 2013).

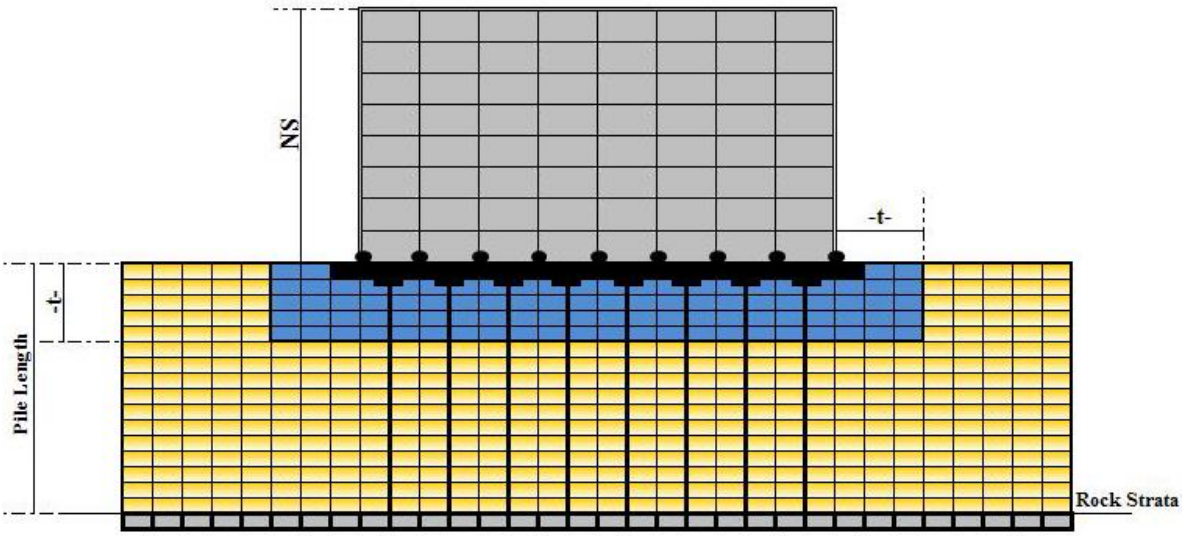

Figure 2.18. Typical Demonstration of Model with Pile (Adir, 2013).

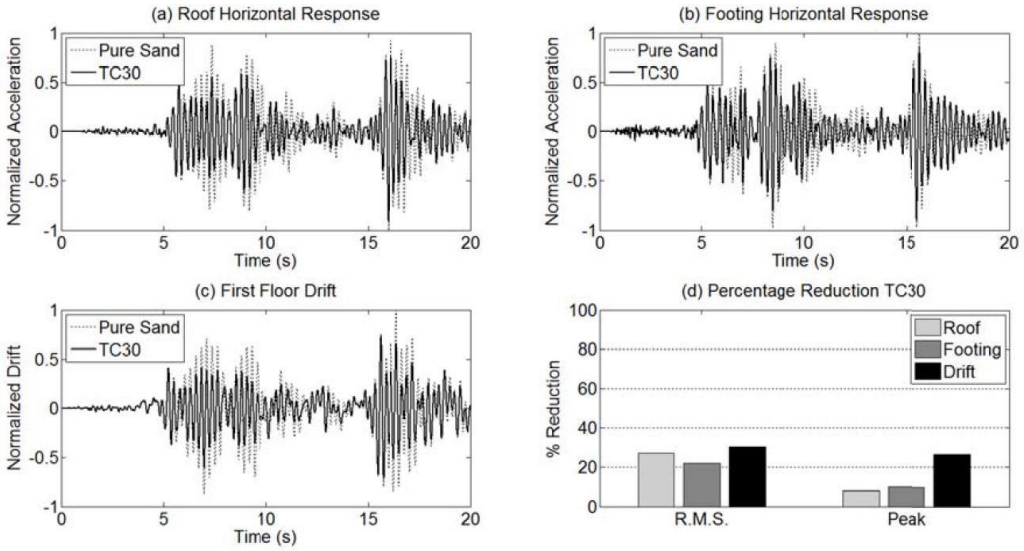

Figure 2.19. Numerical Analysis Results Under 1999 Duzce Earthquake (Adir, 2013).

Results demonstrated that using Tire Waste Soil Mixtures (TWSM) as geotechnical seismic isolation achieved the aim of the study which is the mitigation of the potential seismic hazards using RSM as GSI system. According to the numerical results, 25-30% reduction in RMS acceleration and drift values. Instead of significant decrease in performance parameters, limited effect of proposed GSI system was observed under medium-high rise structures. Thus, low-to-mid rise structures for the proposed system were suggested. However, the study concluded that increasing TC content did not mean to the better behavior of TWSM. Also, adopting pile under structures did not provide better performance with GSI system. Thus, the use of this methodology was not recommended underneath the foundation with piles. On the other hand, Adir (2013) concluded that proposed GSI system should be considered with further numerical and physical modeling to evaluate in-situ conditions.

2.2.1.2. Experimental Study. As previous studies emphasized the needs of experimental study about GSI systems, some experimental studies were done regarding the concept. The first experimental study in the literature about the use of RSM as GSI system was conducted at Bogazici University Kandilli Observatory and Earthquake Research Institute (KOERI). The main aim of the study was determination of the effectiveness of the proposed RSM on the seismic performance of low-to-mid rise buildings by shaking table tests. Up to this study,

there was only numerical analyses about rubber soil mixtures as seismic isolation material. Thus, experimental study was needed to evaluate the response of the buildings under seismic excitations. In the study, 1:10 scaled 3 and 5 story building models were used to represent low and medium rise buildings, respectively. The effects of rubber material type, rubber content and RSM thickness on the effectiveness of the GSI-RSM were evaluated. Shaking table of the KOERI was used for the study. RSM layers were arranged for different percentages as 10%, 20% and 30% with RSM thicknesses of 10 and 15 cm thicknesses. As input ground motions, the 1999 Kocaeli, 1940 El Centro and 1995 Kobe earthquakes were selected. Time of the earthquakes were scaled as $\sqrt{10}$. Cyclic sinusodial motions were obtained by using free vibration tests data. In overall, 8 cases were conducted for five story building model and 2 cases were performed for three story building model (Goztepe, 2016).

Performance checks of laminar were done in accordance with the previous studies from Prasad *et al.* (2004), Jafarzadeh (2004), Whitman and Lambe (1986), and Ecemis and Kahraman (2012) (Goztepe, 2016). The placement of RSM under the foundation was shown in the sketch as seen in Figure 2.21.

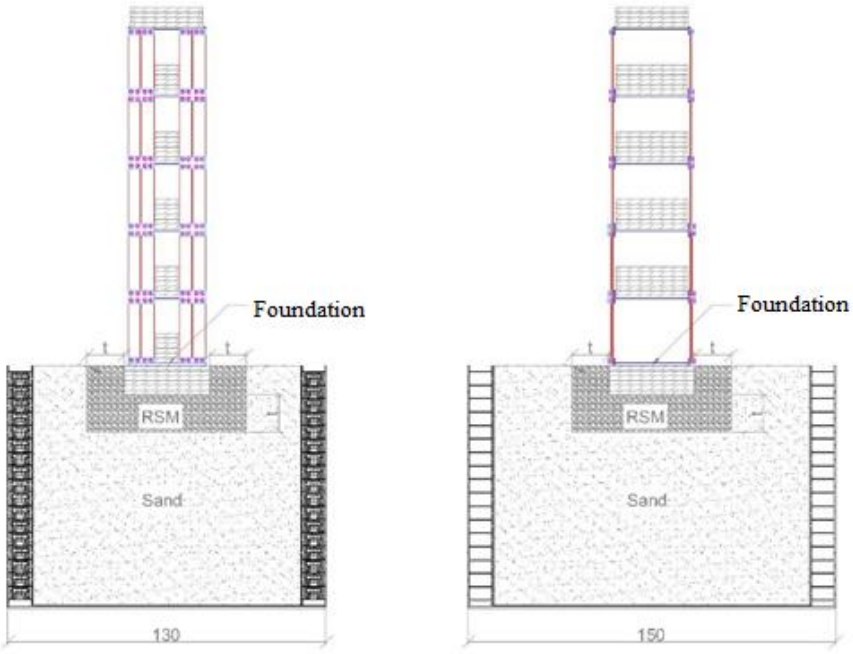

Figure 2.21. The Sectional View of The Models with RSM Layer (Goztepe, 2016).

According to the results obtained from the shaking table tests, the effect of RSM on both three and five story building models were consistent. Also, higher damping ratio and energy absorption capacity were observed in the existence of 30% tire crumb content with 15 cm thickness of rubber material. Due to the low energy dissipation capacity of the sands, rubber materials provided better performance in dissipation of the vibration energy through the deformation of rubber particles. Because of the higher elasticity of the rubber material, large deformations were recovered. Moreover, top floor accelerations and foundation accelerations were reduced up to 30% and 12%, respectively. Arias intensities at top floor and foundation level were decreased up to 61% and 34%. Base shear and base moment values were lowered up to 28%. Demonstrative results of TC30/15 under 1999 Kocaeli earthquake was shown in Figure 2.22.

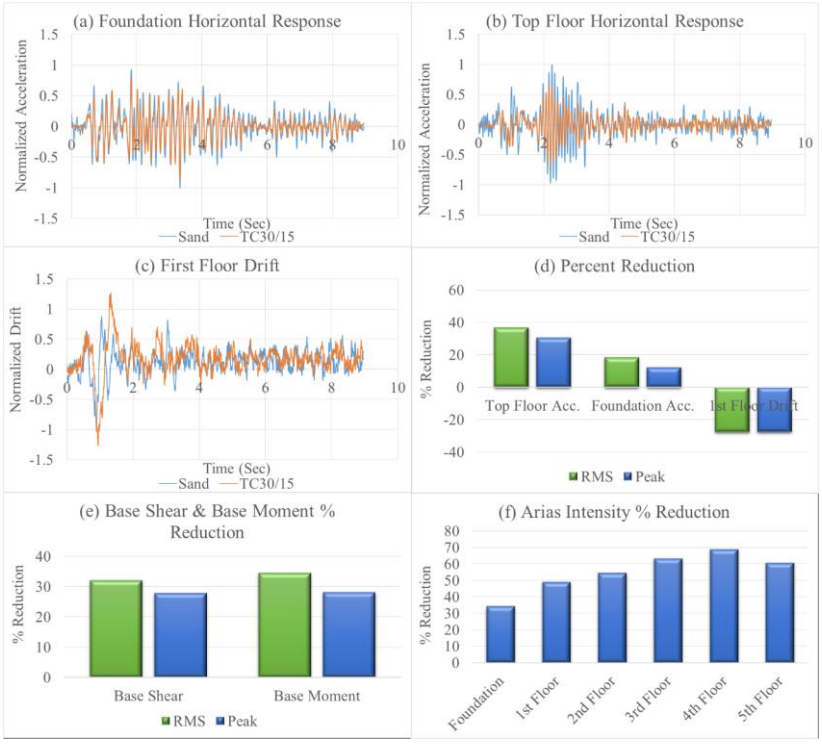

Figure 2.22. (a) Foundation Horizontal Response, (b) Top Floor Horizontal Response, (c) First Floor Drift, (d) Percent Reduction in Top Floor Acceleration, Foundation Acceleration and First Floor Drift, (e) Base Shear and Base Moment and Percent Reduction, (f) Arias Intensity Percent Reduction of TC30/15 for 5 story model under Kocaeli 0.21g EQ (Goztepe, 2016).

In the wake of the comparative and preliminary study, it was concluded that 30% tire crumb with a thickness of 15 cm rubber material demonstrated the best performance in minimizing the potential seismic hazards. It was recommended that the it is necessary to investigate the behavior of the RSM for distinctive number of stories. Also, real scaled building model is needed (Goztepe, 2016).

As it is mentioned in the section, rubber has great capability of being used as isolator in seismic protection of structures. However, due to its drawbacks, which are bouncing and rocking, use of pure rubber is not recommended for RSM. Also, use of scrap-tire in RSM is also limited in civil engineering application.

2.2.2. GSI with Geosynthetics

In the last decades, geosynthetics became part of construction material in civil engineering. They are composed of polymer fibers that are used with soil, rock or other materials. Geosynthetic products include geowebs, geogrids, geonets, geomeshes, geocomposites (geomembrane and geotextile couple) and geotextiles. Geosynthetics are resistant materials to biological and chemical decompositions. When compared to conventional construction techniques, geosynthetics have advantages on providing improvement in engineering performance, reduction in costs and ensurance in safety (Holtz, 2003). The main functions of the geosynthetics can be classified as separating the geomaterials, strengthening the soil deposit, providing drainage, filtering the control of soil particles and retarding the flow of the fluid as seen in Table 2.1 (Gohil *et al.*, 2009; Holtz, 2003).

Geotextiles are the largest group of synthetic materials and permeable textile material including webs, mats, nets, grids and sheets. Geotextiles and geogrids are commonly applied in retaining wall constructions by reinforcing the soil (Holtz, 2003; Gohil *et al.,* 2009). Possibility of slope failures can be prevented by increasing bond tensile strength. They provide drainage by preventing the penetration of coarse particles into lower soil strata that are softer than upper soil.

Table 2.1. Representative Applications of Geotextiles (Gohil *et al.*, 2009; Holtz, 2003).

Primary Function	Application	Secondary Functions
Separation	Unpaved roads (temporary and permanent)	Filter, drains, reinforcement
	Paved roads (secondary and primary)	Filter, drains
	Construction access roads	Filter, drains, reinforcement
	Working platforms	Filter, drains, reinforcement
	Railroads (new construction)	Filter, drains, reinforcement
	Railroads (rehabilitation)	Filter, drains, reinforcement
	Landfill covers	Drains, reinforcement
	Preloading (stabilization)	Drains, reinforcement
	Marine causeways	Filter, drains, reinforcement
	General fill areas	Filter, drains, reinforcement
	Paved and unpaved parking facilities	Filter, drains, reinforcement
	Cattle corrals	Filter, drains, reinforcement
	Coastal and river protection	Filter, drains, reinforcement
	Sports fields	Filter, drains
Drainage-transmission	Retaining walls	Separation, filter
	Vertical drains	Separation, filter
	Horizontal drains	Reinforcement
	Below membranes (drainage of gas and water)	Reinforcement
	Earth dams	Filter
	Below concrete (decking and slabs)	—
Reinforcement	Pavement overlays	—
	Concrete overlays	—
	Subbase reinforcement in roadways and railways	Filter
	Retaining structures	Drains
	Membrane support	Separation, drains, filter
	Embankment reinforcement	Drains
	Fill reinforcement	Drains
	Foundation support	Drains
	Soil encapsulation	Drains, filter separation
	Net against rockfalls	Drains
	Fabric retention systems	Drains
	Sandbags	—
	Reinforcement of membranes	—
	Load redistribution	Separation
	Bridging nonuniformity soft soil areas	Separation
	Encapsulated hydraulic fills	Separation
	Bridge piles for fill placement	—
Filter	Trench drains	Separation, drains
	Pipe wrapping	Separation, drains
	Base course drains	Separation, drains
	Frost protection	Separation, drainage, reinforcement
	Structural drains	Separation, drains
	Toe drains in dams	Separation, drains
	High embankments	Drains
	Filter below fabric-form	Separation, drains
	Silt fences	Separation, drains
	Silt screens	Separation
	Culvert outlets	Separation
	Reverse filters for erosion control:	
	Seeding and mulching	
	Beneath gabions	
	Ditch amoring	
	Embankment protection, coastal	
	Embankment protection, rivers and streams	
	Embankment protection, lakes	
	Vertical drains (wicks)	Separation

Geotextiles are mostly used in drainage, filteration and erosion control (Gohil *et al.,* 2009). They can be combined with geomembranes that are capable of reducing the ground motions transmitted to overlying structures. This combination is called as geocomposite or couple, which are more advantageous than as single. Also, these combinations can be made with geotextile-geonets, geotextile-geogrids, geotextile-geomembranes, geomembrane-geonets and geotextile-polymeric cores (Holtz, 2003; Yegian and Lahlaf, 1992; Yegian *et al.,* 1999).

Ling and Liu (2001) investigated the reinforcement of concrete pavement by using geosynthetics and concluded that geosynthetics were reliable materials in increasing stiffness, bearing capacity and the life of concrete layer.

Haijani (2003) suggested that more increase in number of reinforcement layers is provided, more increase in bearing capacity is observed regarding a range of effective depths.

A parametric study which was conducted by Ghazavi and Lavasan (2008) found out that distance between reinforcing layers and footing, depth and width of synthetic layers play an important role on bearing capacity, and geogrid layers provide an increase in bearing capacity. Moreover, better performance in geosynthetic reinforcement was observed when the desired depth was provided for reinforcement layers in terms of bearing capacity (Sharma *et al.,* 2009).

In addition to the above mentioned properties, geosynthetics can be used as seismic isolator owing to the fact that they are capable of absorbing seismic energy and transmit reduced horizontal and vertical earthquake excitations to the superstructure when geosynthetics are placed under the foundation of overlying structure. They are also cost-effective and practical aspects in high-seismic regions when compared to conventional structural base isolation systems (Yegian and Lahlaf, 1992; Yegian *et al.,* 1999). One of the most common techniques in base isolation is sliding that provides restriction in transmission of shear forces to overlying structure by friction. However, high maintenance and installation cost of conventional base isolators overweight its advantages in reduction of transmitted

forces (Tsang, 2008). Therefore, geosynthetics can be considered in seismic base isolation due to its low-cost operating and installation system.

Selection of the geocomposites is a quite important task. Geotextile and geomembrane couples are the most common type of geosynthetic seismic isolation system. Concept of this geocomposites is to create a smooth layer between structure and soil to dissipate seismic energy sliding. Limitation in displacement caused by sliding is important aspects to take into consideration in design. Dynamic shear strength tests and rigid block tests were conducted by Yegian and Lahlaf (1992) and Yegian *et al.* (1995) using shaking table with different frequencies of ground motions. Results of shaking table tests concluded that transmitted acceleration to the structure without any reduction until resistance of liner interface was overcome by exerted force as seen in Figure 2.23 and Figure 2.24 (Yegian and Lahlaf, 1992). Moreover, larger dynamic friction angles were observed instead of that under static conditions. The friction angle values can be seen in Table 2.2 and Table 2.3 (Yegian and Lahlaf, 1992).

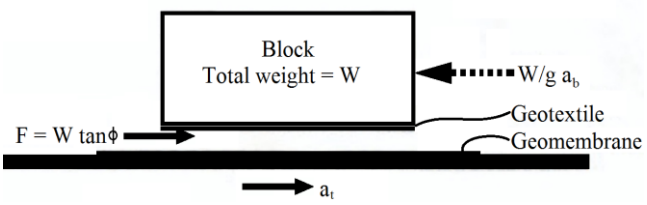

Figure 2.23. Free Body Diagram of the Rigid Block Experiment (Yegian and Lahlaf, 1992).

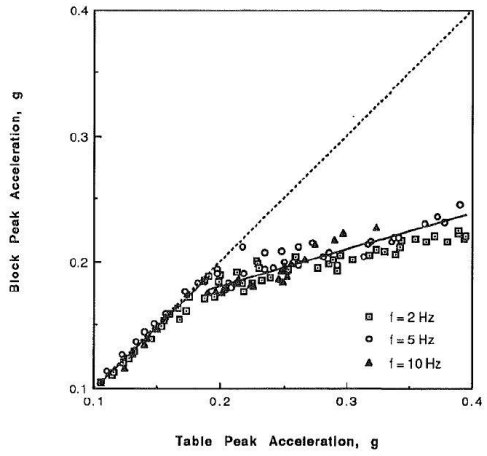

Figure 2.24. Shaking Table Test Results (Yegian and Lahlaf, 1992).

Table 2.2. Dynamic Friction Angles (Yegian and Lahlaf, 1992).

Interface condition (1)	Acceleration transmitted to block at first observation of sliding (2)	Peak dynamic friction angle (3)	Acceleration transmitted to the block after sliding is initiated (4)	Residual dynamic friction angle (5)
Geomembrane[a]/geotextile[b] dry	0.2 g	11.3°	0.19 g[c]–.24 g[d]	10.7–13.5°
Geomembrane[a]/geotextile[b] submerged	0.19 g	10.7°	0.17 g[c]–.23 g[d]	9.6–13°

[a]Gundle HD60: hard, smooth HDPE.
[b]Polyfelt TS700: Nonwoven, continuous filament, needlepunched geotextile.
[c]At first observation of sliding.
[d]At table acceleration of 0.4 g.

Table 2.3. Static Friction Angles (Yegian and Lahlaf, 1992).

Interface condition (1)	Peak angle of friction ϕ (2)	tan ϕ (3)	Residual angle of friction ϕ (4)	tan ϕ (5)
Geomembrane[a]/geotextile[b] dry	10.7°	0.19	10.0°	0.18
Geomembrane[a]/geotextile[b] submerged	9.6°	0.17	8.5°	0.15

[a]Gundle HD60: hard, smooth HDPE.
[b]Polyfelt TS700: Nonwoven, continuous filament, needlepunched geotextile.

Yegian and Kadakal (2004) proposed that friction coefficients and slip displacements have to be low in order to provide mitigation of seismic damages. In their study, four different type of geosynthetic couples were considered. Geotextile/HDPE (High Density Polyethylene), PTFE/PTFE (Polypropylene), UHMWPE/UHMWPE (Ultra-High Molecular Weight Polyproethylene) and geotextile/UHMWPE were selected in cyclic load tests. According to the test results, geotextile/UHMWPE was found as the most reliable case. As a result of these tests, there needs further detailed tests to evaluate the effects of the type of geocomposites in distinctive conditions so that the most suitable case can be observed. Moreover, several shaking table tests conducted on two different smooth geomembrane concluded that transmitted force is limited between two geomembranes and thus, expanded tests were suggested to investigate in detail (Yegian and Kadakal, 2004; Yegian and Catan 2004). Four types of synthetic material were used in the shaking table tests to evaluate dynamic behavior of sliding surfaces. List of synthetic liners investigated for suitability can be seen in Table 2.4 (Yegian and Kadakal, 2004).

Table 2.4. List of Synthetic Liners Used by Yegian and Kadakal (2004).

Interface	Description	Friction coefficient[a]
Geotextile/HDPE	A high-strength nonwoven geotextile, "Typar 3601" against 1.5 mm smooth HDPE (high density polyethylene)	0.15–0.3
PTFE/PTFE	Two sheets of 1.5 mm thickness PTFE (polypropylene)	0.08– 0.15
UHMWPE/UHMWPE	Two layers of 6.4 mm thick UHMWPE (ultrahigh molecular weight polyethylene) "TIVAR 88-2 AntiStatic"	0.09–0.25
Geotextile/UHMWPE	Typar 3601 geotextile against TIVAR 88-2, 6.4 mm thick UHMWPE	0.06–0.08

[a]Range depends on number of cycles, normal stress, and sliding velocity.

Cyclic load tests were conducted to determine friction coefficients of specified synthetic liner surfaces. In these tests, influence of normal stress, number of cycles, and sliding velocity were examined. Shaking table tests were used to conduct displacement-controlled and velocity-control cyclic load tests as seen in Figure 2.25.

Displacement-controlled cyclic load tests are not useful in obtaining relevant information about dynamic response of the structure using plastic interface of four selected synthetic liners. Hence, rigid block tests are utilized to estimate dynamic response of the system considering permanent deformations, transmitted accelerations, and the effects of frequency and amplitude of the excitation. Dynamic transmissibility and slip characteristics of different geosynthetic surfaces can be observed by rigid block tests as seen in Figure 2.26. Earthquake and harmonic excitation as table accelerations were used to evaluate dynamic response of the liners (Kavazanjian *et al.*, 1991; Yegian and Lahlaf, 1992; Yegian *et al.*, 1995; Yegian *et al.*, 1999; Yegian and Kadakal, 2004).

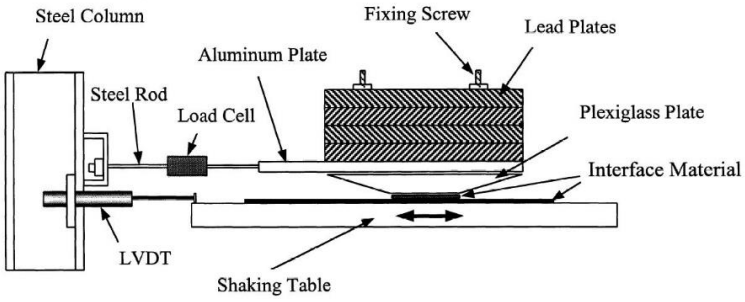

Figure 2.25. Schematic Demonstration of the Cyclic Load Test Setup (Yegian and Kadakal, 2004).

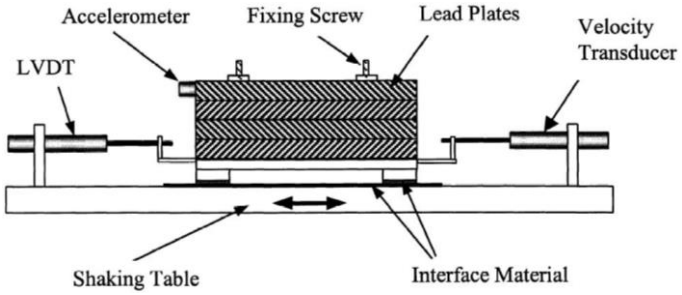

Figure 2.26. Schematic Demonstration of the Rigid Block Test Setup (Yegian and Kadakal, 2004).

Another study was conducted on shaking table facility of Bogazici University Kandilli Observatory and Earthquake Research Institute (Sekman, 2016). Suitable geosynthetic couples were found by rigid block tests as seen in Figure 2.27. As earthquake motion, El Centro, Kobe and Kocaeli earthquakes were selected with varying acceleration amplitudes.

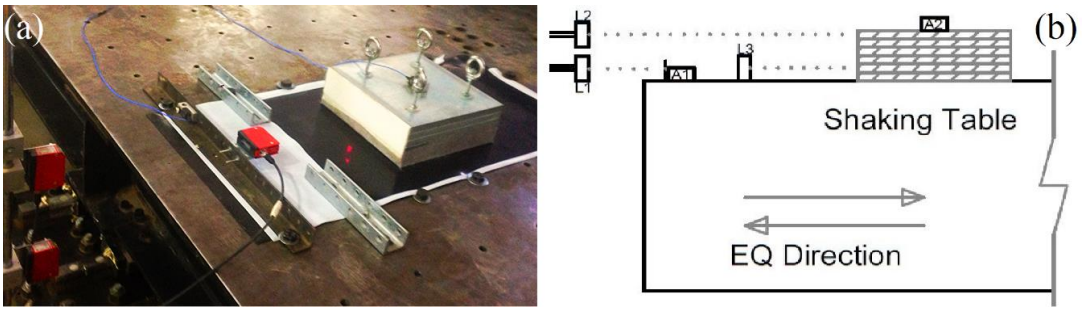

Figure 2.27. (a) A View of Rigid Block Test Setup and (b) Experimental Setup Layout of the Rigid Block Experiment (Sekman, 2016).

In order to determine the dynamic properties of the geosynthetic materials, three different geomembrane-geotextile configurations were used in shaking table tests. Dynamic friction angles of the three geomembrane/geotextile configurations were calculated in the first observation of sliding as seen in Table 2.5. Average of the friction angles was taken to clearify discrepancy among the three geomembrane-geotextile (GG) couples. In the first observation of sliding, dynamic friction angle (ϕ_d) was observed as minimal in the presence of PTFE/SF44 (Sekman, 2016).

Table 2.5. Block Acceleration (a_b) and Dynamic Friction Angles (ϕ_d) of the Three Geomembrane/Geotextile Configurations at the First Observation of Sliding (Sekman, 2016).

Shaking Table Motions	PTFE/SF 44		PTFE/SF 56		HDPE/SF 44	
	a_b (g)	φ_d (^{o})	a_b (g)	φ_d (^{o})	a_b (g)	φ_d (^{o})
1 Hz	0.132	7.510	0.127	7.260	0.261	14.630
2 Hz	0.111	6.320	0.123	7.030	0.244	13.700
3 Hz	0.098	5.600	0.128	7.290	0.219	12.350
4 Hz	0.108	6.180	0.111	6.360	0.223	12.580
5 Hz	0.086	4.890	0.126	7.150	0.214	12.090
El Centro Eq.	0.132	7.530	0.139	7.910	—[1]	—[1]
Kobe Eq.	0.119	6.760	0.115	6.550	0.299	16.640
Kocaeli Eq.	0.115	6.550	0.142	8.090	—[1]	—[1]
Avg.	0.112	6.418	0.126	7.205	0.243	13.665

That the limitation of transmitted accelerations after sliding initiated which means residual acceleration is the other criteria for GG couple. Measured peak table (A_t) and peak block (A_b, residual acceleration) accelerations were illustrated in Table 2.6 under different ground motions for three different geosynthetic couples. Threshold acceleration values for initiation of the GSI system were determined as 0.11g for PTFE/SF44 (GSI2), 0.13g for PTFE/SF56 (GSI3) and 0.24g for HDPE/SF44 (GSI1). Percentage (%) reduction parameters were used to make comparison the effectiveness of geosynthetic couples. Reduction percentages were computed with 100% minus the ratio between the peak block acceleration and peak table acceleration. According to experimental results as seen in Table 2.6, the proposed GSI system provides better response at higher acceleration values in accordance with rigid block experiments. Percentage reduction parameters were indicated in Figure 2.28 under selected eight input motions respectively 1 Hz, 2 Hz, 3 Hz, 4 Hz, 5 Hz, Kocaeli earthquake (1999), Kobe earthquake (1995) and El Centro earthquake (1940). Additionally, the peak slip displacements (D_s) were given in the Table 2.6 regarding given input ground motions.

[1] Depth of the GSI: depth from the foundation of the building model.

Table 2.6. Measured Peak Table Accelerations (A_t), Peak Block (Residual) Accelerations (A_b) and Slip Displacements (D_s) (Sekman, 2016).

PTFE/SF44								
	1 Hz	2 Hz	3 Hz	4 Hz	5 Hz	El Centro Eq. (1940)	Kobe Eq. (1995)	Kocaeli Eq. (1999)
A_t	0.34	0.63	0.76	0.67	0.79	0.34	0.69	0.21
A_b	0.19	0.20	0.19	0.20	0.21	0.15	0.18	0.14
% Reduction	45	69	74	70	74	57	74	36
D_s	6.99	3.81	7.29	2.57	3.82	0.47	2.98	0.50
PTFE/SF56								
	1 Hz	2 Hz	3 Hz	4 Hz	5 Hz	El Centro Eq. (1940)	Kobe Eq. (1995)	Kocaeli Eq. (1999)
A_t	0.32	0.62	0.77	0.68	0.82	0.33	0.74	0.24
A_b	0.20	0.21	0.21	0.21	0.22	0.17	0.19	0.16
% Reduction	38	67	73	69	73	50	74	34
D_s	4.08	6.08	7.76	5.08	4.69	0.45	2.83	0.31
HDPE/SF44								
	1 Hz	2 Hz	3 Hz	4 Hz	5 Hz	El Centro Eq. (1940)	Kobe Eq. (1995)	Kocaeli Eq. (1999)
A_t	0.35	0.63	0.77	0.67	0.81	0.32	0.78	0.24
A_b	0.30	0.33	0.33	0.35	0.35	0.28	0.33	0.24
% Reduction	12	48	57	48	56	13	58	0
D_s	1.14	3.77	3.99	5.45	9.87	0.15	1.36	0.16

Figure 2.29 indicated the peak block acceleration with respect to peak table acceleration under eight given ground motions. The block acceleration appeared as identical to the shaking table acceleration until sliding during these tests. Slip displacements of the block with PTFE/SF44 under cyclic sinusoidal motion with 1 Hz and 5 Hz and Kobe Earthquake (1995) are shown in Figure 2.30.

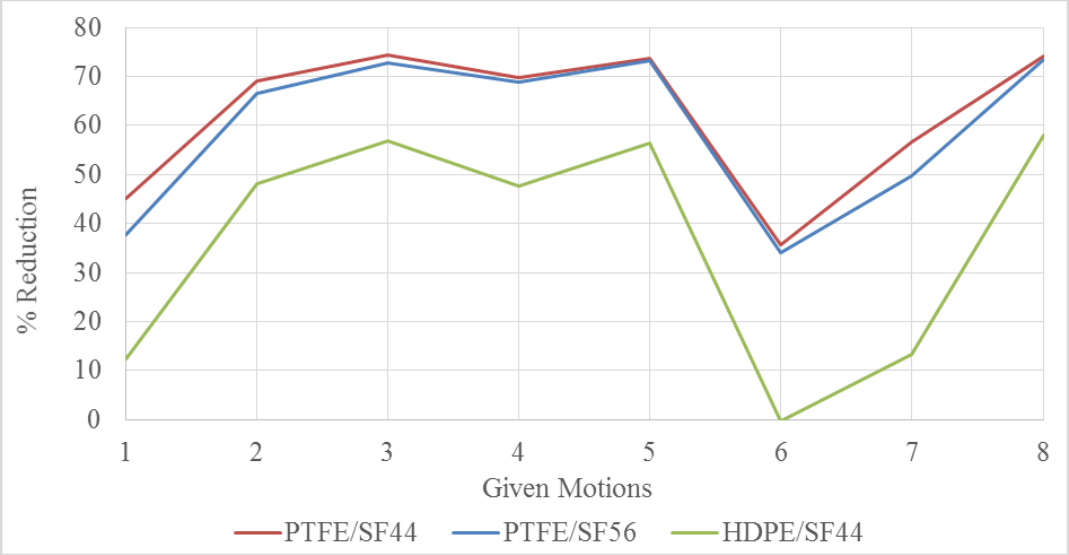

Figure 2.28. % Reduction under Eight Different Shaking Table Motions Respectively 1 Hz, 2 Hz, 3 Hz, 4 Hz, 5 Hz, Kocaeli earthquake (1999), Kobe earthquake (1995) and El Centro earthquake (1940) (Sekman, 2016).

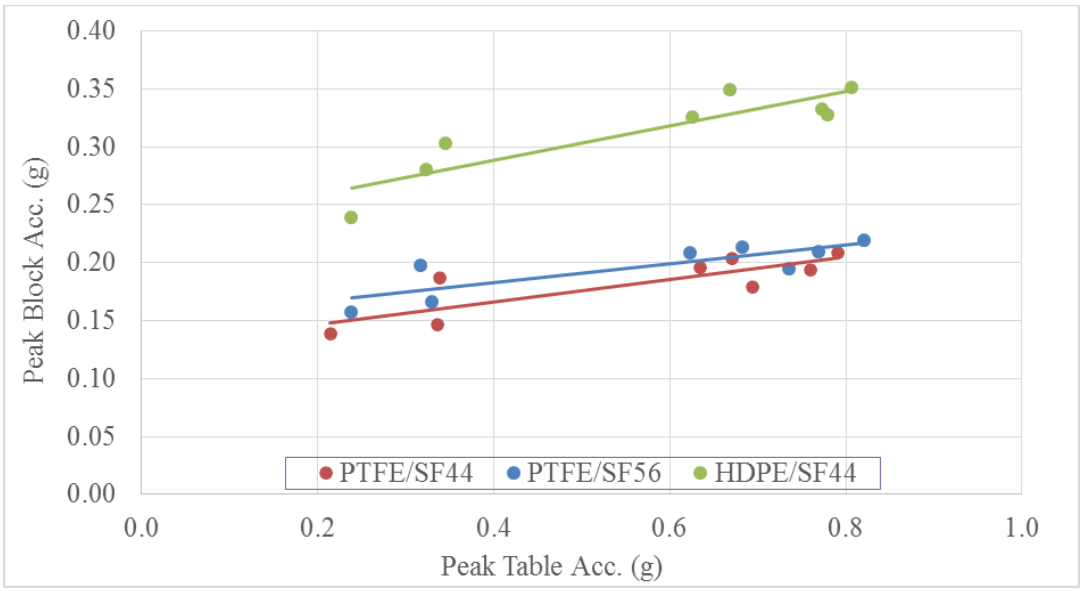

Figure 2.29. Peak Block Accelerations versus Peak Table Accelerations under Eight Different Shaking Table Motions Respectively 1 Hz, 2 Hz, 3 Hz, 4 Hz, 5 Hz, Kocaeli earthquake (1999), Kobe earthquake (1995) and El Centro earthquake (1940) (Sekman, 2016).

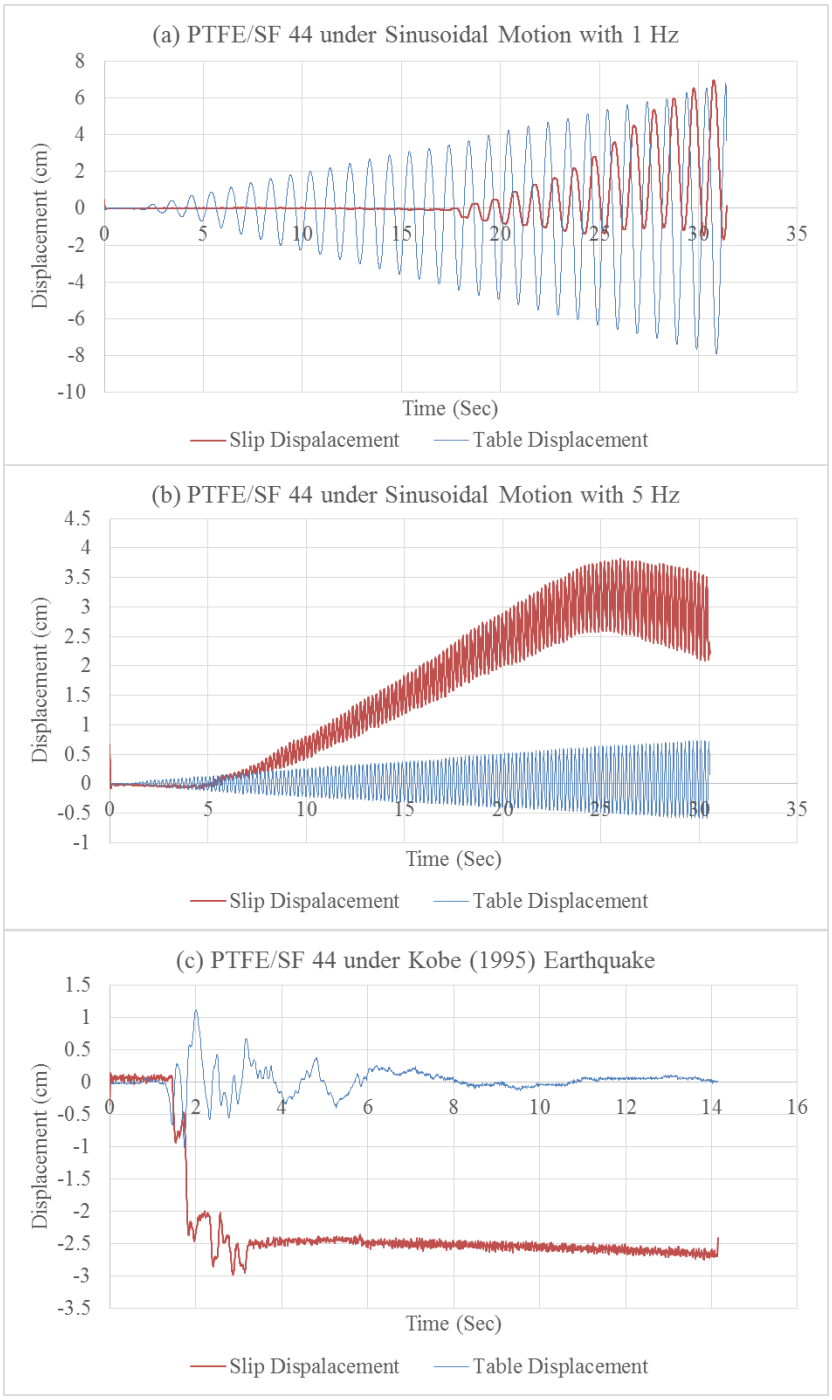

Figure 2.30. (a) Slip Displacements of the Block under 1 Hz Cyclic Sinusoidal Motion, (b) Slip Displacements of the Block under 5 Hz Cyclic Sinusoidal Motion, and (c) Slip Displacements of the Block under Kobe (1995) Earthquake (Sekman, 2016).

Transmitted acceleration were limited by geomembrane-geotextile (GG) after sliding initiated. PTFE/SF44 (GSI2) exhibited minimum residual dynamic friction angle that reduces the transmitted acceleration more than others do (Sekman, 2016).

Aformentioned results provided the information during the input and material selection for the shaking table experiments. Moreover, the friction between the geomembrane and geotextile are verified with the former studies about the GSI with geosynthetics. According to the results of the shaking table tests on a geomembrane/geotextile system, limitation of shear stress transmitted from a geomembrane to a geotextile could be observed. Therefore, any structure or a soil deposit resting on the geotextile can experience only a limiting acceleration by relative displacement initiated along the geomembrane-geotextile interface (Sekman, 2016).

In the following parts, types of GSI with geosynthetics as soil and foundation isolations were introduced and detailed information was given.

2.2.2.1. Soil Isolation with Geosynthetics. The technique that the synthetic liner is placed within the soil profile to absorb earthquake energy is commonly known as *soil isolation*. Slip deformations provide reduction in earthquake energy through sliding along synthetic liner interface. In this system, soil above the liner is isolated from underlying soil deposit under seismic excitation. Soil isolation can be used in the construction of reclaimed land, slopes and embankments (Tsang, 2008; Yegian and Catan 2004). In addition, curved shaped liners provide restoring force against gravitational force to return original position after sliding. Permanent deformations related to slip movement limits the use of soil isolation. Therefore, curved shaped liners are used instead of horizontal liners to reduce slip deformations (Yegian and Catan, 2004; Suresh *et al.*, 2015). Liners are placed along the shaking direction due to uniaxial shaking table tests. They used two types of curved liners in their studies as seen in Figure 2.31a and Figure 2.31b. If the depth of penetration of synthetic liner (D) and horizontal length of isolated soil mass (H) were small, reduction in absorption of seismic energy became more difficult for cylindrical shaped liner. On the other hand, it is provided that the development of further studies will be larger in real field compared to laboratory tests. According to the conducted shaking table tests results, tube shaped liners exhibited

more reliable results and more practical than cylindrical shaped liners in application area. Tests results demonstrated that more increase in table acceleration was observed, more effective results were obtained in the use of tub shaped liner (Yegian and Catan, 2004).

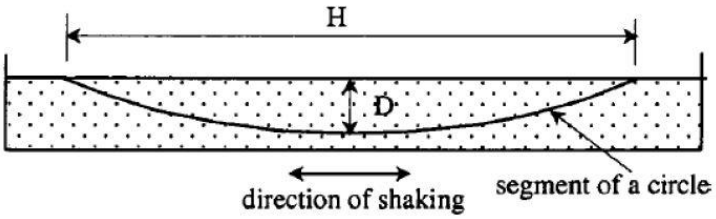

(a) Cylindrical-Shaped Liner, H/D = 6.6

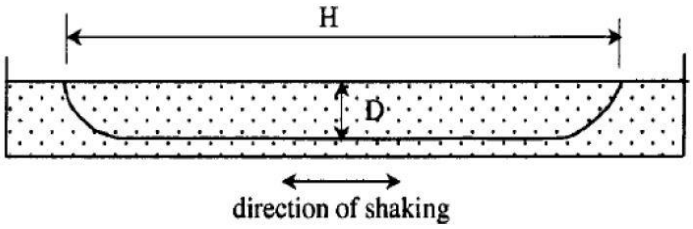

(b) Tub-Shaped Liner, H/D = 9

Figure 2.31. Cylindrical and Tub-Shaped Soil Isolation Systems (Yegian and Catan, 2004).

Selected models for cylindrical and tub-shaped synthetic liners within the soil in soil isolation are shown in Figure 2.32.

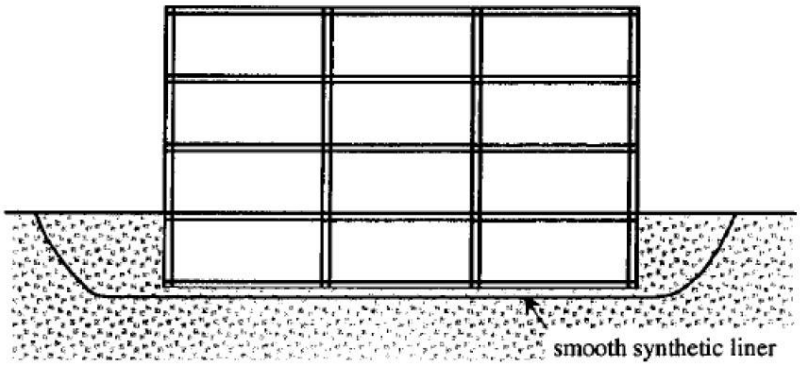

Figure 2.32. Soil Isolation System Demonstration (Yegian and Catan, 2004).

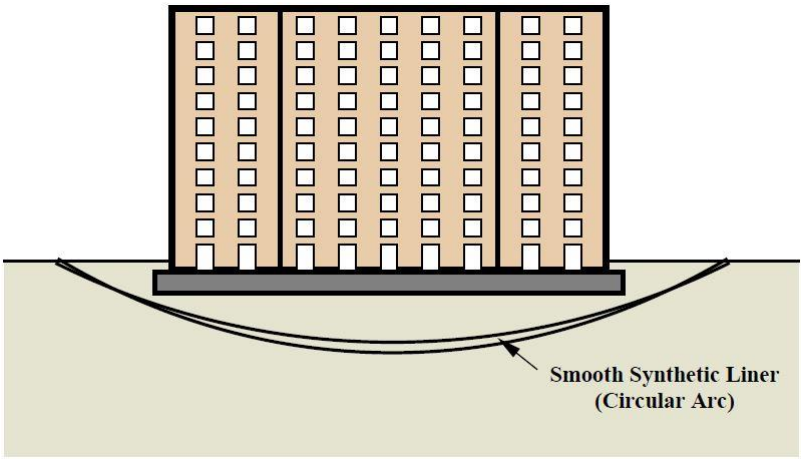

Figure 2.33. Schematic Drawing of Cylindrical Shaped Soil Isolation System (Tsang, 2008).

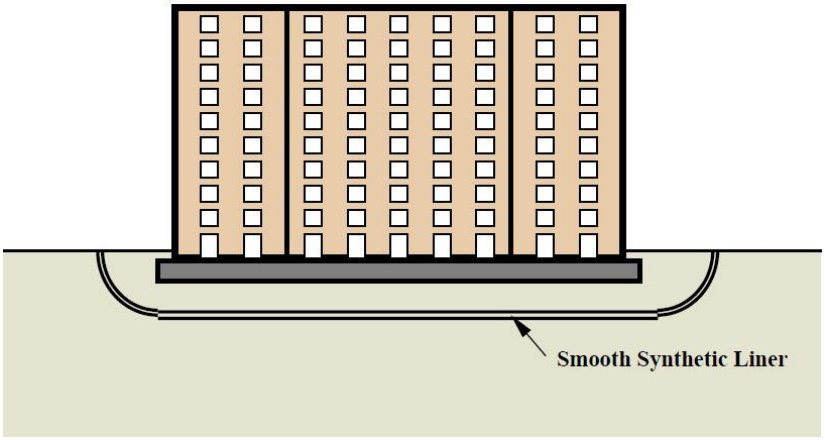

Figure 2.34. Schematic Drawing of Tub Shaped Soil Isolation System (Tsang, 2008).

As a result of the test results, curved shaped synthetic liners provide reduction in transmitted acceleration to overlying structure through sliding within limits. Yegian and Catan (2004) performed sensitivity analysis to determine effectiveness of synthetic liners on soil isolation. They provide a graph that demonstrates the peak transmitted accelerations as a function of H/D ratio with the limitation of penetration depth which is equals to or greater than 3 m (Figure 2.35).

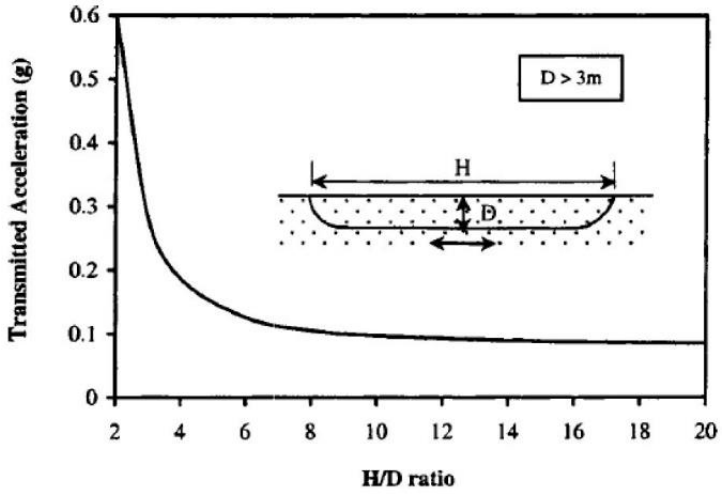

Figure 2.35. Transmitted Acceleration as A Function of H/D Ratio (Yegian and Catan, 2004).

The geometry of isolation liner, type and properties of soil deposit, and type of seismic excitation play an important role in soil isolation. Further research on soil isolation provides different types of isolation system to examine optimal geometry of using synthetic liners. Outside of proposed soil isolation systems, trapezoidal and compound trapezoidal liner were evaluated as seen in Figure 2.36 and Figure 2.37 (Georgarakos *et al.*, 2005; Tsang, 2008).

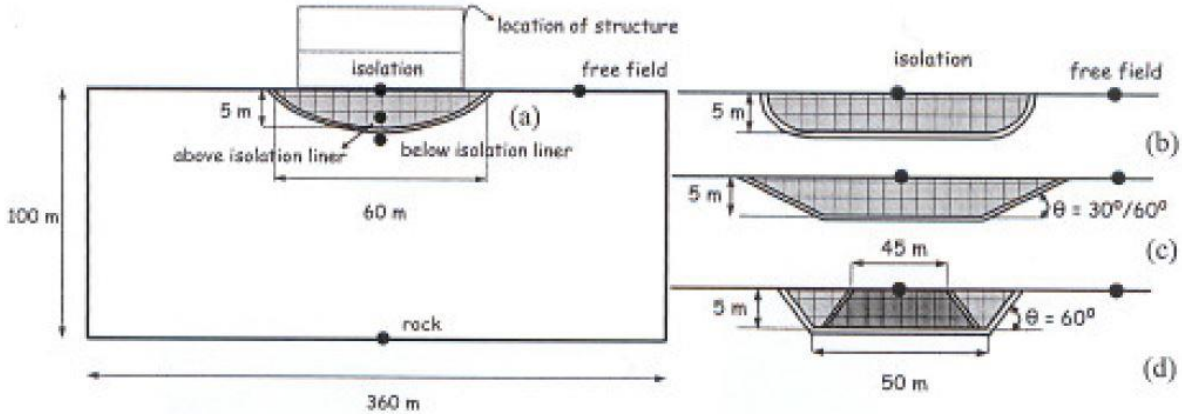

Figure 2.36. In-soil Isolation Systems: (a) Cylindrical, (b) Tub, (c) Trapezoidal, (d) Compound Trapezoidal Liner Geometry (Georgarakos *et al.*, 2005).

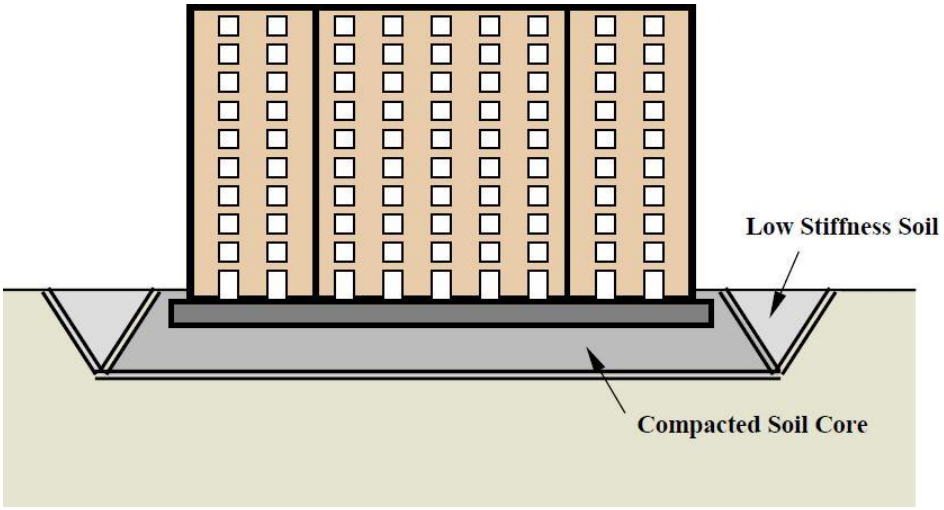

Figure 2.37. Schematic Drawing of Trapezoidal Shaped Soil Isolation System (Tsang, 2008).

According to the conducted study, cylindrical and compound trapezoidal soil isolation types were found as the most efficient liner geometries. Instead of limited displacements, these two types of liner demonstrated considerable alleviation in seismic excitation on the surface without any failure. The results showed that magnitude of transmitted acceleration, slip displacements and soil deformations are directly based on the geometry of used synthetic liner. However, further analysis are needed to evaluate benefits of soil isolation systems on structures (Georgarakos *et al.*, 2005).

Consequences of the another study, numerical experiments showed that trapezoidal soil isolation is an effective technique in case of an extreme seismic loading as seen in Figure 2.38. As the acceleration amplitude increases, effectiveness of the isolation system reduces. Acceleration time histories, moment-curvature relationship and story drifts were compared and the results illustrated that soil isolation is promising way of cost-effective seismic isolation technique. However, slip displacements may occur on synthetic liner while cutting off transmitting acceleration to the superstructure. On the other hand, ensurance in survivability was proven by tests (Tsatsis *et al.*, 2013).

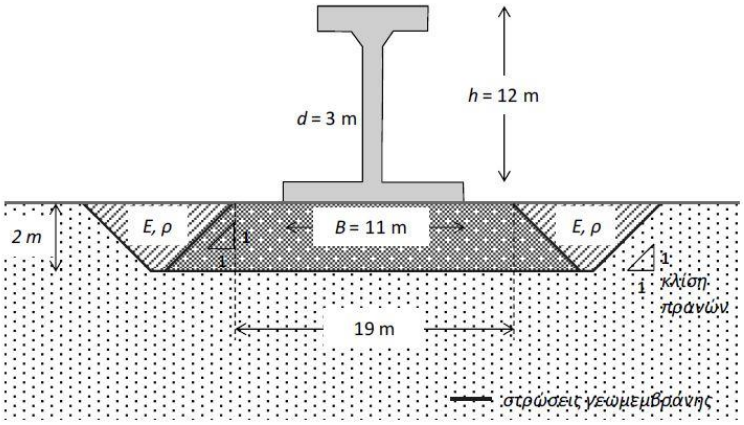

Figure 2.38. Schematic Illustration of In-Soil Isolation System (Tsatsis *et al.*, 2013).

Moreover, bond between soil and synthetic liners is need to be efficient to minimize relative displacement between the liner and soil. Sliding of isolated soil mass over geosynthetic should be avoided to obtain better resutls. Thus, friction angle between soil and geosynthetic was studied by several researchers. As a result of a study, observed range of friction angle between PVC geomembrane and three different types of sand was about 32° to 40° (Ling *et al.*, 2002). Between gravel and geotextile, conducted pullout tests concluded that friction angle varies between 37° to 53° (Perkins and Cuelho, 1999). Frictional resistance between two geosynthetics is generally less than that of between soil and geosynthetics. It is suggested that if there are two geosynthetics in contact, sliding movement is not possible (Tsang, 2008).

In addition to the above mentioned points, creep and stress relaxation are also significant factor in design for a long service life. If there is high creep rates, it is due to the high temperature and high level of exerted load that cause rupture and deformations on geosynthetics. In the presence of soft soil as isolated soil mass, stress relaxation is likely to be observed in synthetic liner. Installation is an another factor that causes failures in geosynthetics. In case of a damage while installation, strength loss is able to be observed. Functionality of geosynthetics that are sensitive to be damaged can be affected by cuts, tears and punctures observed during installation process. Also, geosynthetics should be avoided from exposure to sunlight due to degradation caused by ultraviolet attack (Tsang, 2008).

Furthermore, bathtub is a damaging effect caused by trapped water between geomembrane and geotextile due to the impermeability of geomembrane. If soil is not compacted enough, then liner should be efficient to infiltrate water into the soil. Otherwise, premature failures may be observed (Tsang, 2008).

As mentioned in the block tests conducted by Sekman (2016), HDPE-SF44 couple corresponds to the GSI 1. Additionally, PTFE-SF44 geotextile-geomembrane couple was defined as GSI 2. Lastly, PTFE-SF56 liner was described as GSI 3. Sekman(2016) performed shaking table experiments by using these three GG couples under three and five story building models. Scaled model buildings for three and five story under proposed GSI system were shown in Figure 2.39.

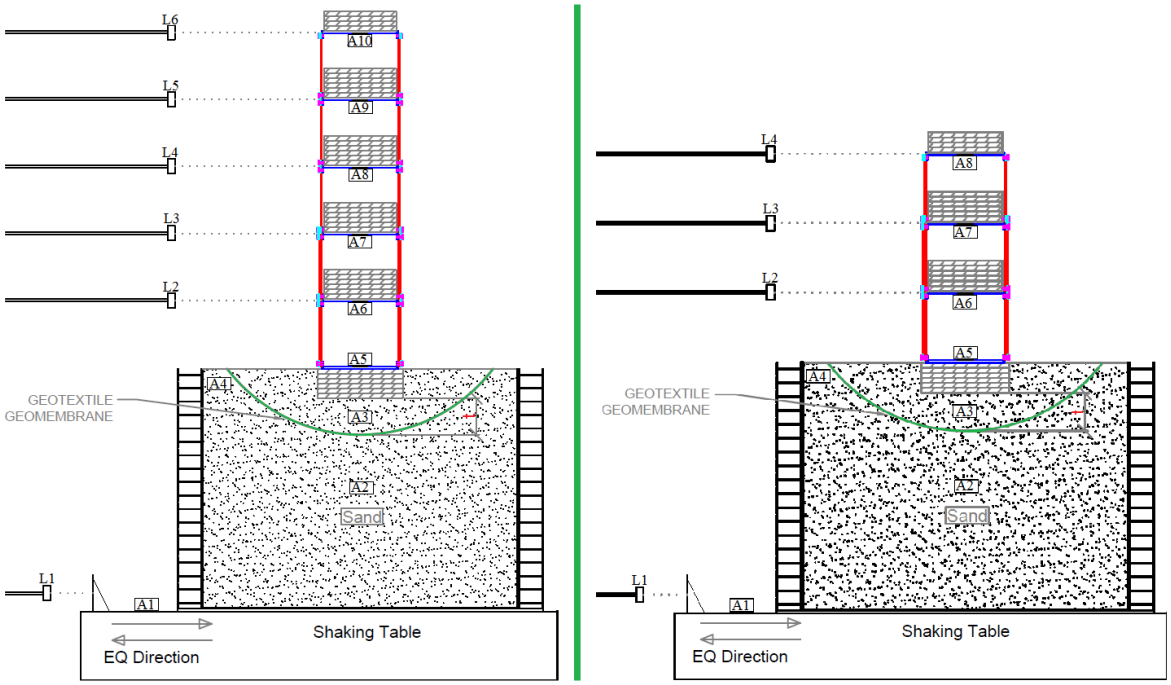

Figure 2.39. Sketch of Proposed GSI System Experiment Setup with 5-story and 3-Story Scaled Building Models (Sekman, 2016).

According to the results given by the study of Sekman (2016), the proposed GSI system exhibited great beneficial effect on the seismic performance of the 3-story and 5-story scaled building models. Among the GSI types, GSI 2 worked better with penetration depth of 15 cm. On the other hand, GSI 3 exhibited more reliable results with penetration

depth of 10 cm. It was observed that discrepancy between GSI depth and GSI type was related to the friction coefficient of the GSI materail. Also, it was concluded that GSI materials having lower friction coefficients had more tendency to lower the transmitted accelerations to the overlying buildings through sliding with increasing GSI depth and curvature. Lower friction coefficients provided less friction forces. Thus, isolated soil mass became bigger. The proposed GSI system exhibited more reduction under cyclic sinusodial motion at frequency values which was very close to the natural frequency of the building. Moreover, proposed GSI system could not provided sufficient enhancement in performance under Kobe earthquake due to the very high spectral values and long duration. In the higher PGA values than 0.8g, geocomposites were not effective due to the permanent slip displacements. On the other hand, damping of the system was improved in general. When compared to the conventional seismic isolation systems, natural period was not shifted. However, the obtained spectral accelerations were dropped at the natural period of the building model.

Performance indicator parameters were also evaluated at the end of the tests. Top floor and foundation level of the building models were reduced up to 26% and 28%, respectively. Additionally, first floor drifts were alleviated up to 16%. It means, soft story phenamenon was substantailly mitigated. Furthermore, top floor Arias intensity, foundation level Arias intensity, base shear and base moment were decreased up to, 51%, 23%, 26% and 22%, respectively. For example, representative results of GSI 1 with 10 cm depth were shown in Figure 2.40 (Sekman, 2016).

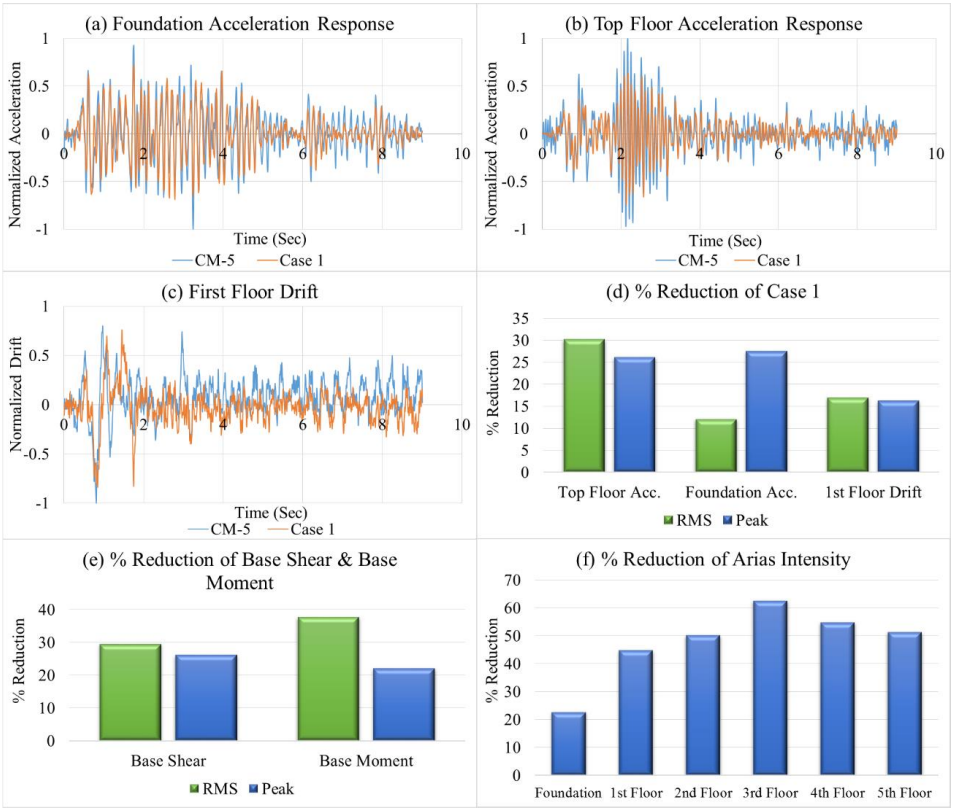

Figure 2.40. (a) Foundation, (b) Top Floor Horizontal Acceleration Response, (c) First Floor Drift, (d) % Reduction of Experimental Results, (e) % Reduction of Base Shear and Base Moment and (f) % Reduction of Arias Intensity of Experimental Results under Kocaeli Earthquake (Sekman, 2016).

Above mentioned numerical and experimental studies demonstrated that proposed GSI system provided efficiency under seismic excitations and played an important role on mitigation of seismic hazards on low-to-mid rise buildings for developing countries. However, geosynthetics are very sensitive materials and directly affected from surroundings and natural phenomena. Thus, necessary protection techniques should be taken into consideration. Also, soil isolation provides beneficial function in application, however, with several drawbacks. There is a possibility of occurance of excessive slip displacement at synthetic liner. In addition, curve shaped liners provide gravitational restoring force to bring the isolated soil mass to its original position. However, it can be difficult, expensive and impractical way to give a cylindrical shape to the synthetic liner in field applications. Soil isolation was recommended to be used in the soils that is prone to liquify during seismic excitations. (Tsatsis *et al.*, 2013; Kumar *et al.*, 2015; Sekman, 2016).

2.2.2.2. Foundation Isolation with Geosynthetics. A seismic isolation technique that is described as placement of the synthetic liner underneath the foundation of a structure. Working principle is same as conventional base isolation. However, entire building is separated from ground by geosynthetic liner in foundation isolation. Absorption of energy and transmission of ground motion forces are supplied by smooth geosynthetic liner underneath the foundation of the building sliding movement. Also, behavior of foundation isolation is similar to the Fricion Pendulum System (FPS) which is a conventional structural seismic isolation techniques. Use of geosynthetic materials in seismic isolation systems for application in earthquake hazard mitigation is shown in Figure 2.41 and Figure 2.42 (Yegian *et al.*, 1999; Yegian and Kadakal, 2004; Edincliler and Sekman, 2016; Suresh *et al.*, 2015).

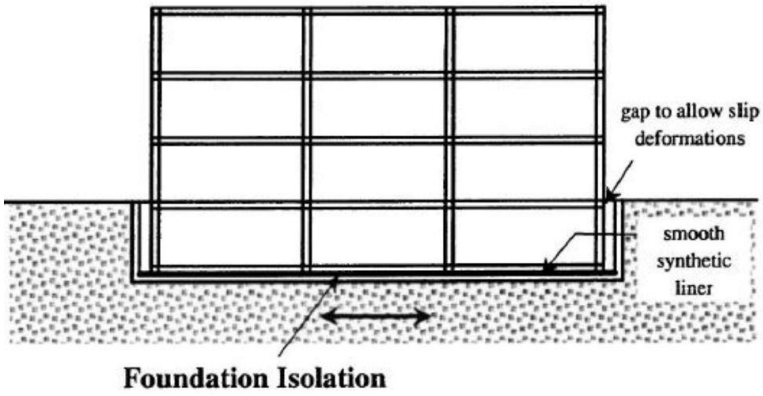

Figure 2.41. Schematic Illustration of Foundation Isolation System (Yegian *et al.*, 1999).

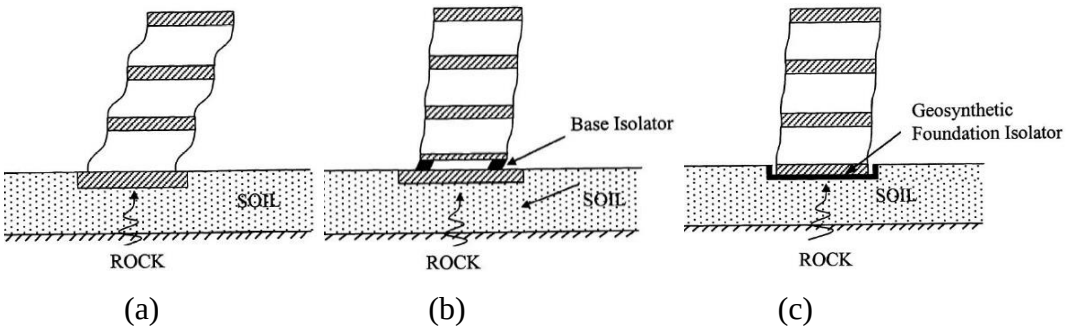

Figure 2.42. (a) Ordinary Structure Subjected to Earthquake, (b) Structure with Conventional Base Isolation Subjected to Earthquake, (c) Structure with Geosynthetic Base Isolation Subjected to Earthquake (Yegian *et al.*, 1999).

The following figure illustrates the comparison of the structural responses between with and without foundation isolation under seismic excitation as seen in Figure 2.43 (Yegian *et al.*, 1999).

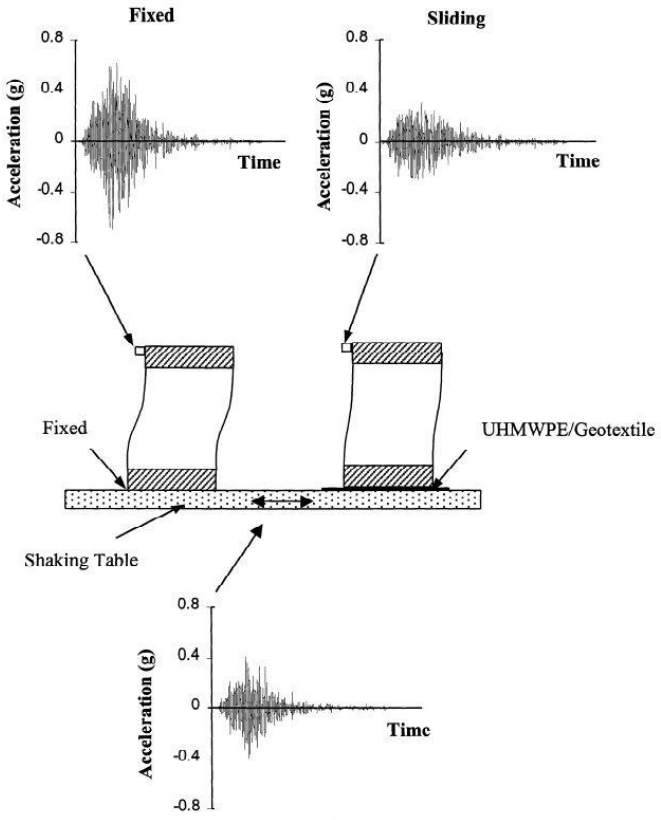

Figure 2.43. Seismic Responses of Building with and without Foundation Isolation Subjected to 0.8g PGA (Yegian *et al.*, 1999).

Some requirements should be met for foundation isolation material (Yegian and Kadakal 2004; Gohil *et al.*, 2009).

- In general, friction coefficients between 0.05 and 0.15 are satisfying values for isolation concept to minimize accelerations transmitted through sliding surface.
- The static friction coefficient should be larger than the dynamic friction coefficient.
- The friction coefficients should be insensitive to velocity, normal stress, sliding distance, moisture and temperature.

- Geosynthetic materials are needed to be resistant to chemical and biological attacks, and to long-term creep effects.
- To provide functionality of the structures during seismic excitation, maximum and permanent slip displacements should be substantially small.

Moreover, influence of inertial effects which may cause deformations that are different from the results obtained from rigid block tests has to be taken into consideration. Thus, dynamic response of a single story building model on foundation isolation was investigated. Also, harmonic and earthquake type table accelerations were used to measure dynamic responses with fixed and isolated cases. Test setup of the model was demonstrated in Figure 2.44 (Yegian *et al.*, 1999; Yegian and Kadakal, 2004; Suresh *et al.*, 2015).

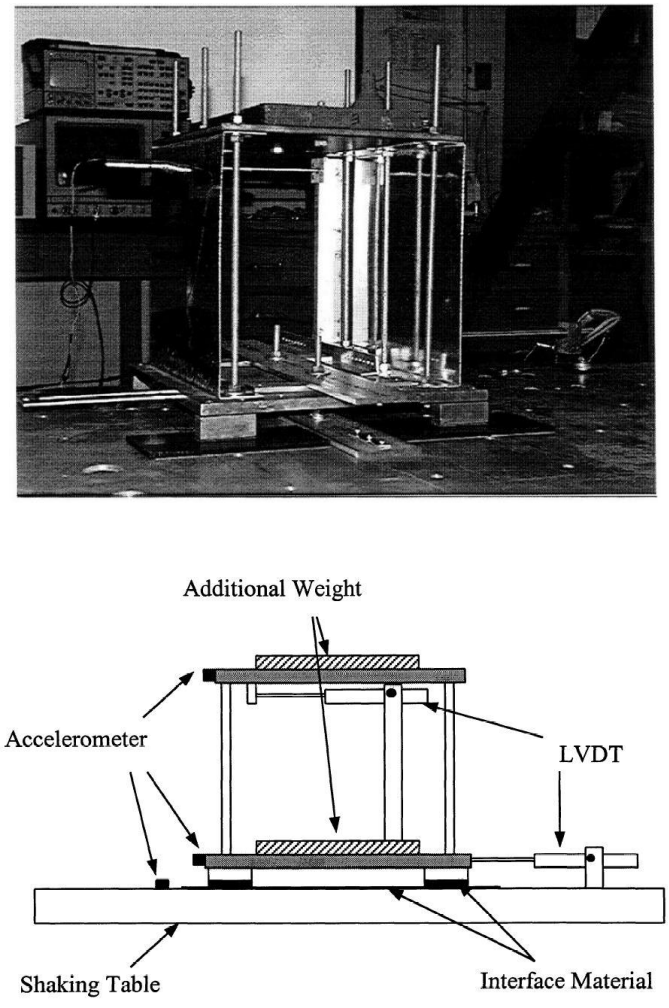

Figure 2.44. Schematic Demonstration of the Building Model Structure (Yegian and Kadakal, 2004).

According to the test results, geotextile over an Ultra-High Molecular Weight Polyethylene (geotextile/UHMWPE) gave better and suitable results on frictional interfaces in foundation isolation application. In the single-story model test, dynamic response of the model on foundation isolations illustrated lower response when compared to fixed based model on shaking table (Yegian and Kadakal, 2004).

A research was conducted to evaluate dynamic behavior of a seismic isolation system by using composite liner including high strength geotextile and an ultra-high molecular weight polyethylene (UHMWPE) geomembrane. Three and five story model buildings were used to represent low and medium rise buildings (Figure 2.45). In the study, Typar-3601 type geotextile and TYVAR 88-2 (6.4 mm thick) geomembrane were used under the model buildings. After the setup of the experiment, free vibration tests were applied for each building. Then, some harmonic and random excitations were applied for fixed based and isolated based model building. (Kalpakci, 2013).

Figure 2.45. Three and Five Story Model Buildings (Kalpakci, 2013).

When all the harmonic and random motion test results for three and five story model building were taken into consideration, it was concluded that maximum reduction was obtained at vicinity of natural frequency of the model structures. Under harmonic motion, proposed system was not triggered even if the frequencies were twice of the natural frequency of the superstructure. However, the composite liner system was initiated even though the frequency of the initiation was not close enough to the natural frequency of the

model building under random motions. Besides, the efficiency of the system was enhanced with an increase in maximum acceleration under random excitations. For these motions, proposed system reached up to 90% reduction percentage under either reverse or strike-slip fault mechanism. Also, at least 20% reduction was observed during the experiments. In general, the proposed composite liner system improved the performance of the system by reducing the effects of motions at frequencies close to the vicinity of the natural frequency of the superstructure, and reducing the spectral accelerations at that frequencies instead of alleviating the whole transmitted accelerations. Furthermore, it was suggested that large scale tests on composite liner systems should be conducted to evaluate this concept in detail. Also, that study was performed considering the base of the model as rigid. However, further studies should be performed to investigate soil-structure interaction by simulation of foundation and soil together (Kalpakci, 2013).

In the latest study, a 1:10 scaled 5-story building model test was conducted to investigate the effects of geosynthetic liners on seismic performance of mid-rise building shaking table tests. The effects of the geosynthetic liner placed underneath the foundation of the overlying mid-rise structure was evaluated as proposed GSI method. Shaking table facility at Bogazici University was used in the experiments. As an input motion, 1940 El Centro earthquake was selected. Basically, that system was chosen with an idea of transformation of the input motions to slip displacements via sliding by the assistance of synthetic liner. Junifor HDPE 1 mm thick geomembrane and 300 gr/m^2 non-woven geotextile which corresponded to GSI 1 from block test were selected as GSI materials that will be utilized under the superstructure. Experimental setup sketch was shown in Figure 2.46. Four performance indicator parameters were investigated at the end of the experiment. Seismic energy was dissipated through friction between geomembrane and geotextile materials. Effects of placing the geosynthetic couple on top floor horizontal acceleration, spectral acceleration, story drifts and arias intensities were evaluated. Top floor horizontal response of the proposed GSI system were illustrated in Figure 2.47 (Edincliler and Sekman, 2016).

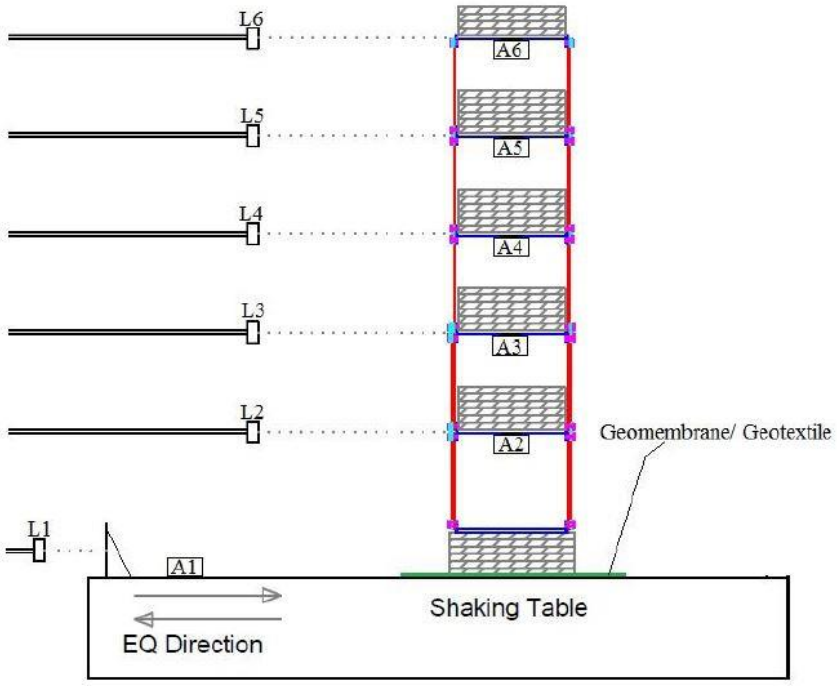

Figure 2.46. Schematic Demonstration of the 5-Story Building Model (Edincliler and Sekman, 2016).

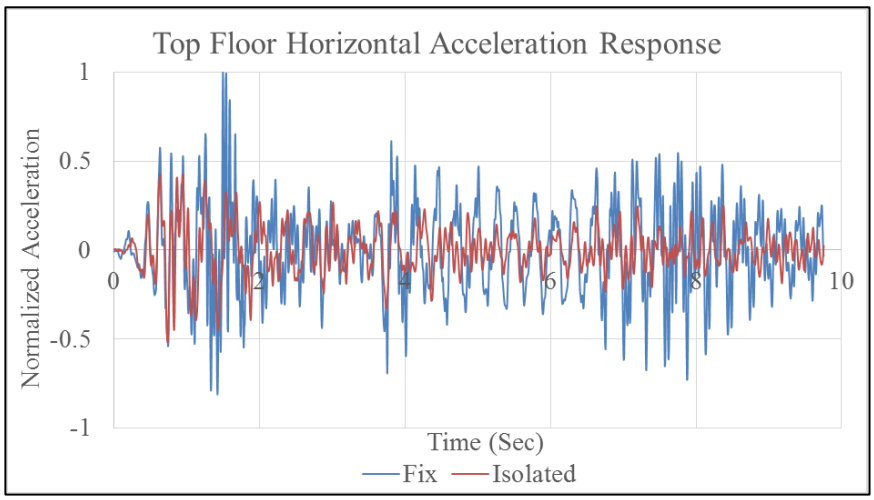

Figure 2.47. Top Floor Horizontal Acceleration Response (Edincliler and Sekman, 2016).

As a result of the mentioned study, up to 65% reduction was observed in the spectral acceleration results. Transmitted accelerations, story drifts and Arias intensities underwent reduction up to 64%, 22% and 83%, respectively. Consequently, application of geosynthetics as foundation isolation provided beneficial effect on seismic response of 5-story building

model. Additionally, damping of the system was substantially increased. Furthermore, foundation isolation by using geosynthetics provides better and cost-effective opportunities in the application area. Also, GSI with geosynthetics can be a good alternative to mitigate seismic hazards under different earthquake motions for developed countries. All the experimental studies on foundation isolation with geosynthetics were performed on rigid base (Yegian *et al.,* 1999; Yegian and Kadakal, 2004; Edincliler and Sekman, 2016; Edincliler *et al.,* 2016).

2.3. Experimental Techniques

In geotechnical earthquake engineering application, several methods such as dynamic soil element tests, reduced-scale model tests and full-scale field tests were studied to investigate performance of the soil under seismic excitation. In order to understand the behavior of the structures, laboratory tests are necessary techniques to investigate either static or dynamic response of the system due to their economical benefits and realistic informations about the ground behavior. In the geotechnical earthquake engineering application, 1-g gravity field on shaking table and N-g gravity field in centrifuge are conducted as two laboratory tests. Boundary effects of the models can be found in the both 1-g shaking table tests and centrifuge tests. Case histories provides relevant data during earthquakes, however, it jeopardizes the society. In model tests, identification of the failure mechanisms and verification of the analytical and constitutive models can be provided. Thus, physical modeling techniques against large earthquakes can provide several records of observations about the response and potential failures of the system (Bhattacharya *et al.*, 2012; Jafarzadeh, 2004; Turan *et al.*, 2009).

Necessary steps for either 1-g or N-g gravitational field tests can be defined as follows (Bhattacharya *et al.*, 2012):

- Deduction in logical non-dimensional groups considering the behaviour of model and prototype scale.
- Ensurance in scaling laws between prototype scale and model.
- Identification of scaling laws in case of satisfaction, violation and special consideriation.

In the following parts, centrifuge and shaking table tests are introduced.

2.3.1. Centrifuge Tests (N-G Gravity Field)

Geotechnical centrifuge uses a scaled model by testing a 1:N scale model at N times earth's gravity that is created by centrifugal force as seen in Figure 2.48. The main advantage of the centrifuge tests is to produce a gravitational stress field similar to expected in situ tests that is developed in the simulation model of prototype stress state. It provides reproduction of the same stress and strain level within the scaled model. Linear dimensions are defined by a factor of 1/N and stress is defined by a factor of unity (Bhattacharya *et al.*, 2012).

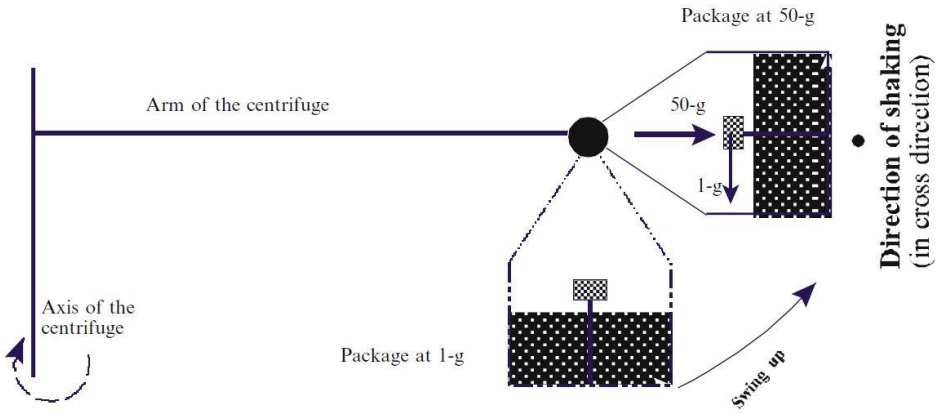

Figure 2.48. Schematic Diagram Showing the Working Principle of A Geotechnical Centrifuge (Bhattacharya *et al.*, 2012).

It is the oldest testing technique and provides valuable data from dynamic and earthquake models. By considering centrifugal force, effect of increasing the weight is likely to be obtained. However, some researchers proposed that there are insufficient evidences of quantitative centrifugal test results or corroboration between prototype data and centrifugal data, although the cost of the centrifuge model tests produced only a small fraction of the total cost of research. Excessive length of centrifuge running time is needed to initiate the large model tests. Also, in terms of seismic response of undrained cohesive soils, centrifuge tests does not provides critical results. Moreover, main problems observed in centrifuge tests are unsatisfaction of all scaling laws and unavailability of numerious instruments in measuring the response of soil. Thus, further researches on large scaled model tests should be conducted (Schofield, 1981; Hushmand *et al.,* 1988; Turan *et al.,* 2009; Ecemis and Kahraman, 2012; Bhattacharya *et al.,* 2012).

2.3.2. Shaking Table Tests (1-G Gravity Field)

There is an another technique to investigate the response of the structures to evaluate their seismic performance by testing at one times earth's gravity. This technique is commonly known as shaking table or earthquake shaking table as seen in Figure 2.49. Generally, test specimens are fixed to the table and then shaken until the failure occurs. Shaking table tests provide large amplitudes, multi-axis input motions and easier experimental measurements in order to understand the basic mechanism of the failure condition. Another advantage of using shaking table tests is observation of liquefaction, post-earthquake settlement and foundation response. Shaking tables provide availability of instrumentation, compaction and placement of the soil. It is a 1-g gravitational field test so that it is not possible to produce higher gravitational field on shaking table tests. However, some behaviors about high normal stresses can be observed on shaking table by very loose soil placement. Several researches were carried out about reduced scaled embankment models, flow failure mechanism of liquefied soil deposits and behavior of underground structures under liquefaction. Cost of actuators for shaking table increases with the increase of loading increments. Actual earthquake data can be reproduced by shaking table (Prasad *et al.,* 2004).

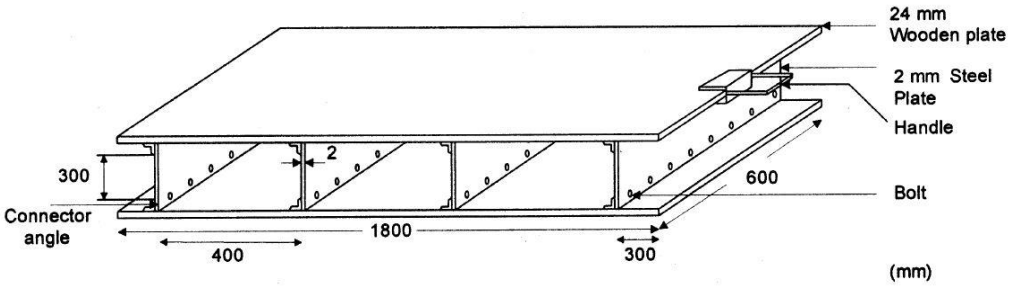

Figure 2.49. Schematic Demonstration of Manuel Shaking Table (Prasad *et al.*, 2004).

Soil deposit underlying a prototype structure has an infinite lateral movement as seen in Figure 2.50. On the other hand, model tests are conducted within finite size so that difficulties in adopting the boundary conditions of the soil within finite dimensions of a container. An ideal container should include large dimensions, flexibility and transparency due to the requirements of confinement that obstruct the mounting of the model on shaking table. Working principle of the model container is shear beam and this is similar to beam theory of Euler-Bernoulli as shown in Figure 2.51. Accordingly, system will have an infinite lateral extent and finite depth of soil profile. Prasad *et al.* (2004) and Bhattacharya *et al.* (2012) stated that direct placement of the model on shaking table presents better solution. According to their researches, soil container limits the dissipation of the energy caused by seismic waves due to the restricted dimensions of soil layer in soil container. Additionally, boundary conditions results in inaccuracies on dynamic response caused by P wave propagation (Lombardi and Bhattacharya, 2012 ; Bhattacharya *et al.*, 2012).

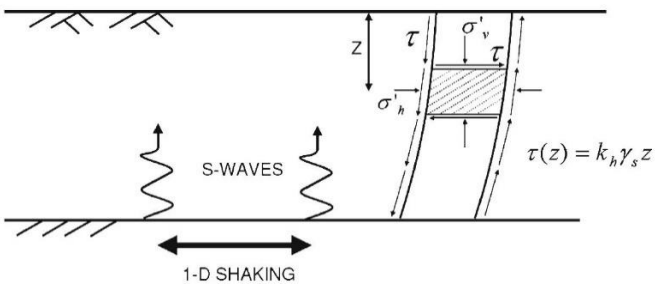

Figure 2.50. Infinite Lateral Extent of Soil Deposit with Finite Depth under Base shaking (Lombardi and Bhattacharya, 2012; Bhattacharya *et al.*, 2012).

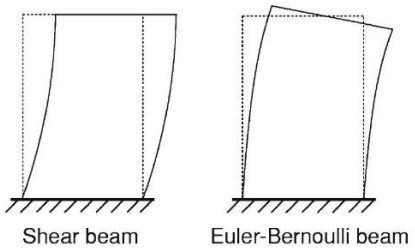

Figure 2.51. Comparison of Shear Beam with Euler-Bernoulli Beam Theory (Lombardi and Bhattacharya, 2012; Bhattacharya *et al.*, 2012).

There are different types of soil container that is needed to discuss. All following types of container presents different advantages and disadvantages with different design requirements. Rigid container, rigid container with flexible boundaries, rigid container with hinged end-walls, equivalent shear beam (ESB) container, laminar container and active boundary container are types of soil container that is used in geotechnical earthquake engineering applications.

In the determination of ground motion characteristics and behavior of a system under dynamic excitation, soil containers are commonly used in centrifuge and shaking table tests. Soil containers are commonly divided into two categories, rigid and flexible containers, as given below .

2.3.3. Rigid Soil Container

A schematic diagram of a rigid soil container is shown in Figure 2.52 and Figure 2.53. End walls of the rigid box have higher stiffness values when compared to layers of existing soil. In order to provide development of the shear stresses in vertical plane between container and soil deposit, layers of the sand is glued onto the box to ensure roughness of the side walls and the base of the container. Roughness assists the base shaking through the soil layer. Thus, very smooth side walls are needed to provide plain strain conditions by using grease or oil on the surfaces of the container. This smoothness can also be obtained by implementing the glass on the side walls (Bhattacharya *et al.*, 2012).

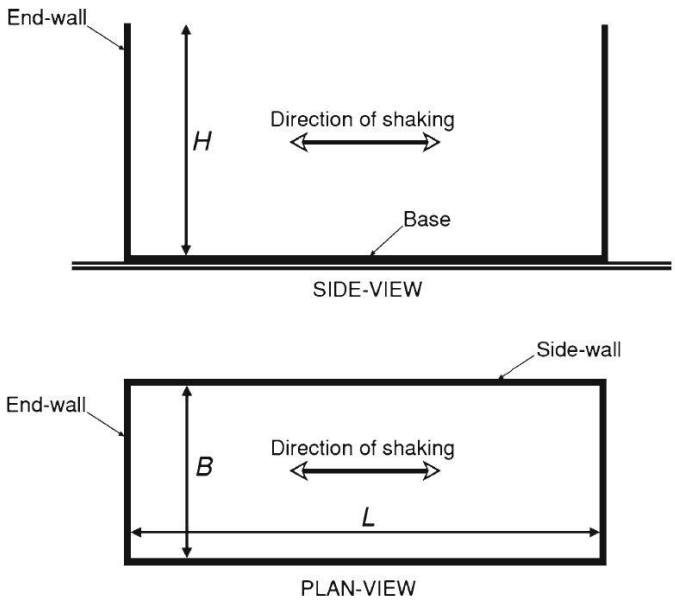

Figure 2.52. Schematic Demonstration of A Rigid Container (Bhattacharya *et al.*, 2012).

Several researches emphasized on the design requirements of the ratio between the length and the height of the container. Numerical studies conducted to investigate boundary effects concluded that the desired length of the container should be 1.5 - 2.0 times the height of the container. Table 2.7 demonstrates and summarizes the conducted studies on rigid containers (Bhattacharya *et al.*, 2012).

Table 2.7. Example of Rigid Soil Containers Found in the Literature (Bhattacharya *et al.*, 2012).

Shape	Shaking direction	*L-B-H* [mm]	*L/H*	Side-walls	Base & end-walls	Testing	Reference
Rectangular	1-D	597-270-150	4.0	Teflon	Rough sand paper	Centrifuge	Adalier and Elgamal (2002)
Rectangular	1-D	500-565-190	2.6	No-details	No-details	Centrifuge	Whitman and Lambe (1986)
Rectangular (Fig. 8.11a)	2-D	712-432-440	1.6	Smooth plastic membrane	Base covered by sand-glue mixture.	Centrifuge	Ng et al. (2004)
Rectangular (Fig. 8.11c)	1-D	1,500-400-1,000	1.5	Perspex and wood plates	Terram geotextile membrane	Shaking table	Norton (2008)
Rectangular (Fig. 8.11b)	1-D	450-240-400	1.1	Perspex	PTFE (poly-tetra-fluoro-ethylene) sheets	Shaking table	Dash (2010)

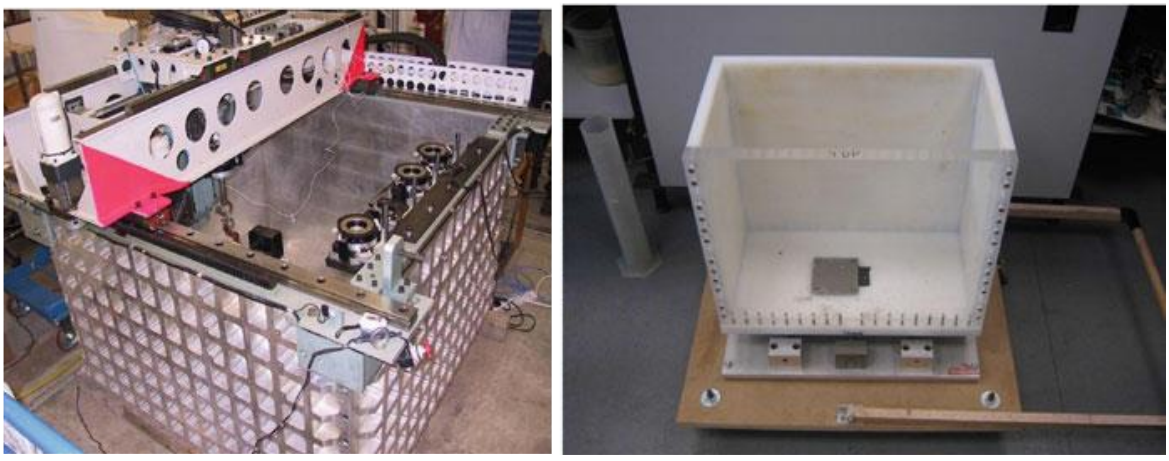

(a) (b)

(c)

Figure 2.53. Examples of Rigid Containers. (a) Rigid Box Used in Centrifuge At The Hong Kong University, (b) Rigid Box Used in Small Shaking Table at University of Bristol, (c) Rigid Box Used in The Shaking Table at University of Oxford (Bhattacharya *et al.*, 2012).

A series of various tests was conducted using the shaking table at University of Bristol. Demonstration of shaking table and soil container was shown in the Figure 2.54. According the conducted study, the presence of the foam provides dissipation of the seismic energy considering artificial boundaries. Substantial increase on the thickness of the foam results in higher absorption level of the energy. Similarity between displacement values between the accelerometers at different distances explained that horizontal section remained horizontal during shaking. Moreover, rigid container does not limit the reflection of the seismic waves from the rigid boundary (Lombardi and Bhattacharya, 2012).

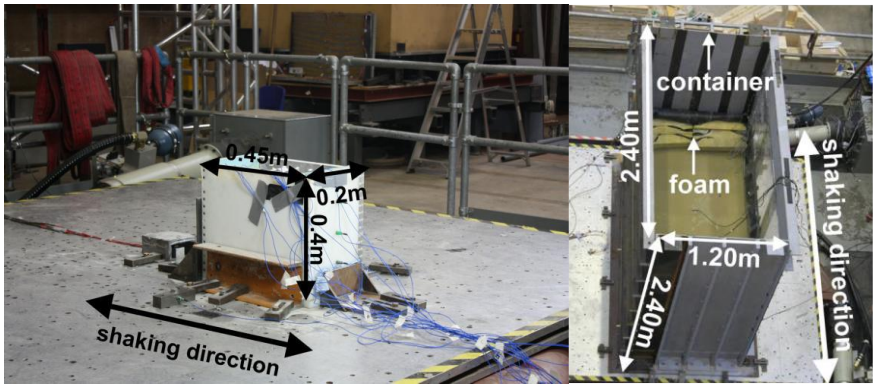

(a) (b)

Figure 2.54. (a) Small Soil Container Considered, (b) Larger Soil Container Used for Validation of the Results (Lombardi and Bhattacharya, 2012).

2.3.3.1. Rigid Soil Container with Flexible Boundary. When flexible boundaries such as sponge material are provided along the end-walls of the container, limitation of the reflection of seismic waves can be provided as seen in Figure 2.55. Reduction of the reflection of the waves and stiffness of the end-wall constitutes the benefits of the rigid container with flexible boundaries. Main advantage of using soft material in the end-walls can be explained as alleviation in wave propagation and P-wave generation. However, there are some limitations in usage of rigid box with flexible boundaries. Uncertainity in unkown exact boundary conditions of sponge causes difficulties in the either analytical or numerical model. Soft materials only diminishes the reflection of the seismic waves not totally prevent. Some examples of rigid container with flexible boundaries can be seen in the Table 2.8 (Bhattacharya *et al.*, 2012).

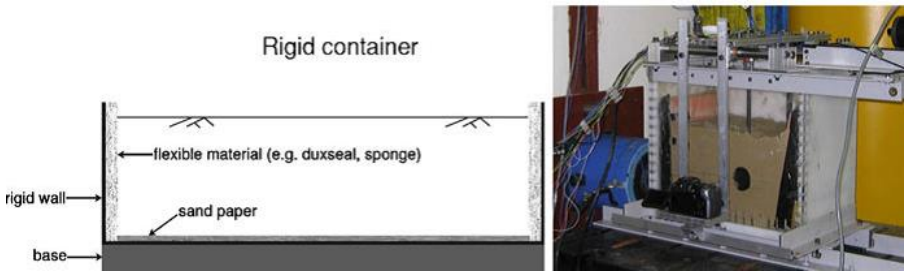

Figure 2.55. Schematic Demonstration of the Rigid Box with Flexible Boundaries and Laboratory Test Conducted in the University of Bristol (Bhattacharya *et al.*, 2012).

Table 2.8. Example of Rigid Soil Containers Found in the Literature (Bhattacharya *et al.*, 2012).

Shape	Shaking direction	*L-B-H* [mm]	*L/H*	Side-walls	End-walls	Testing	Reference
Rectangular	1-D	4,270-910-1,220	3.5	Tempered plate-glass	Hinged to the box	Shaking table	Fishman et al. (1995)
Rectangular (Fig. 8.12b)	1-D	450-240-400	1.1	Perspex	Sponge (30 and 60 mm thick at top and bottom respectively)	Shaking table	Dash (2010)
Rectangular	1-D	1,920-440-600	3.2	Acrylic plate	Sponge (50 mm thick)	Shaking table	Ha et al. (2011)

2.3.3.2. Rigid Soil Container with Hinged End-Walls. In this type of rigid soil container, the end-walls are desinged to rotate about base by hinged connection as seen in Figure 2.56. In order to provide movement, two end-walls should be connected to each other by tie rod. However, there occurs some lateral earth pressure permitted by occurred strain in the walls (Bhattacharya *et al.*, 2012).

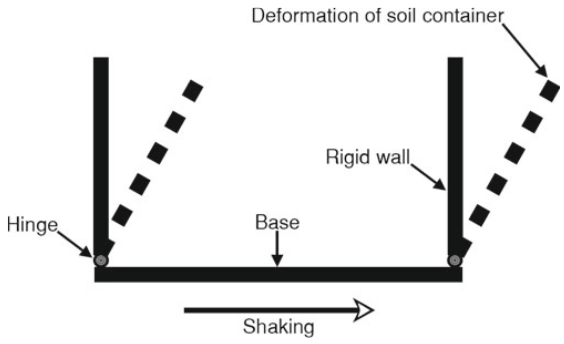

Figure 2.56. Schematic Demonstration of the Rigid Box with Hinged End-Walls (Bhattacharya *et al.*, 2012).

2.3.4. Flexible Soil Containers

Flexible soil containers are more commonly used soil containers in many studies. In the following parts, types of flexible soil containers are introduced.

2.3.4.1. Equivalent Shear Beam (ESB) Container. Setting the rigid frames on each other using rubber layers that has proper stiffness is known as equivalent shear beam (Jafarzadeh, 2004). In this type of container design, end-walls of the container and the existing soil deposit have the same shear stiffness as seen in Figure 2.57 and Figure 2.58. Behavior of the soil and end-walls is assumed as shear beams. Interaction between soil and container is ignored due to the similarity. Boundary conditions of the ESB should be as followings:

- Dynamic stiffness between boundary and adjacent soil must matched to mitigate reflection of the seismic waves.
- Friction between boundary and adjacent soil must be the same so as to maintain similarity in the shear stresses.
- Frictionless surface at the side walls must be provided to sustain plane strain condition

Table 2.9 demonstrates the example of equivalent shear beam container in the literature. One limitation about ESB is that soil behaves highly non-linear under cyclic loading at large strains (Bhattacharya *et al.*, 2012).

Figure 2.57. Schematic Demonstration of the Equivalent Shear Beam (Jafarzadeh, 2004).

Figure 2.58. Examples of Equivalent Shear Beam Container (Jafarzadeh, 2004).

Table 2.9. Example of Equivalent Shear Beam in the Literature (Bhattacharya *et al.*, 2012).

Shape	Shaking	*L-B-H* [mm]	*L/H*	1-g/N-g	Reference
Rectangular	1-D	2,000-750-1,750	1.1	1-g	Carvalho et al. (2010)
Rectangular	1-D	1,200-550-800	1.5	1-g	Dar (1993)
Rectangular	1-D	4,270-910-1,220	3.5	1-g	Fishman et al. (1995)
Rectangular	1-D	4,800-1,000-1,200	4	1-g	Crewe et al. (1995)
Rectangular	1-D	560-250-226	2.5	N-g	Zeng and Schofield (1996)
Rectangular	1-D	800-350-600	1.3	N-g	Madabhushi et al. (1998)

2.3.4.2. Active Boundaries Container. Working principle of an active boundaries container is similar to the that of laminar box. However, external actuators are attached to each layer of the laminar box as shown in Figure 2.59. Achievement of the desired results is provided by actuator exerting different pressure on each laminate. This type of container should be use in the presence of sharp change in the stiffness of the soil under shaking. Also, active boundaries container can be used for liquefaction applications (Bhattacharya *et al.*, 2012).

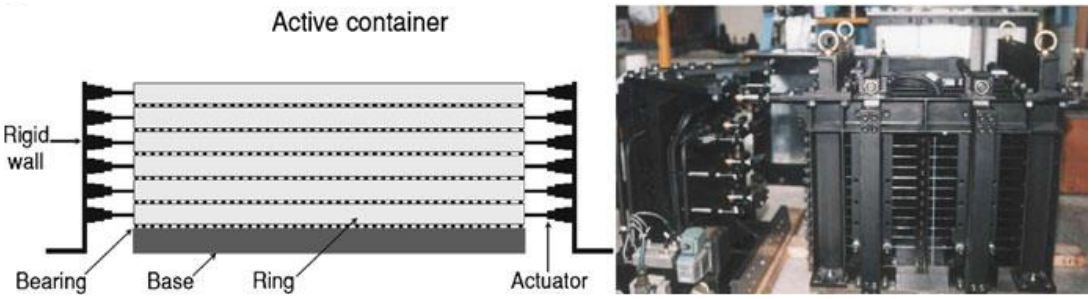

Figure 2.59. Examples of Active Boundaries Container (Bhattacharya *et al.*, 2012).

2.3.4.3. Laminar Box (Flexible Container). The simplest and the oldest techniques in geotechnical engineering modeling are rigid of fixed-wall box due to its efficiency in gaining relevant data for simulated conditions. However, rigid boxs are not sufficient and give irrelevant and inaccurate results in the case of critical response parameters due to the reflection of seismic stress waves back to the soil. On the other hand, flexible containers are capable of solving these problems and can be used as a good alternative. Also, stiffness of the soil is proportional to the walls. Setting each layer on the other to move easily on each other is availible in laminar shear box (Jafarzadeh, 2004). Frictions between each layers are minimized by using roller bearings. Related to the movement of the soil inside, each layer moves accordingly. Schematic illustration of a laminar box is shown in the Figure 2.60 (Prasad *et al.*, 2004).

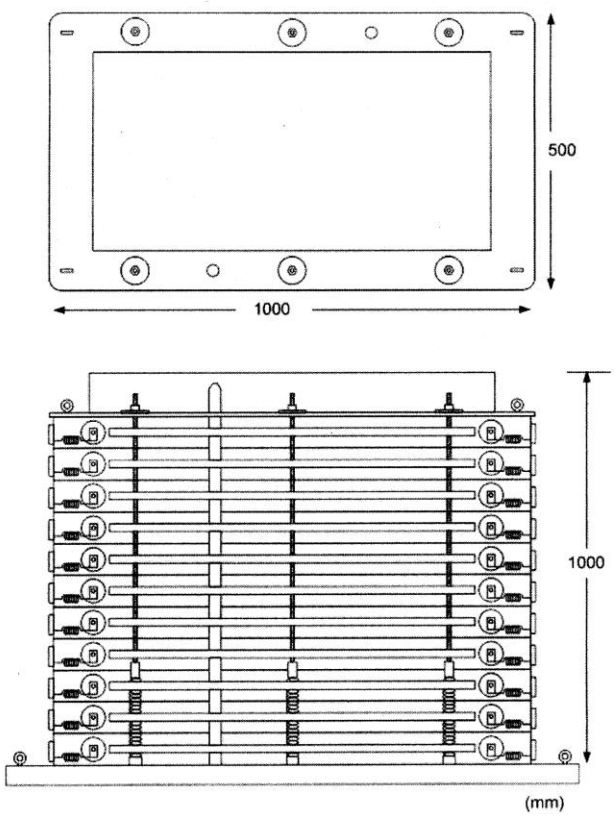

Figure 2.60. Details of A Laminar Shear Box (Prasad *et al.*, 2004).

In a laminar box, a large scale soil speciment provides better results about boundary conditions in free-field soil. Base excitations are the best simulated on a laminar box which is a flexible soil container under earthquake actions as seen in Figure 2.61. It gives more

realistic results about shear deformations of the free-field boundary conditions (Cheung *et al.*, 2013).

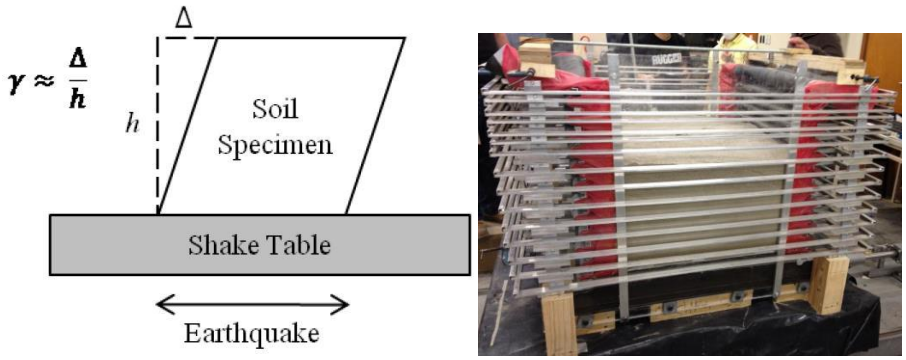

Figure 2.61. Shear Deformations on the Soil in A Laminar Box in the Study (Cheung *et al.*, 2013).

Laminar box has an advantage on the reduction in lateral buckling and lateral friction by roller bearings. Design principle of the laminar box is to provide mitigation in lateral stiffness of the container so as to enable the response of soil-box system by the bearing and steel external frame as seen in Figure 2.62 and Figure 2.63 (Prasad *et al.*, 2004; Bhattacharya *et al.*, 2012).

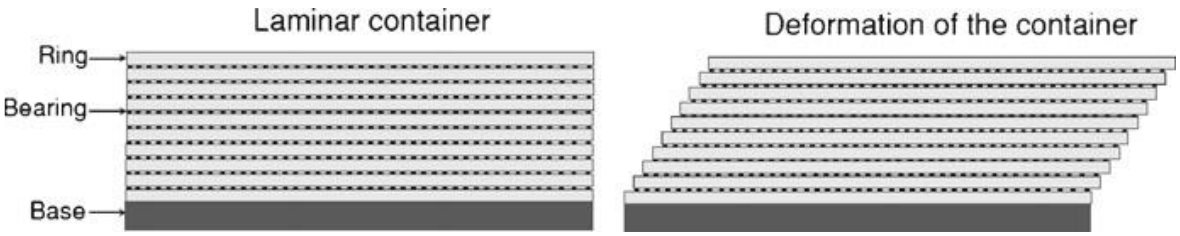

Figure 2.62. Shematic Diagram of Laminar Box (Prasad *et al.*, 2004; Bhattacharya *et al.*, 2012).

Figure 2.63. Examples of Laminar Containers (Prasad *et al.*, 2004; Bhattacharya *et al.*, 2012).

For a laboratory test, following requirements are needed to be taken into consideration (Jafarzadeh, 2004; Chunxia *et al.*, 2008; Ecemis and Kahraman, 2012):

- Size of a laminar box is large enough to simulate large-scale laboratory tests and has to be light enough.
- Each frame of laminar box has sufficient stiffness to ignore distortion of the frame itself.
- Restriction of the lateral displacements during shaking has to be provided by laminar shear box.
- Laminar box is constructed to prevent breakdown of the system.
- Friction between the frames is reduced enough to provide similarity between deformations of soil and frames.
- Resonance effect has to be taken into consideration by avoiding intersection of the fundamental period of the laminar shear box and soil deposit.
- Integrity of the laminar box has to be maintained during the shaking.
- Waterproofing of the laminar box has to be provided during placement of the soil and seismic loading.

- The mass of the laminar box should be less enough to drive soil deformations by the soil mass rather than inertia of the box.
- Soil stresses and strains should be the same before and during the shaking process.
- A laminar box has to be strong and stable against dynamic forces and moments.
- Movement of soil in transverse direction should be permitted.
- Dilatation of the frames should be prevented.
- Connection between bearings and groove should be done well.

Another example of laminar shear box is demonstrated in the Figure 2.64 and Figure 2.65 (Chunxia *et al.*, 2008).

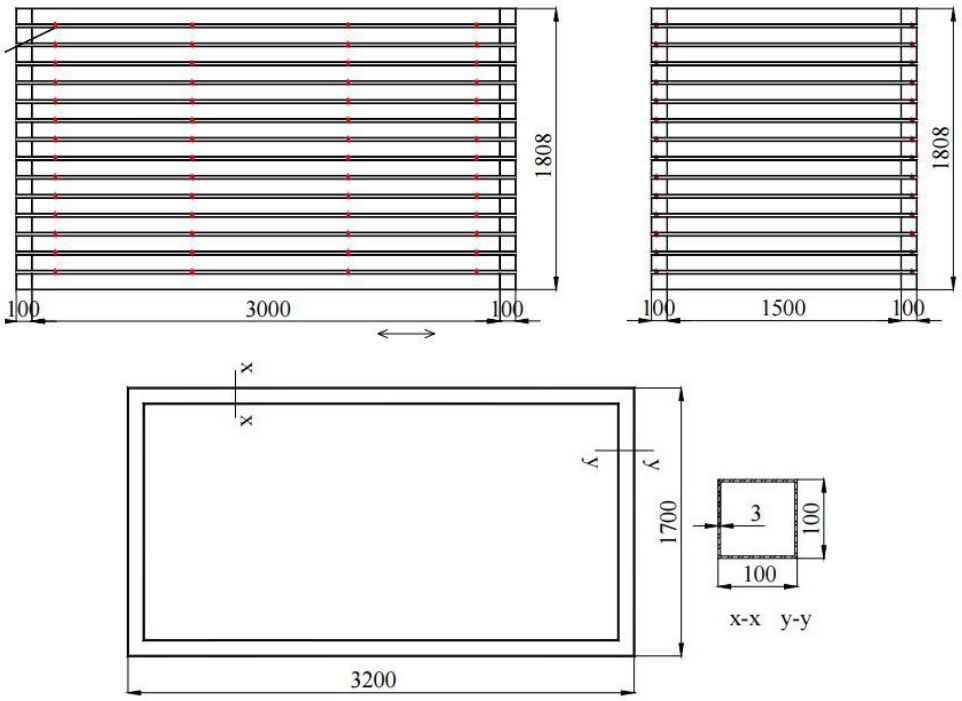

Figure 2.64. Design Drawing of the Laminar Box (Chunxia *et al.*, 2008).

Figure 2.65. Empty Laminar Shear Box on the Shaking Table (Chunxia *et al.*, 2008).

Disassembled parts of a typical laminar box and attachment of a shaking table is shown in Figure 2.66 (Jafarzadeh, 2004).

Figure 2.66. Disassembled Parts of A Laminar Box (Jafarzadeh, 2004).

Factors affecting the performance of a laminar box are shown in followings (Jafarzadeh, 2004; Prasad *et al.*, 2004) :

- Inertia effect of the box,
- Friction effect induced by roller bearings and surface of the layers,
- Membrane effect, and

- Wall effect of the box.

Additionally, a comparative research was conducted on flexible containers for both centrifuge and shaking table tests. A typical demonstration of used laminar box in the study was shown in Figure 2.67. Summary of the laminar shear box designs is illustrated on the Table 2.10 (Turan *et al.*, 2008).

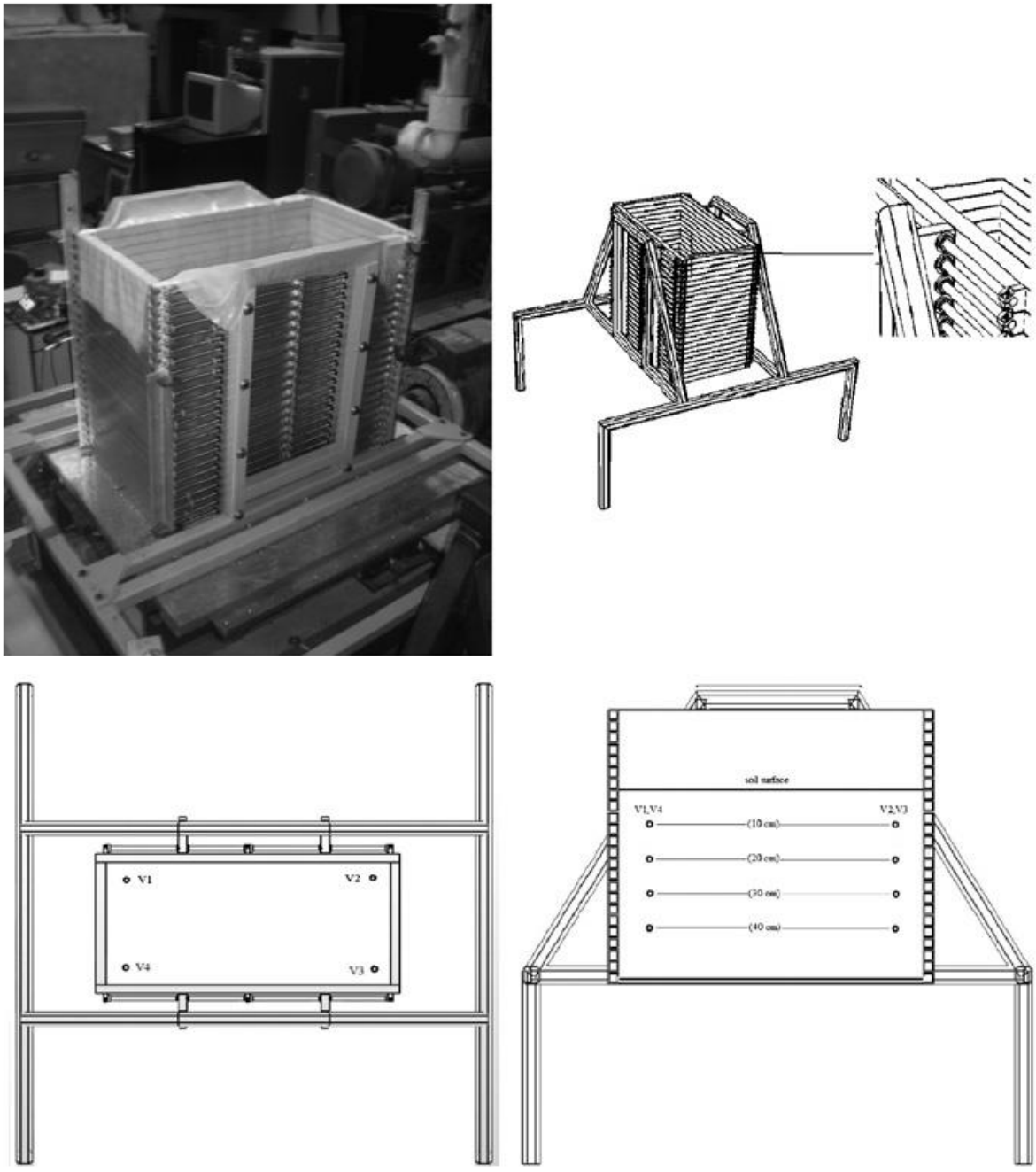

Figure 2.67. Schematic View of Used Laminar Box (Turan *et al.*, 2008).

Table 2.10. Summary of Available Flexible Container (Laminar Box) Designs (Turan *et al.*, 2008).

Reported by	Dimensions ($W \times L \times H$) (mm^3)	Use in	Direction of operation	Shape	Description[a]
Gibson [3]	$350 \times 900 \times 470$	1-G	1-D	Rectangular	1, 4, 6
Prasad et al. [2]	$500 \times 1000 \times 1000$	1-G	1-D	Rectangular	1, 4, 6
Meymand [4]	2280×2130 (D,H)	1-G	2-D	Circular	3, 4, 6
Ueng and Chen [5]	$1888 \times 1888 \times 1520$	1-G	2-D	Rectangular	2, 4, 6
Van Laak et al. [6]	$254 \times 457 \times 254$	N-G	1-D	Rectangular	1, 4, 6
Pamuk et al. [7]	$355 \times 710 \times 355$	N-G	1-D	Rectangular	1, 4, 6
Shen et al. [8]	584×500 (D,H)	N-G	2-D	12-sided polygon	1, 4, 6
Takahashi et al. [9]	$200 \times 450 \times 325$	N-G	1-D	Rectangular	1, 4, 5

[a] *Note*: 1. A stack of laminae separated by bearings; 2. Laminae supported by a frame and move independently; 3. Container hanging on the top lamina supported by a frame; 4. Entire container placed on shaking table; 5. Active; 6. Passive.

According to the another study, shaking table test that has 240 ball bearings was conducted using laminar box that has 6.2 m height as seen in Figure 2.68 (Thevanayagam and Ecemis, 2006).

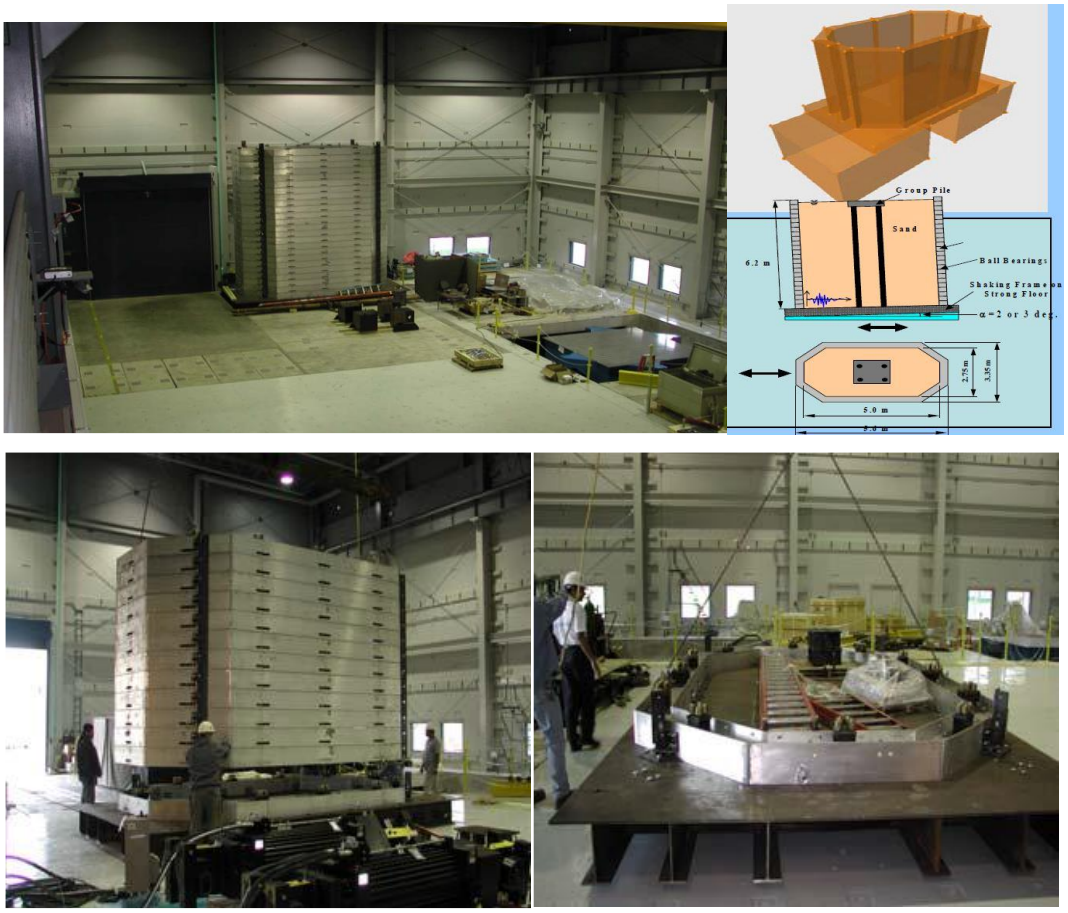

Figure 2.68. Laminar Box on Shaking Table (Thevanayagam and Ecemis, 2006).

According to the results of performed studies, effect of friction were found as negligible due to the substantially low friction between rollers and frames. Also, similar loading conditions were observed under field loading. Placement of transducers into the box provided to gain soil properties well. Moreover, transfer of the weight of laminar box through the table was provided using external frame system (Prasad *et al.*, 2004; Turan *et al.*, 2008). Effects of inertia and boundary were found as acceptable by Ecemis and Kahraman (2012). However, Prasad *et al.* (2004) and Turan *et al.* (2008) founded the effects of boundary as negligible.

Liquefaction effects were considered in a study with one and two dimensional shaking table tests to investigate the actual effects of the earthquakes in liquefaction and water pressure change in soil specimen within a laminar box as seen in Figure 2.69. Consequently, two-dimensional test results overhelmed the one dimensional test results in terms of pore water pressure generation and liquefaction occurance. Higher pore water pressure values were observed in the two dimensional shaking table test results. Moreover, large settlement occured in liquefied sand specimen. Also, liquefaction phenomenon was observed at shallower depths of the specimen while pore water pressure dissipation was slower (Chen *et al.*, 2004).

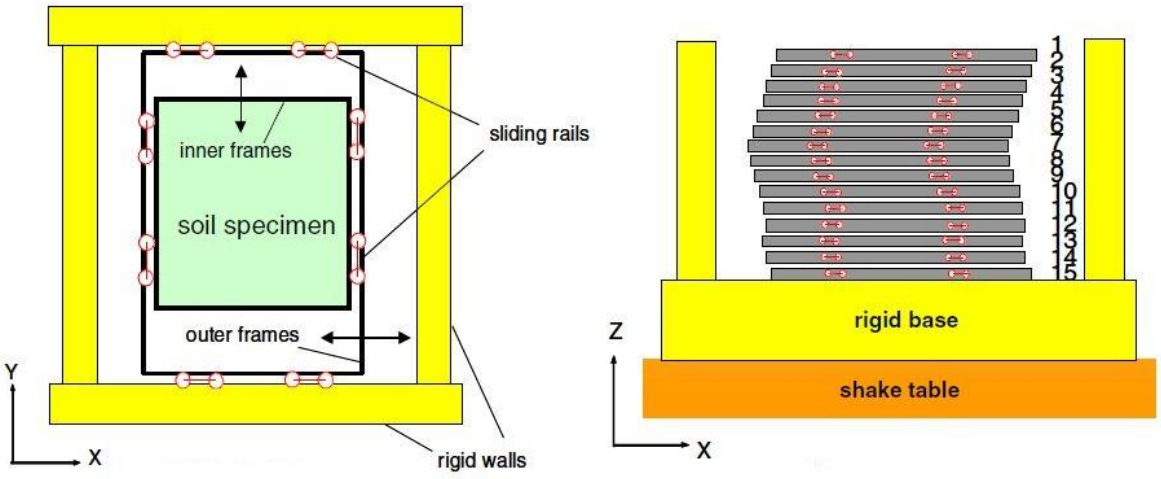

Figure 2.69. Schematic Demonstration of the Biaxial Laminar Shear Box (Chen *et al.*, 2004).

Sekman (2016) and Goztepe (2016) designed a laminar box with a dimensions of 1.3 meter long, 1.1m in width and 1.0m in depth as seen in Figure 2.70. Dimensions of the laminar box were determined by considering the maximum loading capacity of the shaking table. Also considering possible torsion problem during one-directional shaking, the geometry of laminar box was decided as rectangular instead of a square geometry (Sekman, 2016; Goztepe, 2016).

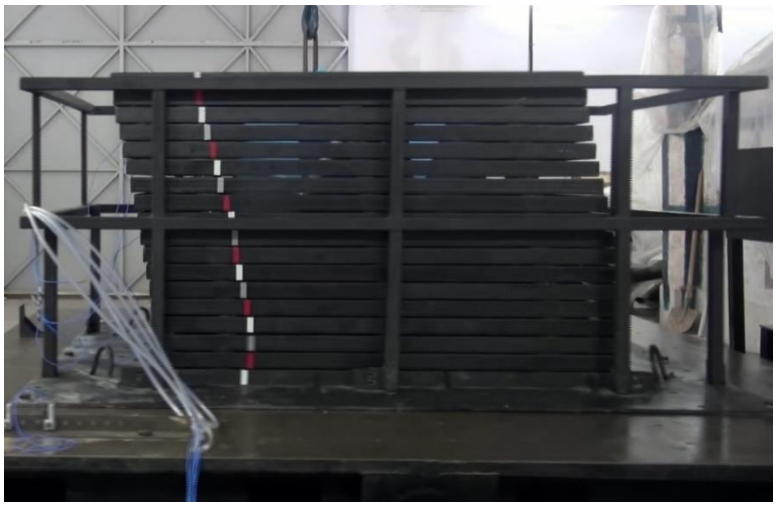

Figure 2.70. Side View of Unidirectional Laminar Box (Sekman, 2016; Goztepe, 2016).

The laminar box is composed of layers, ball bearings, base plate, side guides and internal membrane components. In total, there are 18 sliding layers and 324 roller bearings to provide sliding of the laminates. Steel material was used instead of aluminum I-beam due to the problems about availability and welding. Roller bearings and rubber stoppers were used to overcome sliding and stopping the mechanism of the laminates. The use of roller bearings provided reduction in friction forces between layers by six sets of roller bearings per laminate. Three roller bearings were placed side by side in each set. Bearing houses were constructed from stainless steel. Rubber strips were placed at both ends of these bearing houses as seen in Figure 2.71 (Sekman, 2016; Goztepe, 2016).

Figure 2.71. View of Roller Bearing House with Rubber Strip Stopper (Sekman, 2016; Goztepe, 2016).

Before starting the experiments, performance checks recommended by Prasad *et al.* (2004), Jafarzadeh (2004) and Bhattacharya *et al.* (2012) have to be performed. In the following parts, these performance checks were given in detail.

- Inertia Effect

Pulse absorbtion effects of rubber material provided restriction of clashing of rollers causing additional inertia effect. The lowest layer was fixed on a steel base that was fixed to shaking table. The side guides were made of steel tube sections to provide precaution against unexpected incident. Smooth membrane was attached in the laminar box to provide avoidance of soil leakage between two layers. Additionally, membrane and sidewalls of the box was greased to provide prevention from additional friction forces (Sekman, 2016; Goztepe, 2016).

Mass of the box contributed to the inertia effect. Inside the soil, the measured acceleration should be less than the actual acceleration caused by the inertia of the box. A specified correction factor can be applied for recorded acceleration so as to elucidate the

effect. Considering m_1 and m_2 as the mass of soil within a layer and the layer of box, respectively, then, total dynamic force (F_d) is given as,

$$F_d = (m_1 + m_2).a \quad (2.1)$$

On the other hand, the entire force should be transferred onto the soil. Therefore, if the soil without container is desired, then,

$$F_d = m_1.a' \quad (2.2)$$

Equating the above two equations, then, actual acceleration in soil is obtained as,

$$a' = \left(\frac{m_1+m_2}{m_1}\right).a \quad (2.3)$$

a' = the acceleration of the soil without the influence of the container

a = the measured acceleration

m_1 = weight of soil in the container

m_2 = weight of total laminates

$$a' = (1.3) \text{ x } a \quad (2.4)$$

The influence coefficient was computed about 1.3 and this coefficient was normal up to 1.5 (Sekman, 2016; Goztepe, 2016).

- Friction Effect

Static pullout tests were performed so that friction forces of the roller bearings could be determined to initiate the motion of the layers of laminar box. Measurements were done with the load cells that had 50 kg load capacity by attaching the laminates and applying the static forces on each layer. The friction force that measured at every laminate was a function of the coefficient of friction between the layers and the laminate weight. Laminate weight increases top-down due to added weight of each layer. The measured friction forces were shown in Figure 2.72 (Sekman, 2016; Goztepe, 2016).

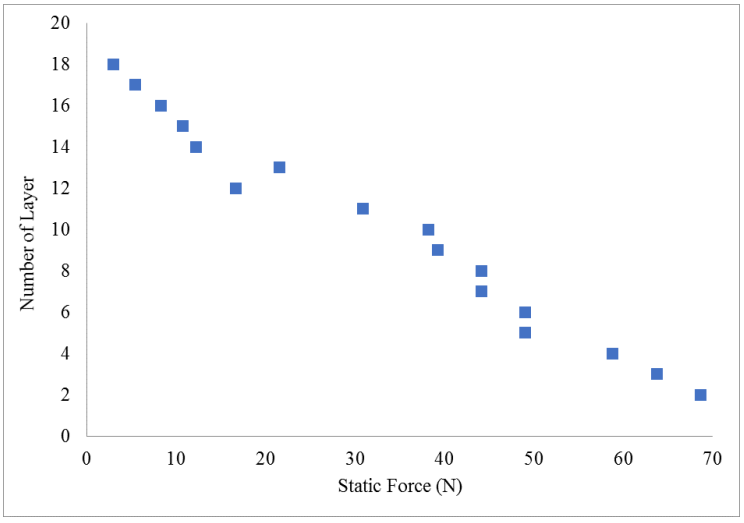

Figure 2.72. Measured Friction Forces from Pullout Test (Sekman, 2016; Goztepe, 2016).

For the initiation of the motion, the maximum force required was measured as 69 N at the bottom layer. The average friction force of all layers was about 33 N. Also, the average coefficient of friction was measured as 0.07. When the laminar box was filled with soil, resistance near the bottom was obtained as 10.5 kN of which almost 0.006 of this resistance was equal to static friction. Thereby, static friction force was neglected (Sekman, 2016; Goztepe, 2016).

- Membrane Effect

In mentioned study, 1.0 mm thick rubber membrane was used as seen the Figure 2.73. Its stiffness was sufficiently small compared to that of soil. Hence, it did not affect the performance of soil mass. Moreover, its effect was localized near the edge rather than center that the effect of membrane was negligible (Sekman, 2016; Goztepe, 2016).

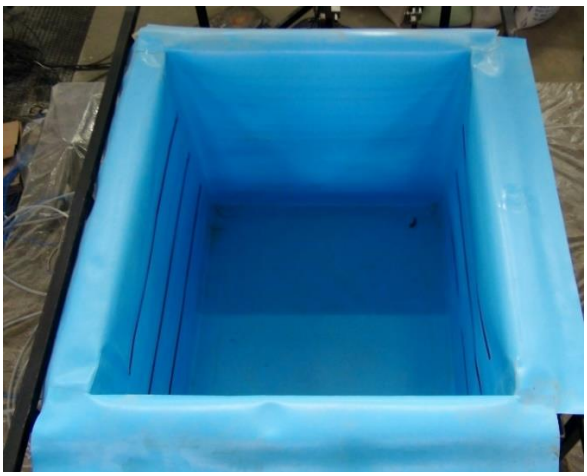

Figure 2.73. A View of Thin Rubber Membrane Located Inside the Laminar Box (Sekman, 2016; Goztepe, 2016).

- Boundary Effect

The performance of the boundaries of laminar box was investigated by performing a series of shaking table tests. Some parts were performed without soil to determine the natural behavior of the laminar box.

3. MATERIALS AND METHODS

The main aim of shaking table experiments is to evaluate the effectiveness of the proposed foundation isolation system with geosynthetics. The effects of the proposed system on 1:10 scaled three and five story building models were evaluated with two different configuration of GG couples as curve shaped and straight liners. This section consists of materials and methods, experimental setup including sample preparation, instrumentation, input ground motion selection, and performing shaking table experiments.

3.1. Shaking Table Facilities

Shaking table test facilities at Bogazici University were used for this study. Uniaxial hyraulic shaking table which provides longitudinal horizontal movement generated by a servo-hydraulic actuator was utilized. Shaking table has 3m x 3m dimensions with a maximum payload capacity of 10 tons considering 2g acceleration. The shaking table is ideally suited for seismic applications due to the stroke capacity of +/- 12 cm (24 cm total stroke). The actuator has a 3-stage servo-valve controlled by an analog inner-loop control system (displacement based), and a digital outer-loop control system (acceleration feedback based) controlled by the newly modified computer-based software system.

3.2. Measuring Instruments

In the measurement of the acceleration response, ±3g capacity accelerometers and ±20g capacity accelerometers were used. Leuze ODSL 96B M/V6.XL-1200-S12 optical distance sensors (ODS) with 150 - 1200 mm measurement range and ±2% absolute measurement accuracy were utilized in measuring displacements. 32 channel dynamic data

logger was used for data acquisition. Sample rate were taken as 1000 sample/sec and 500 sample/sec. for cyclic sinusodial motions and for earthquake motions, respectively.

3.3. Sand Properties

Silivri Sand which is locally found around Istanbul region was used in the experiments. The grain-size distribution of the sand was determined according to the American Standard Test Method (ASTM) of D422 as seen in Figure 3.1. In accordance with the Unified Soil Classification System (USCS), the sand material is classified as poorly graded sand (SP). Also, bulk unit weight of the sand was found as 16.5 kN/m^3.

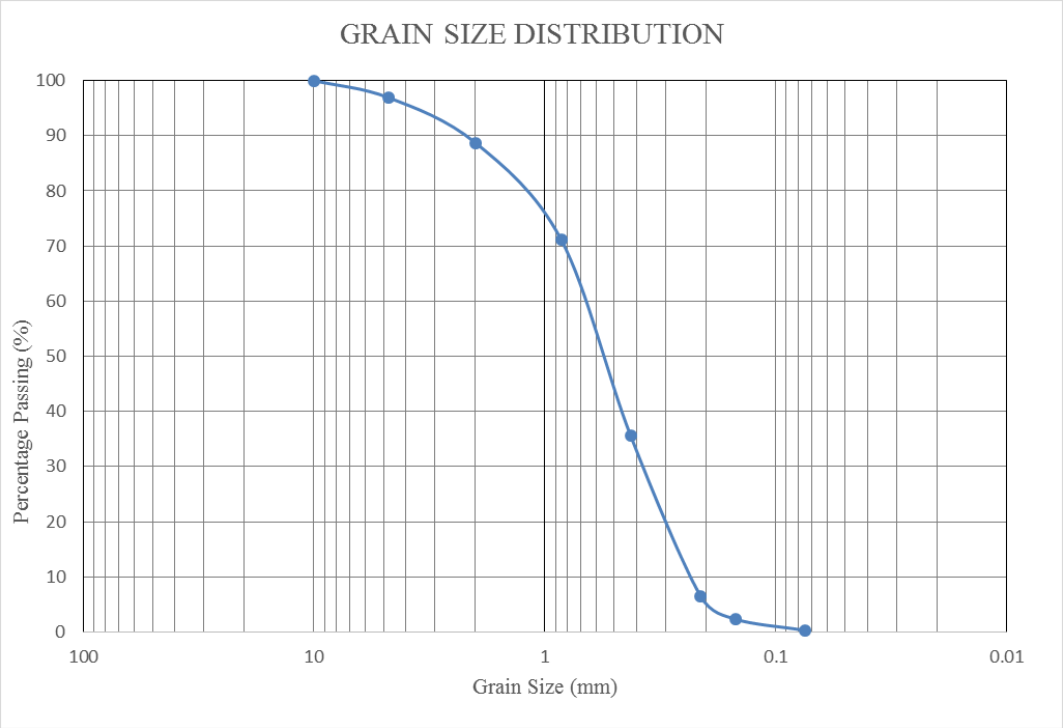

Figure 3.1. Grain Size Distribution of the Silivri Sand.

3.4. Input Ground Motions

Kocaeli (1999), El Centro (Imperial Valley-02) (1940) and, Kobe (1995) earthquakes have been selected for the shaking table tests. Horizontal component of the earthquakes were used due to the uniaxial behavior of the shaking table. Hazard condition of the site, frequency content and applicability to the shaking table were considered during the selection of earthquakes. From different destructive earthquake motions, scaled Kocaeli (1999), El Centro (1940) and Kobe (1995) were used as seen in Figure 3.2. The basic specifications of the earthquakes were tabulated in Table 3.1. PEER Ground Motion Database Center was used in obtaining earthquake data.

Table 3.1. Information About The Given Earthquakes (PEER).

Earthquake Name	Date	Station Name	Earthquake Magnitude	PGA (g)	PGV (cm/sec)	PGD (cm)
Kocaeli, Turkey	17.8.1999	Izmit	7.51	0.22	27.02	14.61
Imperial Valley	19.8.1940	El Centro	6.95	0.31	31.74	18.01
Kobe, Japan	16.1.1995	KJMA	6.90	0.82	77.83	18.87

Furthermore, cyclic sinusoidal motions have been used with different frequencies. Frequencies of the cyclic sinusoidal motion were determined according to the modal frequencies obtained from free vibration tests.

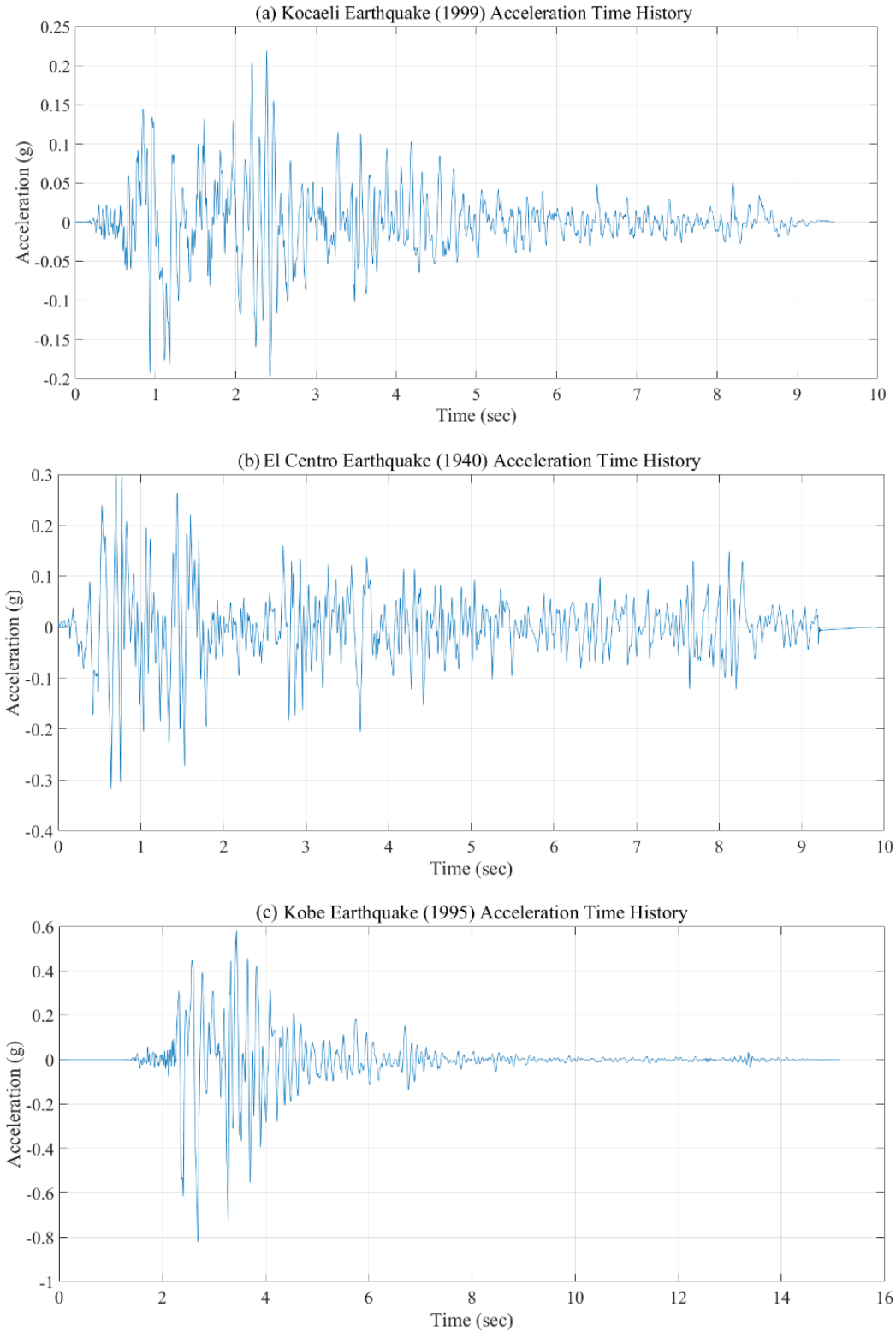

Figure 3.2. Time History of the Scaled Earthquakes as Input Motions. (a) Kocaeli Earthquake, (b) El Centro Earthquake, (c) Kobe Earthquake.

3.5. Experimental Setup and Preperation

The laminar box was designed and constructed in accordance with the literature in order to provide more precise results (Sekman, 2016; Goztepe, 2016). The same laminar box that was designed with 1.3 meters towards the direction of shaking by 1.1 meters with 1.0 meter depth was used as seen in the Figure 3.3. Dimensions of the laminar box were determined by considering the maximum loading capacity of the shaking table. The geometry of laminar box was designed as a rectangular shape instead of a square geometry due to the possible torsion problem during one directional shaking.

Figure 3.3. Side View of Unidirectional Laminar Box.

As mentioned in Section 2, Laminar box consists of 18 laminates and 324 ball bearings, base plate, the side guides and internal membrane components (Sekman, 2016).

In this study, performance checks were repeated according to procedure mentioned in Section 2. Four different performance tests including the inertia of the laminar box, friction between the layers, stiffness of the membrane, and boundary conditions were performed for the constructed laminar box to analyze reliability of the box.

For the performance check of laminar box boundaries, instrumentation layout of the laminar box without soil was shown in Figure 3.4. Four accelerometers and four optical distance sensors (ODS) were mounted conjugately on the front side of the laminar box. Accelerometers were marked as “A” and ODSs were tagged as “L”. A1 and L1 were oriented to provide data from the shaking table for checking the given input. The rest of them were placed from bottom to top as seen in the Figure 3.4. Cyclic sinusoidal motion of 0.5 Hz with 0.05g, 1 Hz with 0.30g, 2 Hz with 0.50g, 3 Hz with 0.60g, 4 Hz with 0.70g, and 5 Hz with 0.80g were applied to the empty laminar box via shaking table for the check of the performance of the laminar box. The performance check results showed that flexible boundaries of the laminar box functioned properly.

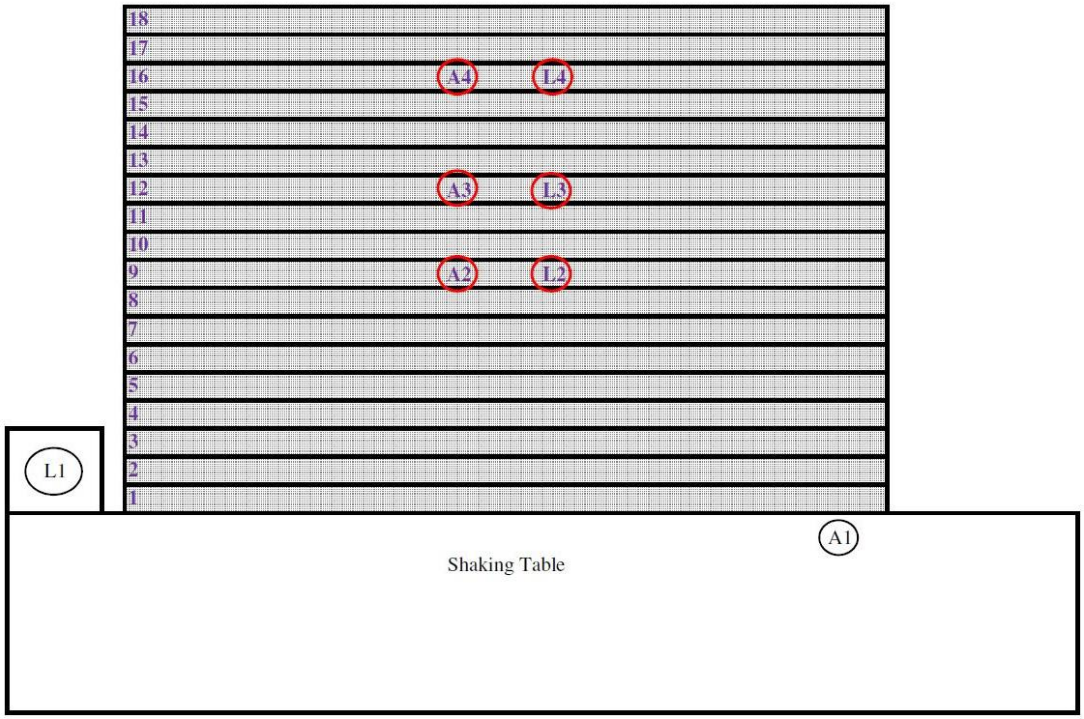

Figure 3.4. Instrumentation Layout of the Empty Laminar Box.

The Figure 3.5a and Figure 3.5b demonstrated the measured accelerations and displacements results from the cyclic sinusoidal motion with 0.5 Hz. Required case was decrease in acceleration and displacement values when the seismic wave moved upward. Thus, both acceleration and displacement values attenuated from bottom to top.

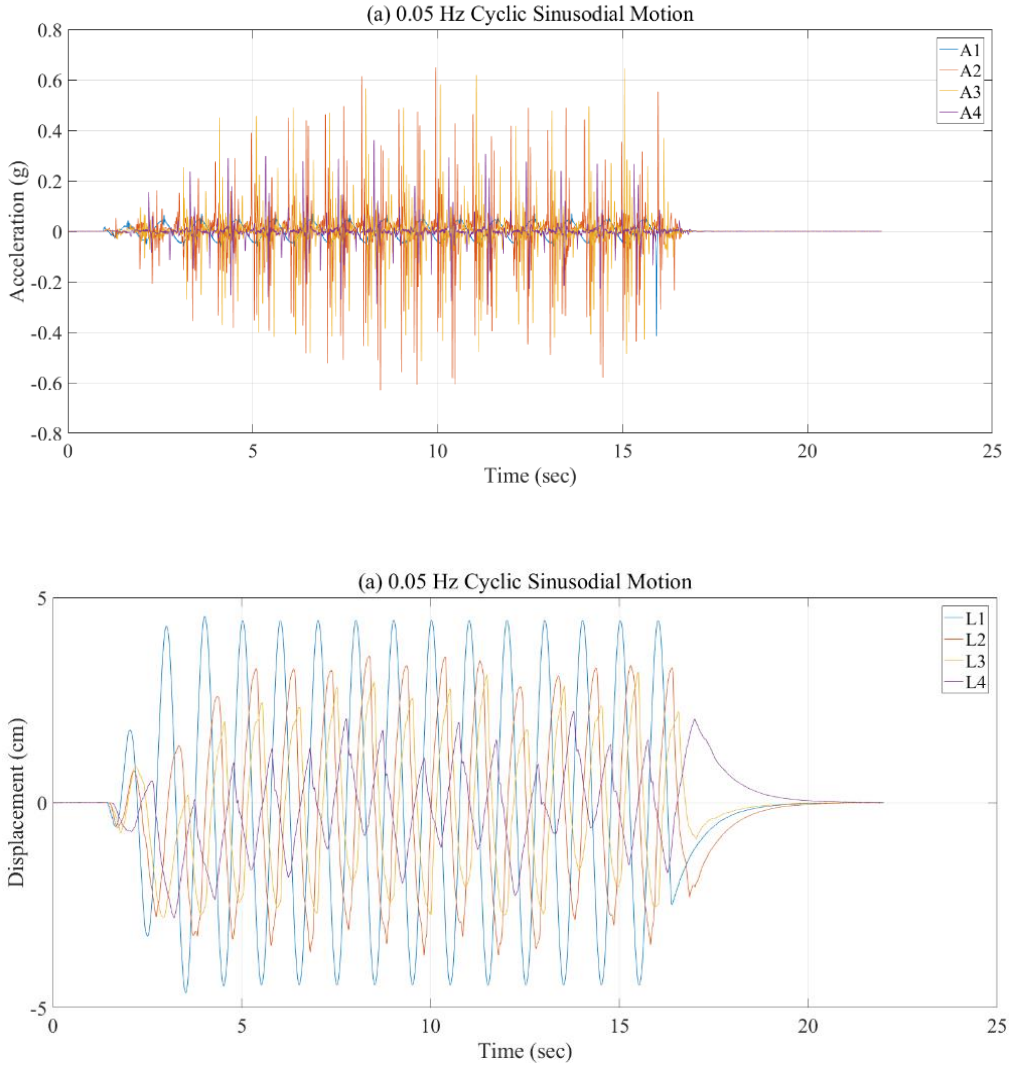

Figure 3.5. (a) Acceleration vs. Time, (b) Displacement vs. Time Under 0.5 Hz Cyclic Sinusodial Motion.

Three ODS and 11 accelerometers were placed to evaluate the response of the soil deposit. Three ODS and three accelerometers A2, L2, A3, L3 and A4, L4 were mounted on three different layers from bottom to top. Accelerometers A7, A8, A9, and A10 were placed on a same horizontal plane whose height is 1/2 of the total height of the laminar box with

the 15 cm avoidance away from the sides as seen in the Figure 3.6b. The rest of the accelerometers A5, A6, A11 and A12 were located at midpoint of the box with the height of 1/4, 2/4, 3/4 and 4/4 of the total height from the ground, respectively as seen in the Figure 3.6a.

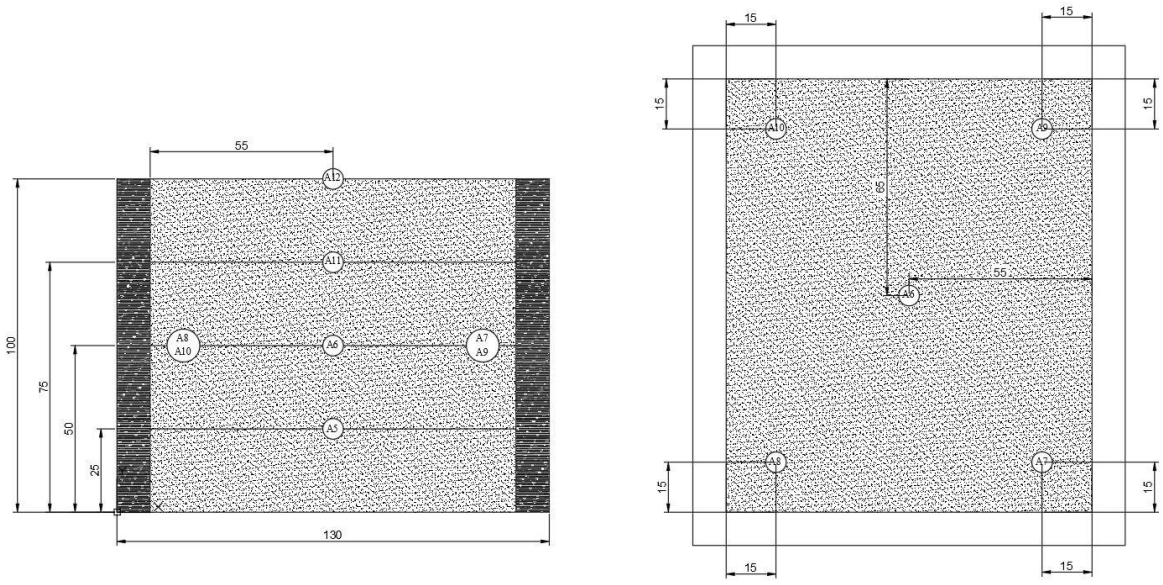

Figure 3.6. (a) Section, (b) Top View of Instrumentation Layout of the Laminar Box Filled with Sand.

Cyclic sinusoidal motions that have 0.5 Hz with 0.1g, 1 Hz with 0.3g, 2 Hz with 0.5g, 3 Hz with 0.6g, 4 Hz with 0.7g and 5 Hz with 0.8g, and Kocaeli earthquake (1999), El Centro earthquake (1940), and Kobe earthquake (1995) motions were applied to the laminar box to provide linearity in soil behavior. The readings of accelerometers were compared in order to evaluate the influence of the box boundaries as seen in Figure 3.7. The comparison was done with the accelerometers A6, A7, A8, A9, and A10 which were at the same horizontal plane. Almost identical acceleration values were obtained due to the same location of the accelerometers at the same horizontal level. Figure 3.7a shows the acceleration values of A6, A7, A8, A9, and A10 under 0.5 Hz cyclic sinusoidal motion. Measured accelerations from A6, A7, A8, A9, and A10 under 1 Hz sinusoidal motion and Kobe earthquake (1995) were indicated in Figure 3.7b and Figure 3.7c. As required, there was no substantial discrepancy among A6, A7, A8, A9, and A10 under different shaking table motions.

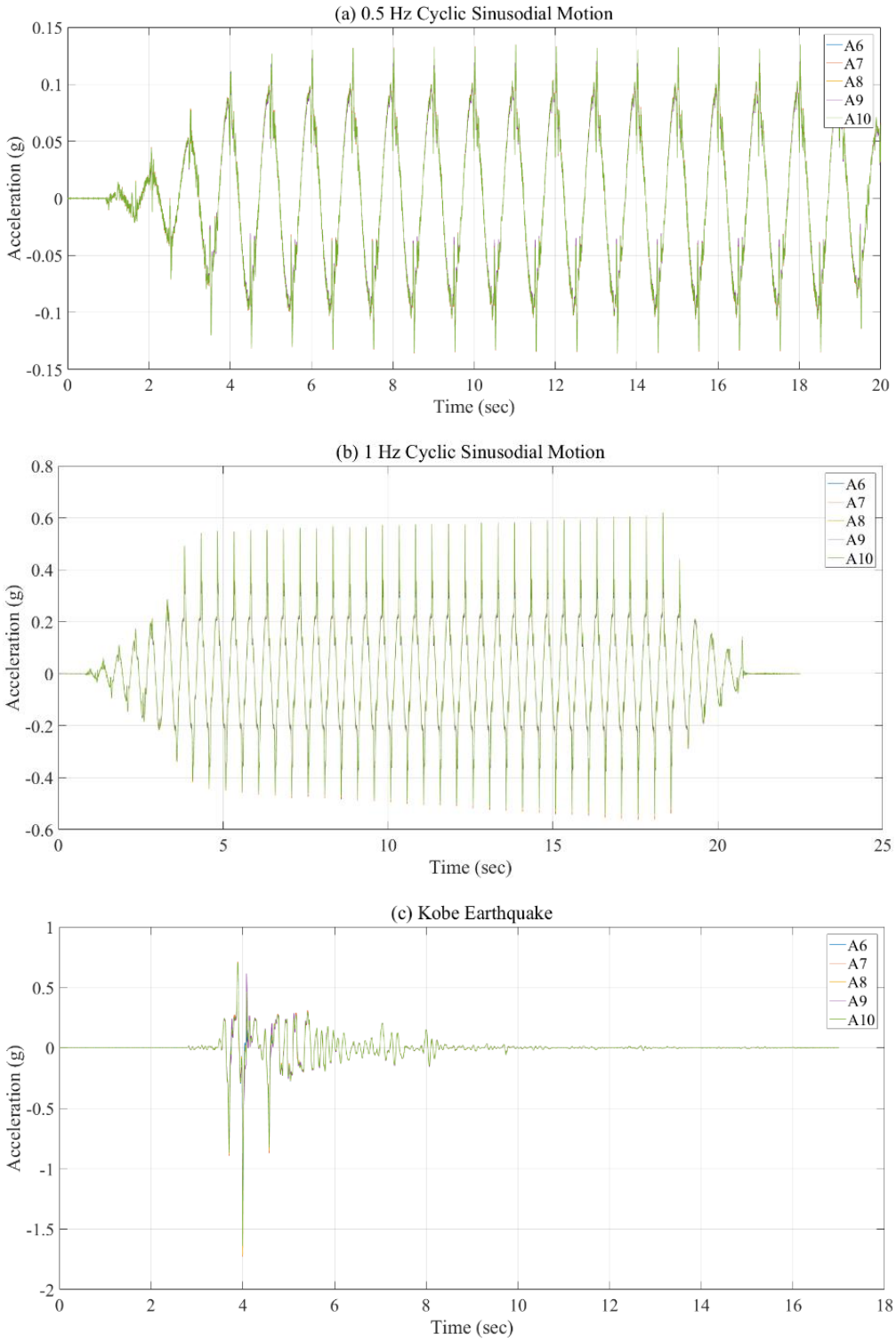

Figure 3.7. (a) Acceleration vs. Time Graph Under 0.5 Hz Cyclic Sinusodial Motion, (b) Acceleration vs. Time Graph Under 1 Hz Cyclic Sinusodial, (c) Acceleration vs. Time Graph Under Kobe Earthquake of Laminar Box filled with Sand.

3.6. Scaled Building Model

For the purpose of the representation of low and medium rise buildings, model buildings were selected as three and five story buildings similar to building models of Sekman (2016) and Goztepe (2016). The dimensions of the laminar box were restricted by the scale factor of the building model. The laminar box dimensions did not allow the construction of full-scale buildings so that a 1:10 scale factor (L=10) was determined considering maximum allowable dimensions for the building model. In order to provide easiness in manufacture and reliability, a 1:10 scale factor was used. In model designing process, similitude requirements were taken from Harris and Sabnis (1999) section 2.5. Material specifications were not scaled due to the use of available material in manufacturing the building. The scale factors for different required parameters were given in Table 3.2. Some physical quantities, such as acceleration and strain, remain the same even after scaling (Harris and Sabnis, 1999; Iai, 1989)

Table 3.2. Scaling Parameters given by Harris and Sabnis (1999), and Iai (1989).

Parameter	1:10 Scaled Model/Prototype	
Length	L	1/10
Time	$\sqrt{L}$	$\sqrt{10}$
Mass	L^2	1/100
Displacement	L	1/10
Acceleration	1	1
Stress	1	1
Strain	1	1
Force	L^2	1/100
Frequency	$1/\sqrt{L}$	$1/\sqrt{10}$
Density	1	1

Figure 3.8. 1:10 Scaled Model of Five Story Building Model.

In the previous study, building models were designed and constructed as seen in Figure 3.8. As a brief explanation of the building, steel columns having 26.5 cm x 5 cm x 0.5 cm dimensions were connected with metric 8 bolts to floors. Floors were made with a dimension of 30 cm x 30 cm x 1 cm. Also, the weight of the floors were made with a dimension of 30 cm x 30 cm x 2 cm. Four flanges were welded on every floor were used as connection apparatus in the attachment of the columns. Foundation was made with a dimension of 35 cm x 35 cm x 2 cm. The final height of the five-story building was 135 cm without foundation, and three-story building was 81 cm without foundation (Goztepe, 2016; Sekman, 2016).

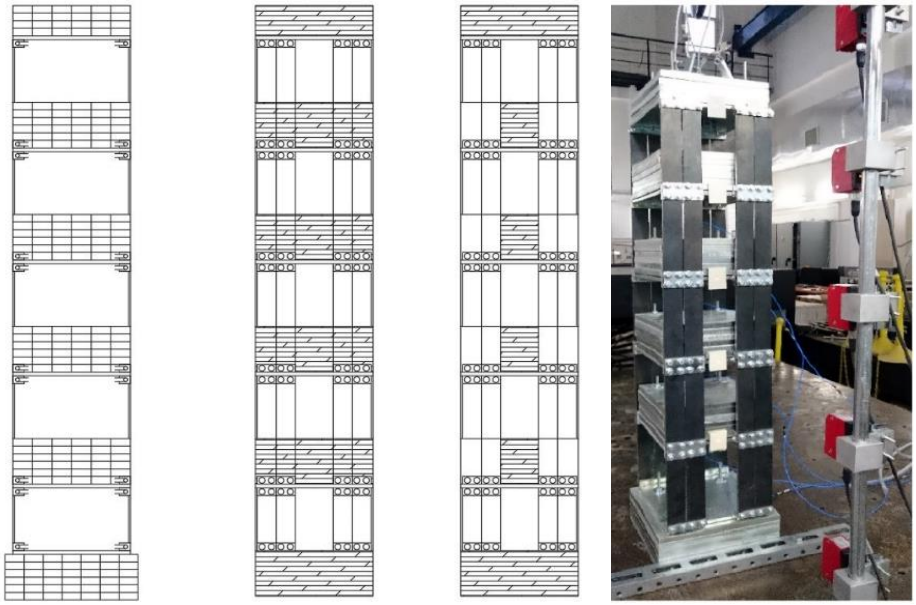

Figure 3.9. 1:10 Scaled Model of Five Story Building Model.

3.7. GSI with Geosynthetics

The concept of the proposed GSI system is the transformation of ground motions to slip displacement by creating an additional geosynthetics layer beneath the structure. Two geosynthetic layers were arranged in the way that one on the top of the other. Moreover, main requirements for determination of suitable geosynthetic material were listed in the study conducted by Yegian and Kadakal (2004). When all these requirements and the literature were taken into consideration, commercially available two geomembranes and two geotextiles were prepared to utilize. Geomembranes were chosen as 1.0 mm thick PTFE sheet and 1.0 mm thick HDPE (junifol PEHD) that are illustrated in Figure 3.10a and Figure 3.10b, respectively. Selected geosynthetic couples were defined as following (Sekman, 2016) :

- GSI 1 : Junifol HDPE 1 mm geomembrane with Typar DuPont SF44 nonwoven geotextile
- GSI 2 : PTFE 1 mm geomembrane with Typar DuPont SF44 nonwoven geotextile
- GSI 3 : PTFE 1 mm geomembrane with Typar DuPont SF56 nonwoven geotextile

(a)

(b)

Figure 3.10. (a) 1mm Thick Junifol HDPE Geomembrane, (b) 1 mm Thick PTFE Geomembrane Sheets.

Geotextiles were 150 and 190 gr/m^2 nonwoven geotextile (Typar DuPont SF 44 and SF 56) as seen in the Figure 3.11.

The selection of above mentioned geotextile-geomembrane (GG) couples was done according to the Section 2 as seen in Table 3.3.

(a)

(b)

Figure 3.11. (a) Typar DuPont SF44 , (b) Typar DuPont SF56 Nonwoven Geotextiles.

Table 3.3. Measured Peak Table Accelerations (A_t), Peak Block (Residual Acceleration) Accelerations (A_b) and Slip Displacements (D_s) (Sekman, 2016).

PTFE/SF44								
	1 Hz	2 Hz	3 Hz	4 Hz	5 Hz	El Centro Eq. (1940)	Kobe Eq. (1995)	Kocaeli Eq. (1999)
A_t	0.34	0.63	0.76	0.67	0.79	0.34	0.69	0.21
A_b	0.19	0.20	0.19	0.20	0.21	0.15	0.18	0.14
% Reduction	45	69	74	70	74	57	74	36
D_s	6.99	3.81	7.29	2.57	3.82	0.47	2.98	0.50
PTFE/SF56								
	1 Hz	2 Hz	3 Hz	4 Hz	5 Hz	El Centro Eq. (1940)	Kobe Eq. (1995)	Kocaeli Eq. (1999)
A_t	0.32	0.62	0.77	0.68	0.82	0.33	0.74	0.24
A_b	0.20	0.21	0.21	0.21	0.22	0.17	0.19	0.16
% Reduction	38	67	73	69	73	50	74	34
D_s	4.08	6.08	7.76	5.08	4.69	0.45	2.83	0.31
HDPE/SF44								
	1 Hz	2 Hz	3 Hz	4 Hz	5 Hz	El Centro Eq. (1940)	Kobe Eq. (1995)	Kocaeli Eq. (1999)
A_t	0.35	0.63	0.77	0.67	0.81	0.32	0.78	0.24
A_b	0.30	0.33	0.33	0.35	0.35	0.28	0.33	0.24
% Reduction	12	48	57	48	56	13	58	0
D_s	1.14	3.77	3.99	5.45	9.87	0.15	1.36	0.16

3.8. Applied Ground Motions

Input motions exerted on shaking table that were applied for proposed GSI system experiments were divided into two categories which were earthquake and cyclic sinusoidal motions. According to free vibration tests, cyclic sinusoidal motion frequencies of the 5-story building model were obtained as 27.55 Hz, 24.05 Hz, 18.68 Hz, 11.65 Hz, and 3.67 Hz. Cyclic sinusoidal motion frequencies of the 3-story building model were obtained as 25.4 Hz, 17.17 Hz, and 5.57 Hz. In order to exert the earthquake motions on the proposed GSI system and building models, duration of the earthquake input data was scaled 1:10 by multiplying duration with a scaling factor of $\sqrt{10}$ in the accordance with the similitude rules taken from Iai (1989). Time history and response spectrum graphs of the scaled earthquake motions are shown in the Figure 3.12, Figure 3.13, and Figure 3.14, respectively.

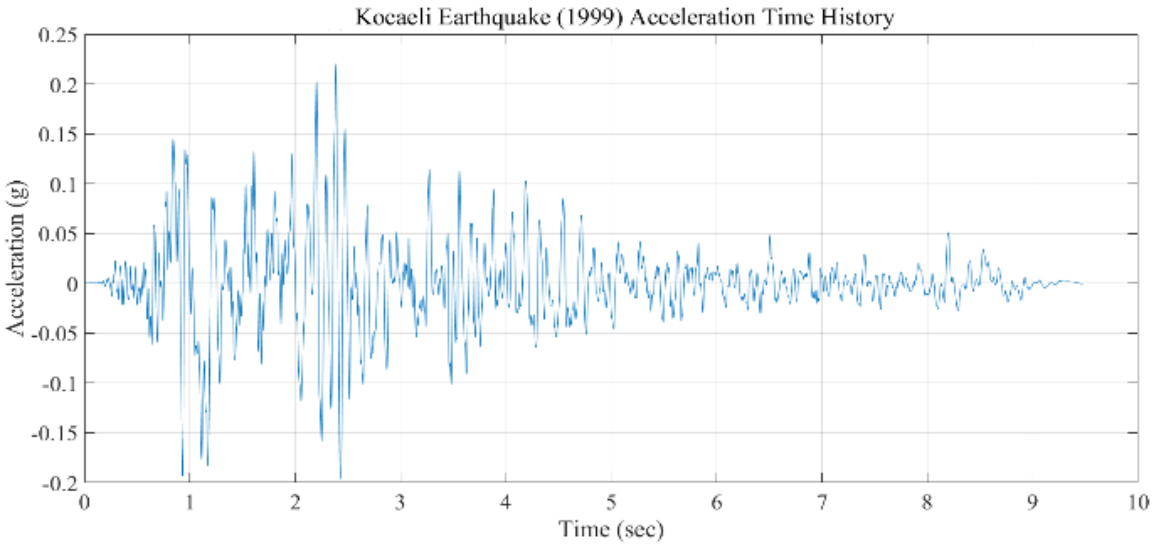

(a)

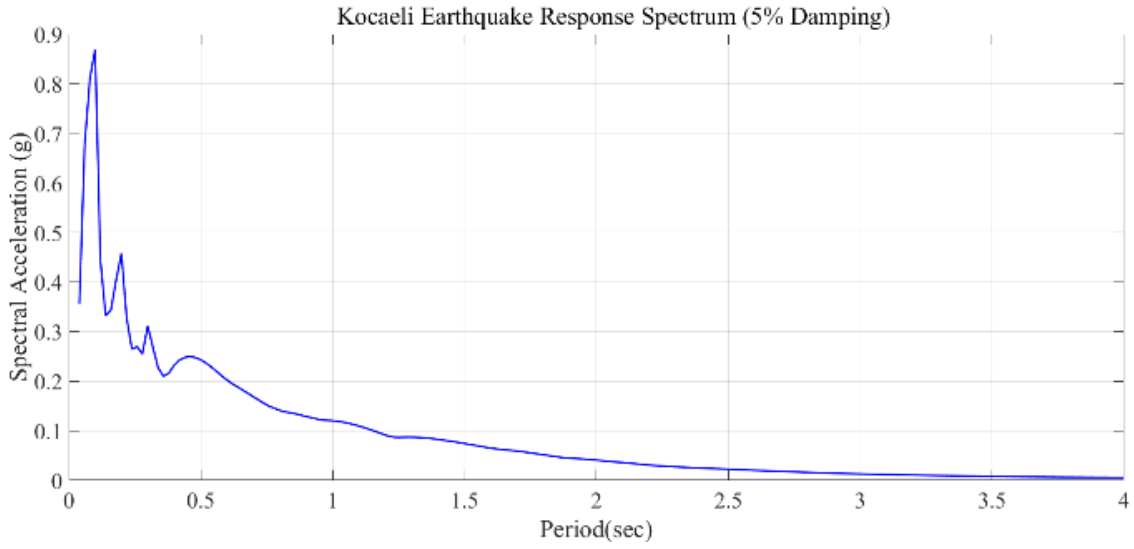

(b)

Figure 3.12. (a) Acceleration Time History, (b) Response Spectrum of Kocaeli Earthquake (1999).

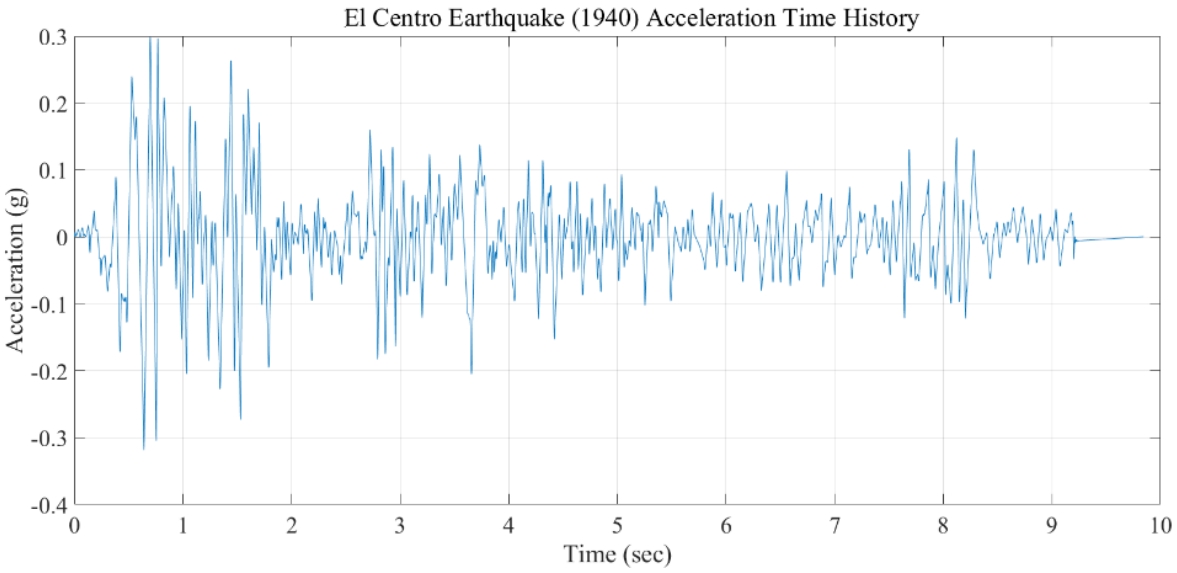

(a)

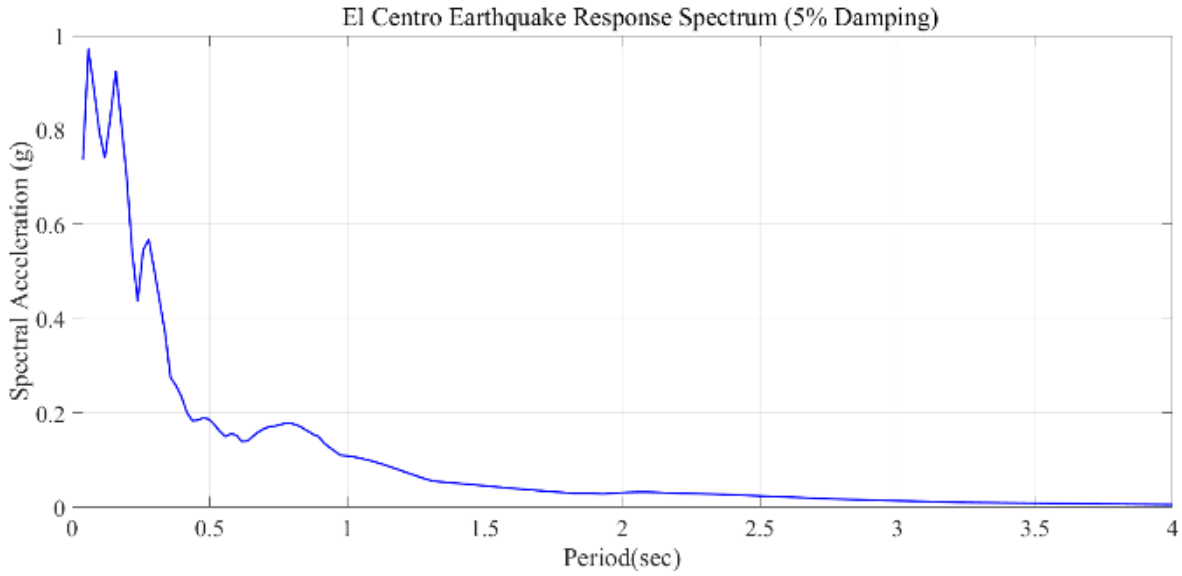

(b)

Figure 3.13. (a) Acceleration Time History, (b) Response Spectrum of El Centro Earthquake (1940).

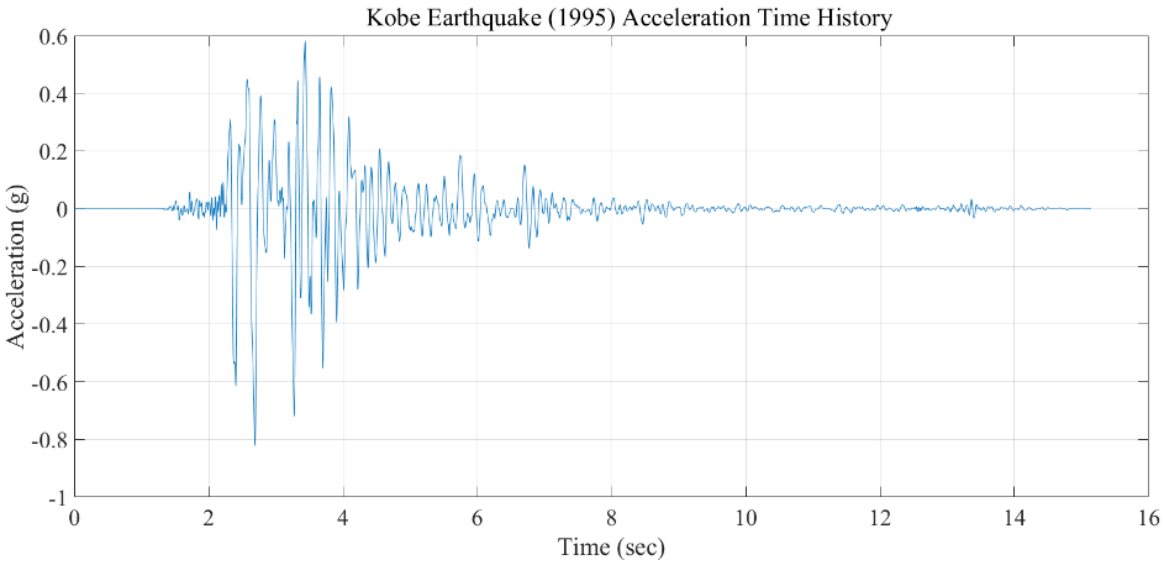

(a)

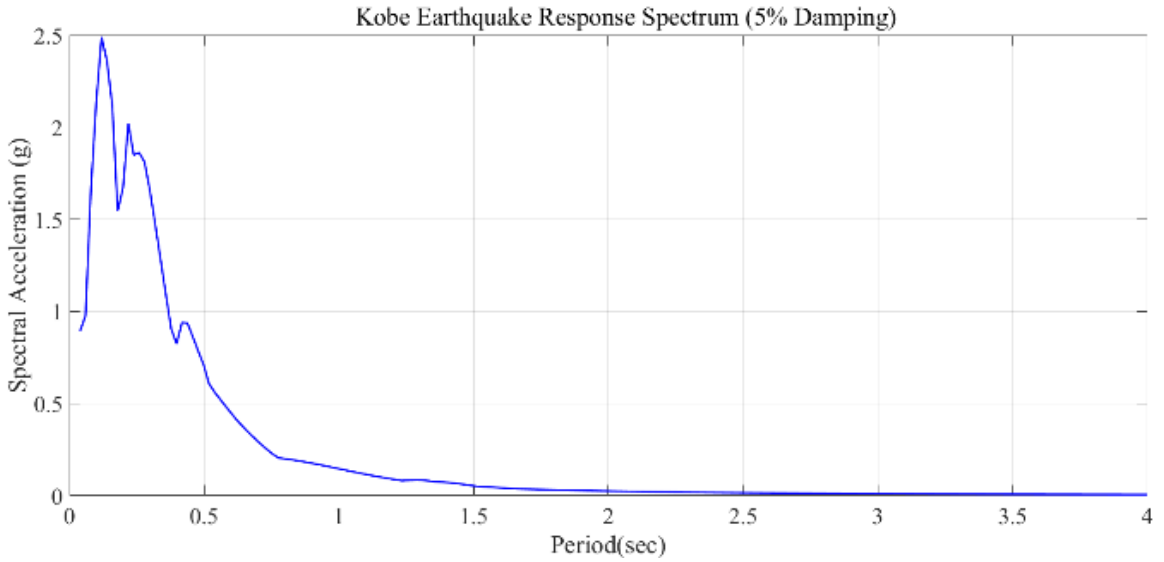

(b)

Figure 3.14. (a) Acceleration Time History, (b) Response Spectrum of Kobe Earthquake (1995).

3.9. Soil Sample Preparation and Instrumentation

In order to obtain a compacted unit weight of sand as 16.5 kN/m^3, approximately 2.5 tons of Silivri Sand were used. At each quarter of the depth of the laminar box, roughly 0.6

tons of Silivri sand was used in each level of equal layers as seen in the Figure 3.15. Compaction was done after completing filling of the sand at each quarter in depth of the box. At first, manual compaction was done by a rectangular shaped rigid spongy material. After manual compaction, soil was placed and compaction was done by giving 9 Hz sinusodial motion to the system within 30 seconds (El-Emam and Bathurst, 2004). After compaction, leveling was done in order to provide smoothness and the same elevation through the whole area as seen in Figure 3.15.

Figure 3.15. Soil Sample Preperation and Compaction.

Accelerometers were placed at the midpoint of each floor to measure transmitted accelerations. The only difference from the free surface was A12 which was the surface accelerometer. It was shifted to the endwall of the box and A25 was placed in the isolated soil mass nearby the foundation of the building. Six ODS were utilized for measuring story displacements. Sketch of experiment setup with five-story and three-story building models are shown in Figure 3.16. Five and three-story buildings were prepared with the same order

using curve shaped liner. ODS were placed on frame toward each floor of the building model. Likewise, 20g capacity accelerometers were mounted on midpoint of every floor and 3g accelerometers were placed in soil. Moreover, locations of the in-soil accelerometers were identified carefully in order to investigate the effect of the GSI. Figure 3.17 demonstrated representative illustration of five and three story buildings with straight liner.

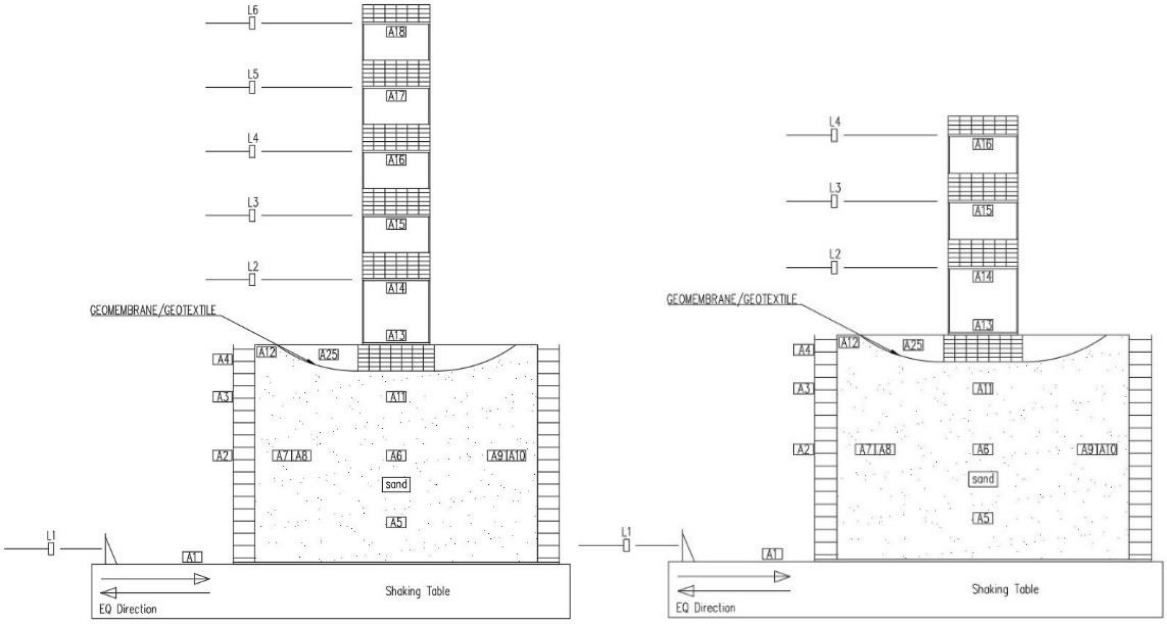

Figure 3.16. Sketch of Experiment Setup for proposed GSI System with Five Story and Three Story Building Model using Curve Shaped Liner.

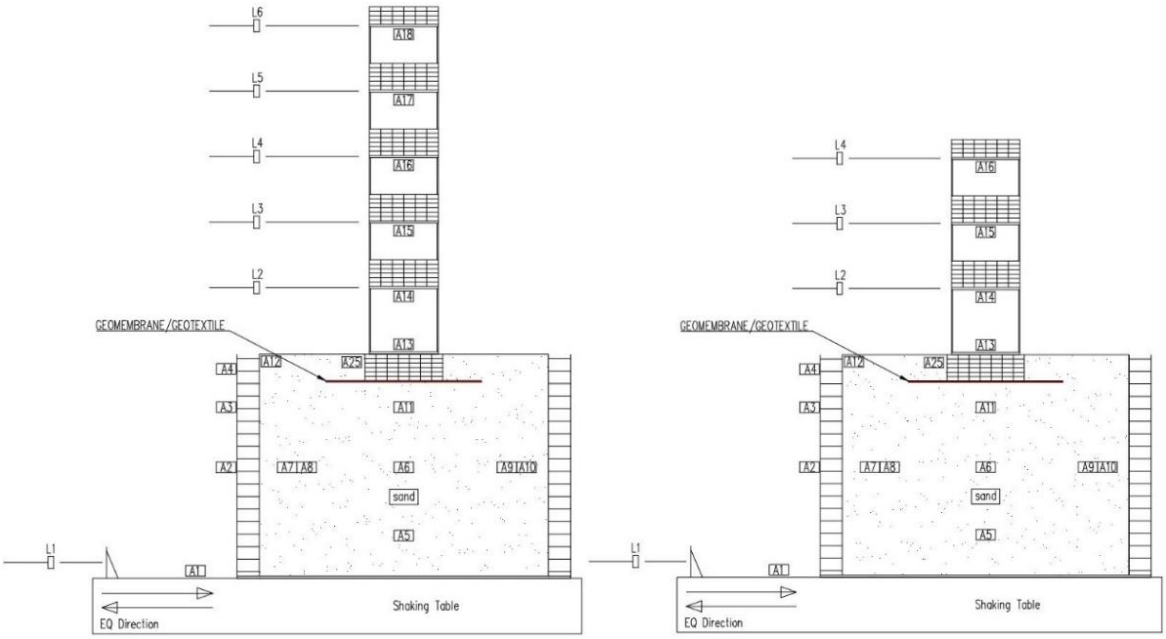

Figure 3.17. Sketch of Experiment Setup for proposed GSI System with Five Story and Three Story Building Model using Straight Liner.

4. EXPERIMENTAL RESULTS

Series of shaking table tests were conducted to evaluate the effects of different parameters including the number of stories, configuration type of GG liners and types of GSI material on seismic performance of low and medium rise buildings under different earthquake motions and cyclic sinusodial motions. Two different 1:10 scaled building models were respectively used as three and five story to represent low and medium rise buildings under same earthquake motion with different ground motion characteristics. Comparative study were performed among 12 cases considering the given parameters under proposed GSI system as seen in Table 4.1 and Table 4.2. Approximately 300 experiments were conducted. These experiments include performance checks of the laminar box, determination of the resonance and fundamental frequencies of the model buildings by free vibration tests, and seismic performance of the defined cases. Some of the conducted experiments were repeated to check the accuracy of the results, and one of them was used for each case.

Effects of two different configuration types of GG couples were evaluated . First eight cases were used to simulate curve shaped liner (CL) which has two different arrangements. Due to the width of the foundation, CL1 corresponds to the curve shaped liner taken as 3B (3x35cm) while CL2 was arranged as 2B (2x35). Secondly, the last four cases were for simulating foundation isolation with the straight liner described as SL. Straight liner has a dimension of 70x70 cm that comes from 2B (2x35). In the determination of used synthetic liners, H/D ratios from Yegian and Catan (2004), and Sekman (2016) were also taken into consideration. H/D ratio of 6 corresponds to CL2 while CL1 is referred to H/D ratio of 9. This means, H/D ratio of curve shaped liner was within the limits defined by Yegian and Catan (2004).

Shaking table tests were conducted under real PGA values of Kocaeli (0.22g), El Centro (0.35g) and Kobe (0.8g) earthquakes and the same earthquakes with increasing PGA values.

Table 4.1. The Cases to Conduct Experiments for Proposed GSI System using Curve Shaped Liners in Foundation Isolation.

Case No	Number of Story	Configuration Type	Type of the GSI Material	Cyclic Sinusoidal Motions	Kocaeli Eq. (1999)	El Centro Eq. (1940)	Kobe Eq. (1995)
CM-5	5	-	-	27.55 Hz 24.05 Hz 18.38 Hz 11.65 Hz 3.67 Hz	0.22 g 0.34 g 0.50 g	0.35 g 0.46 g 0.55 g 0.72 g 0.81 g 0.89 g	0.74 g 0.80 g 0.89 g
Case 1	5	CL1	GSI 1				
Case 2	5	CL2	GSI 1				
Case 3	5	CL2	GSI 2				
Case 4	5	CL1	GSI 2				
Case 5	5	CL2	GSI 3				
Case 6	5	CL1	GSI 3				
CM-3	3	-	-	25.4 Hz 17.17 Hz 5.57 Hz			
Case 7	3	CL1	GSI 3				
Case 8	3	CL2	GSI 3				

Table 4.2. The Cases to Conduct Experiments for Proposed GSI System using Straight Liner in Foundation Isolation.

Case No	Number of Story	Configuration Type	Type of the GSI Material	Cyclic Sinusoidal Motions	Kocaeli Eq. (1999)	El Centro Eq. (1940)	Kobe Eq. (1995)
CM-5	5	-	-	27.55 Hz 24.05 Hz 18.38 Hz 11.65 Hz 3.67 Hz	0.22 g 0.34 g 0.50 g	0.35 g 0.46 g 0.55 g 0.72 g 0.81 g 0.89 g	0.74 g 0.80 g 0.89 g
Case 9	5	SL	GSI 1				
Case 10	5	SL	GSI 2				
Case 11	5	SL	GSI 3				
CM-3	3	-	-	25.4 Hz 17.17 Hz 5.57 Hz			
Case 12	3	SL	GSI 3				

Selected geosynthetic couples were defined as following (Sekman, 2016) :

- GSI 1 : Junifol HDPE 1 mm geomembrane with Typar DuPont SF44 nonwoven geotextile
- GSI 2 : PTFE 1 mm geomembrane with Typar DuPont SF44 nonwoven geotextile
- GSI 3 : PTFE 1 mm geomembrane with Typar DuPont SF56 nonwoven geotextile

Similar to the performance parameters in previos studies, four parameters such as top floor horizontal acceleration, foundation horizontal acceleration and first floor story drift regarding root-mean-square (RMS) and peak values of them were considered. The reason for the selection of first story as story drift is due to the collapse of the building caused by soft story which occurs at the first story. Representation of the results were identified by reduction percentage compared to the identical fixed based models due to the better understanding of the comparative study.

In addition, there are more performance parameters indicated in this study. Arias intensity to evaluate seismic energy dissipation, peak spectral acceleration to observe reduction in spectral acceleration, and period lengthening to investigate period shift effect were selected as performance indicator parameters. These parameters were calculated for the each case. Comparative study was performed between unisolated and isolated buildings and the results of each case were presented in the following parts.

4.1. Unisolated 5-Story Building

Mentioned three performance indicator parameters were evaluated for 5-story building model under Kocaeli, Kobe and El Centro earthquakes as shown in Figure 4.1, Figure 4.2 and Figure 4.3, respectively. Maximum foundation acceleration, maximum top floor acceleration and first floor drift were measured as 0.27g, 1.03g, and 0.017, respectively in the case of Kocaeli Earthquake.

The maximum foundation and top floor acceleration values were obtained as 1.02g and 1.22g under Kobe earthquake, respectively. On the other hand, maximum foundation acceleration was observed as 0.35g while top floor was exposed to maximum acceleration as 0.95g under El Centro earthquake. Furthermore, the maximum first story drift values appeared as 0.0568 and 0.0197 under Kobe and El Centro earthquakes, respectively.

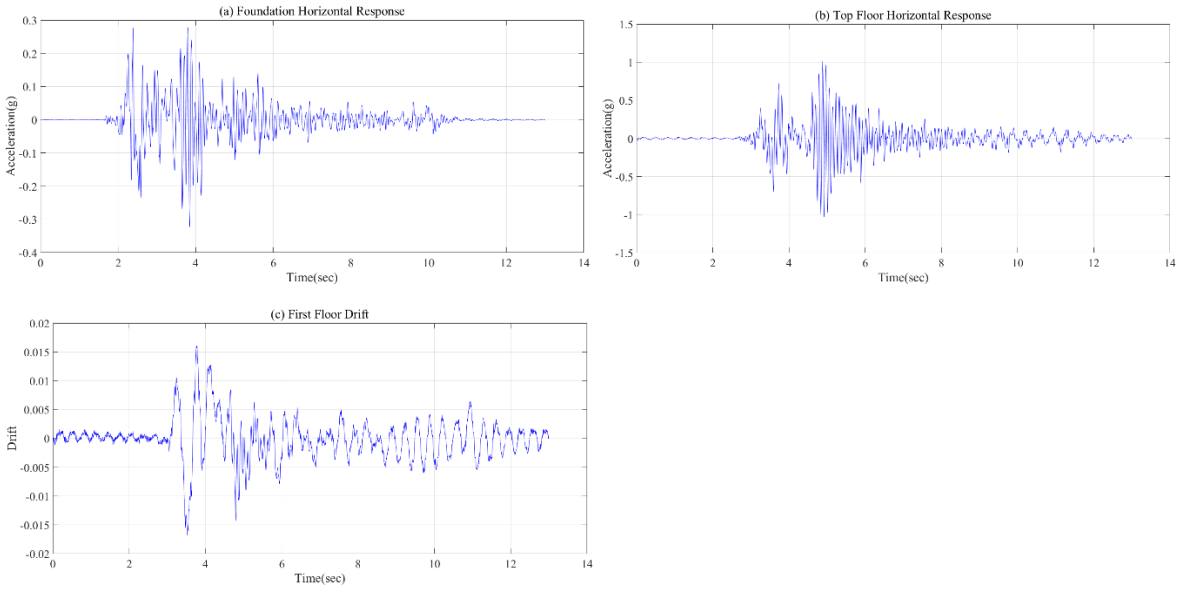

Figure 4.1. (a) Foundation Horizontal Acceleration Response, (b) Top Floor Horizontal Acceleration Response and (c) First Floor Drift of 5-story building model under Kocaeli Earthquake.

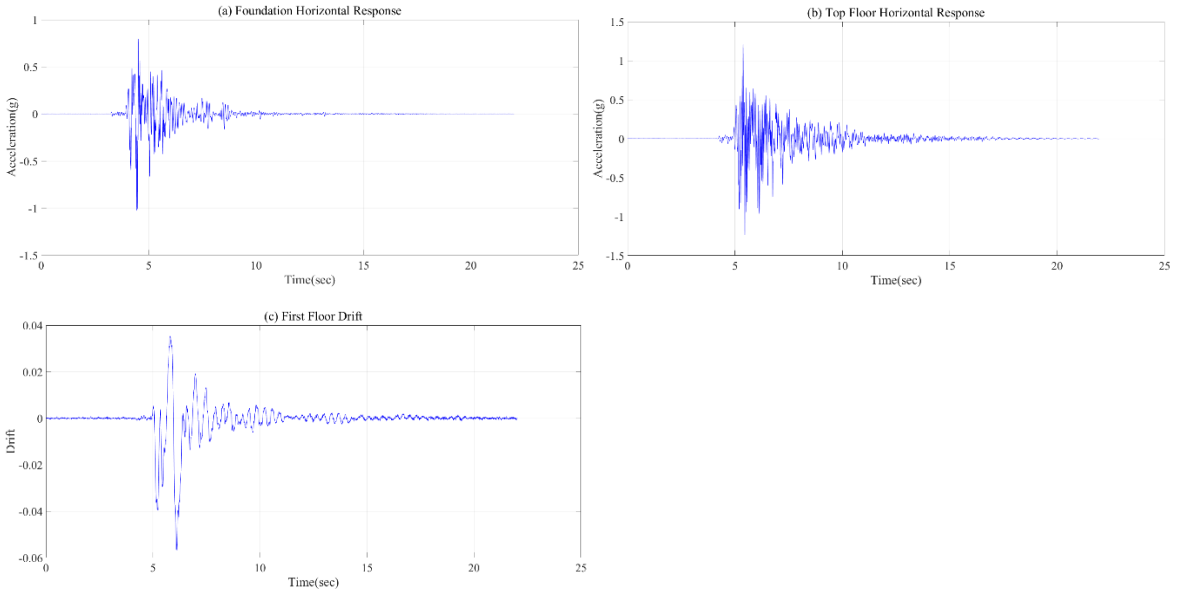

Figure 4.2. (a) Foundation Horizontal Acceleration Response, (b) Top Floor Horizontal Acceleration Response and (c) First Floor Drift of 5-story building model under Kobe Earthquake.

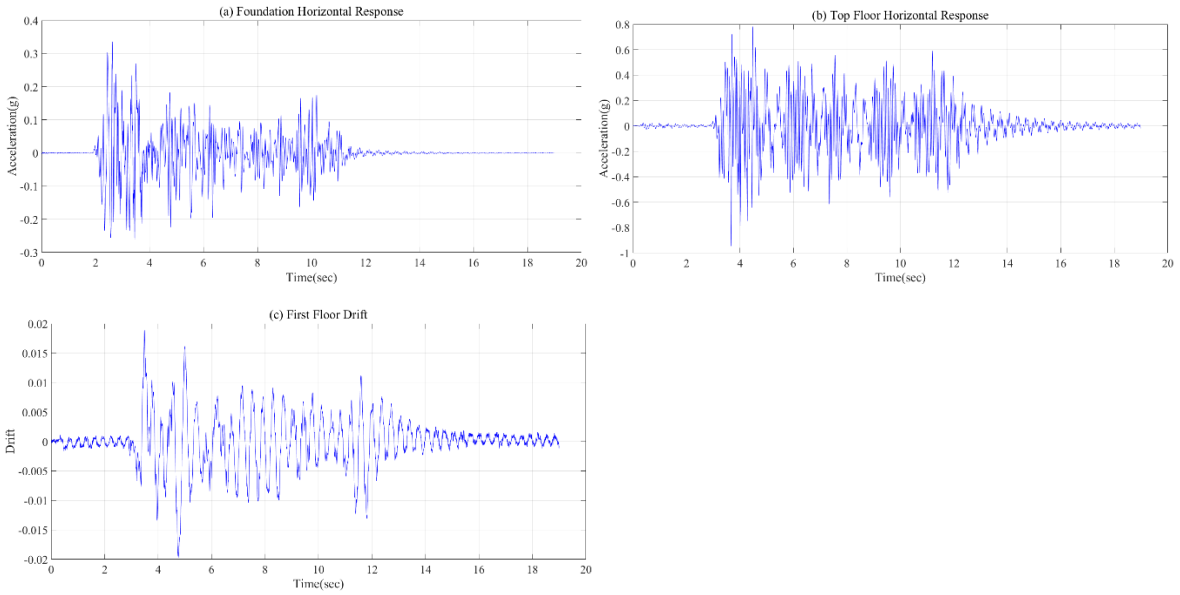

Figure 4.3. (a) Foundation Horizontal Acceleration Response, (b) Top Floor Horizontal Acceleration Response and (c) First Floor Drift of 5-story building model under El Centro Earthquake.

4.2. Soil Response to the Seismic Motions

Soil exhibits different seismic responses under different seismic ground motions. Types of soil and soil characteristics affect the behavior of the soil deposit under earthquake excitations. Silivri sand was used in this study as soil deposit of the overlying building models. The peak acceleration were measured from accelerometer (A11) placed just under the synthetic liner, and accelerometers (A12 and A25) placed at the foundation level. The values were obtained under the Kocaeli, Kobe and El Centro earthquakes with real PGA values, and cyclic sinusodial motions with 11.65 Hz and 17.17 Hz frequency values for five and three story building model, respectively as summarized in Table 4.3. Variations of acceleration responses between two different accelerometer were presented in a percentage. Moreover, reduction percentages of accelerations due to the application of the proposed GSI system were demonstrated in Table 4.4 regarding the cases for curve shaped liners (CL).

Table 4.3. Soil Response to the Seismic Motions.

Soil Response to the Seismic Motion					
Seismic Motions	Peak Acceleration (g)			Variation of Acceleration (%)	
	A1	A11	A12	From A1 to A11	From A11 to A12
Kocaeli Earthquake	0.225	0.218	0.303	-3	28
El Centro Earthquake	0.363	0.250	0.306	-45	18
Kobe Earthquake	0.837	0.845	1.025	1	18
Cyclic Sinusodial Motion	0.370	0.432	0.661	14	35

From deeper soil to surface, acceleration values were decreased substantially. It means, the effect of the seismic waves reduced close to surface. The most reductions was observed under Kocaeli earthquake and cyclic sinusodial motions.

Table 4.4. Acceleration Reduction Percentages from A12 to A25 Based on the Proposed Cases.

Acceleration Reduction								
Cases	Input Motion							
	Kocaeli Earthquake		El Centro Earthquake		Kobe Earthquake		Cyclic Sinusodial Motion	
	% Reduction from A12 to A25 (%)							
	RMS	Peak	RMS	Peak	RMS	Peak	RMS	Peak
Case 1	-6.50	-9.28	-19.58	-14.69	-8.64	-9.38	12.14	0.86
Case 2	4.45	-8.34	1.39	-11.42	-0.67	-7.36	14.12	-4.07
Case 3	2.50	-4.03	-6.86	-21.56	-4.18	-21.89	27.15	1.77
Case 4	16.26	1.39	-20.12	-10.57	-12.58	1.15	12.08	-18.94
Case 5	5.43	-6.15	16.26	-10.99	-13.33	-19.51	14.65	-11.90
Case 6	21.68	2.07	0.47	-10.27	0.68	-14.63	15.26	-24.06
Case 7	31.22	2.81	19.47	-0.19	4.64	-8.07	23.29	14.58
Case 8	32.27	8.78	21.84	3.61	3.29	-25.31	24.23	15.40
Case 9	19.72	-5.09	3.68	-11.22	-9.46	-15.93	25.93	16.70
Case 10	-4.51	-2.03	12.70	-24.22	11.43	-19.30	27.62	-1.06
Case 11	17.81	1.83	5.82	-15.07	5.76	-13.15	26.66	-23.96
Case 12	36.34	0.85	11.36	8.94	8.23	-28.02	27.97	-17.69

GSI3-CL2 was the best case under Kocaeli and El Centro earthquakes while the best cases were GSI2-CL1 in peak value and GSI3-CL1 in RMS value under Kobe earthquake. For the cases with straight liner, GSI3-SL was the most efficient case under Kocaeli and El Centro earthquakes. GSI2-SL was the best case under Kobe earthquake. For the cyclic sinusodial motions, the most effective case was observed as GSI3-CL2 for the curve shaped

liner and GSI1-SL for the straight liner. It means, the proposed GSI system was the most efficient on 3-story building model under Kocaeli and El Centro earthquakes. However, Kobe earthquake demonstrated less destructiveness on 5-story building model. The proposed GSI system provided more efficiency with straight liner under cyclic sinusodial motions in RMS values. However, more effective case was observed on 3-story building under cyclic sinusodial motions. In general, GSI 3 appeared to be the most efficient GG couple.

In the following parts, the defined cases were evaluated under different earthquake motions. These test were repeated under cyclic sinusodial motions and different earthquake motions with real PGA values.

4.3. Case 1 - GSI 1 Placed underneath the 5-Story Building Model

Junifol High Density Polyethylene (HDPE) 1 mm geomembrane with Typar DuPont SF44 nonwoven geotextile was defined as GSI 1 couple and tested under Kocaeli, Kobe and El Centro earthquakes. Curve shaped liner was used as GG couple with the configuration type of CL1 as foundation isolation material. Results were illustrated in order of Kocaeli, Kobe and El Centro earthquakes.

4.3.1. Seismic Response of Case 1 under Kocaeli Earthquake

Peak top floor and foundation horizontal acceleration reduction were observed as 6.87% and 2.32%, respectively. On the other hand, reduction in root-mean-square values of these acceleration responses were found as 8.27% and 4.26% respectively as seen in Figure 4.4a and Figure 4.4b. Reduction in the first floor story drift that can cause collapse of building due to the soft story was observed as 84.50% in RMS and 24.56% in peak value as shown in Figure 4.4c and Figure 4.4d. All performance parameters were indicated and summarized in Table 4.5. Moreover, no period shifting was observed in the system. Maximum reduction in Arias intensity was indicated at the top story as 13.26% (Figure 4.4e).

Alleviation in top floor peak spectral acceleration was illustrated as 4.05%. However, maximum reduction in peak spectral acceleration was observed at the fourth story. Additionally, as seen from Figure 4.4f, base shear and base moment exerted on the building at the foundation level were reduced as 6.30% and 6.50%, respectively.

Figure 4.4. (a) Foundation Acceleration Response, (b) Top Floor Acceleration Response, (c) First Floor Drift Response, (d) % Reduction of Case 1, (e) % Reduction of Arias Intensity, (f) % Reduction of Base Shear and Base Moment under Kocaeli Earthquake.

Table 4.5. Horizontal Acceleration, Story Drift, Arias Intensity, Peak Spectral Acceleration, Period Lengthening Ratio, and Base Shear and Base Moment under Kocaeli Earthquake.

Case 1 under Kocaeli (PGA = 0.22 g) Earthquake (1999)												
	Foundation		1st Floor		2nd Floor		3rd Floor		4th Floor		5th Floor	
	RMS	Peak	RMS	Peak	RMS	Peak	RMS	Peak	RMS	Peak	RMS	Peak
Horizontal Acceleration (g)												
Unisolated	0.052	0.323	0.130	0.879	0.152	0.971	0.089	0.534	0.096	0.550	0.172	1.033
Case 1	0.050	0.315	0.119	0.781	0.138	0.929	0.084	0.510	0.090	0.507	0.158	0.962
% Reduction (%)	4.26	2.32	8.38	11.13	8.90	4.36	5.62	4.37	6.65	7.83	8.27	6.87
Horizontal Story Drift												
Unisolated	-	-	0.0020	0.0114	0.0010	0.0104	0.0015	0.0145	0.0015	0.0041	0.0024	0.0012
Case 1	-	-	0.0003	0.0086	0.0013	0.0090	0.0020	0.0155	0.0006	0.0085	0.0024	0.0008
% Reduction (%)	-	-	84.50	24.56	-30.00	13.46	-33.33	-6.90	62.33	-107.32	0.00	36.67
Arias Intensity (g-sec)												
Unisolated	0.0056		0.0352		0.0479		0.0165		0.0193		0.0641	
Case 1	0.0055		0.0318		0.0429		0.0158		0.0181		0.0556	
% Reduction (%)	1.79		9.66		10.44		4.24		6.22		13.26	
Peak Spectral Acceleration (g)												
Unisolated	1.60		3.98		4.68		2.26		2.47		4.94	
Case 1	1.51		3.80		4.49		2.16		2.30		4.74	
% Reduction (%)	5.63		4.52		4.06		4.42		6.88		4.05	
Period Lengthening Ratio												
	Fundamental Period (sec)											
Unisolated	0.100		0.100		0.080		0.080		0.100		0.080	
Case 1	0.100		0.100		0.080		0.080		0.100		0.080	
Ratio	1.00		1.00		1.00		1.00		1.00		1.00	
	Base Shear (kN)				Base Moment (kN-m)							
	RMS		Peak		RMS		Peak					
Unisolated	0.59		3.65		0.41		2.46					
Case 1	0.54		3.42		0.38		2.30					
% Reduction (%)	7.90		6.30		7.32		6.50					

4.3.2. Seismic Response of Case 1 under Kobe Earthquake

Maximum reduction in horizontal acceleration was observed at foundation level as 12.08% in peak value while this reduction percentage was found as 0.95% in RMS value. However, no reduction was observed at top floor. Maximum reduction in story drift was examined at the second floor as 59.6% in peak value and at top floor as 57.4% in RMS value. Furthermore, Arias intensity showed its effects clearly on the first floor with a reduction percentage of 16.9%. However, no alleviation was evaluated at top story. Also, 6.4% and 15.6% reduction were observed at foundation level in Arias intensity and peak spectral acceleration, respectively. All the results of the case were tabulated and graphed in Table 4.6 and Figure 4.5, respectively. Period shift effect was examined at foundation and third story but the maximum period lengthening ratio was indicated as 4.00. Although there was a reduction in base shear as 3.55% in peak value, small amount of increase in base moment in RMS value was occured as 1.50%. On the other hand, small amount of reduction was observed in base moment as 0.61% in peak value as seen in Figure 4.5f.

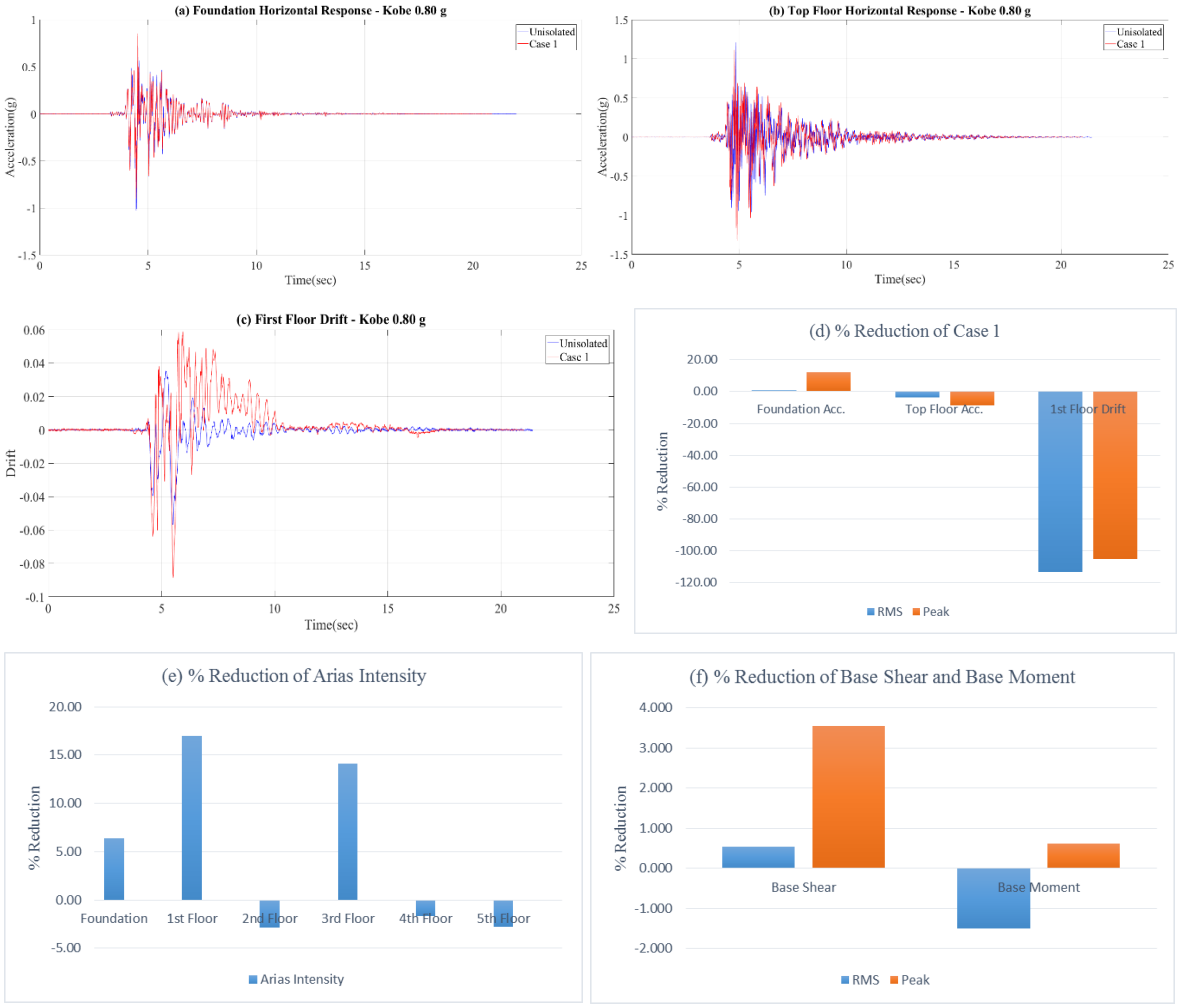

Figure 4.5. (a) Foundation Acceleration Response, (b) Top Floor Acceleration Response, (c) First Floor Drift Response, (d) % Reduction of Case 1, (e) % Reduction of Arias Intensity, (f) % Reduction of Base Shear and Base Moment under Kobe Earthquake.

Table 4.6. Horizontal Acceleration, Story Drift, Arias Intensity, Peak Spectral Acceleration, Period Lengthening Ratio, and Base Shear and Base Moment under Kobe Earthquake.

Case 1 under Kobe (PGA = 0.80 g) Earthquake (1995)												
	Foundation		1st Floor		2nd Floor		3rd Floor		4th Floor		5th Floor	
	RMS	Peak	RMS	Peak	RMS	Peak	RMS	Peak	RMS	Peak	RMS	Peak
Horizontal Acceleration (g)												
Unisolated	0.084	1.025	0.104	1.049	0.095	0.744	0.103	1.015	0.093	0.946	0.128	1.233
Case 1	0.084	0.901	0.097	1.054	0.098	0.725	0.098	1.021	0.096	0.833	0.132	1.341
% Reduction (%)	0.95	12.08	6.76	-0.50	-3.81	2.56	5.03	-0.59	-3.24	11.88	-3.69	-8.70
Horizontal Story Drift												
Unisolated	-	-	0.0030	0.0120	0.0023	0.0109	0.0043	0.0261	0.0030	0.0306	0.0010	0.0190
Case 1	-	-	0.0064	0.0246	0.0044	0.0044	0.0040	0.0339	0.0053	0.0315	0.0004	0.0294
% Reduction (%)	-	-	-113.33	-105.00	-91.30	59.63	6.51	-29.89	-76.67	-2.94	57.40	-54.74
Arias Intensity (g-sec)												
Unisolated	0.0251		0.0377		0.0315		0.0376		0.0303		0.0572	
Case 1	0.0235		0.0313		0.0324		0.0323		0.0308		0.0588	
% Reduction (%)	6.37		16.98		-2.86		14.10		-1.65		-2.80	
Peak Spectral Acceleration (g)												
Unisolated	1.99		2.70		3.80		3.21		2.91		3.71	
Case 1	1.86		2.28		3.59		2.81		3.19		3.64	
% Reduction (%)	6.53		15.56		5.53		12.46		-9.62		1.89	
Period Lengthening Ratio												
	Fundamental Period (sec)											
Unisolated	0.040		0.040		0.080		0.060		0.040		0.080	
Case 1	0.159		0.040		0.080		0.080		0.040		0.040	
Ratio	3.99		1.00		1.00		1.33		1.00		0.50	
	Base Shear (kN)						**Base Moment (kN-m)**					
	RMS		**Peak**				**RMS**		**Peak**			
Unisolated	0.53		5.35				0.34		3.29			
Case 1	0.53		5.16				0.35		3.27			
% Reduction (%)	0.54		3.55				-1.50		0.61			

4.3.3. Seismic Response of Case 1 under El Centro Earthquake

Maximum reduction in horizontal acceleration response was observed at the third floor as 31.91% in peak value. Also, top floor horizontal acceleration response exhibited a reduction as 20.25% in peak value. First story drift demonstrated a reduction percentage of 44.44% at the first floor so that possibility of soft story phenomenon can be minimized. Top floor did not indicate any reduction in story drift parameter. Moreover, great alleviation in Arias intensity and peak spectral acceleration was observed at the third story as 21.22% and 24.67%, respectively. Additionally, there was increase in base shear and base moment in RMS values while reduction was observed in base shear and base moment in peak values.

Results were demonstrated and summarized in Figure 4.6 and Table 4.7. Period was only shifted at the foundation level.

Figure 4.6. (a) Foundation Acceleration Response, (b) Top Floor Acceleration Response, (c) First Floor Drift Response, (d) % Reduction of Case 1, (e) % Reduction of Arias Intensity, (f) % Reduction of Base Shear and Base Moment under El Centro Earthquake.

Table 4.7. Horizontal Acceleration, Story Drift, Arias Intensity, Peak Spectral Acceleration, Period Lengthening Ratio, and Base Shear and Base Moment under El Centro Earthquake.

Case 1 under El Centro (PGA = 0.35 g) Earthquake (1940)												
	Foundation		1st Floor		2nd Floor		3rd Floor		4th Floor		5th Floor	
	RMS	Peak	RMS	Peak	RMS	Peak	RMS	Peak	RMS	Peak	RMS	Peak
Horizontal Acceleration (g)												
Unisolated	0.057	0.336	0.116	0.651	0.140	0.603	0.106	0.633	0.108	0.501	0.172	0.946
Case 1	0.061	0.311	0.116	0.472	0.145	0.538	0.106	0.431	0.114	0.483	0.178	0.755
% Reduction (%)	-7.79	7.52	-0.17	27.43	-3.86	10.68	0.09	31.91	-4.99	3.63	-3.79	20.25
Horizontal Story Drift												
Unisolated	-	-	0.0009	0.0036	0.0024	0.0059	0.0032	0.0183	0.0010	0.0023	0.0018	0.0006
Case 1	-	-	0.0013	0.0020	0.0007	0.0033	0.0037	0.0158	0.0030	0.0024	0.0030	0.0006
% Reduction (%)	-	-	-44.93	44.44	70.00	44.07	-15.63	13.66	-199.00	-4.35	-63.89	-1.82
Arias Intensity (g-sec)												
Unisolated	0.0097		0.0407		0.0596		0.0344		0.0356		0.0895	
Case 1	0.0089		0.0323		0.0507		0.0271		0.0310		0.0761	
% Reduction (%)	8.25		20.64		14.93		21.22		12.92		14.97	
Peak Spectral Acceleration (g)												
Unisolated	1.15		2.28		3.31		2.27		1.53		3.34	
Case 1	1.13		1.99		2.91		1.71		1.44		3.10	
% Reduction (%)	1.74		12.72		12.08		24.67		5.88		7.19	
Period Lengthening Ratio												
	Fundamental Period (sec)											
Unisolated	0.159		0.080		0.080		0.060		0.080		0.080	
Case 1	0.179		0.080		0.080		0.060		0.080		0.080	
Ratio	1.12		1.00		1.00		1.00		1.00		1.00	
	Base Shear (kN)				**Base Moment (kN-m)**							
	RMS		**Peak**		**RMS**		**Peak**					
Unisolated	0.59		3.13		0.42		2.18					
Case 1	0.61		2.56		0.43		1.78					
% Reduction (%)	-3.39		18.21		-2.38		18.35					

4.4. Case 2 - GSI 1 Placed underneath the 5-Story Building Model

Junifol High Density Polyethylene (HDPE) 1 mm geomembrane with Typar DuPont SF44 nonwoven geotextile was used as GSI 1 couple under Kocaeli, Kobe and El Centro earthquakes. Curve shaped liner was used as GG liner with the configuration type of CL2. Results were illustrated in order of Kocaeli, Kobe and El Centro earthquakes.

4.4.1. Seismic Response of Case 2 under Kocaeli Earthquake

Horizontal acceleration underwent reduction at all stories in either peak or RMS values. Maximum reduction of horizontal acceleration response was observed at the third floor as 22.73%. First floor experienced maximum drift reduction as 94.50% in RMS and 60.53% in peak value. Moreover, Arias intensity showed its maximum efficiency at the second story with a reduction of 16.28%. Additionally, maximum reduction in peak spectral acceleration was measured at the third floor as 9.29%. Also, reduction percentages of base shear and base moment were similar to each other as seen in Table 4.8. Demonstration of the results can be seen in Figure 4.7 and Table 4.8. No period shifting was observed on the building model.

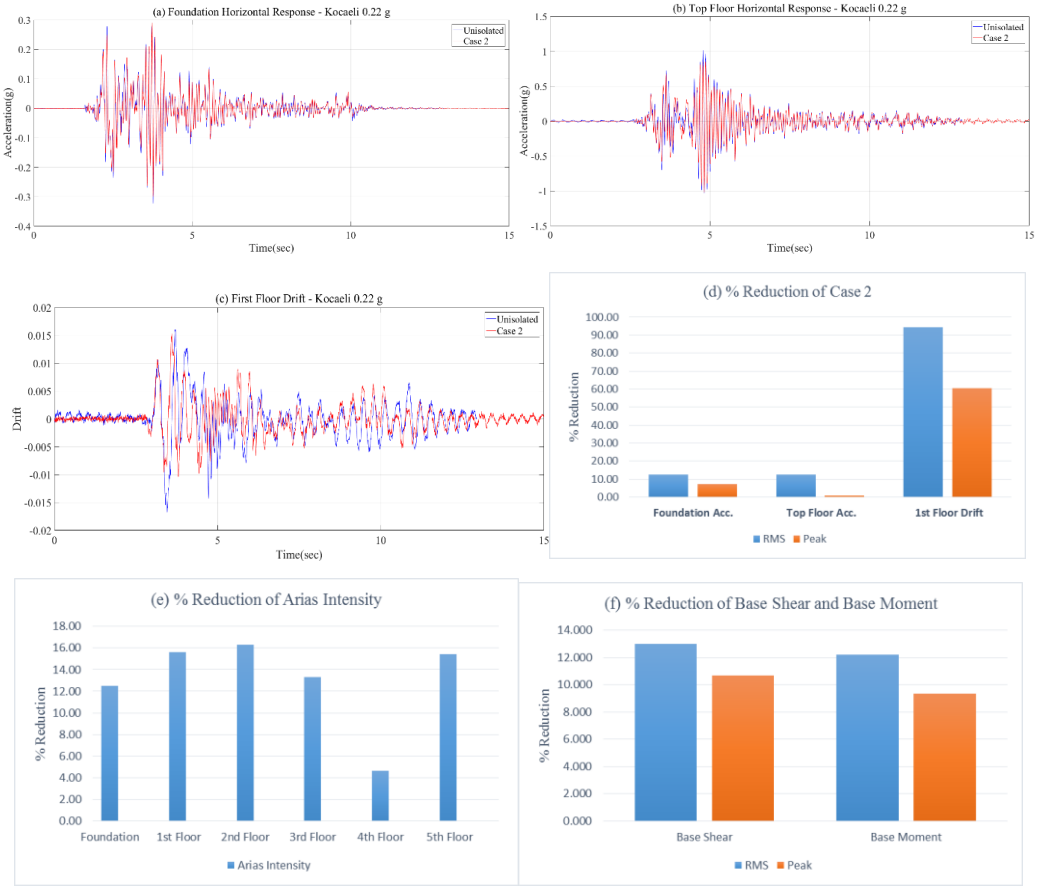

Figure 4.7. (a) Foundation Acceleration Response, (b) Top Floor Acceleration Response, (c) First Floor Drift Response, (d) % Reduction of Case 2, (e) % Reduction of Arias Intensity, (f) % Reduction of Base Shear and Base Moment under Kocaeli Earthquake.

Table 4.8. Horizontal Acceleration, Story Drift, Arias Intensity, Peak Spectral Acceleration, Period Lengthening Ratio, and Base Shear and Base Moment under Kocaeli Earthquake.

Case 2 under Kocaeli (PGA = 0.22 g) Earthquake (1999)												
	Foundation		1st Floor		2nd Floor		3rd Floor		4th Floor		5th Floor	
	RMS	Peak	RMS	Peak	RMS	Peak	RMS	Peak	RMS	Peak	RMS	Peak
Horizontal Acceleration (g)												
Unisolated	0.052	0.323	0.130	0.879	0.152	0.971	0.089	0.534	0.096	0.550	0.172	1.033
Case 2	0.045	0.300	0.111	0.742	0.129	0.904	0.077	0.412	0.088	0.478	0.150	1.024
% Reduction (%)	12.57	7.19	14.38	15.55	14.77	6.93	13.27	22.73	9.04	13.03	12.52	0.92
Horizontal Story Drift												
Unisolated	-	-	0.0020	0.0114	0.0010	0.0104	0.0015	0.0145	0.0015	0.0041	0.0024	0.0012
Case 2	-	-	0.0001	0.0045	0.0016	0.0128	0.0016	0.0073	0.0002	0.0074	0.0015	0.0009
% Reduction (%)	-	-	94.50	60.53	-60.00	-23.08	-6.67	49.66	88.67	-80.49	37.50	24.17
Arias Intensity (g-sec)												
Unisolated	0.0056		0.0352		0.0479		0.0165		0.0193		0.0641	
Case 2	0.0049		0.0297		0.0401		0.0143		0.0184		0.0542	
% Reduction (%)	12.50		15.63		16.28		13.33		4.66		15.44	
Peak Spectral Acceleration (g)												
Unisolated	1.60		3.98		4.68		2.26		2.47		4.94	
Case 2	1.56		3.71		4.25		2.05		2.30		4.54	
% Reduction (%)	2.50		6.78		9.19		9.29		6.88		8.10	
Period Lengthening Ratio												
	Fundamental Period (sec)											
Unisolated	0.100		0.100		0.080		0.080		0.100		0.080	
Case 2	0.100		0.100		0.080		0.080		0.100		0.080	
Ratio	1.00		1.00		1.00		1.00		1.00		1.00	
	Base Shear (kN)						Base Moment (kN-m)					
	RMS			Peak			RMS			Peak		
Unisolated	0.59			3.65			0.41			2.46		
Case 2	0.51			3.26			0.36			2.23		
% Reduction (%)	13.01			10.68			12.20			9.35		

4.4.2. Seismic Response of Case 2 under Kobe Earthquake

Maximum reduction in horizontal acceleration response was observed at the fourth story as 14.32% in peak value. The maximum reduction in story drift was measured as 68.56% in RMS value at top story. On the other hand, maximum reduction in story drift was measured as 38.33% at the first story. Foundation of the building exhibited maximum reduction in Arias intensity as 11.16%. Reduction was only observed at the fourth story as 3.44%. Results were shown in Figure 4.8 and Table 4.9. Period of the foundation and first floor was shifted with a factor of 2 and 1.5, respectively. Maximum reduction was observed in base shear and base moment in peak values as 5.61% and 3.34%, respectively.

Figure 4.8. (a) Foundation Acceleration Response, (b) Top Floor Acceleration Response, (c) First Floor Drift Response, (d) % Reduction of Case 2, (e) % Reduction of Arias Intensity, (f) % Reduction of Base Shear and Base Moment under Kobe Earthquake.

Table 4.9. Horizontal Acceleration, Story Drift, Arias Intensity, Peak Spectral Acceleration, Period Lengthening Ratio, and Base Shear and Base Moment under Kobe Earthquake.

Case 2 under Kobe (PGA = 0.80 g) Earthquake (1995)												
	Foundation		1st Floor		2nd Floor		3rd Floor		4th Floor		5th Floor	
	RMS	Peak	RMS	Peak	RMS	Peak	RMS	Peak	RMS	Peak	RMS	Peak
Horizontal Acceleration (g)												
Unisolated	0.084	1.025	0.104	1.049	0.095	0.744	0.103	1.015	0.093	0.946	0.128	1.233
Case 2	0.078	0.885	0.099	1.040	0.097	0.767	0.098	0.928	0.094	0.810	0.135	1.313
% Reduction (%)	7.70	13.72	3.96	0.84	-2.11	-3.16	5.03	8.55	-0.97	14.32	-5.73	-6.47
Horizontal Story Drift												
Unisolated	-	-	0.0030	0.0120	0.0023	0.0109	0.0043	0.0261	0.0030	0.0306	0.0010	0.0190
Case 2	-	-	0.0024	0.0074	0.0034	0.0217	0.0047	0.0335	0.0037	0.0378	0.0003	0.0155
% Reduction (%)	-	-	20.00	38.33	-47.83	-99.08	-9.30	-28.35	-23.33	-23.53	68.56	18.42
Arias Intensity (g-sec)												
Unisolated	0.0251		0.0377		0.0315		0.0376		0.0303		0.0572	
Case 2	0.0223		0.0364		0.0344		0.0355		0.0323		0.0669	
% Reduction (%)	11.16		3.45		-9.21		5.59		-6.60		-16.96	
Peak Spectral Acceleration (g)												
Unisolated	1.99		2.70		3.80		3.21		2.91		3.71	
Case 2	2.17		3.38		3.91		3.97		2.81		3.90	
% Reduction (%)	-9.05		-25.19		-2.89		-23.68		3.44		-5.12	
Period Lengthening Ratio												
	Fundamental Period (sec)											
Unisolated	0.040		0.040		0.080		0.060		0.040		0.080	
Case 2	0.080		0.060		0.080		0.060		0.040		0.080	
Ratio	2.00		1.50		1.00		1.00		1.00		1.00	
	Base Shear (kN)						**Base Moment (kN-m)**					
	RMS			**Peak**			**RMS**			**Peak**		
Unisolated	0.53			5.35			0.34			3.29		
Case 2	0.52			5.05			0.35			3.18		
% Reduction (%)	1.65			5.61			-1.53			3.34		

4.4.3. Seismic Response of Case 2 under El Centro Earthquake

Reduction in horizontal acceleration response was observed for all the storeys under El Centro earthquake. Maximum peak acceleration value was observed as 23.34% at the third story while maximum RMS value appeared as 14.17% at the first floor. Maximum reduction in story drift was measured at the second story as 72.88% in peak value. A 14.50% reduction was observed as a maximum value in Arias intensity at the first floor. Peak spectral acceleration indicated its maximum reduction at the first floor as 17.54%. Furthermore, summarized results were demonstrated in Figure 4.9 and Table 4.10. Period shifting was obtained at foundation and fourth story as a factor of 1.12 and 4.74, respectively.

Additionally, similarity was observed between the reduction values of base shear and base moment in both peak and RMS values.

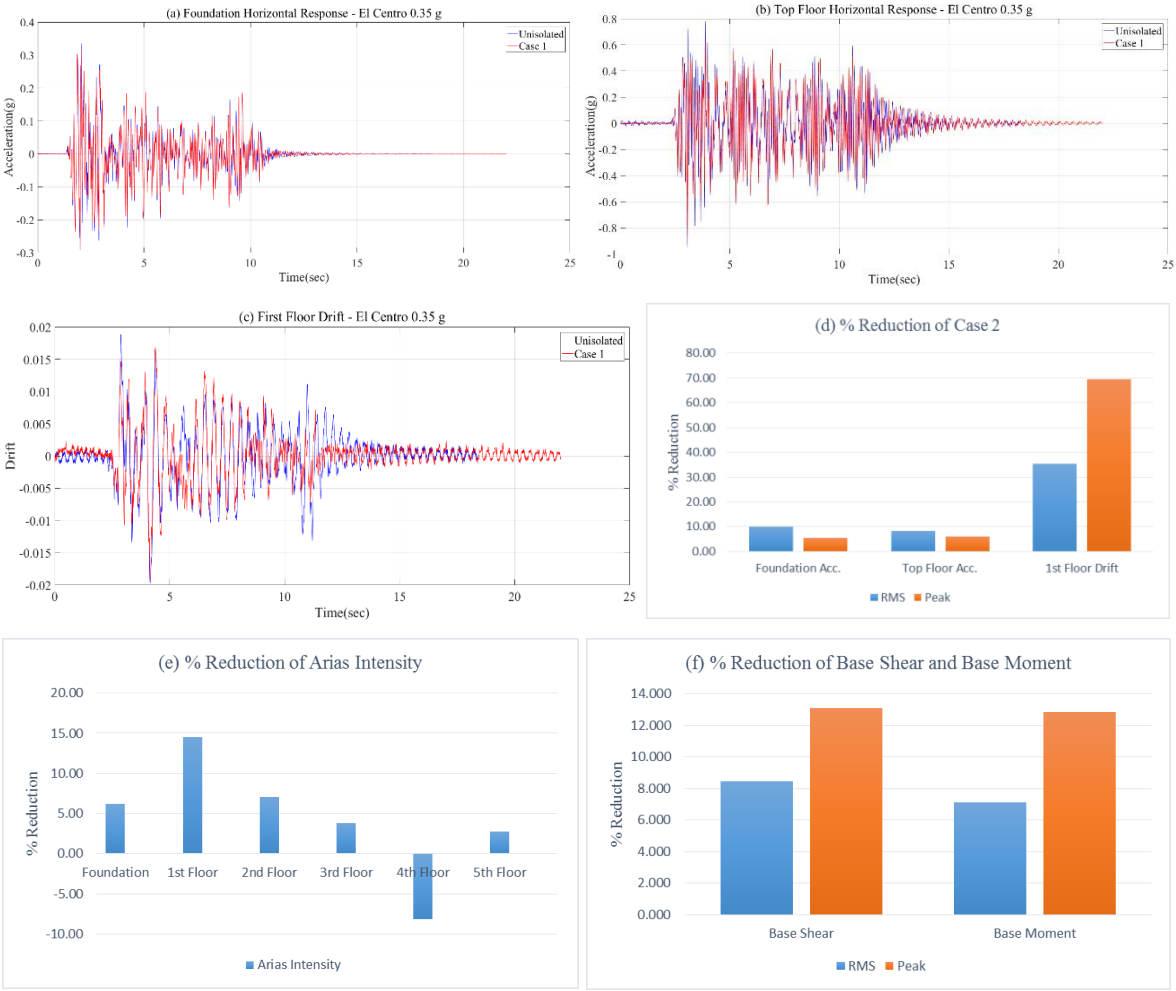

Figure 4.9. (a) Foundation Acceleration Response, (b) Top Floor Acceleration Response, (c) First Floor Drift Response, (d) % Reduction of Case 2, (e) % Reduction of Arias Intensity, (f) % Reduction of Base Shear and Base Moment under El Centro Earthquake.

Table 4.10. Horizontal Acceleration, Story Drift, Arias Intensity, Peak Spectral Acceleration, Period Lengthening Ratio, and Base Shear and Base Moment under El Centro Earthquake.

Case 2 under El Centro (PGA = 0.35 g) Earthquake (1940)												
	Foundation		1st Floor		2nd Floor		3rd Floor		4th Floor		5th Floor	
	RMS	Peak	RMS	Peak	RMS	Peak	RMS	Peak	RMS	Peak	RMS	Peak
Horizontal Acceleration (g)												
Unisolated	0.057	0.336	0.116	0.651	0.140	0.603	0.106	0.633	0.108	0.501	0.172	0.946
Case 2	0.051	0.318	0.099	0.536	0.125	0.561	0.097	0.485	0.105	0.419	0.157	0.890
% Reduction (%)	10.09	5.56	14.17	17.60	10.36	6.97	8.93	23.34	3.33	16.40	8.40	5.97
Horizontal Story Drift												
Unisolated	-	-	0.0009	0.0036	0.0024	0.0059	0.0032	0.0183	0.0010	0.0023	0.0018	0.0006
Case 2	-	-	0.0006	0.0011	0.0014	0.0016	0.0027	0.0144	0.0018	0.0093	0.0025	0.0007
% Reduction (%)	-	-	35.34	69.44	41.67	72.88	15.63	21.31	-80.00	-304.35	-38.89	-18.18
Arias Intensity (g-sec)												
Unisolated	0.0097		0.0407		0.0596		0.0344		0.0356		0.0895	
Case 2	0.0091		0.0348		0.0554		0.0331		0.0385		0.0870	
% Reduction (%)	6.19		14.50		7.05		3.78		-8.15		2.79	
Peak Spectral Acceleration (g)												
Unisolated	1.15		2.28		3.31		2.27		1.53		3.34	
Case 2	1.12		1.88		2.80		2.00		1.86		2.76	
% Reduction (%)	2.61		17.54		15.41		11.89		-21.57		17.37	
Period Lengthening Ratio												
	Fundamental Period (sec)											
Unisolated	0.159		0.080		0.080		0.060		0.080		0.080	
Case 2	0.179		0.080		0.080		0.060		0.378		0.080	
Ratio	1.12		1.00		1.00		1.00		4.74		1.00	
	Base Shear (kN)						**Base Moment (kN-m)**					
	RMS			**Peak**			**RMS**			**Peak**		
Unisolated	0.59			3.13			0.42			2.18		
Case 2	0.54			2.72			0.39			1.90		
% Reduction (%)	8.47			13.10			7.14			12.84		

4.5. Case 3 - GSI 2 Placed underneath the 5-Story Building Model

Polytetrafluoroethylene (PTFE) 1 mm geomembrane with Typar DuPont SF44 nonwoven geotextile was used as GSI 2 couple under Kocaeli, Kobe and El Centro earthquakes. Curve shaped liner was used as GG couple with the configuration type of CL2. Results were illustrated in order of Kocaeli, Kobe and El Centro earthquakes.

4.5.1. Seismic Response of Case 3 under Kocaeli Earthquake

Maximum reduction in RMS and peak value of horizontal acceleration response was observed as 18.26% at the second floor and 14.72% at the fourth floor, respectively. First story revealed maximum reduction in drift as 92.50% in RMS value and 40.35% in peak value. 17.78% reduction was observed as the maximum value of Arias intensity at the top floor. In addition, maximum reduction value of peak spectral acceleration was observed as 13.46% at the second story. Figure 4.10 and Table 4.11 illustrated the results in detail. Besides, period shifting was observed at only third story with a factor of 1.25. Furthermore, larger reduction values were observed in RMS values.

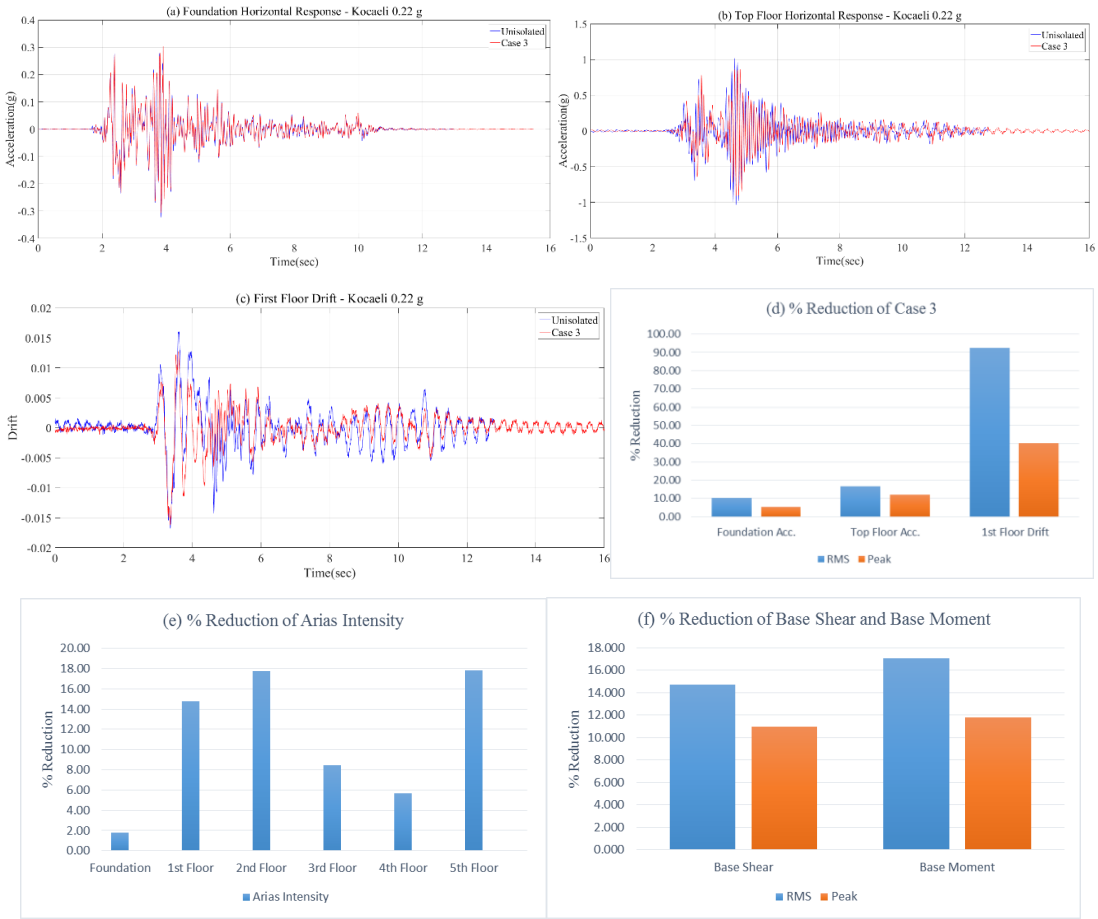

Figure 4.10. (a) Foundation Acceleration Response, (b) Top Floor Acceleration Response, (c) First Floor Drift Response, (d) % Reduction of Case 3, (e) % Reduction of Arias Intensity, (f) % Reduction of Base Shear and Base Moment under Kocaeli Earthquake.

Table 4.11. Horizontal Acceleration, Story Drift, Arias Intensity, Peak Spectral Acceleration, Period Lengthening Ratio, and Base Shear and Base Moment under Kocaeli Earthquake.

Case 3 under Kocaeli (PGA = 0.22 g) Earthquake (1999)												
	Foundation		1st Floor		2nd Floor		3rd Floor		4th Floor		5th Floor	
	RMS	Peak	RMS	Peak	RMS	Peak	RMS	Peak	RMS	Peak	RMS	Peak
Horizontal Acceleration (g)												
Unisolated	0.052	0.323	0.130	0.879	0.152	0.971	0.089	0.534	0.096	0.550	0.172	1.033
Case 3	0.046	0.306	0.108	0.766	0.124	0.859	0.077	0.497	0.084	0.469	0.143	0.909
% Reduction (%)	10.25	5.30	16.77	12.83	18.26	11.53	13.50	6.86	12.47	14.72	16.48	11.97
Horizontal Story Drift												
Unisolated	-	-	0.0020	0.0114	0.0010	0.0104	0.0015	0.0145	0.0015	0.0041	0.0024	0.0012
Case 3	-	-	0.0002	0.0068	0.0015	0.0075	0.0016	0.0137	0.0008	0.0095	0.0025	0.0010
% Reduction (%)	-	-	92.50	40.35	-50.00	27.88	-6.67	5.52	45.00	-131.71	-4.17	15.00
Arias Intensity (g-sec)												
Unisolated	0.0056		0.0352		0.0479		0.0165		0.0193		0.0641	
Case 3	0.0055		0.0300		0.0394		0.0151		0.0182		0.0527	
% Reduction (%)	1.79		14.77		17.75		8.48		5.70		17.78	
Peak Spectral Acceleration (g)												
Unisolated	1.60		3.98		4.68		2.26		2.47		4.94	
Case 3	1.61		3.78		4.05		1.97		2.32		4.35	
% Reduction (%)	-0.63		5.03		13.46		12.83		6.07		11.94	
Period Lengthening Ratio												
	Fundamental Period (sec)											
Unisolated	0.100		0.100		0.080		0.080		0.100		0.080	
Case 3	0.100		0.100		0.080		0.100		0.100		0.080	
Ratio	1.00		1.00		1.00		1.25		1.00		1.00	
	Base Shear (kN)						Base Moment (kN-m)					
	RMS			Peak			RMS			Peak		
Unisolated	0.59			3.65			0.41			2.46		
Case 3	0.50			3.25			0.34			2.17		
% Reduction (%)	14.72			10.96			17.07			11.79		

4.5.2. Seismic Response of Case 3 under Kobe Earthquake

Maximum reduction percentage in acceleration response was obtained at the fourth story as 18.92% in peak value while maximum RMS value was observed at foundation level with reduction value of 6.04%. Maximum reduction in story drift was observed as 22.92% in RMS value at top story. On the other hand, only the first floor of the building exhibited reduction in horizontal story drift which was 8.33% in peak value. Moreover, maximum reduction in Arias intensity appeared as 11.95% at foundation level. More promising result in reduction of peak spectral acceleration was revealed at fourth story as 15.12%. Tabulated results and graphical demonstration of results were shown in Table 4.12 and Figure 4.11. The factors of period shift were 2 and 1.5 at foundation and first story of the building. It

means period of foundation and first story of isolated building was shifted to 2 and 1.5 times greater than unisolated case. Similarity was observed between the reduction values of base shear and base moment in peak value.

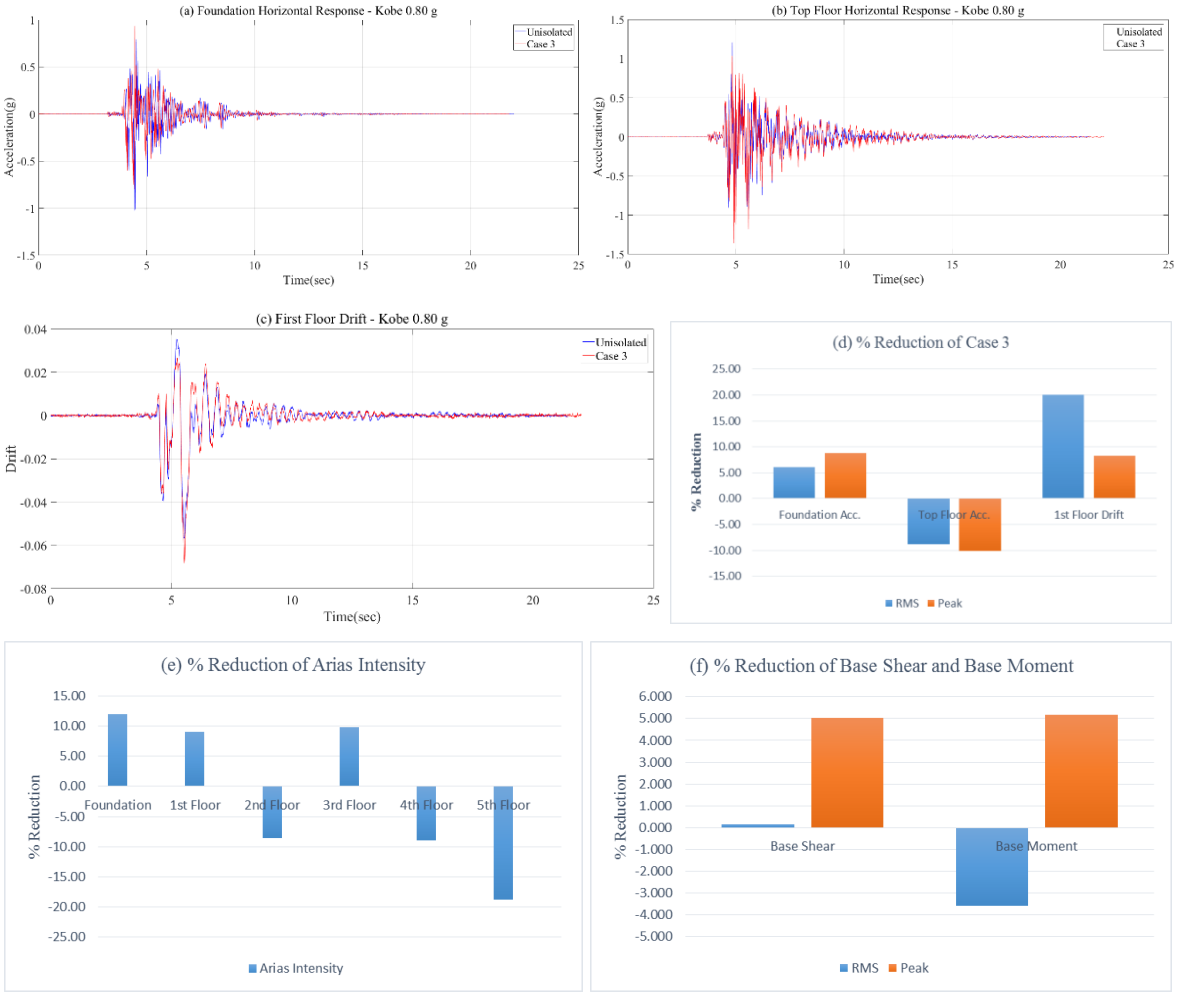

Figure 4.11. (a) Foundation Acceleration Response, (b) Top Floor Acceleration Response, (c) First Floor Drift Response, (d) % Reduction of Case 3, (e) % Reduction of Arias Intensity, (f) % Reduction of Base Shear and Base Moment under Kobe Earthquake.

Table 4.12. Horizontal Acceleration, Story Drift, Arias Intensity, Peak Spectral Acceleration, Period Lengthening Ratio, and Base Shear and Base Moment under Kobe Earthquake.

Case 3 under Kobe (PGA = 0.80 g) Earthquake (1995)												
	Foundation		1st Floor		2nd Floor		3rd Floor		4th Floor		5th Floor	
	RMS	Peak	RMS	Peak	RMS	Peak	RMS	Peak	RMS	Peak	RMS	Peak
Horizontal Acceleration (g)												
Unisolated	0.084	1.025	0.104	1.049	0.095	0.744	0.103	1.015	0.093	0.946	0.128	1.233
Case 3	0.079	0.935	0.099	1.141	0.099	0.716	0.098	0.859	0.097	0.767	0.139	1.359
% Reduction (%)	6.04	8.77	4.64	-8.80	-4.12	3.73	5.13	15.40	-4.42	18.92	-8.86	-10.15
Horizontal Story Drift												
Unisolated	-	-	0.0030	0.0120	0.0023	0.0109	0.0043	0.0261	0.0030	0.0306	0.0010	0.0190
Case 3	-	-	0.0024	0.0110	0.0039	0.0184	0.0047	0.0351	0.0040	0.0368	0.0008	0.0211
% Reduction (%)	-	-	20.00	8.33	-69.57	-68.81	-9.30	-34.48	-33.33	-20.26	22.92	-11.05
Arias Intensity (g-sec)												
Unisolated	0.0251		0.0377		0.0315		0.0376		0.0303		0.0572	
Case 3	0.0221		0.0343		0.0342		0.0339		0.033		0.0679	
% Reduction (%)	11.95		9.02		-8.57		9.84		-8.91		-18.71	
Peak Spectral Acceleration (g)												
Unisolated	1.99		2.70		3.80		3.21		2.91		3.71	
Case 3	2.32		2.51		3.86		2.79		2.47		4.04	
% Reduction (%)	-16.58		7.04		-1.58		13.08		15.12		-8.89	
Period Lengthening Ratio												
	Fundamental Period (sec)											
Unisolated	0.040		0.040		0.080		0.060		0.040		0.080	
Case 3	0.080		0.060		0.080		0.060		0.040		0.080	
Ratio	2.00		1.50		1.00		1.00		1.00		1.00	
	Base Shear (kN)				**Base Moment (kN-m)**							
	RMS		**Peak**		**RMS**		**Peak**					
Unisolated	0.53		5.35		0.34		3.29					
Case 3	0.53		5.08		0.35		3.12					
% Reduction (%)	0.17		5.05		-3.59		5.17					

4.5.3. Seismic Response of Case 3 under El Centro Earthquake

Horizontal acceleration response of the system was reduced mostly at the third floor with a reduction percentage of 33.90% as a peak value. On the other hand, reduction in the RMS value was the highest at the first story with a reduction of 9.16%. Additionally, the maximum reduction in story drift was observed at the fourth story as 59.13% in peak value while 57.64% reduction value was measured at the first story in RMS value. Reduction in Arias intensity at the first story appeared as maximum with a reduction of 21.87%. Moreover, a value of 24.17% reduction in peak spectral acceleration was measured at the second floor. Figure 4.12 and Table 4.13 showed the summarized results. Foundation, first story and fourth story revealed period shifts. However, maximum period shift was observed

at the fourth story as 4.49 times increase in period. Similar reduction percentages were observed in base shear and base moment in peak value as 21.73% and 21.56%, respectively.

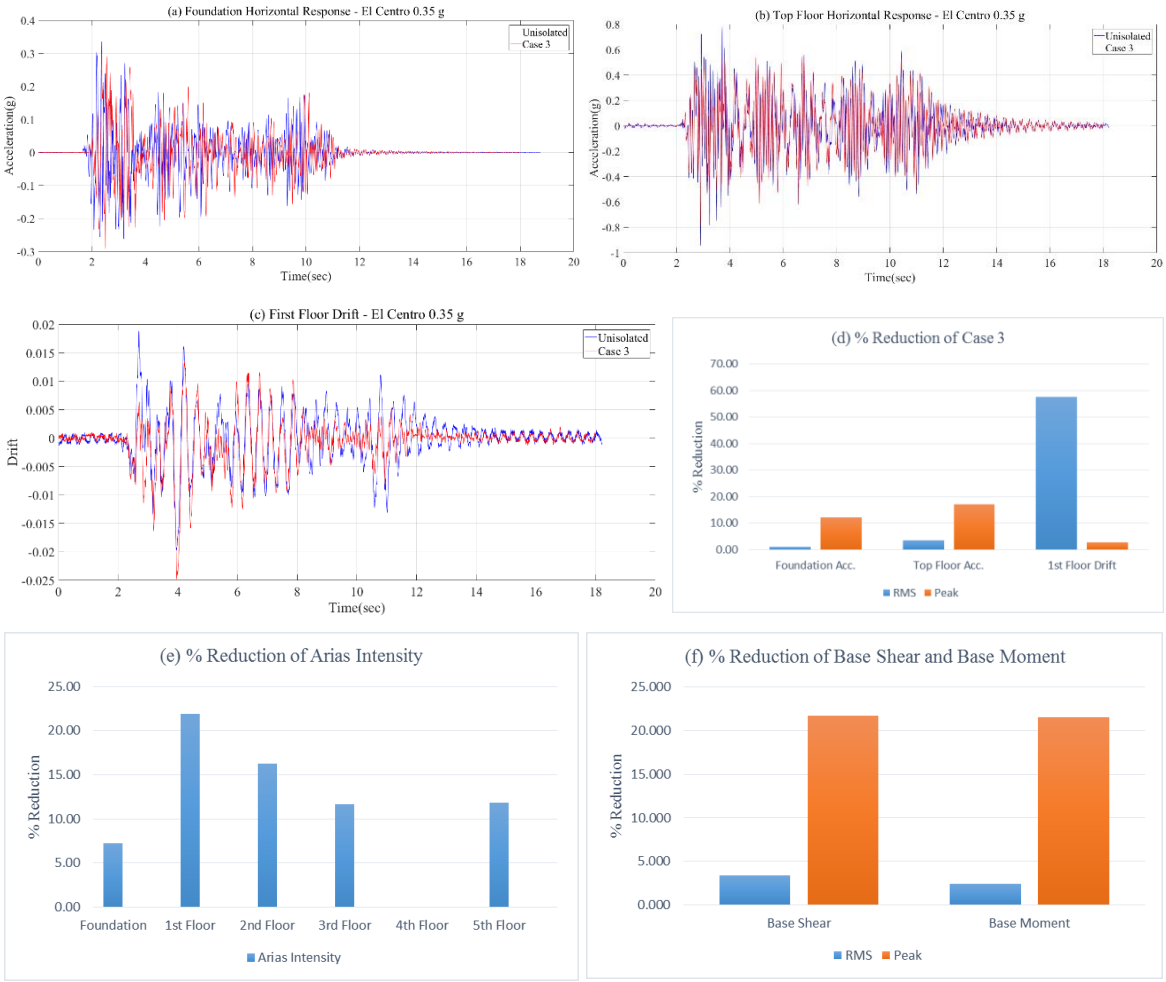

Figure 4.12. (a) Foundation Acceleration Response, (b) Top Floor Acceleration Response, (c) First Floor Drift Response, (d) % Reduction of Case 3, (e) % Reduction of Arias Intensity, (f) % Reduction of Base Shear and Base Moment under El Centro Earthquake.

Table 4.13. Horizontal Acceleration, Story Drift, Arias Intensity, Peak Spectral Acceleration, Period Lengthening Ratio, and Base Shear and Base Moment under El Centro Earthquake.

Case 3 under El Centro (PGA = 0.35 g) Earthquake (1940)												
	Foundation		1st Floor		2nd Floor		3rd Floor		4th Floor		5th Floor	
	RMS	Peak	RMS	Peak	RMS	Peak	RMS	Peak	RMS	Peak	RMS	Peak
Horizontal Acceleration (g)												
Unisolated	0.057	0.336	0.116	0.651	0.140	0.603	0.106	0.633	0.108	0.501	0.172	0.946
Case 3	0.056	0.295	0.105	0.455	0.132	0.520	0.103	0.418	0.111	0.403	0.166	0.784
% Reduction (%)	1.06	12.31	9.16	30.05	5.93	13.82	3.48	33.90	-2.68	19.71	3.50	17.18
Horizontal Story Drift												
Unisolated	-	-	0.0009	0.0036	0.0024	0.0059	0.0032	0.0183	0.0010	0.0023	0.0018	0.0006
Case 3	-	-	0.0004	0.0035	0.0019	0.0053	0.0024	0.0125	0.0017	0.0009	0.0026	0.0003
% Reduction (%)	-	-	57.64	2.78	20.83	10.17	25.00	31.69	-70.00	59.13	-44.44	43.64
Arias Intensity (g-sec)												
Unisolated	0.0097		0.0407		0.0596		0.0344		0.0356		0.0895	
Case 3	0.0090		0.0318		0.0499		0.0304		0.0356		0.0789	
% Reduction (%)	7.22		21.87		16.28		11.63		0.00		11.84	
Peak Spectral Acceleration (g)												
Unisolated	1.15		2.28		3.31		2.27		1.53		3.34	
Case 3	1.12		1.78		2.51		1.96		1.74		2.54	
% Reduction (%)	2.61		21.93		24.17		13.66		-13.73		23.95	
Period Lengthening Ratio												
	Fundamental Period (sec)											
Unisolated	0.159		0.080		0.080		0.060		0.080		0.080	
Case 3	0.179		0.100		0.080		0.060		0.358		0.080	
Ratio	1.12		1.25		1.00		1.00		4.49		1.00	
	Base Shear (kN)						**Base Moment (kN-m)**					
	RMS		**Peak**				**RMS**		**Peak**			
Unisolated	0.59		3.13				0.42		2.18			
Case 3	0.57		2.45				0.41		1.71			
% Reduction (%)	3.39		21.73				2.38		21.56			

4.6. Case 4 - GSI 2 Placed underneath the 5-Story Building Model

Polytetrafluoroethylene (PTFE) 1 mm geomembrane with Typar DuPont SF44 nonwoven geotextile was used as GSI 2 couple under Kocaeli, Kobe and El Centro earthquakes. Curve shaped liner was used as GG couple with the configuration type of CL1. Results were illustrated in order of Kocaeli, Kobe and El Centro earthquakes.

4.6.1. Seismic Response of Case 4 under Kocaeli Earthquake

Third floor revealed maximum reduction in acceleration response as 21.15% in peak value while maximum reduction in RMS value was measured as 26.30% at the second floor. First floor of the building exhibited the best results in horizontal story drift with reduction of 92.50% in RMS value and 63.16% in peak value. Maximum reduction in Arias intensity was observed as 16.28% at the second story. Peak spectral acceleration was reduced mostly at the top floor with a reduction of 13.16%. Results were shown in Figure 4.13 and Table 4.14. Furthermore, no period shifting was observed in the building. Similarly, close values were obtained in base shear and base moment results in either RMS or peak values.

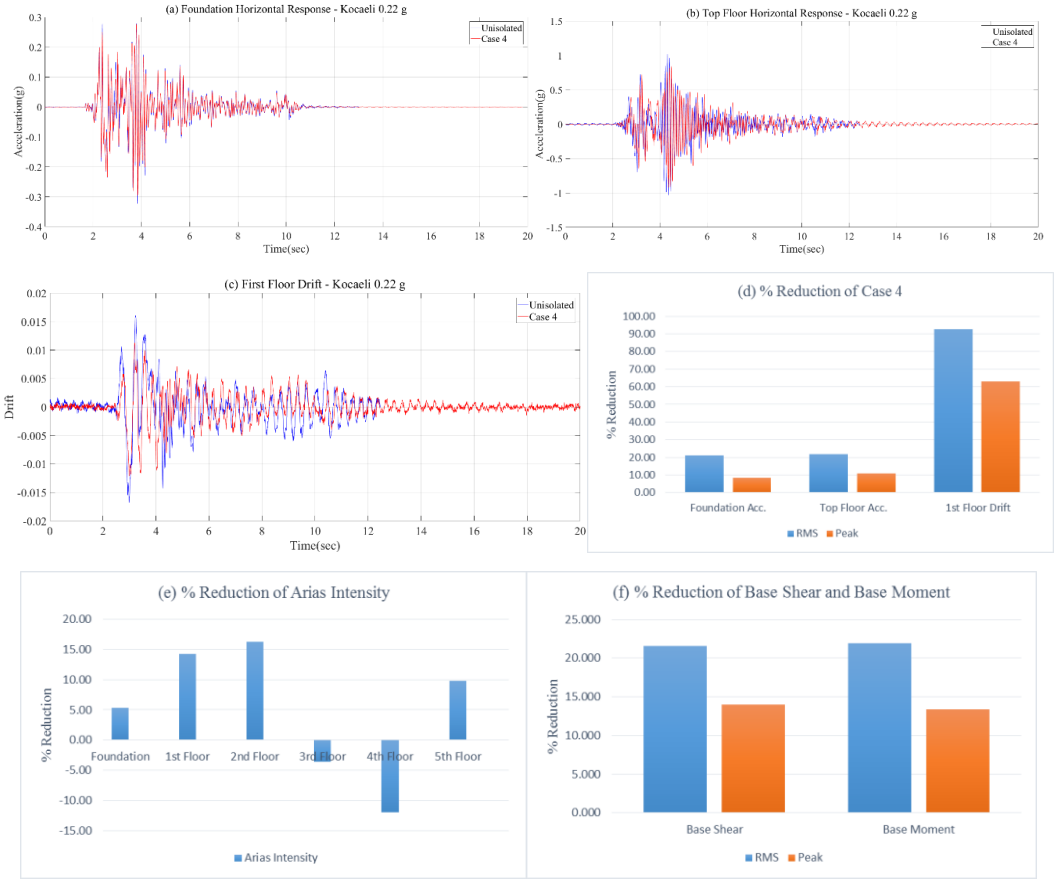

Figure 4.13. (a) Foundation Acceleration Response, (b) Top Floor Acceleration Response, (c) First Floor Drift Response, (d) % Reduction of Case 4, (e) % Reduction of Arias Intensity, (f) % Reduction of Base Shear and Base Moment under Kocaeli Earthquake.

Table 4.14. Horizontal Acceleration, Story Drift, Arias Intensity, Peak Spectral Acceleration, Period Lengthening Ratio, and Base Shear and Base Moment under Kocaeli Earthquake.

Case 4 under Kocaeli (PGA = 0.22 g) Earthquake (1999)												
	Foundation		1st Floor		2nd Floor		3rd Floor		4th Floor		5th Floor	
	RMS	Peak	RMS	Peak	RMS	Peak	RMS	Peak	RMS	Peak	RMS	Peak
Horizontal Acceleration (g)												
Unisolated	0.052	0.323	0.130	0.879	0.152	0.971	0.089	0.534	0.096	0.550	0.172	1.033
Case 4	0.041	0.296	0.097	0.720	0.112	0.839	0.073	0.421	0.082	0.491	0.134	0.921
% Reduction (%)	21.08	8.30	25.31	18.11	26.30	13.65	17.89	21.15	14.76	10.69	21.78	10.85
Horizontal Story Drift												
Unisolated	-	-	0.0020	0.0114	0.0010	0.0104	0.0015	0.0145	0.0015	0.0041	0.0024	0.0012
Case 4	-	-	0.0002	0.0042	0.0010	0.0097	0.0013	0.0075	0.0011	0.0074	0.0021	0.0008
% Reduction (%)	-	-	92.50	63.16	4.00	6.73	13.33	48.28	26.67	-80.49	12.50	33.33
Arias Intensity (g-sec)												
Unisolated	0.0056		0.0352		0.0479		0.0165		0.0193		0.0641	
Case 4	0.0053		0.0302		0.0401		0.0171		0.0216		0.0578	
% Reduction (%)	5.36		14.20		16.28		-3.64		-11.92		9.83	
Peak Spectral Acceleration (g)												
Unisolated	1.60		3.98		4.68		2.26		2.47		4.94	
Case 4	1.53		3.61		4.07		2.02		2.22		4.29	
% Reduction (%)	4.38		9.30		13.03		10.62		10.12		13.16	
Period Lengthening Ratio												
	Fundamental Period (sec)											
Unisolated	0.100		0.100		0.080		0.080		0.100		0.080	
Case 4	0.100		0.100		0.080		0.080		0.100		0.080	
Ratio	1.00		1.00		1.00		1.00		1.00		1.00	
	Base Shear (kN)						**Base Moment (kN-m)**					
	RMS			**Peak**			**RMS**			**Peak**		
Unisolated	0.59			3.65			0.41			2.46		
Case 4	0.46			3.14			0.32			2.13		
% Reduction (%)	21.54			13.97			21.95			13.41		

4.6.2. Seismic Response of Case 4 under Kobe Earthquake

Maximum reduction values of horizontal acceleration response in either RMS or peak value were observed at foundation level of the building. A 10.07% reduction value was measured in RMS value while a 14.68% reduction was observed in peak value. Moreover, maximum reduction in horizontal story drift was obtained from top story of the building as 80.12% in RMS value and 25.79% in peak value. Foundation of the building revealed maximum reduction value in Arias intensity as 11.55%. Additionally, maximum reduction in peak spectral acceleration was observed as 14.33% at the third floor. Table 4.15 and Figure 4.14 illustrated the detailed overview of the results. Period shift occured only at foundation level as a factor of 2. Similarity was observed between RMS and peak values of the reduction

values in base shear. Also, maximum reduction in base moment was observed as 1.52% in peak value.

Figure 4.14. (a) Foundation Acceleration Response, (b) Top Floor Acceleration Response, (c) First Floor Drift Response, (d) % Reduction of Case 4, (e) % Reduction of Arias Intensity, (f) % Reduction of Base Shear and Base Moment under Kobe Earthquake.

Table 4.15. Horizontal Acceleration, Story Drift, Arias Intensity, Peak Spectral Acceleration, Period Lengthening Ratio, and Base Shear and Base Moment under Kobe Earthquake.

Case 4 under Kobe (PGA = 0.80 g) Earthquake (1995)												
	Foundation		1st Floor		2nd Floor		3rd Floor		4th Floor		5th Floor	
	RMS	Peak	RMS	Peak	RMS	Peak	RMS	Peak	RMS	Peak	RMS	Peak
Horizontal Acceleration (g)												
Unisolated	0.084	1.025	0.104	1.049	0.095	0.744	0.103	1.015	0.093	0.946	0.128	1.233
Case 4	0.076	0.875	0.094	1.154	0.095	0.719	0.095	0.884	0.094	0.849	0.133	1.375
% Reduction (%)	10.07	14.68	9.28	-9.96	0.11	3.29	8.42	12.92	-1.51	10.29	-4.00	-11.51
Horizontal Story Drift												
Unisolated	-	-	0.0030	0.0120	0.0023	0.0109	0.0043	0.0261	0.0030	0.0306	0.0010	0.0190
Case 4	-	-	0.0021	0.0117	0.0038	0.0189	0.0040	0.0239	0.0044	0.0435	0.0002	0.0141
% Reduction (%)	-	-	30.00	2.50	-65.22	-73.39	6.98	8.43	-46.67	-42.16	80.12	25.79
Arias Intensity (g-sec)												
Unisolated	0.0251		0.0377		0.0315		0.0376		0.0303		0.0572	
Case 4	0.0222		0.0339		0.0343		0.0344		0.0341		0.0676	
% Reduction (%)	11.55		10.08		-8.89		8.51		-12.54		-18.18	
Peak Spectral Acceleration (g)												
Unisolated	1.99		2.70		3.80		3.21		2.91		3.71	
Case 4	2.11		2.38		3.86		2.75		2.55		3.95	
% Reduction (%)	-6.03		11.85		-1.58		14.33		12.37		-6.47	
Period Lengthening Ratio												
	Fundamental Period (sec)											
Unisolated	0.040		0.040		0.080		0.060		0.040		0.080	
Case 4	0.080		0.040		0.080		0.060		0.040		0.080	
Ratio	2.00		1.00		1.00		1.00		1.00		1.00	
	Base Shear (kN)						**Base Moment (kN-m)**					
	RMS			**Peak**			**RMS**			**Peak**		
Unisolated	0.53			5.35			0.34			3.29		
Case 4	0.51			5.13			0.34			3.24		
% Reduction (%)	4.13			4.11			0.32			1.52		

4.6.3. Seismic Response of Case 4 under El Centro Earthquake

Maximum reduction in horizontal acceleration response was observed as 19.85% in peak value. However, no reduction was measured in RMS value. Fourth story of the building exhibited maximum reduction in story drift as 63.04% in peak value. On the other hand, RMS value demonstrated maximum reduction as 29.77 at the first story. Moreover, maximum reduction in Arias intensity was observed at the first story as 12.53%. Maximum reduction in peak spectral acceleration was found at top floor as 19.46%. Results were tabulated and graphed in Table 4.16 and Figure 4.15, respectively. Period shift of the building was determined at foundation and fourth floor of the building. Maximum period

shift was observed at the fourth story as a factor of 4.74. Again, similar values were obtained in the reduction percentages of base shear and base moment in peak values.

Figure 4.15. (a) Foundation Acceleration Response, (b) Top Floor Acceleration Response, (c) First Floor Drift Response, (d) % Reduction of Case 4, (e) % Reduction of Arias Intensity, (f) % Reduction of Base Shear and Base Moment under El Centro Earthquake.

Table 4.16. Horizontal Acceleration, Story Drift, Arias Intensity, Peak Spectral Acceleration, Period Lengthening Ratio, and Base Shear and Base Moment under El Centro Earthquake.

Case 4 under El Centro (PGA = 0.35 g) Earthquake (1940)												
	Foundation		1st Floor		2nd Floor		3rd Floor		4th Floor		5th Floor	
	RMS	Peak	RMS	Peak	RMS	Peak	RMS	Peak	RMS	Peak	RMS	Peak
Horizontal Acceleration (g)												
Unisolated	0.057	0.336	0.116	0.651	0.140	0.603	0.106	0.633	0.108	0.501	0.172	0.946
Case 4	0.064	0.344	0.126	0.579	0.159	0.560	0.127	0.507	0.137	0.468	0.203	0.904
% Reduction (%)	-12.57	-2.20	-8.90	11.04	-13.58	7.18	-19.08	19.85	-26.16	6.74	-18.19	4.51
Horizontal Story Drift												
Unisolated	-	-	0.0009	0.0036	0.0024	0.0059	0.0032	0.0183	0.0010	0.0023	0.0018	0.0006
Case 4	-	-	0.0006	0.0056	0.0017	0.0050	0.0033	0.0121	0.0016	0.0009	0.0023	0.0003
% Reduction (%)	-	-	29.77	-55.56	29.17	15.25	-3.13	33.88	-60.00	63.04	-27.78	41.82
Arias Intensity (g-sec)												
Unisolated	0.0097		0.0407		0.0596		0.0344		0.0356		0.0895	
Case 4	0.0091		0.0356		0.0566		0.0360		0.0480		0.0903	
% Reduction (%)	6.19		12.53		5.03		-4.65		-34.83		-0.89	
Peak Spectral Acceleration (g)												
Unisolated	1.15		2.28		3.31		2.27		1.53		3.34	
Case 4	1.12		1.89		2.77		2.05		1.99		2.69	
% Reduction (%)	2.61		17.11		16.31		9.69		-30.07		19.46	
Period Lengthening Ratio												
	Fundamental Period (sec)											
Unisolated	0.159		0.080		0.080		0.060		0.080		0.080	
Case 4	0.179		0.080		0.080		0.060		0.378		0.080	
Ratio	1.12		1.00		1.00		1.00		4.74		1.00	
	Base Shear (kN)						**Base Moment (kN-m)**					
	RMS		**Peak**				**RMS**		**Peak**			
Unisolated	0.59		3.13				0.42		2.18			
Case 4	0.69		2.86				0.50		1.99			
% Reduction (%)	-16.95		8.63				-19.05		8.72			

4.7. Case 5 - GSI 3 Placed underneath the 5-Story Building Model

Polytetrafluoroethylene (PTFE) 1 mm geomembrane with Typar DuPont SF56 nonwoven geotextile was used as GSI 3 couple under Kocaeli, Kobe and El Centro earthquakes. Curve shaped liner was used as GG couple the configuration type of CL2. Results were illustrated in order of Kocaeli, Kobe and El Centro earthquakes.

4.7.1. Seismic Response of Case 5 under Kocaeli Earthquake

All the performance indicator parameters showed reduction trend in all stories. However, period shifting was not observed. In RMS values, maximum reductions in horizontal acceleration and story drift were measured as 18.72% at the second story and 85.05% at the first story, respectively. On the other hand, maximum reductions in acceleration response and story drift were observed as 10.89% at the third floor and 55% at top floor, respectively. Maximum reduction in Arias intensity appeared as 14.20% at top story. Moreover, a reduction of 10.53% in peak spectral acceleration was observed at the top story. Reduction values in base shear and base moment appeared as similar to each other. Results can be evaluated in Table 4.17 and Figure 4.16.

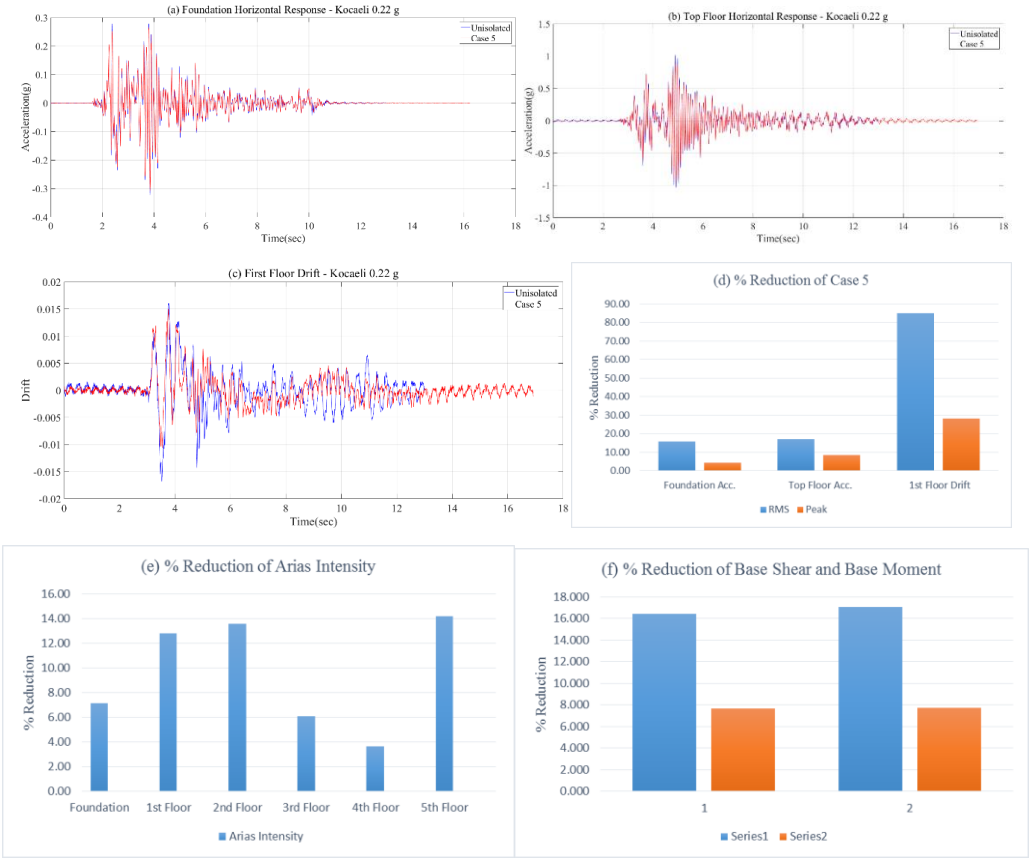

Figure 4.16. (a) Foundation Acceleration Response, (b) Top Floor Acceleration Response, (c) First Floor Drift Response, (d) % Reduction of Case 5, (e) % Reduction of Arias Intensity, (f) % Reduction of Base Shear and Base Moment under Kocaeli Earthquake.

Table 4.17. Horizontal Acceleration, Story Drift, Arias Intensity, Peak Spectral Acceleration, Period Lengthening Ratio, and Base Shear and Base Moment under Kocaeli Earthquake.

Case 5 under Kocaeli (PGA = 0.22 g) Earthquake (1999)												
	Foundation		1st Floor		2nd Floor		3rd Floor		4th Floor		5th Floor	
	RMS	Peak	RMS	Peak	RMS	Peak	RMS	Peak	RMS	Peak	RMS	Peak
Horizontal Acceleration (g)												
Unisolated	0.052	0.323	0.130	0.879	0.152	0.971	0.089	0.534	0.096	0.550	0.172	1.033
Case 5	0.044	0.308	0.106	0.788	0.123	0.901	0.075	0.476	0.083	0.528	0.142	0.946
% Reduction (%)	15.86	4.52	18.31	10.32	18.72	7.24	15.19	10.89	14.14	4.09	17.18	8.40
Horizontal Story Drift												
Unisolated	-	-	0.0020	0.0114	0.0010	0.0104	0.0015	0.0145	0.0015	0.0041	0.0024	0.0012
Case 5	-	-	0.0003	0.0082	0.0011	0.0120	0.0015	0.0092	0.0012	0.0067	0.0028	0.0005
% Reduction (%)	-	-	85.05	28.07	-10.00	-15.38	0.00	36.55	20.00	-63.41	-16.67	55.00
Arias Intensity (g-sec)												
Unisolated	0.0056		0.0352		0.0479		0.0165		0.0193		0.0641	
Case 5	0.0052		0.0307		0.0414		0.0155		0.0186		0.0550	
% Reduction (%)	7.14		12.78		13.57		6.06		3.63		14.20	
Peak Spectral Acceleration (g)												
Unisolated	1.60		3.98		4.68		2.26		2.47		4.94	
Case 5	1.53		3.71		4.19		2.05		2.27		4.42	
% Reduction (%)	4.38		6.78		10.47		9.29		8.10		10.53	
Period Lengthening Ratio												
	Fundamental Period (sec)											
Unisolated	0.100		0.100		0.080		0.080		0.100		0.080	
Case 5	0.100		0.100		0.080		0.080		0.100		0.080	
Ratio	1.00		1.00		1.00		1.00		1.00		1.00	
	Base Shear (kN)				Base Moment (kN-m)			
	RMS		Peak		RMS		Peak	
Unisolated	0.59		3.65		0.41		2.46	
Case 5	0.49		3.37		0.34		2.27	
% Reduction (%)	16.43		7.67		17.07		7.72	

4.7.2. Seismic Response of Case 5 under Kobe Earthquake

Maximum reduction in horizontal acceleration response was observed as 11.77% in peak value at the fourth story. In addition, horizontal story drift of second floor was reduced in isolated case with a reduction of 19.27% in peak value while this percentage was 10% in RMS at the first story. First floor experienced maximum reduction in Arias intensity as 16.71%. Moreover, maximum reduction in peak spectral acceleration was observed as 13.71% at fourth story. All mentioned results were tabulated and graphed in Table 4.18 and Figure 4.17. Only foundation of the proposed building underwent period shifting with a factor of 2. Reduction percentages in base shear and base moment were similar in peak values.

Figure 4.17. (a) Foundation Acceleration Response, (b) Top Floor Acceleration Response, (c) First Floor Drift Response, (d) % Reduction of Case 5, (e) % Reduction of Arias Intensity, (f) % Reduction of Base Shear and Base Moment under Kobe Earthquake.

Table 4.18. Horizontal Acceleration, Story Drift, Arias Intensity, Peak Spectral Acceleration, Period Lengthening Ratio, and Base Shear and Base Moment under Kobe Earthquake.

Case 5 under Kobe (PGA = 0.80 g) Earthquake (1995)												
	Foundation		1st Floor		2nd Floor		3rd Floor		4th Floor		5th Floor	
	RMS	Peak	RMS	Peak	RMS	Peak	RMS	Peak	RMS	Peak	RMS	Peak
Horizontal Acceleration (g)												
Unisolated	0.084	1.025	0.104	1.049	0.095	0.744	0.103	1.015	0.093	0.946	0.128	1.233
Case 5	0.086	0.921	0.102	1.092	0.101	0.682	0.103	0.903	0.098	0.835	0.138	1.199
% Reduction (%)	-1.90	10.17	1.84	-4.12	-6.24	8.32	0.10	11.04	-5.29	11.77	-7.84	2.75
Horizontal Story Drift												
Unisolated	-	-	0.0030	0.0120	0.0023	0.0109	0.0043	0.0261	0.0030	0.0306	0.0010	0.0190
Case 5	-	-	0.0027	0.0166	0.0027	0.0088	0.0049	0.0311	0.0039	0.0284	0.0012	0.0213
% Reduction (%)	-	-	10.00	-38.33	-17.39	19.27	-13.95	-19.16	-30.00	7.19	-21.70	-12.11
Arias Intensity (g-sec)												
Unisolated	0.0251		0.0377		0.0315		0.0376		0.0303		0.0572	
Case 5	0.0225		0.0314		0.0307		0.0324		0.0290		0.0576	
% Reduction (%)	10.36		16.71		2.54		13.83		4.29		-0.70	
Peak Spectral Acceleration (g)												
Unisolated	1.99		2.70		3.80		3.21		2.91		3.71	
Case 5	2.01		2.48		3.72		2.77		2.81		3.74	
% Reduction (%)	-1.01		8.15		2.11		13.71		3.44		-0.81	
Period Lengthening Ratio												
	Fundamental Period (sec)											
Unisolated	0.040		0.040		0.080		0.060		0.040		0.080	
Case 5	0.080		0.040		0.080		0.060		0.040		0.080	
Ratio	2.00		1.00		1.00		1.00		1.00		1.00	
	Base Shear (kN)						**Base Moment (kN-m)**					
	RMS		**Peak**				**RMS**		**Peak**			
Unisolated	0.53		5.35				0.34		3.29			
Case 5	0.55		4.99				0.36		3.06			
% Reduction (%)	-3.00		6.73				-5.09		6.99			

4.7.3. Seismic Response of Case 5 under El Centro Earthquake

Reduction percentages for horizontal acceleration were similar to each other among the stories. Maximum reduction was observed at the third story as 39.36% in peak value. On the other hand, RMS value showed maximum reduction as 33.28% at the first story. Moreover, maximum reduction in story drift was observed at the fourth floor as 35.65% in peak value while maximum reduction was measured as 67.22% at top floor in RMS value. Maximum reduction in Arias intensity was obtained as 29.48% at the first floor. Maximum alleviation in peak spectral acceleration appeared as 36.56% at the second floor. Illustration of the results can be seen in Figure 4.18 and Table 4.19. Period shift reached its maximum

value at the fourth floor with a reduction of 5.24%. Results of reduction in base shear and base moment values were very close to each other in either RMS or peak values.

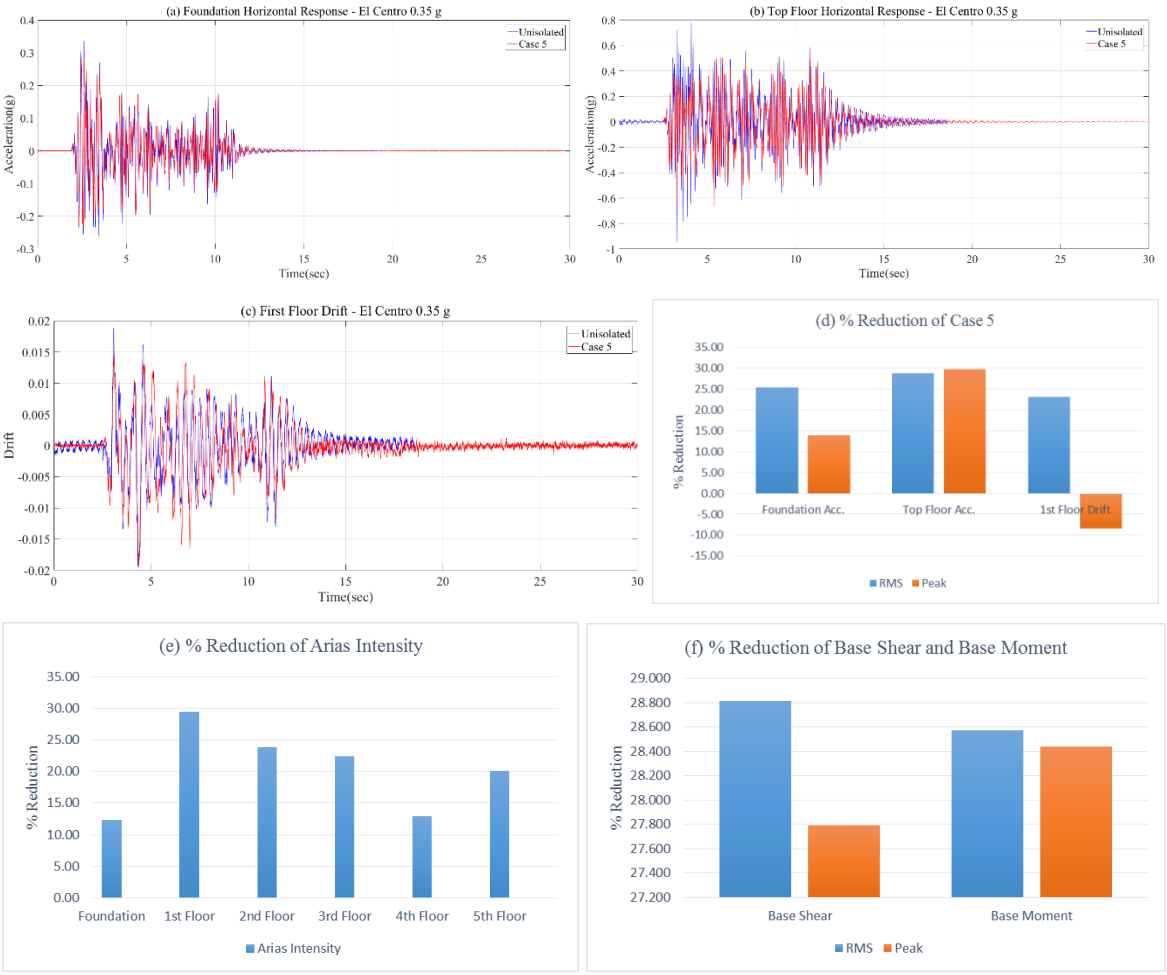

Figure 4.18. (a) Foundation Acceleration Response, (b) Top Floor Acceleration Response, (c) First Floor Drift Response, (d) % Reduction of Case 5, (e) % Reduction of Arias Intensity, (f) % Reduction of Base Shear and Base Moment under El Centro Earthquake.

Table 4.19. Horizontal Acceleration, Story Drift, Arias Intensity, Peak Spectral Acceleration, Period Lengthening Ratio, and Base Shear and Base Moment under El Centro Earthquake.

Case 5 under El Centro (PGA = 0.35 g) Earthquake (1940)												
	Foundation		1st Floor		2nd Floor		3rd Floor		4th Floor		5th Floor	
	RMS	Peak	RMS	Peak	RMS	Peak	RMS	Peak	RMS	Peak	RMS	Peak
Horizontal Acceleration (g)												
Unisolated	0.057	0.336	0.116	0.651	0.140	0.603	0.106	0.633	0.108	0.501	0.172	0.946
Case 5	0.042	0.289	0.077	0.401	0.097	0.499	0.075	0.384	0.080	0.396	0.122	0.664
% Reduction (%)	25.49	14.01	33.28	38.34	30.52	17.25	29.89	39.36	25.79	20.93	28.86	29.80
Horizontal Story Drift												
Unisolated	-	-	0.0009	0.0036	0.0024	0.0059	0.0032	0.0183	0.0010	0.0023	0.0018	0.0006
Case 5	-	-	0.0007	0.0039	0.0010	0.0057	0.0025	0.0105	0.0013	0.0015	0.0006	0.0005
% Reduction (%)	-	-	23.08	-8.33	58.75	3.39	21.88	42.62	-30.00	35.65	67.22	12.73
Arias Intensity (g-sec)												
Unisolated	0.0097		0.0407		0.0596		0.0344		0.0356		0.0895	
Case 5	0.0085		0.0287		0.0454		0.0267		0.0310		0.0715	
% Reduction (%)	12.37		29.48		23.83		22.38		12.92		20.11	
Peak Spectral Acceleration (g)												
Unisolated	1.15		2.28		3.31		2.27		1.53		3.34	
Case 5	1.11		1.77		2.45		1.44		1.62		2.60	
% Reduction (%)	3.48		22.37		25.98		36.56		-5.88		22.16	
Period Lengthening Ratio												
	Fundamental Period (sec)											
Unisolated	0.159		0.080		0.080		0.060		0.080		0.080	
Case 5	0.179		0.080		0.080		0.060		0.418		0.080	
Ratio	1.12		1.00		1.00		1.00		5.24		1.00	
	Base Shear (kN)				**Base Moment (kN-m)**			
	RMS		**Peak**		**RMS**		**Peak**	
Unisolated	0.59		3.13		0.42		2.18	
Case 5	0.42		2.26		0.30		1.56	
% Reduction (%)	28.81		27.80		28.57		28.44	

4.8. Case 6 - GSI 3 Placed underneath the 5-Story Building Model

Polytetrafluoroethylene (PTFE) 1 mm geomembrane with Typar DuPont SF56 nonwoven geotextile was used as GSI 3 couple under Kocaeli, Kobe and El Centro earthquakes. Curve shaped liner was used as GG liner with CL1. Results were illustrated in order of Kocaeli, Kobe and El Centro earthquakes.

4.8.1. Seismic Response of Case 6 under Kocaeli Earthquake

Reduction percentages as RMS values were very close to each other in horizontal acceleration responses as seen in Table 4.20. However, maximum reduction in acceleration response was observed as 30.62% at the first floor in RMS value. On the other hand,

maximum reduction value was observed as 11.39% at the third floor in peak value. First floor showed maximum story drift reduction in peak value as 63.16% while first story exhibited a reduction in RMS value as 92.05%. Arias intensity showed its maximum reduction at top floor as 16.22% as seen in Figure 4.19. Reductions in base shear and base moment values were similar to each other in RMS and peak values. About 30% reduction and 10% reduction were observed in RMS and peak values, respectively. Moreover, peak spectral acceleration revealed maximum reduction as 12.55% at the fourth floor. Finally, no period shift was observed.

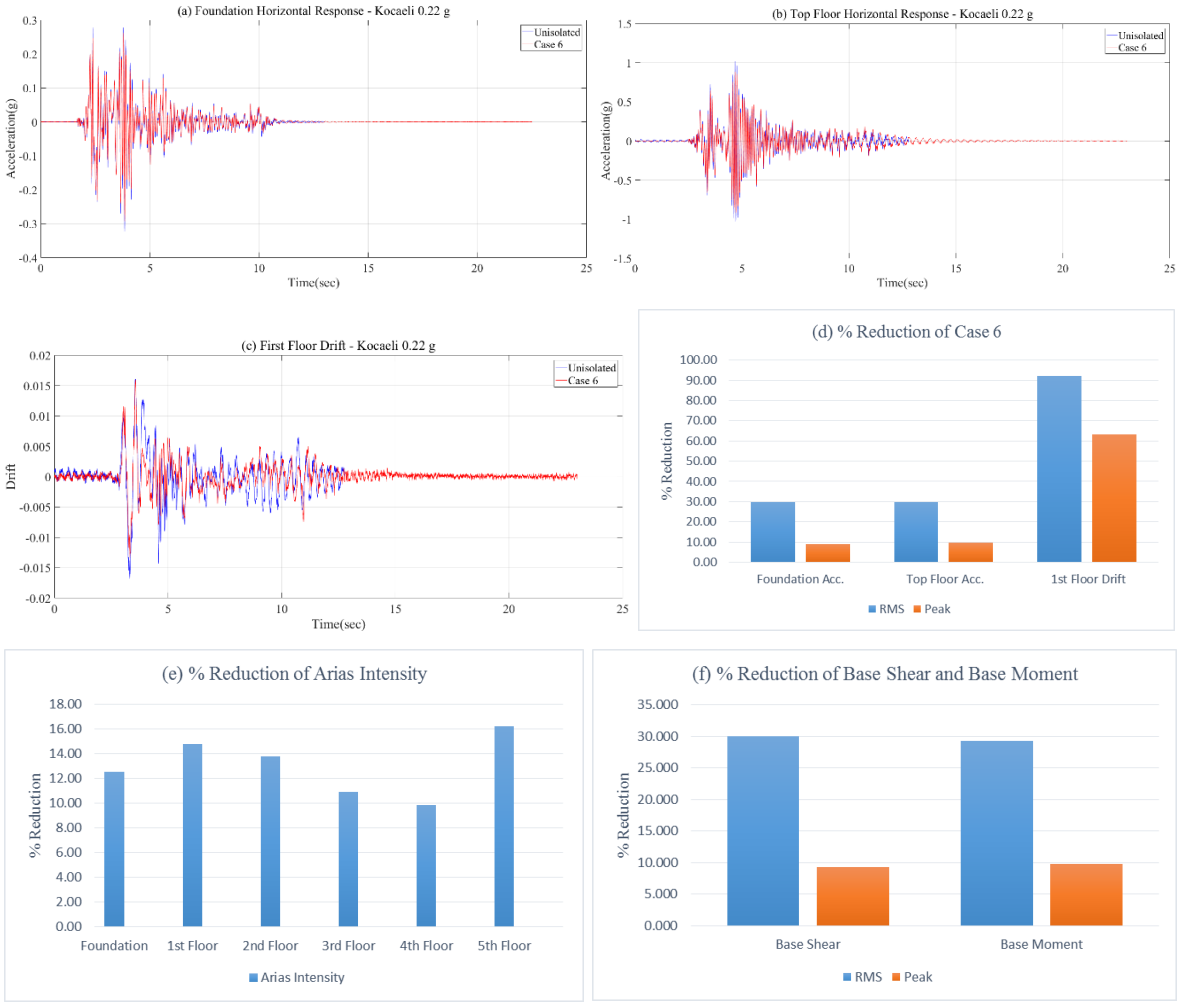

Figure 4.19. (a) Foundation Acceleration Response, (b) Top Floor Acceleration Response, (c) First Floor Drift Response, (d) % Reduction of Case 6, (e) % Reduction of Arias Intensity, (f) % Reduction of Base Shear and Base Moment under Kocaeli Earthquake.

Table 4.20. Horizontal Acceleration, Story Drift, Arias Intensity, Peak Spectral Acceleration, Period Lengthening Ratio, and Base Shear and Base Moment under Kocaeli Earthquake.

Case 6 under Kocaeli (PGA = 0.22 g) Earthquake (1999)												
	Foundation		1st Floor		2nd Floor		3rd Floor		4th Floor		5th Floor	
	RMS	Peak	RMS	Peak	RMS	Peak	RMS	Peak	RMS	Peak	RMS	Peak
Horizontal Acceleration (g)												
Unisolated	0.052	0.323	0.130	0.879	0.152	0.971	0.089	0.534	0.096	0.550	0.172	1.033
Case 6	0.036	0.294	0.090	0.813	0.106	0.879	0.063	0.473	0.069	0.491	0.121	0.935
% Reduction (%)	29.59	8.96	30.62	7.53	30.19	9.54	28.91	11.39	28.59	10.82	29.70	9.53
Horizontal Story Drift												
Unisolated	-	-	0.0020	0.0114	0.0010	0.0104	0.0015	0.0145	0.0015	0.0041	0.0024	0.0012
Case 6	-	-	0.0002	0.0042	0.0012	0.0138	0.0016	0.0167	0.0007	0.0068	0.0015	0.0006
% Reduction (%)	-	-	92.05	63.16	-20.00	-32.69	-6.67	-15.17	54.20	-65.85	37.50	54.17
Arias Intensity (g-sec)												
Unisolated	0.0056		0.0352		0.0479		0.0165		0.0193		0.0641	
Case 6	0.0049		0.0300		0.0413		0.0147		0.0174		0.0537	
% Reduction (%)	12.50		14.77		13.78		10.91		9.84		16.22	
Peak Spectral Acceleration (g)												
Unisolated	1.60		3.98		4.68		2.26		2.47		4.94	
Case 6	1.44		3.59		4.23		2.08		2.16		4.43	
% Reduction (%)	10.00		9.80		9.62		7.96		12.55		10.32	
Period Lengthening Ratio												
	Fundamental Period (sec)											
Unisolated	0.100		0.100		0.080		0.080		0.100		0.080	
Case 6	0.100		0.100		0.080		0.080		0.100		0.080	
Ratio	1.00		1.00		1.00		1.00		1.00		1.00	
	Base Shear (kN)				Base Moment (kN-m)			
	RMS		Peak		RMS		Peak	
Unisolated	0.59		3.65		0.41		2.46	
Case 6	0.41		3.31		0.29		2.22	
% Reduction (%)	30.07		9.32		29.27		9.76	

4.8.2. Seismic Response of Case 6 under Kobe Earthquake

Maximum reduction in acceleration response of the system was measured as 12.96% at the fourth story in peak, and 14.49% at the first story in RMS value. First story was exposed to maximum reduction in story drift in both RMS and peak values as 30% and 12.50%, respectively. Maximum reduction in Arias intensity was observed as 16.98% at the first floor. Moreover, peak spectral acceleration underwent 8.41% reduction at the third story. Results can be examined in Figure 4.20 and Table 4.21. No period shifting was observed on the structure. Additionally, maximum reduction in base shear and base moment was observed as 11% and 9.76% in peak values, respectively.

Figure 4.20. (a) Foundation Acceleration Response, (b) Top Floor Acceleration Response, (c) First Floor Drift Response, (d) % Reduction of Case 6, (e) % Reduction of Arias Intensity, (f) % Reduction of Base Shear and Base Moment under Kobe Earthquake.

Table 4.21. Horizontal Acceleration, Story Drift, Arias Intensity, Peak Spectral Acceleration, Period Lengthening Ratio, and Base Shear and Base Moment under Kobe Earthquake.

Case 6 under Kobe (PGA = 0.80 g) Earthquake (1995)												
	Foundation		1st Floor		2nd Floor		3rd Floor		4th Floor		5th Floor	
	RMS	Peak	RMS	Peak	RMS	Peak	RMS	Peak	RMS	Peak	RMS	Peak
Horizontal Acceleration (g)												
Unisolated	0.084	1.025	0.104	1.049	0.095	0.744	0.103	1.015	0.093	0.946	0.128	1.233
Case 6	0.076	1.040	0.089	1.089	0.085	0.669	0.090	0.909	0.084	0.823	0.117	1.280
% Reduction (%)	10.31	-1.41	14.49	-3.84	9.83	9.98	13.26	10.43	9.60	12.96	8.00	-3.79
Horizontal Story Drift												
Unisolated	-	-	0.0030	0.0120	0.0023	0.0109	0.0043	0.0261	0.0030	0.0306	0.0010	0.0190
Case 6	-	-	0.0021	0.0105	0.0025	0.0136	0.0038	0.0274	0.0037	0.0321	0.0009	0.0199
% Reduction (%)	-	-	30.00	12.50	-8.70	-24.77	11.63	-4.98	-23.33	-4.90	6.69	-4.74
Arias Intensity (g-sec)												
Unisolated	0.0251		0.0377		0.0315		0.0376		0.0303		0.0572	
Case 6	0.0229		0.0313		0.0291		0.0322		0.0281		0.0551	
% Reduction (%)	8.76		16.98		7.62		14.36		7.26		3.67	
Peak Spectral Acceleration (g)												
Unisolated	1.99		2.70		3.80		3.21		2.91		3.71	
Case 6	2.19		2.60		3.67		2.94		2.78		3.66	
% Reduction (%)	-10.05		3.70		3.42		8.41		4.47		1.35	
Period Lengthening Ratio												
	Fundamental Period (sec)											
Unisolated	0.040		0.040		0.080		0.060		0.040		0.080	
Case 6	0.040		0.040		0.080		0.060		0.040		0.080	
Ratio	1.00		1.00		1.00		1.00		1.00		1.00	
	Base Shear (kN)				**Base Moment (kN-m)**							
	RMS		**Peak**		**RMS**		**Peak**					
Unisolated	0.53		5.35		0.34		3.29					
Case 6	0.47		5.16		0.31		3.11					
% Reduction (%)	11.00		3.55		9.76		5.47					

4.8.3. Seismic Response of Case 6 under El Centro Earthquake

As seen in Figure 4.21 and Table 4.22, horizontal acceleration response underwent 31.91% in peak value at the third floor. However, no reduction was found in RMS value. Moreover, maximum reduction in story drift was observed at the second floor as 70% in RMS and 44.44% at the first story in peak value. Maximum reductions in Arias intensity and peak spectral acceleration appeared as 29.73% at the first floor, and 36.56% at the fourth floor, respectively. In addition, similar reduction values between base shear and base moment were observed in peak values as about 27%. Period shift demonstrated maximum reduction at the fourth story with a factor of 5.24.

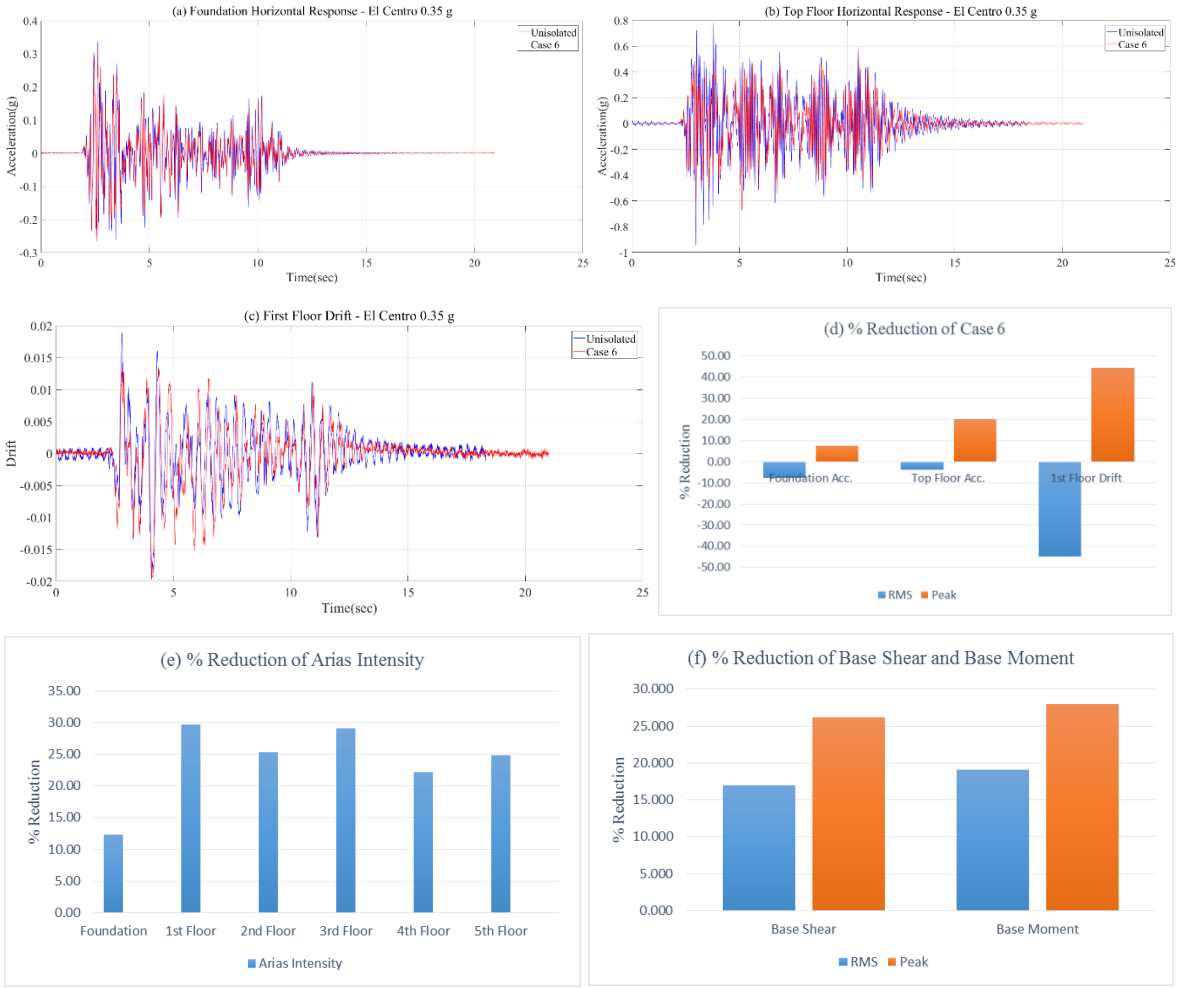

Figure 4.21. (a) Foundation Acceleration Response, (b) Top Floor Acceleration Response, (c) First Floor Drift Response, (d) % Reduction of Case 6, (e) % Reduction of Arias Intensity, (f) % Reduction of Base Shear and Base Moment under El Centro Earthquake.

Table 4.22. Horizontal Acceleration, Story Drift, Arias Intensity, Peak Spectral Acceleration, Period Lengthening Ratio, and Base Shear and Base Moment under El Centro Earthquake.

Case 6 under El Centro (PGA = 0.35 g) Earthquake (1940)												
	Foundation		1st Floor		2nd Floor		3rd Floor		4th Floor		5th Floor	
	RMS	Peak	RMS	Peak	RMS	Peak	RMS	Peak	RMS	Peak	RMS	Peak
Horizontal Acceleration (g)												
Unisolated	0.057	0.336	0.116	0.651	0.140	0.603	0.106	0.633	0.108	0.501	0.172	0.946
Case 6	0.061	0.311	0.116	0.472	0.145	0.538	0.106	0.431	0.114	0.483	0.178	0.755
% Reduction (%)	-7.79	7.52	-0.17	27.43	-3.86	10.68	0.09	31.91	-4.99	3.63	-3.79	20.25
Horizontal Story Drift												
Unisolated	-	-	0.0009	0.0036	0.0024	0.0059	0.0032	0.0183	0.0010	0.0023	0.0018	0.0006
Case 6	-	-	0.0005	0.0048	0.0018	0.0058	0.0031	0.0188	0.0010	0.0006	0.0011	0.0002
% Reduction (%)	-	-	49.83	-33.33	25.00	1.69	3.13	-2.73	1.00	73.48	38.89	67.27
Arias Intensity (g-sec)												
Unisolated	0.0097		0.0407		0.0596		0.0344		0.0356		0.0895	
Case 6	0.0085		0.0286		0.0445		0.0244		0.0277		0.0673	
% Reduction (%)	12.37		29.73		25.34		29.07		22.19		24.80	
Peak Spectral Acceleration (g)												
Unisolated	1.15		2.28		3.31		2.27		1.53		3.34	
Case 6	1.11		1.72		2.39		1.44		1.49		2.50	
% Reduction (%)	3.48		24.56		27.79		36.56		2.61		25.15	
Period Lengthening Ratio												
	Fundamental Period (sec)											
Unisolated	0.159		0.080		0.080		0.060		0.080		0.080	
Case 6	0.179		0.080		0.080		0.060		0.418		0.080	
Ratio	1.12		1.00		1.00		1.00		5.24		1.00	
	Base Shear (kN)						**Base Moment (kN-m)**					
	RMS		**Peak**				**RMS**		**Peak**			
Unisolated	0.59		3.13				0.42		2.18			
Case 6	0.49		2.31				0.34		1.57			
% Reduction (%)	16.95		26.20				19.05		27.98			

4.9. Unisolated Ground with the 3-Story Building

Three performance indicator parameters were evaluated for 3-story building model under Kocaeli, Kobe and El Centro earthquakes as shown in Figure 4.22, Figure 4.23 and Figure 4.24, respectively. Maximum foundation acceleration, top floor acceleration and first floor drift were observed as 0.46g, 0.58g, and 0.0162, respectively in the case of Kocaeli Earthquake.

The maximum foundation and top floor acceleration values were measured as 0.92g and 0.91g under Kobe earthquake, respectively. On the other hand, maximum foundation

acceleration was found as 0.49g while top floor was exposed to maximum acceleration as 0.64g under El Centro earthquake. Furthermore, the maximum first story drift values appeared as 0.0159 and 0.0045 under Kobe and El Centro earthquakes, respectively.

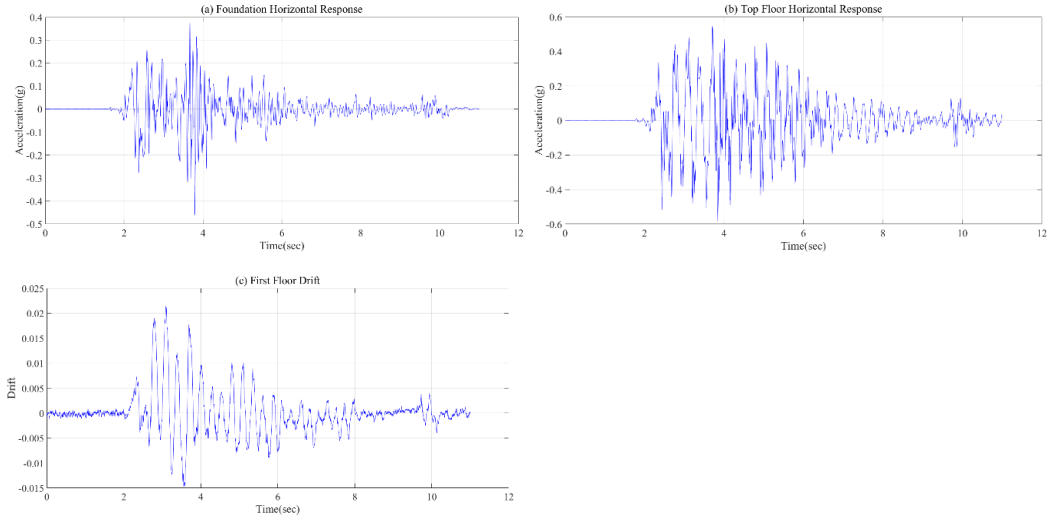

Figure 4.22. (a) Foundation Horizontal Acceleration Response, (b) Top Floor Horizontal Acceleration Response and (c) First Floor Drift of 3-Story Building Model under Kocaeli Earthquake.

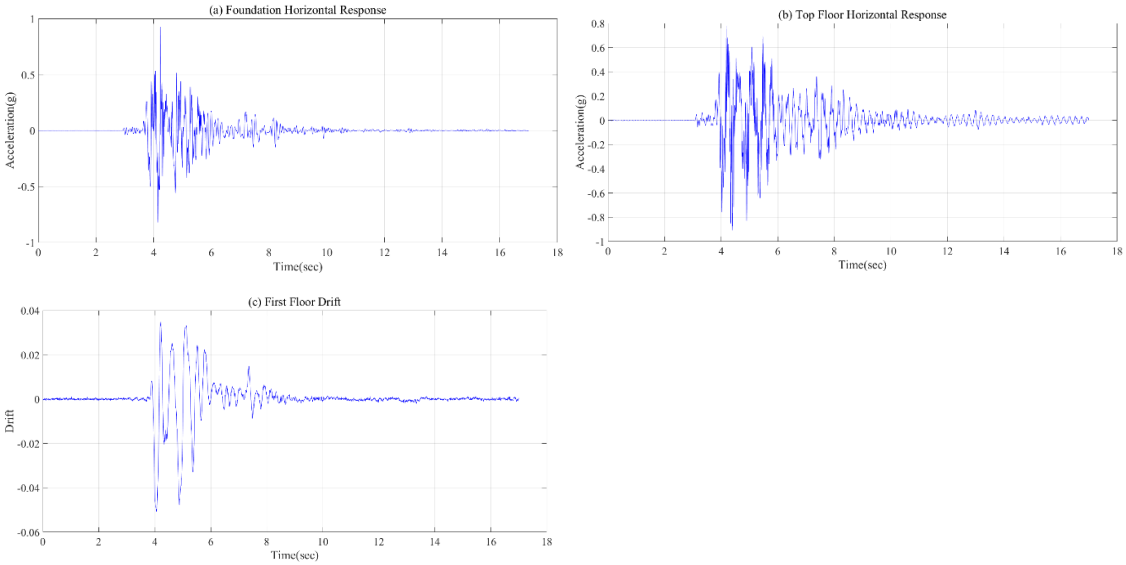

Figure 4.23. (a) Foundation Horizontal Acceleration Response, (b) Top Floor Horizontal Acceleration Response and (c) First Floor Drift of 3-Story Building Model under Kobe Earthquake.

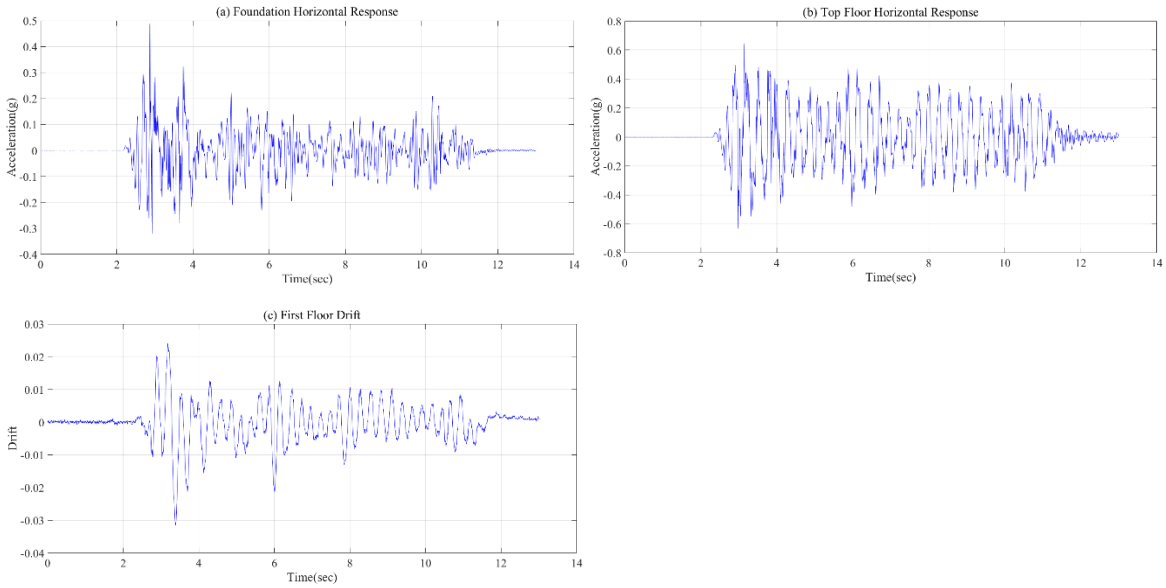

Figure 4.24. (a) Foundation Horizontal Acceleration Response, (b) Top Floor Horizontal Acceleration Response and (c) First Floor Drift of 3-Story Building Model under El Centro Earthquake.

4.10. Case 7 - GSI 3 Placed underneath the 3-Story Building Model

Polytetrafluoroethylene (PTFE) 1 mm geomembrane with Typar DuPont SF56 nonwoven geotextile was used as GSI 3 couple under Kocaeli, Kobe and El Centro earthquakes. Curve shaped liner was used as GG couple with CL1. Results were illustrated in order of Kocaeli, Kobe and El Centro earthquakes.

4.10.1. Seismic Response of Case 7 under Kocaeli Earthquake

When comparison was done, maximum reduction in acceleration response was observed at foundation level as 22.45% in peak value. Also, maximum reduction observed in RMS value revealed as 34.87% at foundation level. There was a huge amount of reduction in story drift as RMS value which was observed as 98.98% at top story. In addition,

maximum reduction was observed at the first floor as 24.07% in peak value. Arias intensity and peak spectral acceleration exhibited reduction as 30.67% at foundation level, and 30.14% at the second story, respectively. Moreover, same reduction values in base shear and base moment were observed as 33.33% in RMS value. However, an 11.76% and 4.35% reduction percentages were observed in base shear and base moment in peak value, respectively. Detailed results can be seen in Figure 4.25 and Table 4.23. Surprisingly, shortening of the period was observed at top story.

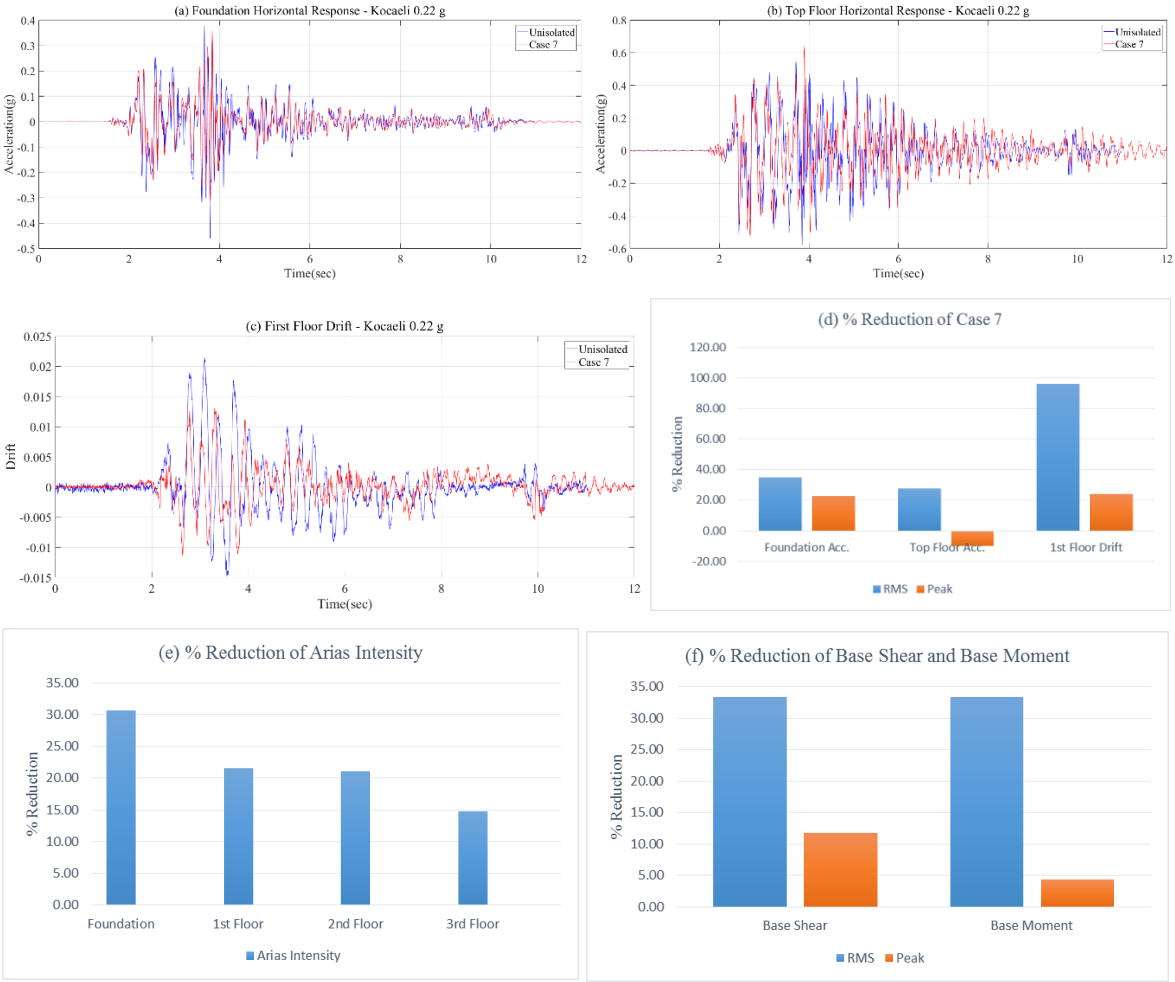

Figure 4.25. (a) Foundation Acceleration Response, (b) Top Floor Acceleration Response, (c) First Floor Drift Response, (d) % Reduction of Case 7, (e) % Reduction of Arias Intensity, (f) % Reduction of Base Shear and Base Moment under Kocaeli Earthquake.

Table 4.23. Horizontal Acceleration, Story Drift, Arias Intensity, Peak Spectral Acceleration, Period Lengthening Ratio, and Base Shear and Base Moment under Kocaeli Earthquake.

Case 7 under Kocaeli (PGA = 0.22 g) Earthquake (1999)								
	Foundation		**1st Floor**		**2nd Floor**		**3rd Floor**	
	RMS	**Peak**	**RMS**	**Peak**	**RMS**	**Peak**	**RMS**	**Peak**
Horizontal Acceleration (g)								
Unisolated	0.065	0.461	0.100	0.477	0.115	0.595	0.137	0.582
Case 7	0.042	0.357	0.069	0.443	0.080	0.475	0.099	0.640
% Reduction (%)	34.87	22.45	30.90	7.19	30.51	20.18	27.82	-10.11
Horizontal Story Drift								
Unisolated	-	-	0.0012	0.0162	0.0013	0.0056	0.1373	0.0122
Case 7	-	-	0.0001	0.0123	0.0003	0.0047	0.0014	0.0149
% Reduction (%)	-	-	95.83	24.07	73.85	16.07	98.98	-22.13
Arias Intensity (g-sec)								
Unisolated	0.0075		0.0176		0.0232		0.0332	
Case 7	0.0052		0.0138		0.0183		0.0283	
% Reduction (%)	30.67		21.59		21.12		14.76	
Peak Spectral Acceleration (g)								
Unisolated	1.71		2.46		3.45		2.45	
Case 7	1.56		1.76		2.41		2.19	
% Reduction (%)	8.77		28.46		30.14		10.61	
Period Lengthening Ratio								
	Fundamental Period (sec)							
Unisolated	0.100		0.040		0.040		0.299	
Case 7	0.100		0.040		0.040		0.259	
Ratio	1.00		1.00		1.00		0.87	
	Base Shear (kN)				**Base Moment (kN-m)**			
	RMS		**Peak**		**RMS**		**Peak**	
Unisolated	0.36		1.87		0.15		0.69	
Case 7	0.24		1.65		0.10		0.66	
Ratio	33.33		11.76		33.33		4.35	

4.10.2. Seismic Response of Case 7 under Kobe Earthquake

In horizontal acceleration response, maximum reduction was observed at the second floor as 15.58% in peak value. On the other hand, RMS value showed maximum reduction as 9.37%. Reduction in story drift was observed only at the first floor in RMS value as 24%.

No reduction was observed in Arias intensity. Moreover, peak spectral acceleration demonstrated reduction only at the second floor as 26.98%. Figure 4.26 and Table 4.24 showed summarized results. Maximum period shift was observed at top floor with a huge factor of 10.95. This means, unisolated case exhibited fundamental period of 0.040 second. Increase in base shear was observed while 4% reduction was obtained in base moment. However, isolated case provided 10 times greater predominant period in contrast to unisolated case.

Figure 4.26. (a) Foundation Acceleration Response, (b) Top Floor Acceleration Response, (c) First Floor Drift Response, (d) % Reduction of Case 7, (e) % Reduction of Arias Intensity, (f) % Reduction of Base Shear and Base Moment under Kobe Earthquake.

Table 4.24. Horizontal Acceleration, Story Drift, Arias Intensity, Peak Spectral Acceleration, Period Lengthening Ratio, and Base Shear and Base Moment under Kobe Earthquake.

Case 7 under Kobe (PGA = 0.80 g) Earthquake (1995)								
	Foundation		1st Floor		2nd Floor		3rd Floor	
	RMS	Peak	RMS	Peak	RMS	Peak	RMS	Peak
Horizontal Acceleration (g)								
Unisolated	0.092	0.925	0.096	0.837	0.118	1.216	0.130	0.909
Case 7	0.083	1.134	0.091	0.760	0.111	1.026	0.129	1.039
% Reduction (%)	9.37	-22.66	5.52	9.27	5.69	15.58	1.08	-14.37
Horizontal Story Drift								
Unisolated	-	-	0.0025	0.0159	0.0023	0.0082	0.0039	0.0183
Case 7	-	-	0.0019	0.0175	0.0029	0.0163	0.0045	0.0282
% Reduction (%)	-	-	24.00	-10.06	-26.09	-98.78	-15.38	-54.10
Arias Intensity (g-sec)								
Unisolated	0.0230		0.0251		0.0377		0.0460	
Case 7	0.0244		0.0290		0.0434		0.0583	
% Reduction (%)	-6.09		-15.54		-15.12		-26.74	
Peak Spectral Acceleration (g)								
Unisolated	1.84		2.66		4.93		2.41	
Case 7	2.24		3.06		3.60		2.62	
% Reduction (%)	-21.74		-15.04		26.98		-8.71	
Period Lengthening Ratio								
	Fundamental Period (sec)							
Unisolated	0.040		0.040		0.040		0.040	
Case 7	0.060		0.040		0.040		0.438	
Ratio	1.50		1.00		1.00		10.95	
	Base Shear (kN)				**Base Moment (kN-m)**			
	RMS		**Peak**		**RMS**		**Peak**	
Unisolated	0.38		3.51		0.15		1.25	
Case 7	0.36		3.60		0.14		1.20	
Ratio	5.76		-2.56		3.58		4.00	

4.10.3. Seismic Response of Case 7 under El Centro Earthquake

Horizontal acceleration response was reduced only at foundation of the building as 6.59%. On the other hand, maximum reduction was observed as 22.22% at foundation level in RMS value. No reduction in story drift was observed in peak value. However, second

story revealed maximum reduction as 60.95% in RMS value. Only reduction was observed at foundation of the building as 12% in Arias intensity. Also, reduction was measured only at foundation level as 10%. Tabulated values and graphical demonstration were shown in Table 4.25 and Figure 4.27, respectively. A reduction was observed in base shear and base moment in RMS values. Additionally, period shifting was observed at top story with a factor of 1.15.

Figure 4.27. (a) Foundation Acceleration Response, (b) Top Floor Acceleration Response, (c) First Floor Drift Response, (d) % Reduction of Case 7, (e) % Reduction of Arias Intensity, (f) % Reduction of Base Shear and Base Moment under El Centro Earthquake.

Table 4.25. Horizontal Acceleration, Story Drift, Arias Intensity, Peak Spectral Acceleration, Period Lengthening Ratio, and Base Shear and Base Moment under El Centro Earthquake.

Case 7 under El Centro (PGA = 0.35 g) Earthquake (1940)								
	Foundation		1st Floor		2nd Floor		3rd Floor	
	RMS	Peak	RMS	Peak	RMS	Peak	RMS	Peak
Horizontal Acceleration (g)								
Unisolated	0.069	0.489	0.101	0.486	0.130	0.597	0.175	0.644
Case 7	0.054	0.456	0.084	0.554	0.110	0.677	0.147	0.655
% Reduction (%)	22.22	6.59	16.90	-13.91	15.25	-13.34	15.64	-1.69
Horizontal Story Drift								
Unisolated	-	-	0.0007	0.0045	0.0021	0.0074	0.0027	0.0158
Case 7	-	-	0.0005	0.0066	0.0008	0.0075	0.0022	0.0191
% Reduction (%)	-	-	27.40	-46.67	60.95	-1.35	18.52	-20.89
Arias Intensity (g-sec)								
Unisolated	0.0100		0.0211		0.0351		0.0634	
Case 7	0.0088		0.0213		0.0368		0.0660	
% Reduction (%)	12.00		-0.95		-4.84		-4.10	
Peak Spectral Acceleration (g)								
Unisolated	1.10		2.03		2.17		2.64	
Case 7	0.99		2.24		2.25		2.84	
% Reduction (%)	10.00		-10.34		-3.69		-7.58	
Period Lengthening Ratio								
	Fundamental Period (sec)							
Unisolated	0.179		0.060		0.040		0.259	
Case 7	0.179		0.060		0.040		0.299	
Ratio	1.00		1.00		1.00		1.15	
	Base Shear (kN)				**Base Moment (kN-m)**			
	RMS		Peak		RMS		Peak	
Unisolated	0.40		1.96		0.17		0.73	
Case 7	0.33		2.06		0.15		0.79	
Ratio	17.18		-5.10		15.68		-8.26	

4.11. Case 8 - GSI 3 Placed underneath the 3-Story Building Model

Polytetrafluoroethylene (PTFE) 1 mm geomembrane with Typar DuPont SF56 nonwoven geotextile was used as GSI 3 couple under Kocaeli, Kobe and El Centro earthquakes. Curve shaped liner was used as GG couple with CL2. Results were illustrated in order of Kocaeli, Kobe and El Centro earthquakes.

4.11.1. Seismic Response of Case 8 under Kocaeli Earthquake

Foundation of the building experienced maximum reduction in acceleration response as 35.48% and 26.58% in RMS and peak value.At top story, 99.13% reduction in story drift was found in RMS value. Also, maximum reduction in story drift was observed at the first story as 25.31% in peak value. Maximum reduction in Arias intensity was obtained as 32% at foundation level. Moreover, peak spectral acceleration showed reduction as 25.61% at the first story. Reduction results can be seen in Figure 4.28 and Table 4.26. No period shifting was observed on the building. Furthermore, same reduction percentages in base shear and base moment were observed as 33.33% in RMS value. However, 10.70% and 1.19% reduction values were obtained in base shear and base moment in peak value, respectively.

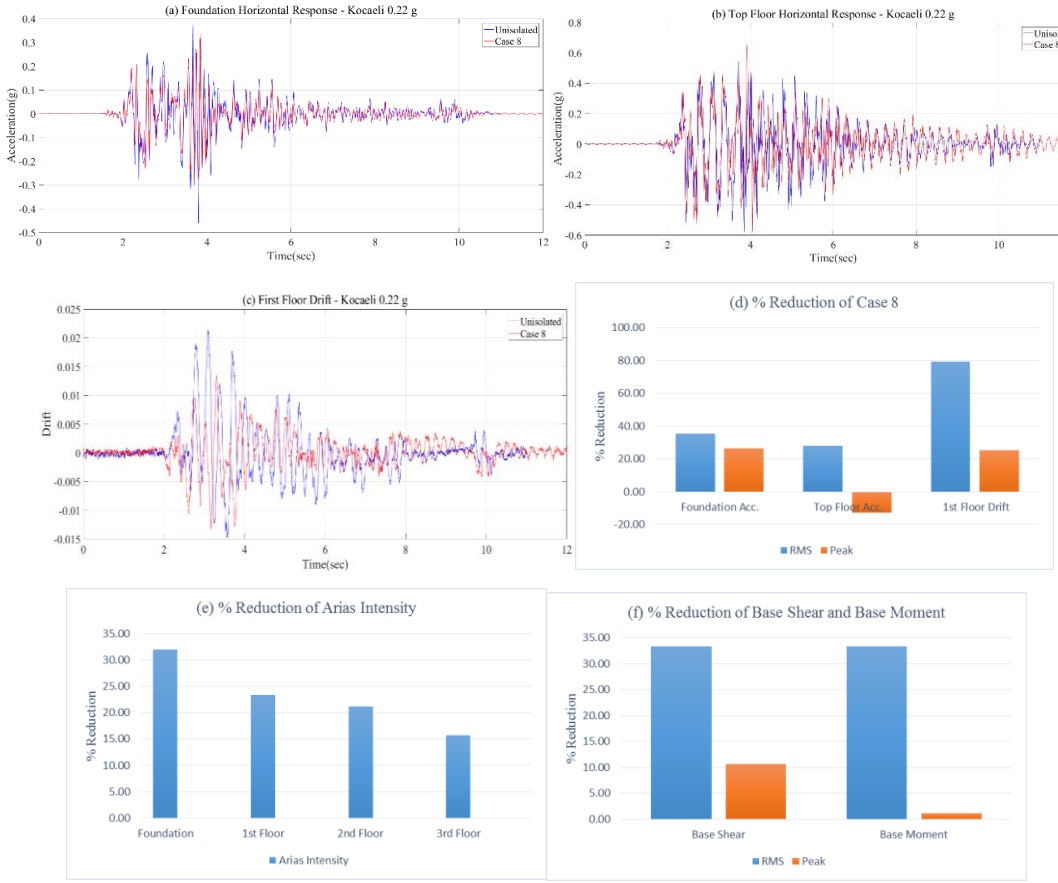

Figure 4.28. (a) Foundation Acceleration Response, (b) Top Floor Acceleration Response, (c) First Floor Drift Response, (d) % Reduction of Case 8, (e) % Reduction of Arias Intensity, (f) % Reduction of Base Shear and Base Moment under Kocaeli Earthquake.

Table 4.26. Horizontal Acceleration, Story Drift, Arias Intensity, Peak Spectral Acceleration, Period Lengthening Ratio, and Base Shear and Base Moment under Kocaeli Earthquake.

Case 8 under Kocaeli (PGA = 0.22 g) Earthquake (1999)								
	Foundation		**1st Floor**		**2nd Floor**		**3rd Floor**	
	RMS	**Peak**	**RMS**	**Peak**	**RMS**	**Peak**	**RMS**	**Peak**
Horizontal Acceleration (g)								
Unisolated	0.065	0.461	0.100	0.477	0.115	0.595	0.137	0.582
Case 8	0.042	0.338	0.068	0.446	0.080	0.517	0.099	0.655
% Reduction (%)	35.48	26.58	31.60	6.48	30.51	13.08	28.19	-12.59
Horizontal Story Drift								
Unisolated	-	-	0.0012	0.0162	0.0013	0.0056	0.1373	0.0122
Case 8	-	-	0.0003	0.0121	0.0007	0.0060	0.0012	0.0109
% Reduction (%)	-	-	79.17	25.31	47.69	-7.14	99.13	10.66
Arias Intensity (g-sec)								
Unisolated	0.0075		0.0176		0.0232		0.0332	
Case 8	0.0051		0.0135		0.0183		0.0280	
% Reduction (%)	32.00		23.30		21.12		15.66	
Peak Spectral Acceleration (g)								
Unisolated	1.71		2.46		3.45		2.45	
Case 8	1.51		1.83		2.58		2.27	
% Reduction (%)	11.70		25.61		25.22		7.35	
Period Lengthening Ratio								
	Fundamental Period (sec)							
Unisolated	0.100		0.040		0.040		0.299	
Case 8	0.100		0.040		0.040		0.279	
Ratio	1.00		1.00		1.00		0.93	
	Base Shear (kN)				**Base Moment (kN-m)**			
	RMS		**Peak**		**RMS**		**Peak**	
Unisolated	0.36		1.87		0.15		0.69	
Case 8	0.24		1.67		0.10		0.69	
Ratio	33.33		10.70		33.33		1.19	

4.11.2. Seismic Response of Case 8 under Kobe Earthquake

Maximum reduction in horizontal acceleration was observed as 18.30% in peak value at the second story. Reduction in story drift was observed as 16% only at foundation level in RMS value. No reduction in Arias intensity was observed. Moreover, reduction in peak

spectral acceleration was increased up to 19.07% only at the second floor. Results can be evaluated in Figure 4.29 and Table 4.27. Period shifting occured only at foundation level with a factor of 1.5. Although a reduction in base shear and base moment was observed in RMS values, an increase in base shear and base moment was observed in peak values.

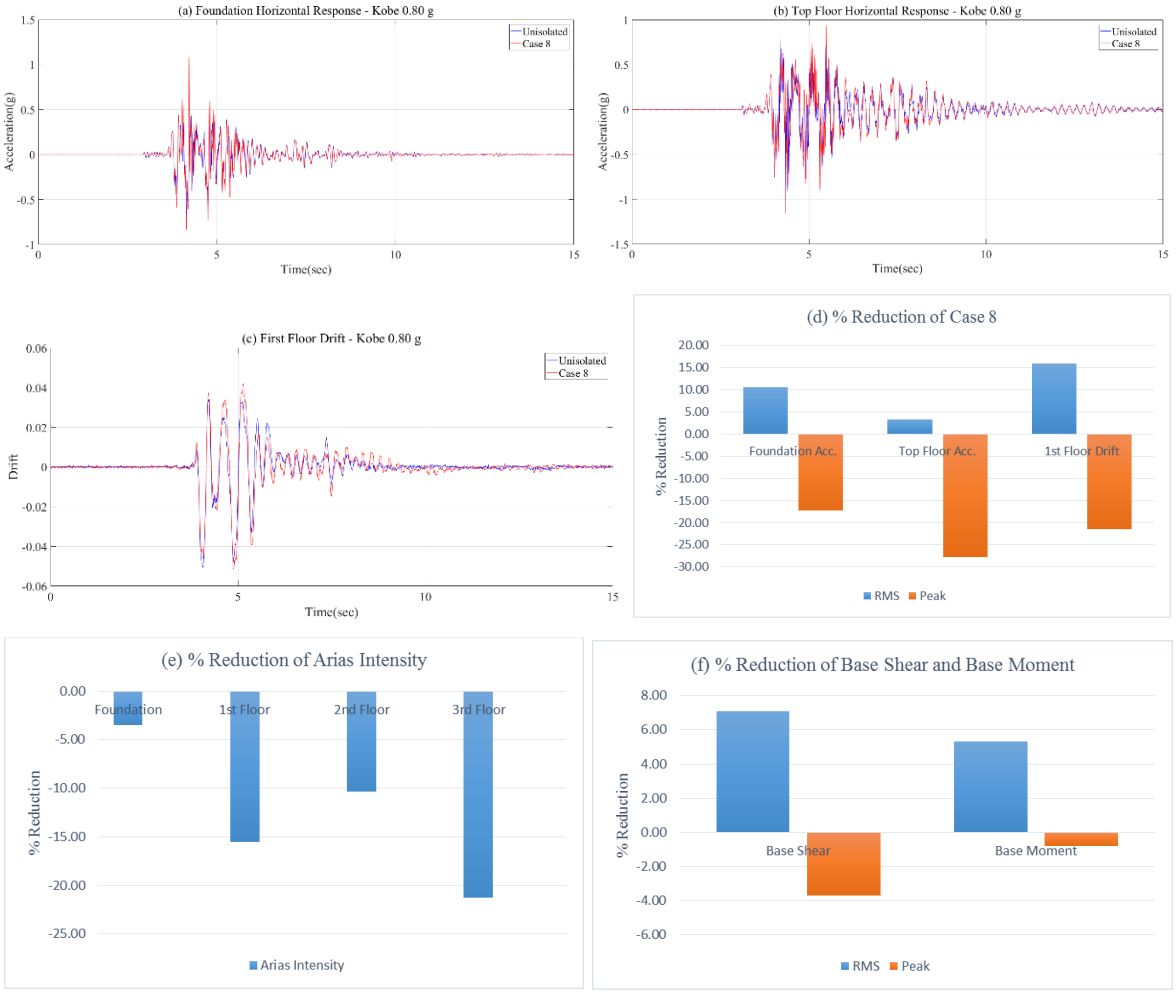

Figure 4.29. (a) Foundation Acceleration Response, (b) Top Floor Acceleration Response, (c) First Floor Drift Response, (d) % Reduction of Case 8, (e) % Reduction of Arias Intensity, (f) % Reduction of Base Shear and Base Moment under Kobe Earthquake.

Table 4.27. Horizontal Acceleration, Story Drift, Arias Intensity, Peak Spectral Acceleration, Period Lengthening Ratio, and Base Shear and Base Moment under Kobe Earthquake.

Case 8 under Kobe (PGA = 0.80 g) Earthquake (1995)								
	Foundation		1st Floor		2nd Floor		3rd Floor	
	RMS	Peak	RMS	Peak	RMS	Peak	RMS	Peak
Horizontal Acceleration (g)								
Unisolated	0.092	0.925	0.096	0.837	0.118	1.216	0.130	0.909
Case 8	0.082	1.085	0.091	0.815	0.109	0.993	0.126	1.161
% Reduction (%)	10.57	-17.32	5.42	2.63	7.65	18.30	3.23	-27.74
Horizontal Story Drift								
Unisolated	-	-	0.0025	0.0159	0.0023	0.0082	0.0039	0.0183
Case 8	-	-	0.0021	0.0193	0.0031	0.0205	0.0043	0.0246
% Reduction (%)	-	-	16.00	-21.38	-34.78	-150.00	-10.26	-34.43
Arias Intensity (g-sec)								
Unisolated	0.0230		0.0251		0.0377		0.0460	
Case 8	0.0238		0.029		0.0416		0.0558	
% Reduction (%)	-3.48		-15.54		-10.34		-21.30	
Peak Spectral Acceleration (g)								
Unisolated	1.84		2.66		4.93		2.41	
Case 8	2.02		3.16		3.99		2.66	
% Reduction (%)	-9.78		-18.80		19.07		-10.37	
Period Lengthening Ratio								
	Fundamental Period (sec)							
Unisolated	0.040		0.040		0.040		0.040	
Case 8	0.060		0.040		0.040		0.040	
Ratio	1.50		1.00		1.00		1.00	
	Base Shear (kN)				**Base Moment (kN-m)**			
	RMS		**Peak**		**RMS**		**Peak**	
Unisolated	0.38		3.51		0.15		1.25	
Case 8	0.36		3.64		0.14		1.26	
Ratio	7.07		-3.70		5.30		-0.80	

4.11.3. Seismic Response of Case 8 under El Centro Earthquake

Acceleration response of foundation of the building demonstrated more reduction than stories with a 25.4% reduction in RMS value while maximum reduction value of acceleration response was observed as 10.62% at foundation level in peak value. Maximum reduction in

story drift appeared as 8.89% at only the first story in peak value. Also, maximum reduction in story drift was observed as 78.08% in RMS value. Moreover, maximum reductions in Arias intensity and peak spectral acceleration were observed at foundation of the building as 14% and 9.09%, respectively. Summarized results can be observed in Figure 4.30 and Table 4.28. Period lengthening occured at top story with a factor of 1.15. Furthermore, similar reduction values were obtained in RMS values for base shear and base moment. On the other hand, reduction in base shear was observed while increase in base moment was obtained in peak values.

Figure 4.30. (a) Foundation Acceleration Response, (b) Top Floor Acceleration Response, (c) First Floor Drift Response, (d) % Reduction of Case 8, (e) % Reduction of Arias Intensity, (f) % Reduction of Base Shear and Base Moment under under El Centro Earthquake.

Table 4.28. Horizontal Acceleration, Story Drift, Arias Intensity, Peak Spectral Acceleration, Period Lengthening Ratio, and Base Shear and Base Moment under El Centro Earthquake.

Case 8 under El Centro (PGA = 0.35 g) Earthquake (1940)								
	Foundation		1st Floor		2nd Floor		3rd Floor	
	RMS	Peak	RMS	Peak	RMS	Peak	RMS	Peak
Horizontal Acceleration (g)								
Unisolated	0.069	0.489	0.101	0.486	0.130	0.597	0.175	0.644
Case 8	0.052	0.437	0.078	0.476	0.104	0.637	0.139	0.645
% Reduction (%)	25.40	10.62	22.56	2.08	20.03	-6.63	20.57	-0.12
Horizontal Story Drift								
Unisolated	-	-	0.0007	0.0045	0.0021	0.0074	0.0027	0.0158
Case 8	-	-	0.0002	0.0041	0.0017	0.0133	0.0018	0.0195
% Reduction (%)	-	-	78.08	8.89	19.05	-79.73	33.33	-23.42
Arias Intensity (g-sec)								
Unisolated	0.0100		0.0211		0.0351		0.0634	
Case 8	0.0086		0.0195		0.0345		0.0615	
% Reduction (%)	14.00		7.58		1.71		3.00	
Peak Spectral Acceleration (g)								
Unisolated	1.10		2.03		2.17		2.64	
Case 8	1.00		1.95		2.00		2.80	
% Reduction (%)	9.09		3.94		7.83		-6.06	
Period Lengthening Ratio								
	Fundamental Period (sec)							
Unisolated	0.179		0.060		0.040		0.259	
Case 8	0.179		0.060		0.040		0.299	
Ratio	1.00		1.00		1.00		1.15	
	Base Shear (kN)				**Base Moment (kN-m)**			
	RMS		Peak		RMS		Peak	
Unisolated	0.40		1.96		0.17		0.73	
Case 8	0.31		1.92		0.14		0.75	
Ratio	21.86		2.04		20.66		-2.34	

4.12. Proposed GSI System using Straight Liner as Foundation Isolation

In order to investigate the effect of configuration type, same geosynthetic couples were placed as straight liner instead of curve shaped liner. Same test procedure was implemented to the three and five story buildings. Case 9, Case 10, Case 11 and Case 12 involves the results of the straight liner (SL) effects on the buildings as a foundation isolation.

4.13. Case 9 - GSI 1 Placed underneath the 5-Story Building Model

Junifol High Density Polyethylene (HDPE) 1 mm geomembrane with Typar DuPont SF44 nonwoven geotextile was used as GSI 1 couple under Kocaeli, Kobe and El Centro earthquakes. Straight liner was used as GG couple having a width of 2B (2x35). Results were illustrated in order of Kocaeli, Kobe and El Centro earthquakes.

4.13.1. Seismic Response of Case 9 under Kocaeli Earthquake

Reduction in acceleration response in RMS values and maximum values were measured as 28.38% at the fourth story. When compared to the peak values in acceleration response on foundation, a 1.86% reduction was observed. First story experienced maximum reduction in horizontal story drift as 66.50% and 36.84% in RMS and peak value, respectively. Maximum reduction in Arias intensity was observed as 2.81% at top story. Peak spectral acceleration showed just a little bit reduction as 0.62%. Results can be seen in Figure 4.31 and Table 4.29. Moreoever, period shifting did not occured in the whole storeys. Also, similar reduction values were obtained in RMS values for base shear and base moment. On the other hand, an increase in base shear and base moment was observed in peak values.

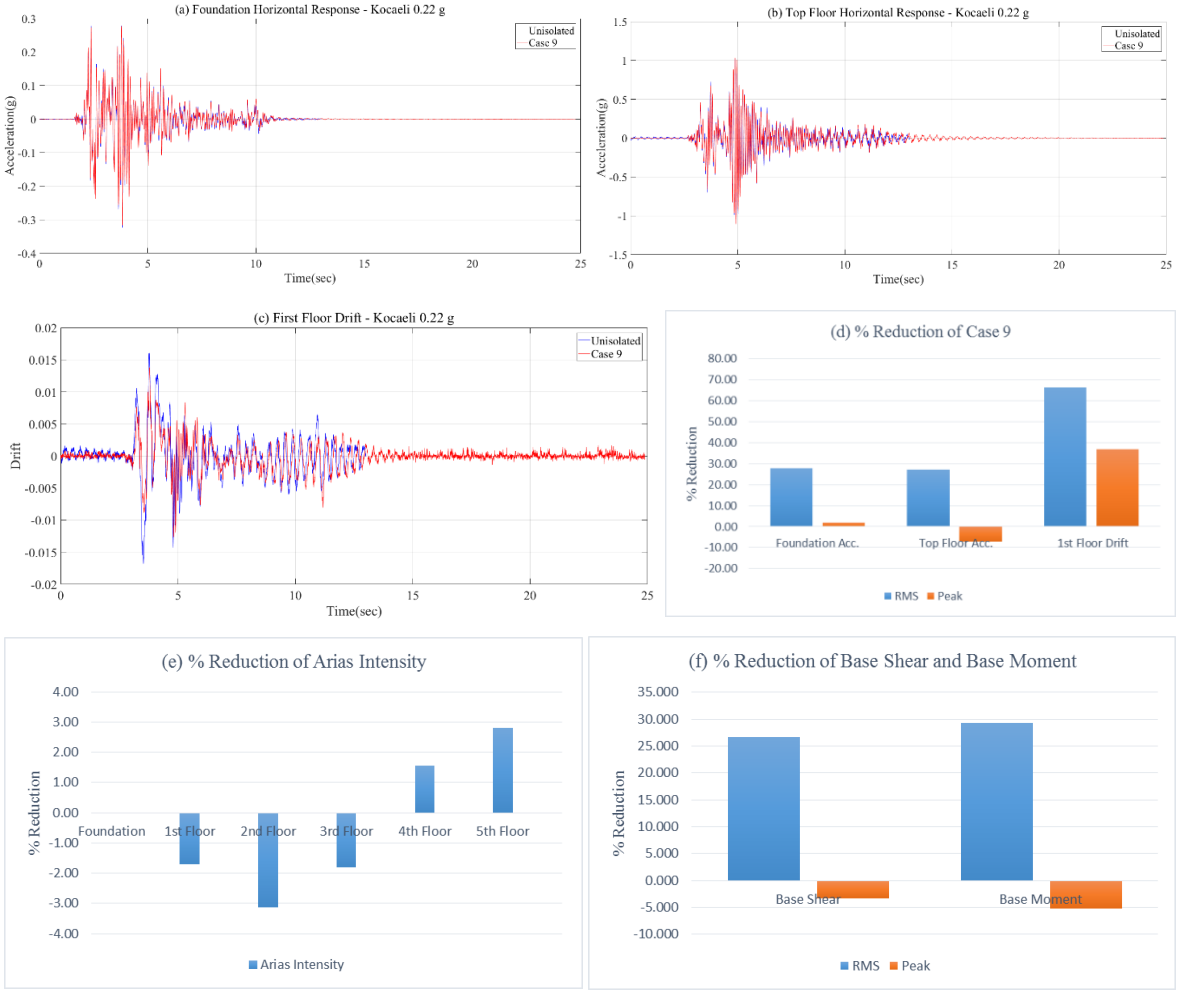

Figure 4.31. (a) Foundation Acceleration Response, (b) Top Floor Acceleration Response, (c) First Floor Drift Response, (d) % Reduction of Case 9, (e) % Reduction of Arias Intensity, (f) % Reduction of Base Shear and Base Moment under Kocaeli Earthquake.

Table 4.29. Horizontal Acceleration, Story Drift, Arias Intensity, Peak Spectral Acceleration, Period Lengthening Ratio, and Base Shear and Base Moment under Kocaeli Earthquake.

Case 9 under Kocaeli (PGA = 0.22 g) Earthquake (1999)												
	Foundation		1st Floor		2nd Floor		3rd Floor		4th Floor		5th Floor	
	RMS	Peak	RMS	Peak	RMS	Peak	RMS	Peak	RMS	Peak	RMS	Peak
Horizontal Acceleration (g)												
Unisolated	0.052	0.323	0.130	0.879	0.152	0.971	0.089	0.534	0.096	0.550	0.172	1.033
Case 9	0.037	0.317	0.095	0.889	0.111	1.003	0.065	0.538	0.069	0.593	0.125	1.106
% Reduction (%)	27.85	1.86	27.23	-1.13	26.76	-3.20	27.11	-0.82	28.38	-7.74	27.32	-7.02
Horizontal Story Drift												
Unisolated	-	-	0.0020	0.0114	0.0010	0.0104	0.0015	0.0145	0.0015	0.0041	0.0024	0.0012
Case 9	-	-	0.0007	0.0072	0.0006	0.0099	0.0016	0.0196	0.0008	0.0046	0.0019	0.0008
% Reduction (%)	-	-	66.50	36.84	42.00	4.81	-6.67	-35.17	46.00	-12.20	20.83	33.33
Arias Intensity (g-sec)												
Unisolated	0.0056		0.0352		0.0479		0.0165		0.0193		0.0641	
Case 9	0.0056		0.0358		0.0494		0.0168		0.0190		0.0623	
% Reduction (%)	0.00		-1.70		-3.13		-1.82		1.55		2.81	
Peak Spectral Acceleration (g)												
Unisolated	1.60		3.98		4.68		2.26		2.47		4.94	
Case 9	1.59		4.09		4.89		2.33		2.48		5.14	
% Reduction (%)	0.62		-2.76		-4.49		-3.10		-0.40		-4.05	
Period Lengthening Ratio												
	Fundamental Period (sec)											
Unisolated	0.100		0.100		0.080		0.080		0.100		0.080	
Case 9	0.100		0.100		0.080		0.080		0.100		0.080	
Ratio	1.00		1.00		1.00		1.00		1.00		1.00	
	Base Shear (kN)				Base Moment (kN-m)			
	RMS		Peak		RMS		Peak	
Unisolated	0.59		3.65		0.41		2.46	
Case 9	0.43		3.77		0.29		2.59	
% Reduction (%)	26.66		-3.29		29.27		-5.28	

4.13.2. Seismic Response of Case 9 under Kobe Earthquake

Maximum reduction in acceleration response was observed as 89.63% and 9.38% at the fourth story in RMS and peak value, respectively. The only reduction in story drift was observed at the fourth story as 26.47%. Also, the maximum reduction in Arias intensity occured only at the foundation level as 4.38% as seen in Figure 4.32. However, no reduction was observed in peak spectral acceleration. Moreover, no period shifting was determined as seen in Table 4.30. In addition, no reduction was observed in base shear and base moment in either RMS or peak values.

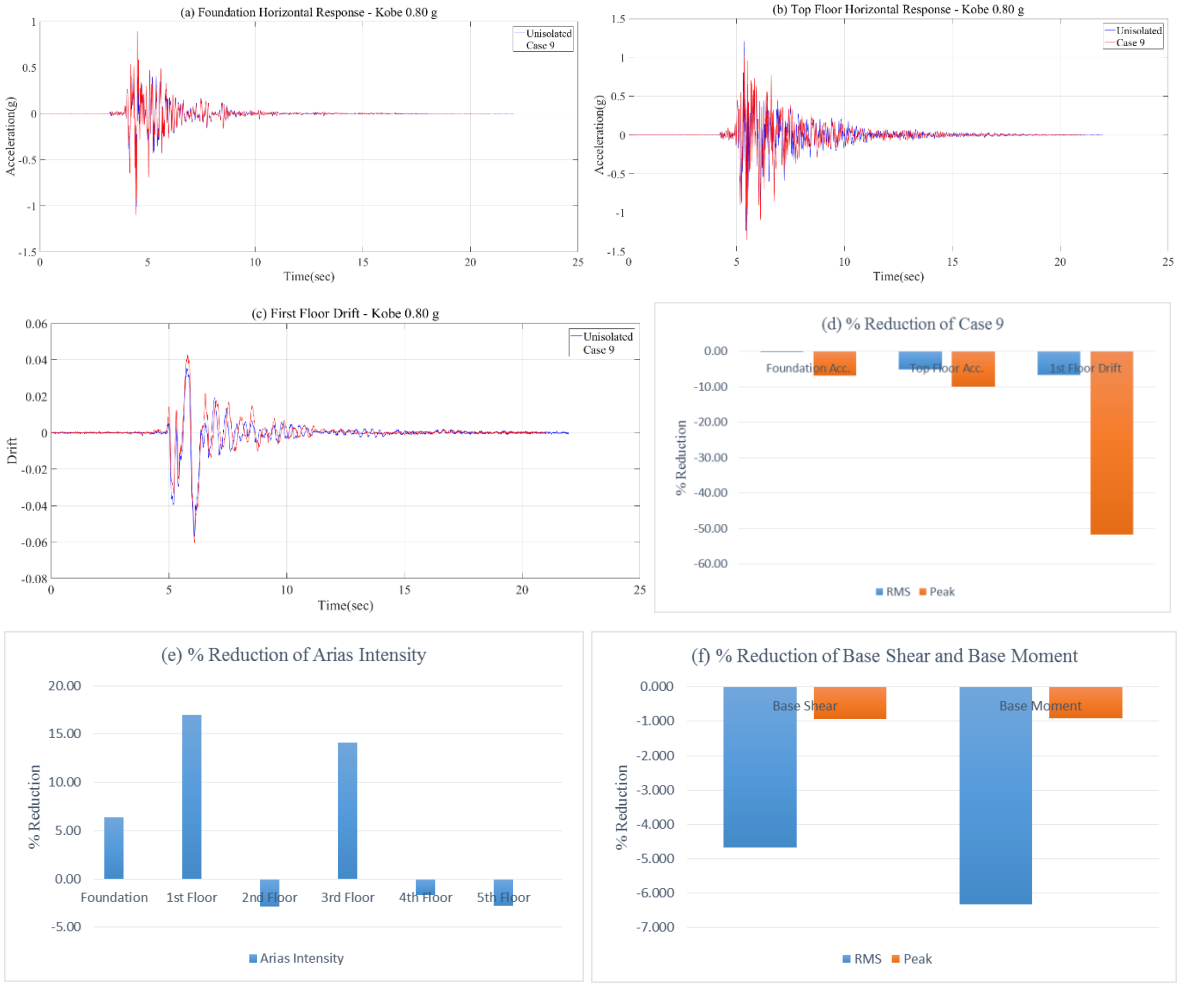

Figure 4.32. (a) Foundation Acceleration Response, (b) Top Floor Acceleration Response, (c) First Floor Drift Response, (d) % Reduction of Case 9, (e) % Reduction of Arias Intensity, (f) % Reduction of Base Shear and Base Moment under Kobe Earthquake.

Table 4.30. Horizontal Acceleration, Story Drift, Arias Intensity, Peak Spectral Acceleration, Period Lengthening Ratio, and Base Shear and Base Moment under Kobe Earthquake.

Case 9 under Kobe (PGA = 0.80 g) Earthquake (1995)												
	Foundation		1st Floor		2nd Floor		3rd Floor		4th Floor		5th Floor	
	RMS	Peak	RMS	Peak	RMS	Peak	RMS	Peak	RMS	Peak	RMS	Peak
Horizontal Acceleration (g)												
Unisolated	0.084	1.025	0.104	1.049	0.095	0.744	0.103	1.015	0.927	0.946	0.128	1.233
Case 9	0.085	1.096	0.106	0.988	0.104	0.730	0.111	1.052	0.096	0.857	0.134	1.357
% Reduction (%)	-0.12	-6.92	-2.42	5.83	-9.51	1.78	-7.74	-3.69	89.63	9.38	-5.18	-10.03
Horizontal Story Drift												
Unisolated	-	-	0.0030	0.0120	0.0023	0.0109	0.0043	0.0261	0.0030	0.0306	0.0010	0.0190
Case 9	-	-	0.0032	0.0182	0.0034	0.0126	0.0052	0.0397	0.0032	0.0225	0.0015	0.0232
% Reduction (%)	-	-	-6.67	-51.67	-47.83	-15.60	-20.93	-52.11	-6.67	26.47	-52.13	-22.11
Arias Intensity (g-sec)												
Unisolated	0.0251		0.0377		0.0315		0.0376		0.0303		0.0572	
Case 9	0.0240		0.0378		0.0361		0.0417		0.0310		0.0604	
% Reduction (%)	4.38		-0.27		-14.60		-10.90		-2.31		-5.59	
Peak Spectral Acceleration (g)												
Unisolated	1.99		2.70		3.80		3.21		2.91		3.71	
Case 9	2.49		3.79		3.93		4.79		3.18		3.92	
% Reduction (%)	-25.13		-40.37		-3.42		-49.22		-9.28		-5.66	
Period Lengthening Ratio												
	Fundamental Period (sec)											
Unisolated	0.040		0.040		0.080		0.060		0.040		0.080	
Case 9	0.040		0.060		0.080		0.060		0.040		0.080	
Ratio	1.00		1.50		1.00		1.00		1.00		1.00	
	Base Shear (kN)				**Base Moment (kN-m)**							
	RMS		**Peak**		**RMS**		**Peak**					
Unisolated	0.53		5.35		0.34		3.29					
Case 9	0.56		5.40		0.36		3.32					
% Reduction (%)	-4.67		-0.93		-6.32		-0.91					

4.13.3. Seismic Response of Case 9 under El Centro Earthquake

Reduction in acceleration response was obtained as 29.96% in peak value. On the other hand, maximum reduction was observed as 26.89% in RMS value. Maximum reduction in story drift was measured as 68.89% on the foundation of the building in peak value. As a root-mean-square value, 50% reduction was observed at the second story. Arias intensity underwent reduction at the fourth story as 38.20%. Moreover, third floor exhibited maximum reduction in peak spectral acceleration as 25.99%. Demonstration of the results was given in Table 4.31 and Figure 4.33. Maximum period shifting was observed at the fourth story with a factor of 6.49. Also, similar reduction percentages were obtained in base shear and base moment in RMS and peak values.

Figure 4.33. (a) Foundation Acceleration Response, (b) Top Floor Acceleration Response, (c) First Floor Drift Response, (d) % Reduction of Case 9, (e) % Reduction of Arias Intensity, (f) % Reduction of Base Shear and Base Moment under El Centro Earthquake.

Table 4.31. Horizontal Acceleration, Story Drift, Arias Intensity, Peak Spectral Acceleration, Period Lengthening Ratio, and Base Shear and Base Moment under El Centro Earthquake.

Case 9 under El Centro (PGA = 0.35 g) Earthquake (1940)												
	Foundation		1st Floor		2nd Floor		3rd Floor		4th Floor		5th Floor	
	RMS	Peak	RMS	Peak	RMS	Peak	RMS	Peak	RMS	Peak	RMS	Peak
Horizontal Acceleration (g)												
Unisolated	0.057	0.336	0.116	0.651	0.140	0.603	0.106	0.633	0.108	0.501	0.172	0.946
Case 9	0.048	0.283	0.094	0.469	0.117	0.611	0.081	0.443	0.079	0.388	0.136	0.743
% Reduction (%)	14.34	15.73	18.84	27.86	16.73	-1.28	24.25	29.96	26.89	22.54	20.58	21.44
Horizontal Story Drift												
Unisolated	-	-	0.0009	0.0036	0.0024	0.0059	0.0032	0.0183	0.0010	0.0023	0.0018	0.0006
Case 9	-	-	0.0016	0.0011	0.0012	0.0061	0.0021	0.0068	0.0016	0.0014	0.0016	0.0014
% Reduction (%)	-	-	-78.37	68.89	50.00	-3.39	34.38	62.84	-60.00	40.87	11.11	-145.45
Arias Intensity (g-sec)												
Unisolated	0.0097		0.0407		0.0596		0.0344		0.0356		0.0895	
Case 9	0.0083		0.0311		0.0478		0.0229		0.0220		0.0653	
% Reduction (%)	14.43		23.59		19.80		33.43		38.20		27.04	
Peak Spectral Acceleration (g)												
Unisolated	1.15		2.28		3.31		2.27		1.53		3.34	
Case 9	1.05		1.84		2.83		1.68		1.29		2.89	
% Reduction (%)	8.70		19.30		14.50		25.99		15.69		13.47	
Period Lengthening Ratio												
	Fundamental Period (sec)											
Unisolated	0.159		0.080		0.080		0.060		0.080		0.080	
Case 9	0.179		0.080		0.080		0.080		0.518		0.080	
Ratio	1.12		1.00		1.00		1.33		6.49		1.00	
	Base Shear (kN)						**Base Moment (kN-m)**					
	RMS		**Peak**				**RMS**		**Peak**			
Unisolated	0.59		3.13				0.42		2.18			
Case 9	0.47		2.51				0.33		1.73			
% Reduction (%)	20.34		19.81				21.43		20.64			

4.14. Case 10 - GSI 2 Placed underneath the 5-Story Building Model

Polytetrafluoroethylene (PTFE) 1 mm geomembrane with Typar DuPont SF44 nonwoven geotextile was used as GSI 2 couple under Kocaeli, Kobe and El Centro earthquakes. Straight liner (SL) was used as GG couple having a width of 2B. Results were illustrated in order of Kocaeli, Kobe and El Centro earthquakes.

4.14.1. Seismic Response of Case 10 under Kocaeli Earthquake

Maximum reduction in horizontal acceleration was observed as 10.53% in peak value and 60.71% in RMS value at the third and second floors, respectively. At the second floor, maximum reduction in story drift was measured as 78.85% in peak value. On the other hand, maximum reduction appeared as 76.50% in RMS value. Maximum reduction in Arias intensity and peak spectral acceleration were observed at top floor of the building as 9.83% and 8.30%, respectively. Again, similarity was observed in base shear and base moment in RMS and peak values. Results can be seen in Figure 4.34 and Table 4.32. No period shift occured on the building.

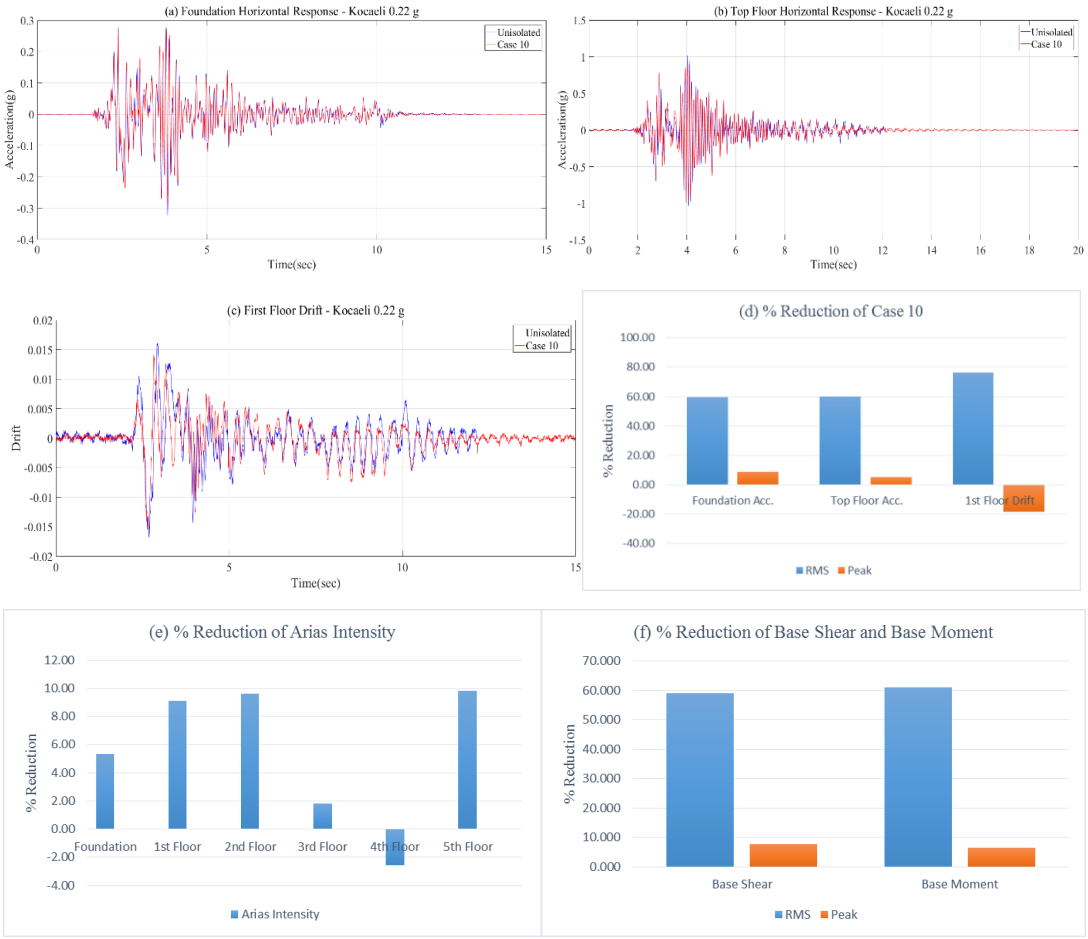

Figure 4.34. (a) Foundation Acceleration Response, (b) Top Floor Acceleration Response, (c) First Floor Drift Response, (d) % Reduction of Case 10, (e) % Reduction of Arias Intensity, (f) % Reduction of Base Shear and Base Moment under Kocaeli Earthquake.

Table 4.32. Horizontal Acceleration, Story Drift, Arias Intensity, Peak Spectral Acceleration, Period Lengthening Ratio, and Base Shear and Base Moment under Kocaeli Earthquake.

Case 10 under Kocaeli (PGA = 0.22 g) Earthquake (1999)												
	Foundation		1st Floor		2nd Floor		3rd Floor		4th Floor		5th Floor	
	RMS	Peak	RMS	Peak	RMS	Peak	RMS	Peak	RMS	Peak	RMS	Peak
Horizontal Acceleration (g)												
Unisolated	0.052	0.323	0.130	0.879	0.152	0.971	0.089	0.534	0.096	0.550	0.172	1.033
Case 10	0.021	0.294	0.051	0.789	0.060	0.906	0.037	0.478	0.040	0.528	0.069	0.978
% Reduction (%)	59.77	8.99	60.54	10.19	60.71	6.77	58.94	10.53	58.11	3.96	59.87	5.36
Horizontal Story Drift												
Unisolated	-	-	0.0020	0.0114	0.0010	0.0104	0.0015	0.0145	0.0015	0.0041	0.0024	0.0012
Case 10	-	-	0.0005	0.0135	0.0003	0.0022	0.0008	0.0137	0.0004	0.0063	0.0013	0.0010
% Reduction (%)	-	-	76.50	-18.42	71.00	78.85	46.00	5.52	74.00	-53.66	45.83	20.83
Arias Intensity (g-sec)												
Unisolated	0.0056		0.0352		0.0479		0.0165		0.0193		0.0641	
Case 10	0.0053		0.0320		0.0433		0.0162		0.0198		0.0578	
% Reduction (%)	5.36		9.09		9.60		1.82		-2.59		9.83	
Peak Spectral Acceleration (g)												
Unisolated	1.60		3.98		4.68		2.26		2.47		4.94	
Case 10	1.56		3.79		4.29		2.08		2.33		4.53	
% Reduction (%)	2.50		4.77		8.33		7.96		5.67		8.30	
Period Lengthening Ratio												
	Fundamental Period (sec)											
Unisolated	0.100		0.100		0.080		0.080		0.100		0.080	
Case 10	0.100		0.100		0.080		0.080		0.100		0.080	
Ratio	1.00		1.00		1.00		1.00		1.00		1.00	
	Base Shear (kN)				Base Moment (kN-m)			
	RMS		Peak		RMS		Peak	
Unisolated	0.59		3.65		0.41		2.46	
Case 10	0.24		3.37		0.16		2.30	
% Reduction (%)	59.07		7.67		60.98		6.50	

4.14.2. Seismic Response of Case 10 under Kobe Earthquake

Maximum values in reduction of acceleration response were observed as 17.15% in peak value and 92.43% in RMS value. At the first story, maximum reduction in story drift was obtained as 46.67% in RMS value while top floor provided maximum reduction as 64.63% in peak value. Arias intensity underwent a 25.27% reduction at the third floor as seen in Table 4.33 and Figure 4.35. Peak spectral acceleration was reduced at the second floor with a reduction of 1.58%. Period shifting occured only at the first floor. In RMS and peak values, similar reduction percentages were observed in base shear and base moment.

Figure 4.35. (a) Foundation Acceleration Response, (b) Top Floor Acceleration Response, (c) First Floor Drift Response, (d) % Reduction of Case 10, (e) % Reduction of Arias Intensity, (f) % Reduction of Base Shear and Base Moment under Kobe Earthquake.

Table 4.33. Horizontal Acceleration, Story Drift, Arias Intensity, Peak Spectral Acceleration, Period Lengthening Ratio, and Base Shear and Base Moment under Kobe Earthquake.

Case 10 under Kobe (PGA = 0.80 g) Earthquake (1995)												
	Foundation		1st Floor		2nd Floor		3rd Floor		4th Floor		5th Floor	
	RMS	Peak	RMS	Peak	RMS	Peak	RMS	Peak	RMS	Peak	RMS	Peak
Horizontal Acceleration (g)												
Unisolated	0.084	1.025	0.104	1.049	0.095	0.744	0.103	1.015	0.927	0.946	0.128	1.233
Case 10	0.066	1.034	0.082	1.080	0.081	0.696	0.075	0.971	0.070	0.784	0.101	1.332
% Reduction (%)	21.68	-0.88	21.16	-2.96	13.95	6.37	27.20	4.33	92.43	17.15	20.47	-8.03
Horizontal Story Drift												
Unisolated	-	-	0.0030	0.0120	0.0023	0.0109	0.0043	0.0261	0.0030	0.0306	0.0010	0.0190
Case 10	-	-	0.0016	0.0047	0.0017	0.0143	0.0036	0.0353	0.0056	0.0103	0.0022	0.0067
% Reduction (%)	-	-	46.67	60.83	26.09	-31.19	16.28	-35.25	-86.67	66.37	-123.12	64.63
Arias Intensity (g-sec)												
Unisolated	0.0251		0.0377		0.0315		0.0376		0.0303		0.0572	
Case 10	0.0217		0.0330		0.0329		0.0281		0.0245		0.0511	
% Reduction (%)	13.55		12.47		-4.44		25.27		19.14		10.66	
Peak Spectral Acceleration (g)												
Unisolated	1.99		2.70		3.80		3.21		2.91		3.71	
Case 10	2.47		2.73		3.74		3.54		3.19		3.75	
% Reduction (%)	-24.12		-1.11		1.58		-10.28		-9.62		-1.08	
Period Lengthening Ratio												
	Fundamental Period (sec)											
Unisolated	0.040		0.040		0.080		0.060		0.040		0.080	
Case 10	0.040		0.060		0.080		0.060		0.040		0.080	
Ratio	1.00		1.50		1.00		1.00		1.00		1.00	
	Base Shear (kN)				**Base Moment (kN-m)**							
	RMS		**Peak**		**RMS**		**Peak**					
Unisolated	0.53		5.35		0.34		3.29					
Case 10	0.42		5.23		0.27		3.17					
% Reduction (%)	21.50		2.24		21.65		3.65					

4.14.3. Seismic Response of Case 10 under El Centro Earthquake

Third and fourth floor showed maximum reduction in acceleration response as 34.89% in peak, and 35.03% in RMS value, respectively. At the first story, maximum reduction in story drift was observed as 70.56% in peak value. On the other hand, maximum reduction in story drift in RMS value was observed at the fourth floor as 66%. Maximum reduction in Arias intensity was measured as 40.17% at the fourth story. Moreover, third story was exposed to maximum reduction in peak spectral acceleration as 36.56%. Table 4.34 and Figure 4.36 illustrated results in detail. Maximum period shift was obtained at the fourth

story with a factor of 6.49. Additionally, similar and larger reduction values were observed in base shear and base moment in RMS and peak values as 30% and 24%, respectively.

Figure 4.36. (a) Foundation Acceleration Response, (b) Top Floor Acceleration Response, (c) First Floor Drift Response, (d) % Reduction of Case 10, (e) % Reduction of Arias Intensity, (f) % Reduction of Base Shear and Base Moment under El Centro Earthquake.

Table 4.34. Horizontal Acceleration, Story Drift, Arias Intensity, Peak Spectral Acceleration, Period Lengthening Ratio, and Base Shear and Base Moment under El Centro Earthquake.

Case 10 under El Centro (PGA = 0.35 g) Earthquake (1940)												
	Foundation		1st Floor		2nd Floor		3rd Floor		4th Floor		5th Floor	
	RMS	Peak	RMS	Peak	RMS	Peak	RMS	Peak	RMS	Peak	RMS	Peak
Horizontal Acceleration (g)												
Unisolated	0.057	0.336	0.116	0.651	0.140	0.603	0.106	0.633	0.108	0.501	0.172	0.946
Case 10	0.043	0.290	0.081	0.436	0.102	0.604	0.070	0.412	0.070	0.370	0.119	0.695
% Reduction (%)	24.25	13.80	29.82	32.94	27.38	-0.25	34.59	34.89	35.03	26.15	30.55	26.57
Horizontal Story Drift												
Unisolated	-	-	0.0009	0.0036	0.0024	0.0059	0.0032	0.0183	0.0010	0.0023	0.0018	0.0006
Case 10	-	-	0.0013	0.0011	0.0016	0.0067	0.0029	0.0144	0.0003	0.0019	0.0011	0.0004
% Reduction (%)	-	-	-44.93	70.56	33.33	-13.56	9.38	21.31	66.00	17.39	38.89	27.27
Arias Intensity (g-sec)												
Unisolated	0.0097		0.0407		0.0596		0.0344		0.0356		0.0895	
Case 10	0.0079		0.0285		0.0446		0.0210		0.0213		0.0614	
% Reduction (%)	18.56		29.98		25.17		38.95		40.17		31.40	
Peak Spectral Acceleration (g)												
Unisolated	1.15		2.28		3.31		2.27		1.53		3.34	
Case 10	1.06		1.83		2.46		1.44		1.16		2.54	
% Reduction (%)	7.83		19.74		25.68		36.56		24.18		23.95	
Period Lengthening Ratio												
	Fundamental Period (sec)											
Unisolated	0.159		0.080		0.080		0.060		0.080		0.080	
Case 10	0.179		0.100		0.080		0.060		0.518		0.080	
Ratio	1.12		1.25		1.00		1.00		6.49		1.00	
	Base Shear (kN)						**Base Moment (kN-m)**					
	RMS		**Peak**				**RMS**		**Peak**			
Unisolated	0.59		3.13				0.42		2.18			
Case 10	0.41		2.41				0.29		1.64			
% Reduction (%)	30.51		23.00				30.95		24.77			

4.15. Case 11 - GSI 3 Placed underneath the 3-Story Building Model

Polytetrafluoroethylene (PTFE) 1 mm geomembrane with Typar DuPont SF56 nonwoven geotextile was used as GSI 3 couple under Kocaeli, Kobe and El Centro earthquakes. Straight liner (SL) was used as GG couple having a width of 2B. Results were illustrated in order of Kocaeli, Kobe and El Centro earthquakes.

4.15.1. Seismic Response of Case 11 under Kocaeli Earthquake

Maximum reduction in acceleration response was observed at foundation level as 16.55% in peak value, and fourth story as 34.30% in RMS value. Top floor was exposed to maximum reduction in story drift either in RMS or peak value. Peak value was observed as 62.50% and RMS value was calculated as 25%. Similarly, fourth story was exposed to maximum reduction in Arias intensity and peak spectral acceleration as 26.94% and 12.15%, respectively. Results can be observed on Table 4.35 and Figure 4.37. Furthermore, no period shift occured on the building. Similarity between the RMS and peak values of base shear and base moment stood out.

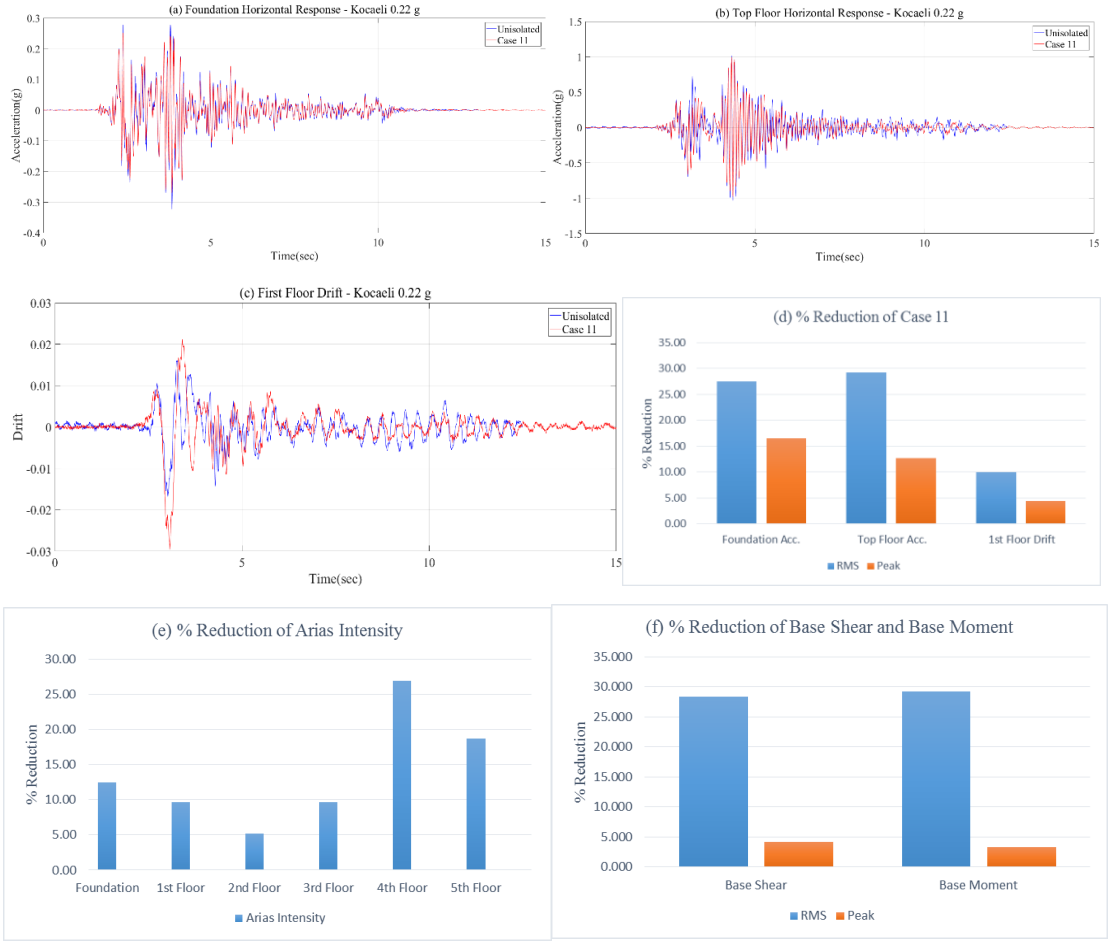

Figure 4.37. (a) Foundation Acceleration Response, (b) Top Floor Acceleration Response, (c) First Floor Drift Response, (d) % Reduction of Case 11, (e) % Reduction of Arias Intensity, (f) % Reduction of Base Shear and Base Moment under Kocaeli Earthquake.

Table 4.35. Horizontal Acceleration, Story Drift, Arias Intensity, Peak Spectral Acceleration, Period Lengthening Ratio, and Base Shear and Base Moment under Kocaeli Earthquake.

Case 11 under Kocaeli (PGA = 0.22 g) Earthquake (1999)												
	Foundation		1st Floor		2nd Floor		3rd Floor		4th Floor		5th Floor	
	RMS	Peak	RMS	Peak	RMS	Peak	RMS	Peak	RMS	Peak	RMS	Peak
Horizontal Acceleration (g)												
Unisolated	0.052	0.323	0.130	0.879	0.152	0.971	0.089	0.534	0.096	0.550	0.172	1.033
Case 11	0.038	0.269	0.095	0.842	0.114	0.946	0.065	0.598	0.063	0.475	0.122	0.902
% Reduction (%)	27.47	16.55	26.85	4.22	25.12	2.57	26.88	-12.07	34.30	13.63	29.18	12.70
Horizontal Story Drift												
Unisolated	-	-	0.0020	0.0114	0.0010	0.0104	0.0015	0.0145	0.0015	0.0041	0.0024	0.0012
Case 11	-	-	0.0018	0.0109	0.0019	0.0124	0.0026	0.0203	0.0020	0.0025	0.0018	0.0005
% Reduction (%)	-	-	10.00	4.39	-90.00	-19.23	-73.33	-40.00	-33.33	39.51	25.00	62.50
Arias Intensity (g-sec)												
Unisolated	0.0056		0.0352		0.0479		0.0165		0.0193		0.0641	
Case 11	0.0049		0.0318		0.0454		0.0149		0.0141		0.0521	
% Reduction (%)	12.50		9.66		5.22		9.70		26.94		18.72	
Peak Spectral Acceleration (g)												
Unisolated	1.60		3.98		4.68		2.26		2.47		4.94	
Case 11	1.47		4.04		4.67		2.28		2.17		4.82	
% Reduction (%)	8.13		-1.51		0.21		-0.88		12.15		2.43	
Period Lengthening Ratio												
	Fundamental Period (sec)											
Unisolated	0.100		0.100		0.080		0.080		0.100		0.080	
Case 11	0.100		0.100		0.080		0.080		0.100		0.080	
Ratio	1.00		1.00		1.00		1.00		1.00		1.00	
	Base Shear (kN)						Base Moment (kN-m)					
	RMS			Peak			RMS			Peak		
Unisolated	0.59			3.65			0.41			2.46		
Case 11	0.42			3.50			0.29			2.38		
% Reduction (%)	28.36			4.11			29.27			3.25		

4.15.2. Seismic Response of Case 11 under Kobe Earthquake

Maximum reduction in acceleration results was observed at the fourth story as 91.25% in RMS value and 8.16% in peak value. Story drift showed maximum reduction at the first and top floor as 75% in peak value, and 43.2% as RMS value, respectively. First story was exposed to maximum reduction in Arias intensity as 16.71%. Moreover, maximum reduction in peak spectral acceleration was observed as 5% at the second floor. These results can be seen from Figure 4.38 and Table 4.36. Period lengthening was observed at the first floor with a factor of 1.5 while shorthening in period at top floor with a factor of 0.50. Similar reduction values were obtained in base shear and base moment. However, a little bit increase was observed in base moment in peak value.

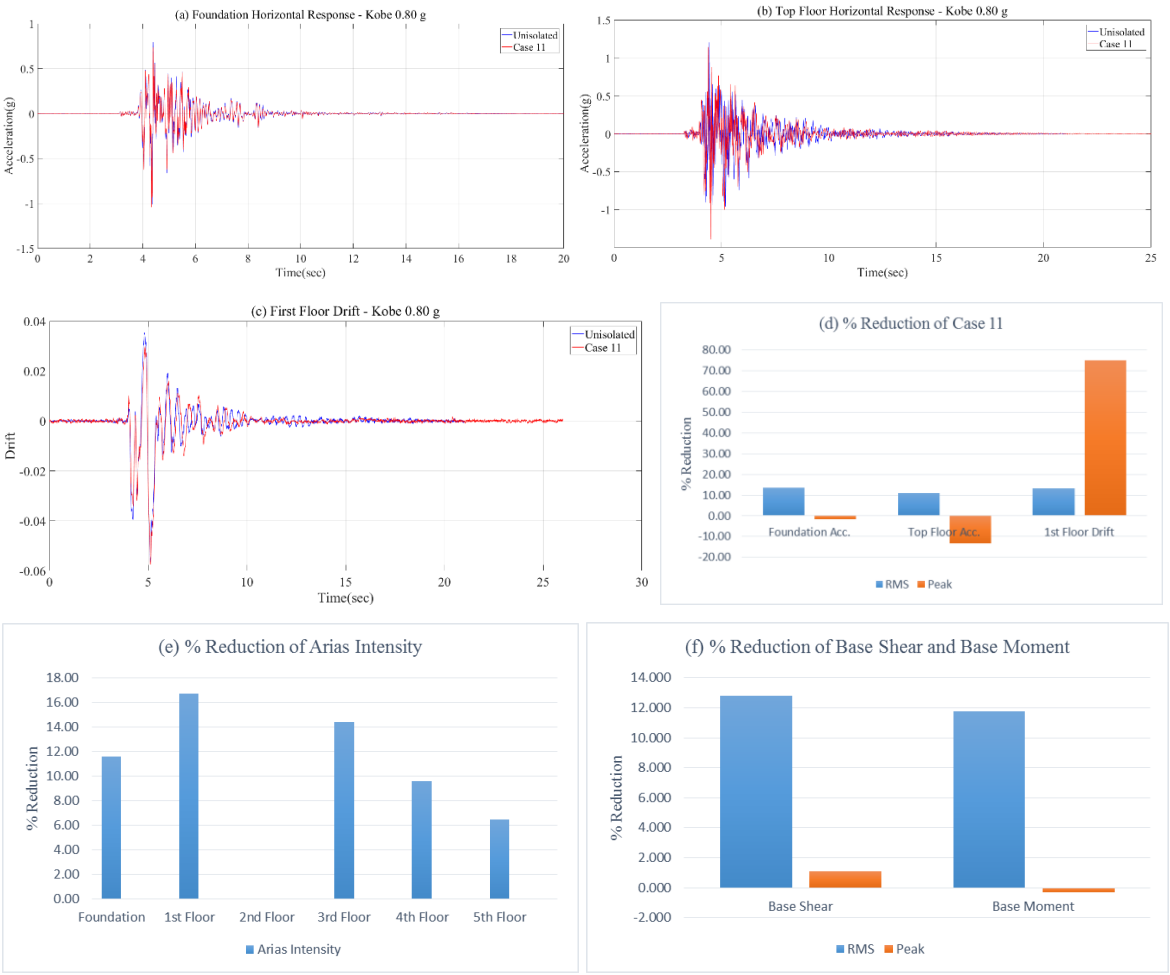

Figure 4.38. (a) Foundation Acceleration Response, (b) Top Floor Acceleration Response, (c) First Floor Drift Response, (d) % Reduction of Case 11, (e) % Reduction of Arias Intensity, (f) % Reduction of Base Shear and Base Moment under Kobe Earthquake.

Table 4.36. Horizontal Acceleration, Story Drift, Arias Intensity, Peak Spectral Acceleration, Period Lengthening Ratio, and Base Shear and Base Moment under Kobe Earthquake.

Case 11 under Kobe (PGA = 0.80 g) Earthquake (1995)												
	Foundation		1st Floor		2nd Floor		3rd Floor		4th Floor		5th Floor	
	RMS	Peak	RMS	Peak	RMS	Peak	RMS	Peak	RMS	Peak	RMS	Peak
Horizontal Acceleration (g)												
Unisolated	0.084	1.025	0.104	1.049	0.095	0.744	0.103	1.015	0.927	0.946	0.128	1.233
Case 11	0.073	1.042	0.087	0.985	0.087	0.721	0.088	0.980	0.081	0.869	0.113	1.396
% Reduction (%)	13.63	-1.65	16.14	6.13	8.03	3.08	14.81	3.48	91.25	8.16	11.14	-13.15
Horizontal Story Drift												
Unisolated	-	-	0.0030	0.0120	0.0023	0.0109	0.0043	0.0261	0.0030	0.0306	0.0010	0.0190
Case 11	-	-	0.0026	0.0030	0.0028	0.0221	0.0043	0.0391	0.0036	0.0384	0.0006	0.0164
% Reduction (%)	-	-	13.33	75.00	-21.74	-102.75	0.00	-49.81	-20.00	-25.49	43.20	13.68
Arias Intensity (g-sec)												
Unisolated	0.0251		0.0377		0.0315		0.0376		0.0303		0.0572	
Case 11	0.0222		0.0314		0.0315		0.0322		0.0274		0.0535	
% Reduction (%)	11.55		16.71		0.00		14.36		9.57		6.47	
Peak Spectral Acceleration (g)												
Unisolated	1.99		2.70		3.80		3.21		2.91		3.71	
Case 11	2.44		2.58		3.61		3.39		3.25		3.59	
% Reduction (%)	-22.61		4.44		5.00		-5.61		-11.68		3.23	
Period Lengthening Ratio												
	Fundamental Period (sec)											
Unisolated	0.040		0.040		0.080		0.060		0.040		0.080	
Case 11	0.040		0.060		0.080		0.060		0.040		0.040	
Ratio	1.00		1.50		1.00		1.00		1.00		0.50	
	Base Shear (kN)						**Base Moment (kN-m)**					
	RMS			**Peak**			**RMS**			**Peak**		
Unisolated	0.53			5.35			0.34			3.29		
Case 11	0.46			5.29			0.30			3.30		
% Reduction (%)	12.80			1.12			11.76			-0.30		

4.15.3. Seismic Response of Case 11 under El Centro Earthquake

Maximum reduction in horizontal acceleration response as 38.35% in peak value was the same as in RMS value at the fourth story. Maximum reduction in story drift was observed as 65.57% at the third floor in peak value. Third floor produced more reduction than other stories with a reduction of 46.80% in Arias intensity and 30.84% in peak spectral acceleration response as seen in Table 4.37 and Figure 4.39. Maximum period shift was observed at the third floor with a factor of 1.33. Similar values in the reduction of base shear and base moment were observed in RMS and peak values that were also similar to each other.

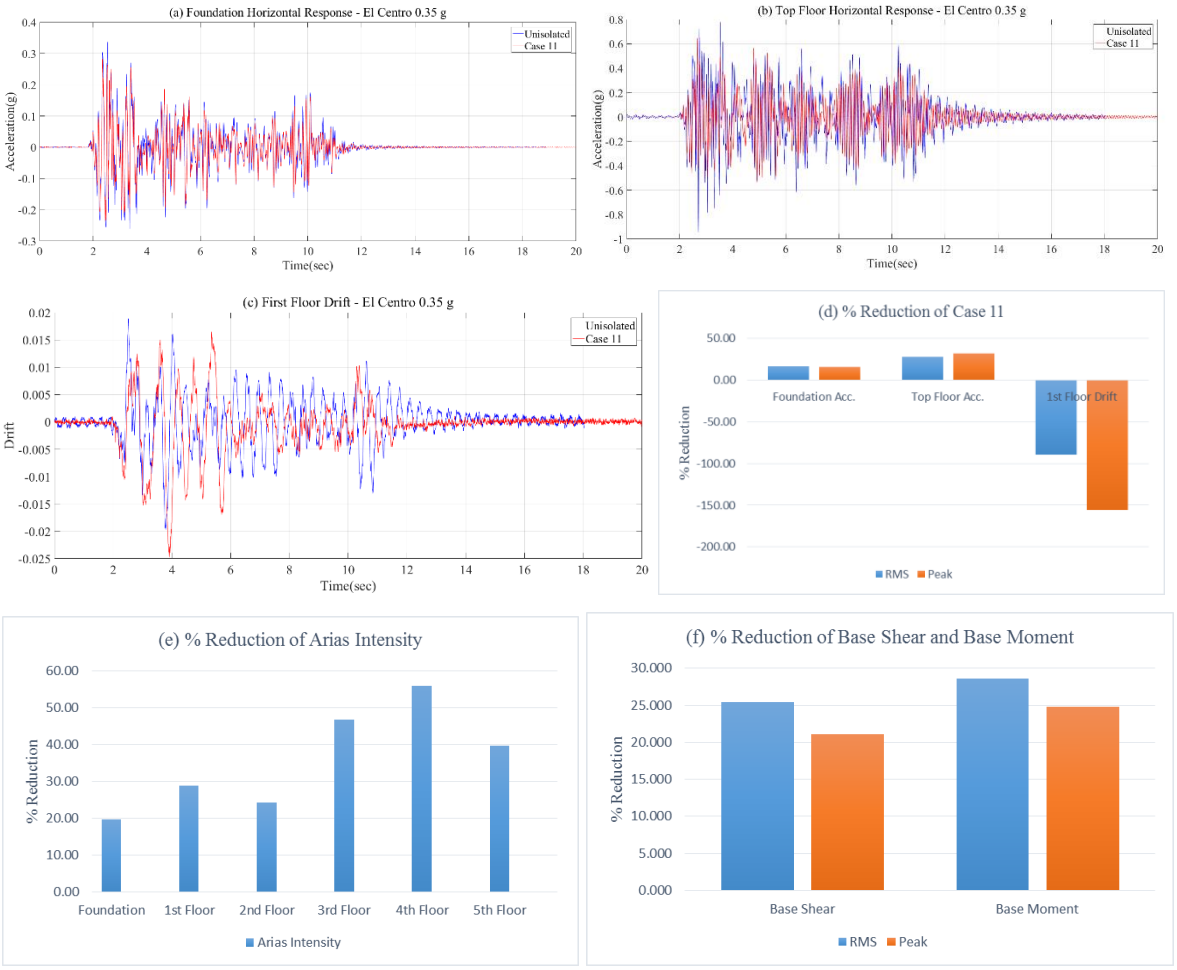

Figure 4.39. (a) Foundation Acceleration Response, (b) Top Floor Acceleration Response, (c) First Floor Drift Response, (d) % Reduction of Case 11, (e) % Reduction of Arias Intensity, (f) % Reduction of Base Shear and Base Moment under El Centro Earthquake.

Table 4.37. Horizontal Acceleration, Story Drift, Arias Intensity, Peak Spectral Acceleration, Period Lengthening Ratio, and Base Shear and Base Moment under El Centro Earthquake.

Case 11 under El Centro (PGA = 0.35 g) Earthquake (1940)												
	Foundation		1st Floor		2nd Floor		3rd Floor		4th Floor		5th Floor	
	RMS	Peak	RMS	Peak	RMS	Peak	RMS	Peak	RMS	Peak	RMS	Peak
Horizontal Acceleration (g)												
Unisolated	0.057	0.336	0.116	0.651	0.140	0.603	0.106	0.633	0.108	0.501	0.172	0.946
Case 11	0.047	0.282	0.091	0.503	0.113	0.651	0.072	0.390	0.067	0.396	0.124	0.645
% Reduction (%)	16.64	16.15	21.61	22.69	19.16	-7.95	32.24	38.35	38.35	21.11	27.76	31.82
Horizontal Story Drift												
Unisolated	-	-	0.0009	0.0036	0.0024	0.0059	0.0032	0.0183	0.0010	0.0023	0.0018	0.0006
Case 11	-	-	0.0017	0.0092	0.0015	0.0054	0.0031	0.0063	0.0020	0.0043	0.0016	0.0002
% Reduction (%)	-	-	-89.52	-155.56	37.50	8.47	3.13	65.57	-100.00	-86.96	11.11	58.18
Arias Intensity (g-sec)												
Unisolated	0.0097		0.0407		0.0596		0.0344		0.0356		0.0895	
Case 11	0.0078		0.0290		0.0451		0.0183		0.0157		0.0541	
% Reduction (%)	19.59		28.75		24.33		46.80		55.90		39.55	
Peak Spectral Acceleration (g)												
Unisolated	1.15		2.28		3.31		2.27		1.53		3.34	
Case 11	1.04		1.85		2.65		1.57		1.07		2.63	
% Reduction (%)	9.57		18.86		19.94		30.84		30.07		21.26	
Period Lengthening Ratio												
	Fundamental Period (sec)											
Unisolated	0.159		0.080		0.080		0.060		0.080		0.080	
Case 11	0.179		0.100		0.080		0.080		0.080		0.080	
Ratio	1.12		1.25		1.00		1.33		1.00		1.00	
	Base Shear (kN)						**Base Moment (kN-m)**					
	RMS		**Peak**				**RMS**		**Peak**			
Unisolated	0.59		3.13				0.42		2.18			
Case 10	0.44		2.47				0.30		1.64			
% Reduction (%)	25.42		21.09				28.57		24.77			

4.16. Case 12 - GSI 3 Placed underneath the 3-Story Building Model

Polytetrafluoroethylene (PTFE) 1 mm geomembrane with Typar DuPont SF56 nonwoven geotextile was used as GSI 3 couple under Kocaeli, Kobe and El Centro earthquakes. Straight liner (SL) was used as GG couple having a width of 2B. Results were illustrated in order of Kocaeli, Kobe and El Centro earthquakes.

4.16.1. Seismic Response of Case 12 under Kocaeli Earthquake

Maximum reduction in acceleration response was observed at the second floor as 48.82% in RMS, and 26.64% in peak value. Large amount of reduction in story drift was observed in the results. Maximum reduction was observed at top story as 98.98% in RMS value and 80.86% in peak value. Maximum reduction in Arias intensity appeared at the second floor as 38.36%. Moreover, a 32.11% reduction was measured at the first floor in peak spectral acceleration. Comparative results can be seen in Figure 4.40 and Table 4.38. A little bit period shift was observed at the top floor with a increasing factor of 1.07. Great reduction percentages were obtained in base shear and base moment, especially in RMS values as about 47%.

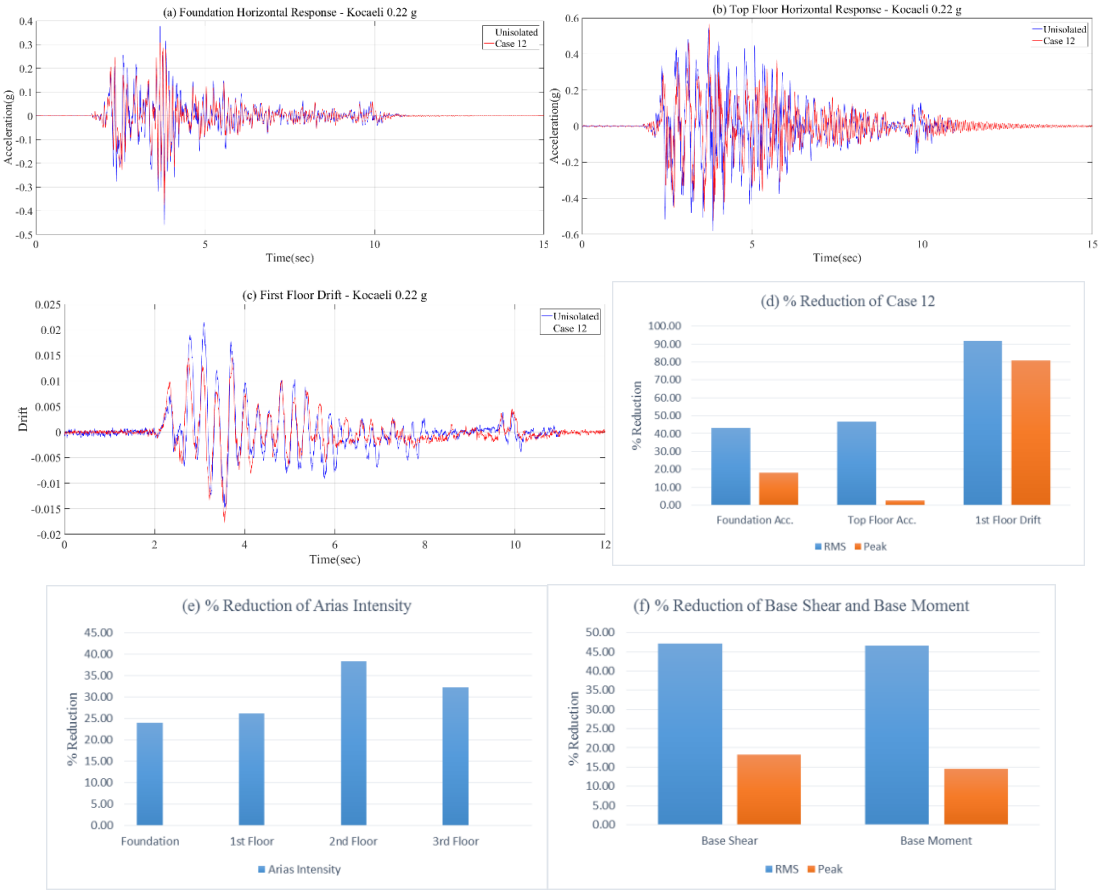

Figure 4.40. (a) Foundation Acceleration Response, (b) Top Floor Acceleration Response, (c) First Floor Drift Response, (d) % Reduction of Case 12, (e) % Reduction of Arias Intensity, (f) % Reduction of Base Shear and Base Moment under Kocaeli Earthquake.

Table 4.38. Horizontal Acceleration, Story Drift, Arias Intensity, Peak Spectral Acceleration, Period Lengthening Ratio, and Base Shear and Base Moment under Kocaeli Earthquake.

Case 12 under Kocaeli (PGA = 0.22 g) Earthquake (1999)								
	Foundation		1st Floor		2nd Floor		3rd Floor	
	RMS	Peak	RMS	Peak	RMS	Peak	RMS	Peak
Horizontal Acceleration (g)								
Unisolated	0.065	0.461	0.100	0.477	0.115	0.595	0.137	0.582
Case 12	0.037	0.377	0.056	0.379	0.059	0.437	0.073	0.567
% Reduction (%)	43.01	18.20	44.10	20.63	48.82	26.64	46.54	2.56
Horizontal Story Drift								
Unisolated	-	-	0.0012	0.0162	0.0013	0.0056	0.1373	0.0122
Case 12	-	-	0.0001	0.0031	0.0011	0.0109	0.0014	0.0067
% Reduction (%)	-	-	91.67	80.86	15.38	-94.64	98.98	45.08
Arias Intensity (g-sec)								
Unisolated	0.0075		0.0176		0.0232		0.0332	
Case 12	0.0057		0.0130		0.0143		0.0225	
% Reduction (%)	24.00		26.14		38.36		32.23	
Peak Spectral Acceleration (g)								
Unisolated	1.71		2.46		3.45		2.45	
Case 12	1.65		1.67		2.50		2.00	
% Reduction (%)	3.51		32.11		27.54		18.37	
Period Lengthening Ratio								
	Fundamental Period (sec)							
Unisolated	0.100		0.040		0.040		0.299	
Case 12	0.100		0.040		0.040		0.319	
Ratio	1.00		1.00		1.00		1.07	
	Base Shear (kN)				Base Moment (kN-m)			
	RMS		Peak		RMS		Peak	
Unisolated	0.36		1.87		0.15		0.69	
Case 12	0.19		1.53		0.08		0.59	
Ratio	47.22		18.18		46.67		14.49	

4.16.2. Seismic Response of Case 12 under Kobe Earthquake

Maximum reduction in acceleration response was observed at the second floor as 9.5% in peak value, and at the first floor as 26.04% in RMS value. At the second floor, maximum reduction was obtained as 66.59% in story drift. On the other hand, the first story was exposed to maximum reduction in Arias intensity as 25.9 %. Moreover, reduction in peak spectral acceleration at the second floor was observed as 38.54%. Also, the results can be

seen in Figure 4.41 and Table 4.39. Almost 10 times greater fundamental period was observed in isolated case with an increasing factor of 10.95 when compared to unisolated case. Furthermore, larger reduction values were obtained in base shear and base moment in RMS values as about 22% when compared to peak values that were 2.85% for base shear and 6.40% for base moment.

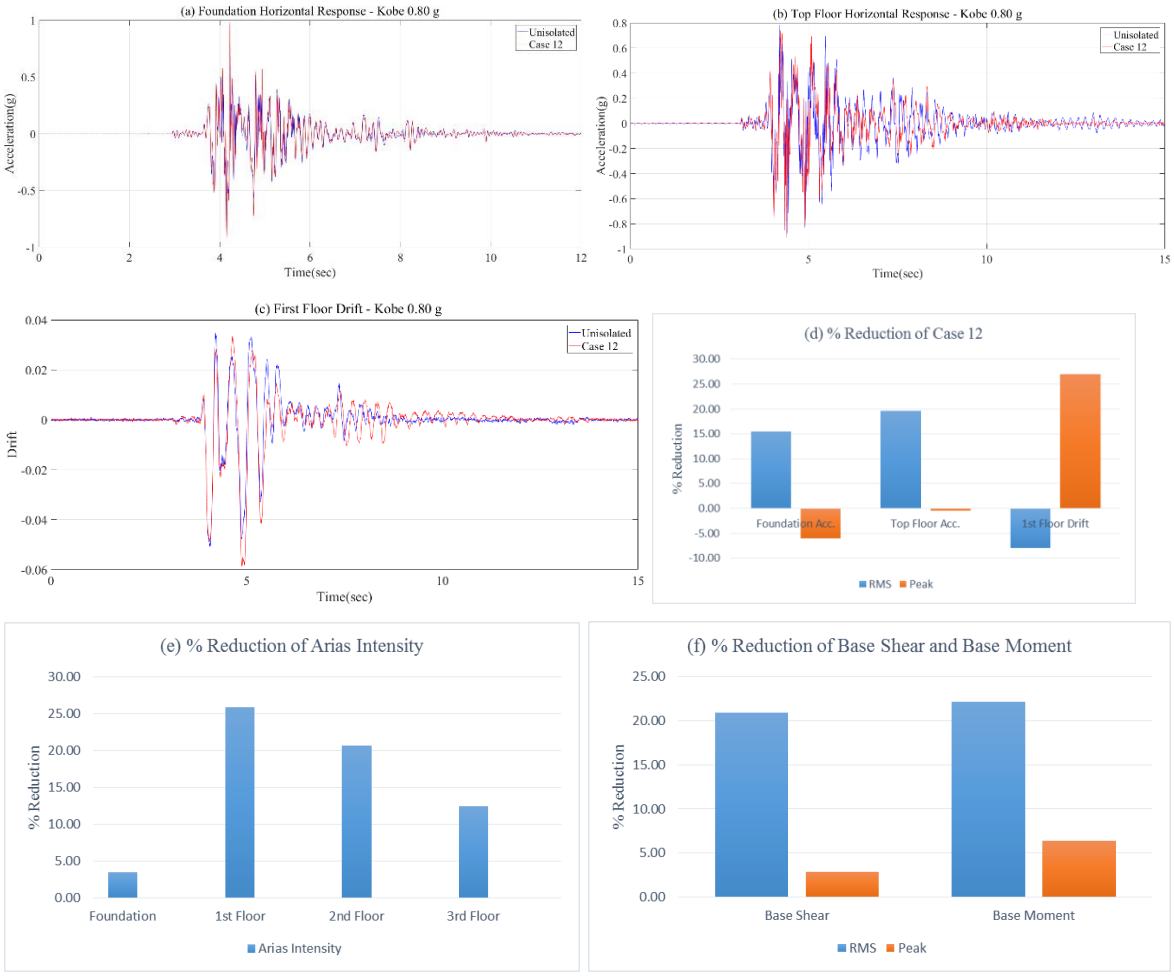

Figure 4.41. (a) Foundation Acceleration Response, (b) Top Floor Acceleration Response, (c) First Floor Drift Response, (d) % Reduction of Case 12, (e) % Reduction of Arias Intensity, (f) % Reduction of Base Shear and Base Moment under Kobe Earthquake.

Table 4.39. Horizontal Acceleration, Story Drift, Arias Intensity, Peak Spectral Acceleration, Period Lengthening Ratio, and Base Shear and Base Moment under Kobe Earthquake.

Case 12 under Kobe (PGA = 0.80 g) Earthquake (1995)								
	Foundation		1st Floor		2nd Floor		3rd Floor	
	RMS	Peak	RMS	Peak	RMS	Peak	RMS	Peak
Horizontal Acceleration (g)								
Unisolated	0.092	0.925	0.096	0.837	0.118	1.216	0.130	0.909
Case 12	0.078	0.981	0.071	0.759	0.090	1.100	0.105	0.913
% Reduction (%)	15.47	-6.07	26.04	9.34	23.45	9.50	19.62	-0.41
Horizontal Story Drift								
Unisolated	-	-	0.0025	0.0159	0.0023	0.0082	0.0039	0.0183
Case 12	-	-	0.0027	0.0116	0.0033	0.0027	0.0041	0.0229
% Reduction (%)	-	-	-8.00	27.04	-43.48	66.59	-5.13	-25.14
Arias Intensity (g-sec)								
Unisolated	0.0230		0.0251		0.0377		0.0460	
Case 12	0.0222		0.0186		0.0299		0.0403	
% Reduction (%)	3.48		25.90		20.69		12.39	
Peak Spectral Acceleration (g)								
Unisolated	1.84		2.66		4.93		2.41	
Case 12	2.10		1.73		3.03		2.34	
% Reduction (%)	-14.13		34.96		38.54		2.90	
Period Lengthening Ratio								
	Fundamental Period (sec)							
Unisolated	0.040		0.040		0.040		0.040	
Case 12	0.040		0.060		0.040		0.438	
Ratio	1.00		1.50		1.00		10.95	
	Base Shear (kN)				**Base Moment (kN-m)**			
	RMS		**Peak**		**RMS**		**Peak**	
Unisolated	0.38		3.51		0.15		1.25	
Case 12	0.30		3.41		0.11		1.17	
Ratio	20.94		2.85		22.15		6.40	

4.16.3. Seismic Response of Case 12 under El Centro Earthquake

Maximum reduction in horizontal acceleration response was observed at the second floor as 32.59% in RMS value and 25.54% in peak value. At the first story, maximum

reduction in story drift was measured as 95.11% which means enormous reduction in occurance of soft story phenomenon. Similarly, second floor was exposed to maximum reduction in Arias intensity and peak spectral acceleration as 40.46% and 23.50%, respectively. Finalized results were tabulated and graphed in Table 4.40 and Figure 4.42, respectively. Maximum period shifting was observed at the second floor with a factor of 7.47. Moreover, larger reduction values in base moment and base shear was observed in RMS values. However, about 15% increase in base shear value was obtained in peak value.

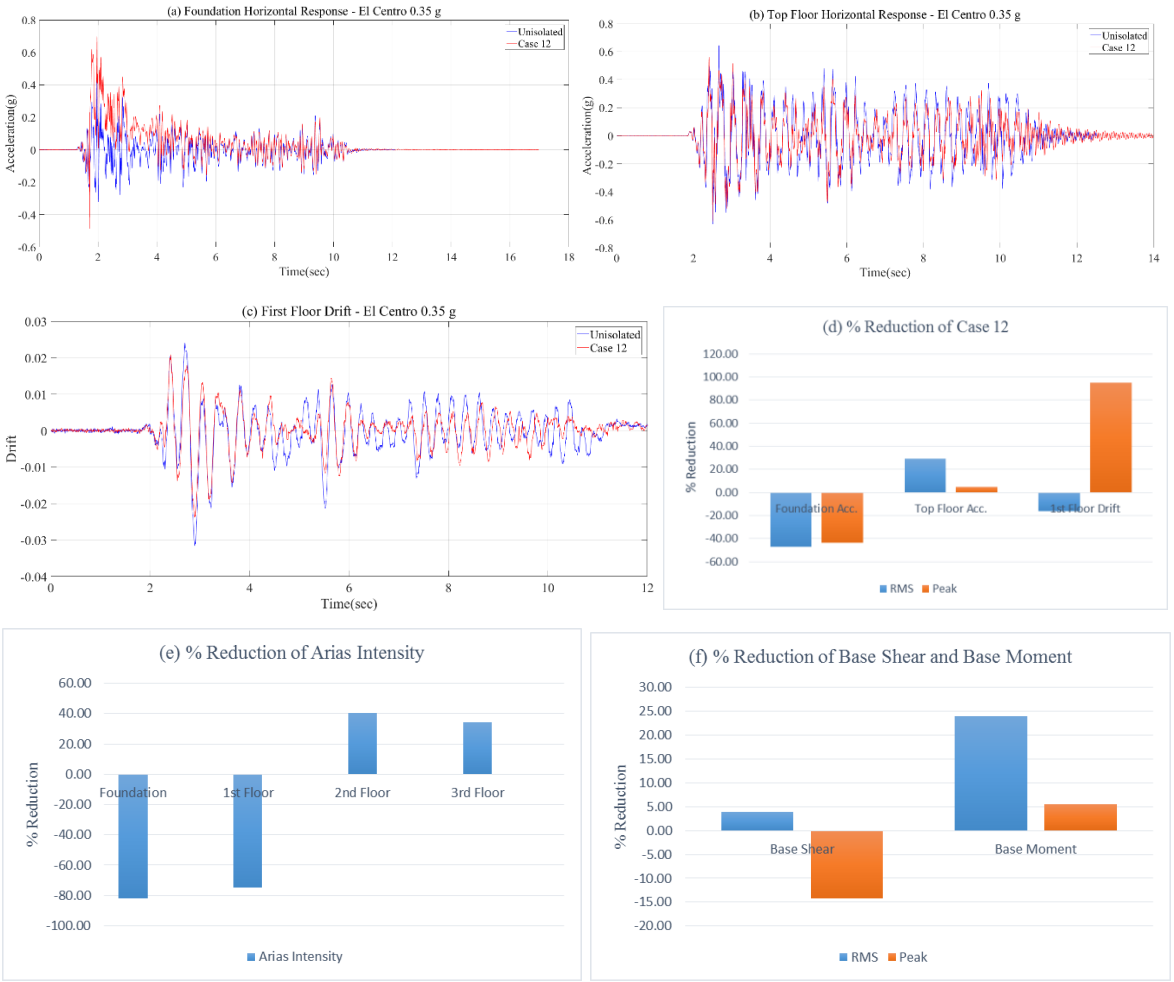

Figure 4.42. (a) Foundation Acceleration Response, (b) Top Floor Acceleration Response, (c) First Floor Drift Response, (d) % Reduction of Case 12, (e) % Reduction of Arias Intensity, (f) % Reduction of Base Shear and Base Moment under El Centro Earthquake.

Table 4.40. Horizontal Acceleration, Story Drift, Arias Intensity, Peak Spectral Acceleration, Period Lengthening Ratio, and Base Shear and Base Moment under El Centro Earthquake.

Case 12 under El Centro (PGA = 0.35 g) Earthquake (1940)								
	Foundation		1st Floor		2nd Floor		3rd Floor	
	RMS	Peak	RMS	Peak	RMS	Peak	RMS	Peak
Horizontal Acceleration (g)								
Unisolated	0.069	0.489	0.101	0.486	0.130	0.597	0.175	0.644
Case 12	0.102	0.701	0.117	0.690	0.088	0.445	0.124	0.613
% Reduction (%)	-47.04	-43.49	-15.90	-41.93	32.59	25.54	29.11	4.87
Horizontal Story Drift								
Unisolated	-	-	0.0007	0.0045	0.0021	0.0074	0.0027	0.0158
Case 12	-	-	0.0009	0.0002	0.0013	0.0152	0.0026	0.0156
% Reduction (%)	-	-	-16.44	95.11	38.10	-105.41	3.70	1.27
Arias Intensity (g-sec)								
Unisolated	0.0100		0.0211		0.0351		0.0634	
Case 12	0.0182		0.0369		0.0209		0.0417	
% Reduction (%)	-82.00		-74.88		40.46		34.23	
Peak Spectral Acceleration (g)								
Unisolated	1.10		2.03		2.17		2.64	
Case 12	1.44		1.78		1.66		2.37	
% Reduction (%)	-30.91		12.32		23.50		10.23	
Period Lengthening Ratio								
	Fundamental Period (sec)							
Unisolated	0.179		0.060		0.040		0.259	
Case 12	0.100		0.060		0.299		0.299	
Ratio	0.56		1.00		7.47		1.15	
	Base Shear (kN)				**Base Moment (kN-m)**			
	RMS		Peak		RMS		Peak	
Unisolated	0.40		1.96		0.17		0.73	
Case 12	0.38		2.24		0.13		0.69	
Ratio	3.95		-14.29		24.04		5.52	

5. PARAMETRIC STUDY

The effects of the GSI type, number of stories, and configuration of GG couples were evaluated in terms of eight performance indicator parameters under different earthquake motions. Shaking table test results were investigated considering these parameters. The effectiveness and efficiency of the proposed GSI system were evaluated among 12 cases. Each experimental case was compared with the others regarding previously defined performance parameters. Benefits and drawbacks of the proposed system were investigated through each parameter for each experimental case regarding the soil-structure interaction (SSI).

In the following parts, seismic responses of the defined cases under Kocaeli, El Centro and Kobe earthquakes with real PGA values and cyclic sinusodial motions were introduced regarding the eight performance parameters which are top story and foundation acceleration responses, first and top story drifts, top floor and foundation Arias intensities, base shear and base moment.

5.1. Seismic Response of the Cases under Earthquake Motions with Real PGA values and Cyclic Sinusodial Motions

Eight performance parameters were evaluated under real PGA values and specified cyclic sinusodial motion. The results of each case were tabulated one by one under Kocaeli, Kobe and El Centro earthquakes. Moreover, frequency values of 11.65 Hz and 17.17 Hz were used for five and three story buildings as cyclic sinusodial motions, respectively.

As seen in Table 5.1, GSI1-CL1 (Case 1) provided better results under Kocaeli earthquake and cyclic sinusodial motions. Case 1 exbihited more efficiency in first story drift under Kocaeli earthquake. However, the lowest Arias intensity results were observed under Kocaeli earthquake compared to Kobe earthquake that produced no efficiency in top

floor Arias intensity. Case 1 provided more promising results in Arias intensity under El Centro earthquake among the other earthquake motions. On the other hand, all the indicator parameters in cyclic sinusodial motions underwent large amount of reduction percentage when compared to the earthquakes. When compared to other earthquakes, GSI 1 worked better under El Centro earthquake in the reduction of base shear and base moment. Furthermore, similarity was observed between the reduction values of base shear and base moment under cyclic sinusodial motions.

Table 5.1. Results of Performance Indicator Parameters for Case 1.

Case 1								
	Ground Motions							
	Kocaeli Earthquake (1999) PGA = 0.22g		El Centro Earthquake (1940) PGA = 0.35g		Kobe Earthquake (1995) PGA = 0.80g		Cyclic Sinusodial Motion 11.65 Hz	
Performance Indicator Parameters	% Reduction (%)							
	RMS	Peak	RMS	Peak	RMS	Peak	RMS	Peak
Top Floor Acceleration	8.27	6.87	-3.79	20.25	-3.69	-8.70	29.96	27.77
Foundation Acceleration	4.26	2.32	-7.79	7.52	0.95	12.08	20.10	15.96
Top Floor Drift	0.00	36.67	-63.89	-1.82	57.40	-54.74	37.33	45.95
First Story Drift	84.50	24.56	-44.93	44.44	-113.33	-105.00	43.96	48.69
Top Floor Arias Intensity	13.26		14.97		-2.8		52.52	
Foundation Arias Intensity	1.79		8.25		6.37		38.17	
Base Shear	7.90	6.30	-3.39	18.21	0.54	3.55	29.48	30.69
Base Moment	7.32	6.50	-2.38	18.35	-1.50	0.61	30.00	30.17

Against the earthquakes, more beneficial results were observed under Kocaeli earthquake for Case 2 (GSI1-CL2) as seen in Table 5.2. Enourmous reduction appeared in first story drift under Kocaeli earthquake. Also, persuasive results were obtained in first story drift under El Centro earthquake. When compared to other earthquakes, base shear and base moment underwent more reduction under El Centro earthquake in peak value, and under Kocaeli earthquake in RMS value. However, top story drift underwent more reduction under Kobe earthquake even than cyclic sinusodial motion.

Table 5.2. Results of Performance Indicator Parameters for Case 2.

Case 2								
	Ground Motions							
	Kocaeli Earthquake (1999) PGA = 0.22g		El Centro Earthquake (1940) PGA = 0.35g		Kobe Earthquake (1995) PGA = 0.80g		Cyclic Sinusodial Motion 11.65 Hz	
Performance Indicator Parameters	% Reduction (%)							
	RMS	Peak	RMS	Peak	RMS	Peak	RMS	Peak
Top Floor Acceleration	12.52	0.92	8.40	5.97	-5.73	-6.47	20.46	17.90
Foundation Acceleration	12.57	7.19	10.09	5.56	7.70	13.72	18.34	3.28
Top Floor Drift	37.50	24.17	-38.89	-18.18	68.56	18.42	10.67	16.89
First Story Drift	94.50	60.53	35.34	69.44	20.00	38.33	26.37	29.84
Top Floor Arias Intensity	15.44		2.79		-16.96		32.66	
Foundation Arias Intensity	12.50		6.19		11.16		29.00	
Base Shear	13.01	10.68	8.47	13.10	1.65	5.61	20.52	17.88
Base Moment	12.20	9.35	7.14	12.84	-1.53	3.34	20.66	19.18

Case 3 (GSI2-CL2) provided huge reduction in the first story drift under Kocaeli earthquake. Also, great reduction values were observed under cyclic sinusodial motion. In overall, great amount of reduction percentages was provided under cyclic sinusodial motion. Under El Centro earthquake, Case 3 produced promising reduction values in top floor drift. However, reduction in foundation Arias intensity values produced by Case 3 under Kobe earthquake was more reliable among the other earthquakes. Additionally, results in base shear and base moment underwent more reduction under El Centro earthquake in peak value, and under Kocaeli earthquake in RMS value as seen in Table 5.3.

Table 5.3. Results of Performance Indicator Parameters for Case 3.

Case 3								
	Ground Motions							
	Kocaeli Earthquake (1999) PGA = 0.22g		El Centro Earthquake (1940) PGA = 0.35g		Kobe Earthquake (1995) PGA = 0.80g		Cyclic Sinusodial Motion 11.65 Hz	
Performance Indicator Parameters	% Reduction (%)							
	RMS	Peak	RMS	Peak	RMS	Peak	RMS	Peak
Top Floor Acceleration	16.48	11.97	3.50	17.18	-8.86	-10.15	53.35	44.08
Foundation Acceleration	10.25	5.30	1.60	12.31	6.04	8.77	33.96	21.14
Top Floor Drift	-4.17	15.00	-44.44	43.64	22.92	-11.05	62.67	57.43
First Story Drift	92.50	40.35	57.64	2.78	20.00	8.33	56.04	51.31
Top Floor Arias Intensity	17.78		11.84		-18.71		76.13	
Foundation Arias Intensity	1.79		7.22		11.95		52.18	
Base Shear	14.72	10.96	3.39	21.73	0.17	5.05	52.17	44.35
Base Moment	17.07	11.79	2.38	21.56	-3.59	5.17	53.20	45.75

Case 4 (GSI2-CL1) provided great reduction values in first story drift and top floor drift under Kocaeli and Kobe earthquakes, respectively. Case 4 was not fully functional under El Centro earthquake. On the other hand, the largest reduction values were observed under cyclic sinusodial motion. However, alleviation under Kocaeli earthquake was larger than cyclic sinusodial motion. Furthermore, GSI 2 functioned more properly under Kocaeli earthquake in reducing the effect of base shear and base moment as seen in Table 5.4.

Table 5.4. Results of Performance Indicator Parameters for Case 4.

Case 4								
	Ground Motions							
	Kocaeli Earthquake (1999) PGA = 0.22g		El Centro Earthquake (1940) PGA = 0.35g		Kobe Earthquake (1995) PGA = 0.80g		Cyclic Sinusodial Motion 11.65 Hz	
Performance Indicator Parameters	% Reduction (%)							
	RMS	Peak	RMS	Peak	RMS	Peak	RMS	Peak
Top Floor Acceleration	21.78	10.85	-18.19	4.51	-4.00	-11.51	31.46	29.14
Foundation Acceleration	21.08	8.30	-12.57	-2.20	10.07	14.68	11.98	-4.13
Top Floor Drift	12.50	33.33	-27.78	41.82	80.12	25.79	38.67	47.97
First Story Drift	92.50	63.16	29.77	-55.56	30.00	2.50	36.26	43.46
Top Floor Arias Intensity	9.83		-0.89		-18.18		53.03	
Foundation Arias Intensity	5.36		6.19		11.55		22.50	
Base Shear	21.54	13.97	-16.95	8.63	4.13	4.11	30.64	30.76
Base Moment	21.95	13.41	-19.05	8.72	0.32	1.52	31.60	32.27

Under the earthquakes, Arias intensity underwent maximum reduction under El Centro earthquake (Table 5.5). Also, Case 5 (GSI3-CL2) provided more reliable reduction values only under Kocaeli earthquake in the first story drift. Moreover, top floor drift underwent more reduction under El Centro earthquake. Larger reduction values in base shear and base moment were observed under El Centro earthquake.

Table 5.5. Results of Performance Indicator Parameters for Case 5.

Case 5								
	Ground Motions							
	Kocaeli Earthquake (1999) PGA = 0.22g		El Centro Earthquake (1940) PGA = 0.35g		Kobe Earthquake (1995) PGA = 0.80g		Cyclic Sinusodial Motion 11.65 Hz	
Performance Indicator Parameters	% Reduction (%)							
	RMS	Peak	RMS	Peak	RMS	Peak	RMS	Peak
Top Floor Acceleration	17.18	8.40	28.86	29.80	-7.84	2.75	35.13	32.57
Foundation Acceleration	15.86	4.52	25.49	14.01	-1.90	10.17	24.60	4.62
Top Floor Drift	-16.67	55.00	67.22	12.73	-21.70	-12.11	36.00	37.84
First Story Drift	85.05	28.07	23.08	-8.33	10.00	-38.33	35.16	18.32
Top Floor Arias Intensity	14.20		20.11		-0.70		56.57	
Foundation Arias Intensity	7.14		12.37		10.36		41.30	
Base Shear	16.43	7.67	28.81	27.80	-3.00	6.73	34.54	32.40
Base Moment	17.07	7.72	28.57	28.44	-5.09	6.99	35.00	34.17

Case 6 (GSI3-CL1) worked better in reducing Arias intensity under El Centro earthquake. On the other hand, GSI 3 functioned well in alleviation of first story drift under Kocaeli earthquake. Moreover, top floor drift underwent more reduction under El Centro earthquake than others. Case 6 was less effective under Kobe earthquake. In overall, results were undergone mostly under cyclic sinusodial motion (Table 5.6). In reducing the values of base shear and base moment, GSI 3 worked more appropriately under El Centro and Kocaeli earthquakes in peak and RMS values, respectively.

Table 5.6. Results of Performance Indicator Parameters for Case 6.

Case 6								
	Ground Motions							
	Kocaeli Earthquake (1999) PGA = 0.22g		El Centro Earthquake (1940) PGA = 0.35g		Kobe Earthquake (1995) PGA = 0.80g		Cyclic Sinusodial Motion 11.65 Hz	
Performance Indicator Parameters	% Reduction (%)							
	RMS	Peak	RMS	Peak	RMS	Peak	RMS	Peak
Top Floor Acceleration	29.70	9.53	-3.79	20.25	8.00	-3.79	44.88	36.19
Foundation Acceleration	29.59	8.96	-7.79	7.52	10.31	-1.41	18.91	-0.43
Top Floor Drift	37.50	54.17	38.89	67.27	6.69	-4.74	37.33	36.49
First Story Drift	92.05	63.16	49.83	-33.33	30.00	12.50	50.55	45.03
Top Floor Arias Intensity	16.22		24.80		3.67		63.74	
Foundation Arias Intensity	12.50		12.37		8.76		21.53	
Base Shear	30.07	9.32	16.95	26.20	11.00	3.55	43.21	36.27
Base Moment	29.27	9.76	19.05	27.98	9.76	5.47	44.60	37.46

Against the earthquakes, it is obvious that all the performance indicator parameters underwent more reduction under Kocaeli earthquake when compared to other earthquakes as seen in Table 5.7. Case 7 (GSI3-CL1) functioned fully in story drift in RMS value under Kocaeli earthquake. Again, GSI 3 was not efficient under Kobe earthquake. However, Arias intensities underwent more reduction under cyclic sinusodial motion. Besides, Case 7 worked better under Kocaeli earthquake in reducing base shear and base moment of the structure when compared to other earthquakes.

Table 5.7. Results of Performance Indicator Parameters for Case 7.

Case 7								
	Ground Motions							
	Kocaeli Earthquake (1999) PGA = 0.22g		El Centro Earthquake (1940) PGA = 0.35g		Kobe Earthquake (1995) PGA = 0.80g		Cyclic Sinusodial Motion 17.17 Hz	
Performance Indicator Parameters	% Reduction (%)							
	RMS	Peak	RMS	Peak	RMS	Peak	RMS	Peak
Top Floor Acceleration	27.82	-10.11	15.64	-1.69	1.08	-14.37	32.33	29.13
Foundation Acceleration	34.87	22.45	22.22	6.59	9.37	-22.66	29.98	23.90
Top Floor Drift	98.98	-22.13	18.52	-20.89	-15.38	-54.10	40.91	33.33
First Story Drift	95.83	24.07	27.40	-46.67	24.00	-10.06	44.00	37.97
Top Floor Arias Intensity	14.76		-4.10		-26.74		49.29	
Foundation Arias Intensity	30.67		12.00		-6.09		45.77	
Base Shear	33.33	11.76	5.76	-2.56	17.18	-5.10	32.28	27.20
Base Moment	33.33	4.35	3.58	4.00	15.68	-8.26	32.35	27.84

Under the earthquakes, GSI 3 worked more appropriately for all the performance indicator parameters under Kocaeli earthquake by exhibiting more reduction when compared to other earthquakes. Case 8 (GSI3-CL2) functioned fully in top story drift in RMS value under Kocaeli earthquake. Again, GSI 3 was not efficient under Kobe earthquake. However, Arias intensities underwent more reduction under cyclic sinusodial motion. When compared to other earthquakes, Case 8 worked better under Kocaeli earthquake in reducing base shear and base moment values as seen in Table 5.8.

Table 5.8. Results of Performance Indicator Parameters for Case 8.

Case 8								
	Ground Motions							
	Kocaeli Earthquake (1999) PGA = 0.22g		El Centro Earthquake (1940) PGA = 0.35g		Kobe Earthquake (1995) PGA = 0.80g		Cyclic Sinusodial Motion 17.17 Hz	
Performance Indicator Parameters	% Reduction (%)							
	RMS	Peak	RMS	Peak	RMS	Peak	RMS	Peak
Top Floor Acceleration	28.19	-12.59	20.57	-0.12	3.23	-27.74	32.76	29.13
Foundation Acceleration	35.48	26.58	25.40	10.62	10.57	-17.32	31.47	28.21
Top Floor Drift	99.13	10.66	33.33	-23.42	-10.26	-34.43	22.73	0.00
First Story Drift	79.17	25.31	78.08	8.89	16.00	-21.38	40.00	31.65
Top Floor Arias Intensity	15.66		3.00		-21.30		48.33	
Foundation Arias Intensity	32.00		14.00		-3.48		46.36	
Base Shear	33.33	10.70	7.07	-3.70	21.86	2.04	33.07	27.35
Base Moment	33.33	1.19	5.30	-0.80	20.66	-2.34	32.94	27.84

Against the earthquakes, GSI1-SL (Case 9) worked more appropriately for all the performance indicator parameters under Kocaeli earthquake by exhibiting more reduction when compared to other earthquakes. However, foundation acceleration and first story drift underwent more reduction under El Centro earthquake in peak value. Moreover, GSI 1 was not efficient under Kobe earthquake. However, Arias intensities underwent more reduction under cyclic sinusodial motion. Furhermore, maximum reduction values in base shear and base moment were observed under El Centro earthquake. Instead of large reduction values in RMS value under Kocaeli earthquake, increase in base shear and base moment values were obtained as seen in Table 5.9.

Table 5.9. Results of Performance Indicator Parameters for Case 9.

Case 9								
	Ground Motions							
	Kocaeli Earthquake (1999) PGA = 0.22g		El Centro Earthquake (1940) PGA = 0.35g		Kobe Earthquake (1995) PGA = 0.80g		Cyclic Sinusodial Motion 11.65 Hz	
Performance Indicator Parameters	% Reduction (%)							
	RMS	Peak	RMS	Peak	RMS	Peak	RMS	Peak
Top Floor Acceleration	27.32	-7.02	20.58	21.44	-5.18	-10.03	29.65	34.25
Foundation Acceleration	27.85	1.86	14.34	15.73	-0.12	-6.92	31.73	21.82
Top Floor Drift	20.83	33.33	11.11	-145.45	-52.13	-22.11	34.67	37.84
First Story Drift	66.50	36.84	-78.37	68.89	-6.67	-51.67	26.37	40.31
Top Floor Arias Intensity	2.81		27.04		-5.59		48.92	
Foundation Arias Intensity	0.00		14.43		4.38		51.89	
Base Shear	26.66	-3.29	20.34	19.81	-4.67	-0.93	29.62	34.05
Base Moment	29.27	-5.28	21.43	20.64	-6.32	-0.91	29.60	34.77

Under the earthquakes, GSI2-SL (Case 10) worked appropriately under all seismic motions. However, foundation acceleration and first story drift underwent more reduction under El Centro earthquake in peak value. Moreover, GSI 2 was more efficient in top floor drift under Kobe earthquake in peak value. However, Arias intensities underwent more reduction under cyclic sinusodial motion. Great reduction percentages were observed under Kocaeli earthquake in base shear and base moment in RMS values. On the other hand, GSI 2 demonstrated larger reduction values under El Centro earthquake in base shear and base moment in peak values (Table 5.10).

Table 5.10. Results of Performance Indicator Parameters for Case 10.

Case 10								
	Ground Motions							
	Kocaeli Earthquake (1999) PGA = 0.22g		El Centro Earthquake (1940) PGA = 0.35g		Kobe Earthquake (1995) PGA = 0.80g		Cyclic Sinusodial Motion 11.65 Hz	
Performance Indicator Parameters	% Reduction (%)							
	RMS	Peak	RMS	Peak	RMS	Peak	RMS	Peak
Top Floor Acceleration	59.87	5.36	30.55	26.57	20.47	-8.03	54.67	37.61
Foundation Acceleration	59.77	8.99	24.25	13.80	21.68	-0.88	27.92	7.65
Top Floor Drift	45.83	20.83	38.89	27.27	-123.12	64.63	57.33	45.95
First Story Drift	76.50	-18.42	-44.93	70.56	46.67	60.83	58.24	43.46
Top Floor Arias Intensity	9.83		31.40		10.66		76.80	
Foundation Arias Intensity	5.36		18.56		13.55		41.32	
Base Shear	59.07	7.67	30.51	23.00	21.50	2.24	53.03	36.77
Base Moment	60.98	6.50	30.95	24.77	21.65	3.65	54.40	38.86

GSI3-SL (Case 11) worked appropriately under Kobe earthquake in reducing first story drift among the earthquakes. However, foundation acceleration and top story drift underwent more reduction under Kocaeli earthquake. Moreover, GSI 3 was more efficient in top story drift under Kobe earthquake in peak value. However, Arias intensities underwent more reduction under cyclic sinusodial motion. GSI 3 provided more promising results under El Centro earthquake in reducing base shear and base moment as seen in Table 5.11.

Table 5.11. Results of Performance Indicator Parameters for Case 11.

Case 11								
	Ground Motions							
	Kocaeli Earthquake (1999) PGA = 0.22g		El Centro Earthquake (1940) PGA = 0.35g		Kobe Earthquake (1995) PGA = 0.80g		Cyclic Sinusodial Motion 11.65 Hz	
Performance Indicator Parameters	% Reduction (%)							
	RMS	Peak	RMS	Peak	RMS	Peak	RMS	Peak
Top Floor Acceleration	29.18	12.70	27.76	31.82	11.14	-13.15	55.12	45.09
Foundation Acceleration	27.47	16.55	16.64	16.15	13.63	-1.65	21.09	-11.83
Top Floor Drift	25.00	62.50	11.11	58.18	43.2	13.68	60	58.11
First Story Drift	10.00	4.39	-89.52	-155.56	13.13	75.00	61.54	50.79
Top Floor Arias Intensity	18.72		39.55		6.47		75.64	
Foundation Arias Intensity	12.50		19.59		11.55		25.67	
Base Shear	28.36	4.11	25.42	21.09	12.80	1.12	52.75	41.85
Base Moment	29.27	3.25	28.57	24.77	11.76	-0.30	54.60	45.85

Case 12 (GSI3-SL) worked more appropriately under Kocaeli earthquake in reducing all the performance indicator parameters among the earthquakes. However, foundation

acceleration and top story drift underwent more reduction under Kocaeli earthquake as seen in Table 5.12. Moreover, GSI 3 was more efficient in first story drift under El Centro earthquake in peak value. However, Arias intensities underwent more reduction under cyclic sinusodial motion. When compared to other earthquakes, GSI 3 showed more efficiency in reducing base shear and base moment under Kocaeli earthquake.

Table 5.12. Results of Performance Indicator Parameters for Case 12.

Case 12								
	Ground Motions							
	Kocaeli Earthquake (1999) PGA = 0.22g		El Centro Earthquake (1940) PGA = 0.35g		Kobe Earthquake (1995) PGA = 0.80g		Cyclic Sinusodial Motion 17.17 Hz	
Performance Indicator Parameters	% Reduction (%)							
	RMS	Peak	RMS	Peak	RMS	Peak	RMS	Peak
Top Floor Acceleration	46.54	2.56	29.11	4.87	19.62	-0.41	50.35	46.05
Foundation Acceleration	43.01	18.20	-47.04	-43.49	15.47	-6.07	49.40	45.49
Top Floor Drift	98.98	45.08	3.70	1.27	-5.13	-25.14	36.36	16.67
First Story Drift	91.67	80.86	-16.44	95.11	-8.00	27.04	60.00	50.63
Top Floor Arias Intensity	32.23		34.23		12.39		67.42	
Foundation Arias Intensity	24.00		-82.00		3.48		66.63	
Base Shear	47.22	18.18	20.94	2.85	3.95	-14.29	51.18	41.11
Base Moment	46.67	14.49	22.15	6.40	24.04	5.52	51.31	42.27

Effects of the proposed GSI system for defined cases were evaluated under Kocaeli, El Centro and Kobe earthquakes with increasing PGA values and cyclic sinusodial motions with varying frequencies. The mentioned eight performance parameters were investigated.

5.2. Effects of the Proposed GSI System on Performance Indicator Parameters under Earthquake Motions with Increasing PGA and Cyclic Sinusodial Motion with Various Frequencies

Investigation of the proposed GSI system was performed considering eight performance indicator parameters under distinctive seismic ground motions. These evaluations were conducted regarding increasing peak ground accelerations and cyclic sinusodial motions with different frequencies of the seismic excitations. Using these results,

effects of acceleration amplitudes and frequency content of the input ground motions on the proposed GSI systems were evaluated.

Input values were given in Table 4.1 and Table 4.2 in Section 4. For Kocaeli earthquakes, 0.22g, 0.34g and 0.50g acceleration amplitudes were used in the experiments. Acceleration amplitudes of 0.35g, 0.46g, 0.55g, 0.72g, 0.81g and 0.89g were used for El Centro earthquake. In the cases of Kobe earthquake, 0.74g, 0.80g and 0.89g as PGA values were used as input motions. As cyclic sinusodial motions, frequency values were taken from the free vibration tests. These are 3.67 Hz, 11.65 Hz, 18.38 Hz, 24.05 Hz and 27.55 Hz for the five story building model. On the other hand, three story building model was tested under 5.57 Hz, 17.17 Hz and 25.4 Hz.

5.2.1. Effects of Proposed GSI System on Top Floor Acceleration

Figure 5.1 demonstrates the graphical representation of the reduction percentages of top floor acceleration in the proposed GSI system using curve shaped liner with varying frequency and amplitude. According to the obtained results, Case 6 which is the couple of Typar DuPont SF56 with PTFE 1 mm geomembrane revealed the best results for the configuration type CL 1 and for the five story building compared to three story building having same configuration type under Kocaeli earthquake. Three story building was influenced in PGA values higher than 0.30g and Case 8 exhibited maximum reduction as 21% at 0.50g. However, Case 3 with CL2 provided better results until 0.35g. Therefore, GSI 3 provided more promising results when looked into overall view of the results. Under Kobe earthquake, only Case 1, Case 5 and Case 6 functioned properly. It means, three story building could not show resistance and other cases including for five story building were not beneficial under Kobe earthquake. Furthermore, GSI 3 was more beneficial geosynthetic couple in the case of Kobe earthquake. Also, Case 5 with CL2 reacted significantly in the reduction of the top floor acceleration. Case 1, Case 5 and Case 6 worked properly until 0.76g, 0.78g and 0.82g, respectively. As seen from Figure 5.1c, three story building did not exhibited resistance against El Centro earthquake in PGA values higher than 0.55g. However, five story building showed more reliable values under the same earthquake. The

most efficient GSI application appeared as Case 1 with CL1. It indicated the maximum reduction as 30% at 0.22g. In overall, workability range of the cases on five story building was between 0.50g and 0.80g. The most effective synthetic liner was observed as GSI 1 when compared to others. GG couples lost their efficiency in PGA values higher than 0.78g for the five story building. Besides, reduction in PGA was observed only in three story building between 20 and 25 Hz. Effective range of the proposed GSI system was observed as 5 and 20 Hz. Three story building demonstrated constant reduction trend throughout the frequency range. Hence, GSI 3 appeared to be the most efficient synthetic liner. However, Case 3 in which GSI 2 was used with CL2 demonstrated maximum reduction of the system at 13 Hz as 45%.

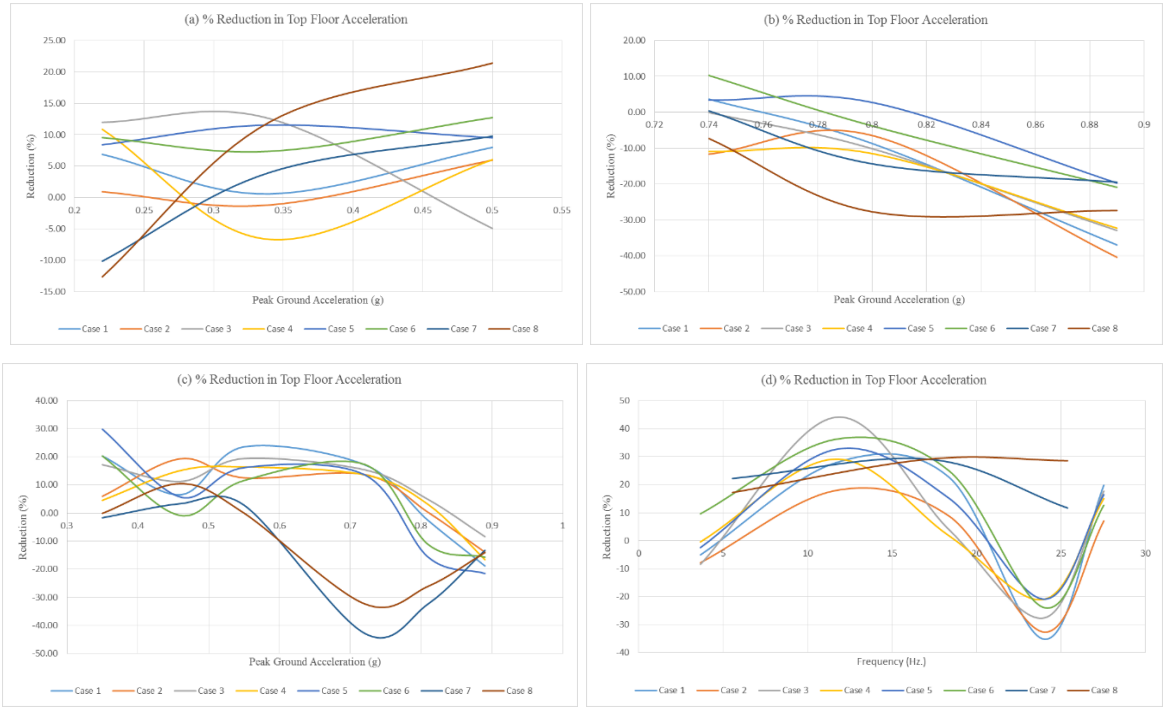

Figure 5.1. Reduction in Top Floor Acceleration under (a) Kocaeli Earthquake, (b) Kobe Earthquake, (c) El Centro Earthquake, (d) Cyclic Sinusodial Motion for GSI-CL.

When the another alternative of proposed GSI system was considered, Figure 5.2 illustrates the effects of the foundation isolation using straight liner. All cases functioned properly and GSI 3 worked more better than others under Kocaeli earthquake. However, Case 9 including GSI 1 as synthetic liner demonstrated resistance against Kocaeli earthquake in PGA values higher than 0.35g. When compared to the configuration type of proposed GSI

system, similarity in the reduction values and behaviors were observed between curved shape liner and straight liner. However, maximum reduction was obtained at 0.50g as 27%. Besides, increase in reduction values stood out with increasing PGA values under Kocaeli earthquake. Similarly, behavior of the proposed GSI system with straight liner was similar to the curve shaped liner. However, only GSI 3 provided reduction under Kobe earthquake until 0.80g. When compared to curve shaped liner, straight liner improved the performance of the GSI 3 and provided a little bit more reduction at 0.74g. Similar behavior was observed between straight liner and curved liner under El Centro earthquake. However, maximum reduction was obtained as 42% in the existance of straight liner while 23% reduction appeared as maximum of curved liner. Moreover, three story building demonstrated more resistance up to 0.75g in straight liner when compared to curved liner. Also, GSI 1 appeared to be the most efficient synthetic couple in reducing the top floor acceleration under El Centro earthquake. The most similar behavior was observed in frequency range. There were no significant differences between curve shaped liner and straight liner under cyclic sinusodial motions.

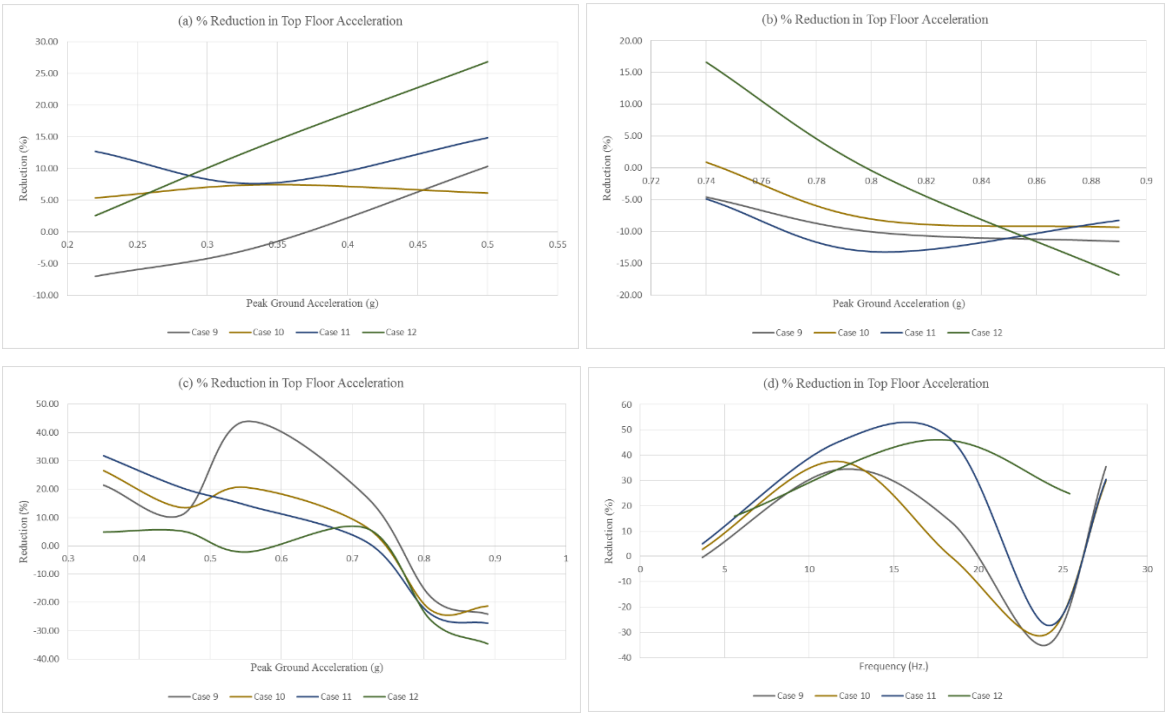

Figure 5.2. Reduction in Top Floor Acceleration under (a) Kocaeli Earthquake, (b) Kobe Earthquake, (c) El Centro Earthquake, (d) Cyclic Sinusodial Motion for GSI-SL.

5.2.2. Effects of Proposed GSI System on Foundation Acceleration

Figure 5.3 illustrates the variation of foundation acceleration with different PGA and frequency values under different ground motions. It was clearly observed that GSI 3 worked more appropriately than the other synthetic couples under Kocaeli earthquake. Also, GG couples on three story building exhibited more reduction than those on five story building in higher PGA values. Maximum reduction was observed as 28% at 0.22g on three story building. Among the cases on five story building, the most efficient one appeared as Case 6 with CL1. GG couples under the five story building lost their effectiveness in PGA values higher than 0.35g. In general, cases with shorter GG liner provided more promising results under Kocaeli earthquake. Furthermore, Case 1, Case 2, Case 3, Case 4 and Case 5 provided similar reduction percentages in the whole PGA range under Kobe earthquake. Also, GSI 1 appeared to be the most efficient synthetic liner type. The presence of CL2 improved the performance of the proposed GSI system under Kobe earthquake. Moreover, three story building underwent more reduction between 0.40 and 0.50g when compared to the five story building under El Centro earthquake. It can be stated from the Case 1, Case 4, Case 6 and Case 7 that synthetic liner with longer GG liner indicated more resistance against earthquake. Additionally, model buildings experienced more reduction with the influence of GSI 3 under El Centro earthquake. Using GSI 3 also improved the performance of the proposed GSI system under cyclic sinusodial motion, especially at higher frequency values. On the other hand, three story building experienced more reduction at lower frequency values. Using the configuration type of CL1 enhanced the results under cyclic sinusodial motion.

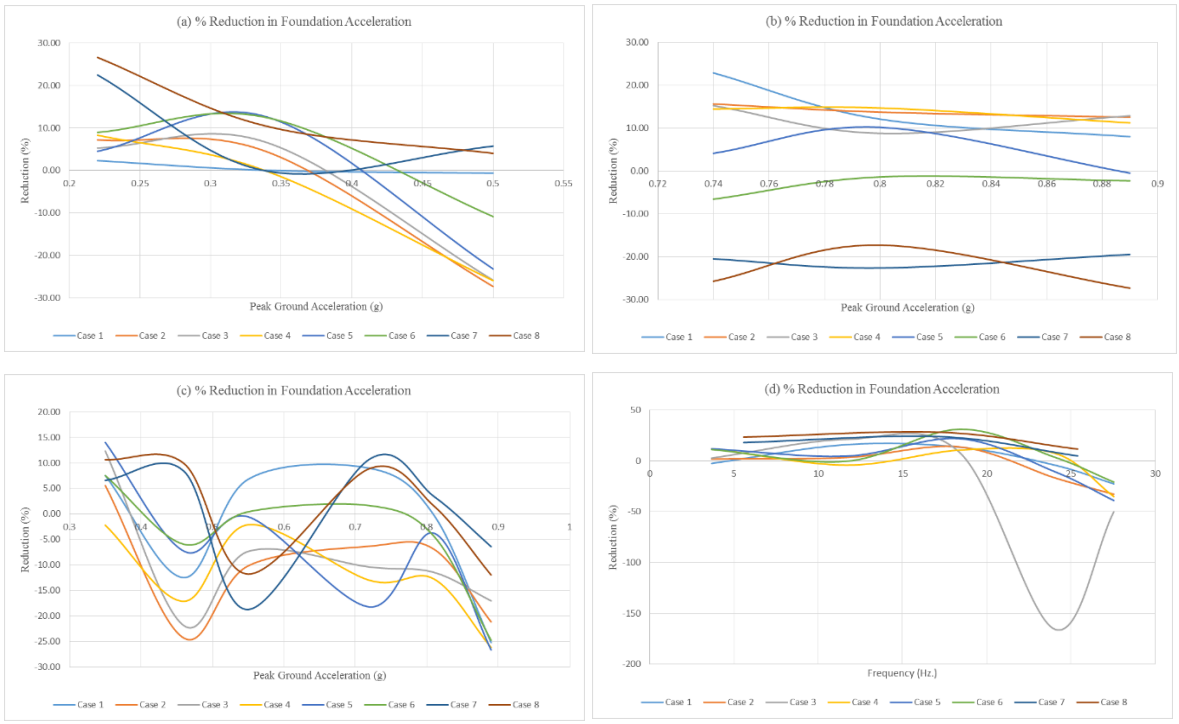

Figure 5.3. Reduction in Foundation Acceleration under (a) Kocaeli Earthquake, (b) Kobe Earthquake, (c) El Centro Earthquake, (d) Cyclic Sinusodial Motion for GSI-CL.

As given in Figure 5.4, GSI 1 provided tremendous reduction about 90% under Kocaeli earthquake by the means of straight liner. The other cases lost their effects in PGA values higher than 0.40 and 0.45g. It was obviously seen that five story building experienced more reduction in the presence of GSI 1 under Kocaeli earthquake. Under Kobe earthquake, only straight liner GSI 2 functioned properly in PGA values higher than 0.80g. The other cases did not work under Kobe earthquake. GSI 2 worked better at higher amplitudes while Case 12 reacted beneficially at lower amplitudes. Also, five story building experienced more reduction at higher PGA values. On the other hand, three story building underwent more reduction at lower PGA values. Furthermore, three story building model exhibited more reliable reduction values when compared to the five story building under cyclic sinusodial motion. On the five story building model, Case 11 provided more promising results than the others. It means, GSI 3 performed more properly than other types of synthetic liner under cyclic sinusodial motion. When comparison was done between curve shaped liner and straight liner, large discreapancies were observed under the seismic ground motions, except Kocaeli earthquake. Better results were obtained in the presence of curved liner instead of straight liner.

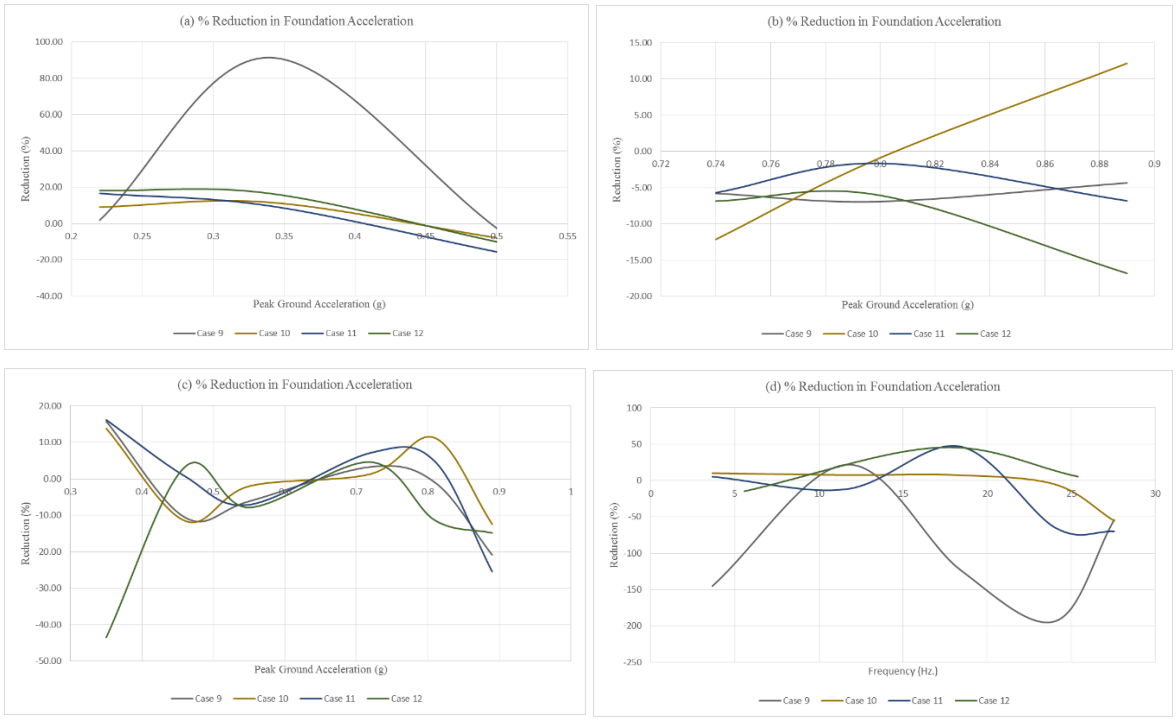

Figure 5.4. Reduction in Foundation Acceleration under (a) Kocaeli Earthquake, (b) Kobe Earthquake, (c) El Centro Earthquake, (d) Cyclic Sinusodial Motion for GSI-SL.

5.2.3. Effects of Proposed GSI System on Top Floor Drift

Figure 5.5 demonstrates the reduction percentages of top floor drift under different seismic excitations. Five story building underwent more reduction than three story building. Also, GSI 3 was seemed to be the most efficient synthetic liner at lower acceleration amplitudes. However, GSI 2 appeared as the most effective geosynthetic couple at higher acceleration amplitudes, especially in PGA values higher than 0.30g. Moreover, synthetic liner with CL1 improved the effectiveness of the proposed GSI system under Kocaeli earthquake. However, GSI 1 was not effective between 0.78 and 0.84g. On the other hand, GSI 2 exhibited more efficiency between 0.78 and 0.84g. Besides, three story building experienced no beneficial effects on top floor drift. However, Case 8 indicated some reduction in PGA values higher than 0.86g under Kobe earthquake. The destructive effects of El Centro earthquake were reduced much more in the presence of GSI 1 liner, especially between 0.50 and 0.80g with a maximum reduction of about 90%. Additionally, three story

building showed reduction in top floor drift only at about 0.80g. However, there was no specific efficiency about the configuration type under El Centro earthquake. Furthermore, the presence of CL1 provided more reliable results under cyclic sinusodial motion as seen in Figure 5.5d. Also, GSI 3 demonstrated more reduction than other synthetic couples, particularly at higher PGA values. It is obvious that five story building experienced more reduction than three story building under cyclic sinusodial motion.

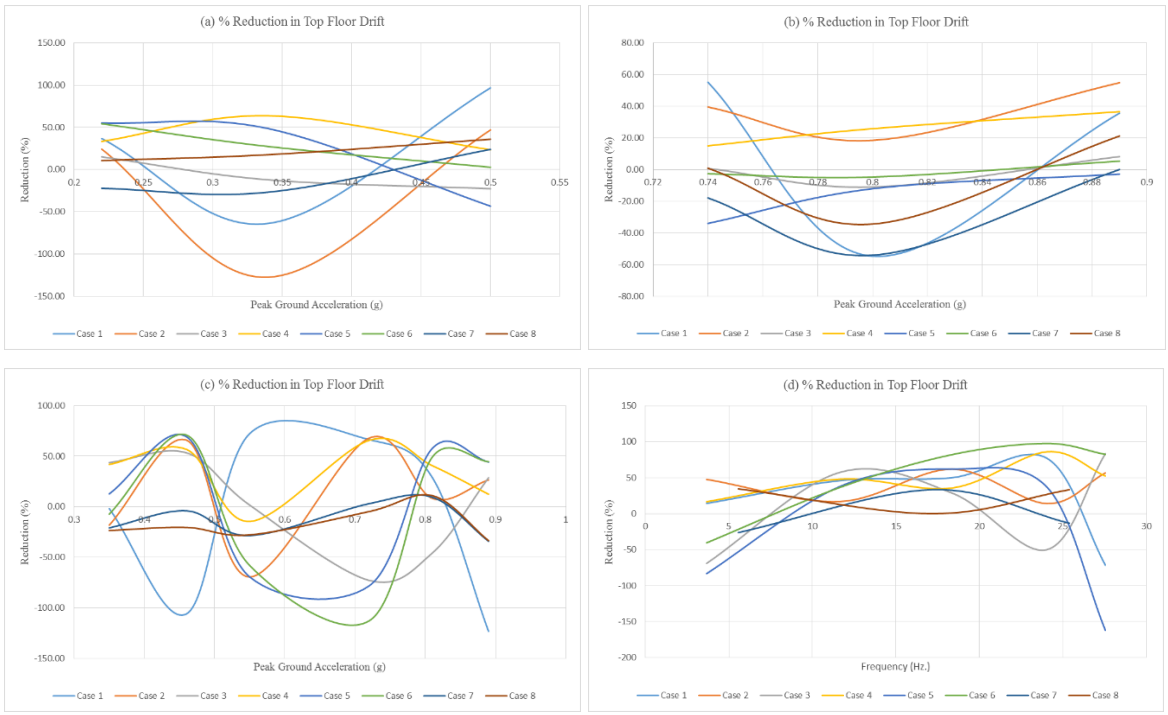

Figure 5.5. Reduction in Top Floor Drift under (a) Kocaeli Earthquake, (b) Kobe Earthquake, (c) El Centro Earthquake, (d) Cyclic Sinusodial Motion for GSI-CL.

Effect of foundation isolation using straight liner with varying acceleration amplitude and frequency contents was illustrated in Figure 5.6. GSI 3 provided more efficiency under Kocaeli earthquake. However, GSI 2 reacted better in top floor drift under Kobe earthquake. Besides, three story building experienced less reduction after 0.45g under Kocaeli earthquake and gained resistance against PGA values higher than 0.86g under Kobe earthquake. Eventhough Case 10 and Case 11 were seemed to be the most two effective GSI system, they lost their effects in PGA values higher than 0.82g under Kobe earthquake. Furthermore, five story building underwent more reduction than three story building under Kocaeli, Kobe and El Centro earthquakes, and cyclic sinusodial motion. GSI 2 provided

more reliable results between 20 and 25 Hz while GSI 3 demonstrated more reduction between 15 and 20 Hz. Under El Centro earthquake, GSI 2 exhibited more reduction at lower PGA values. On the other hand, GSI 3 improved the performance of the GSI system at higher PGA values under El Centro earthquake. Only similarity in behavior and reduction percentages between curved and straight liner was observed under cyclic sinusodial motion. Although there were some differencies between the configuration types, curve shaped liner was seemed to be more efficient configuration type.

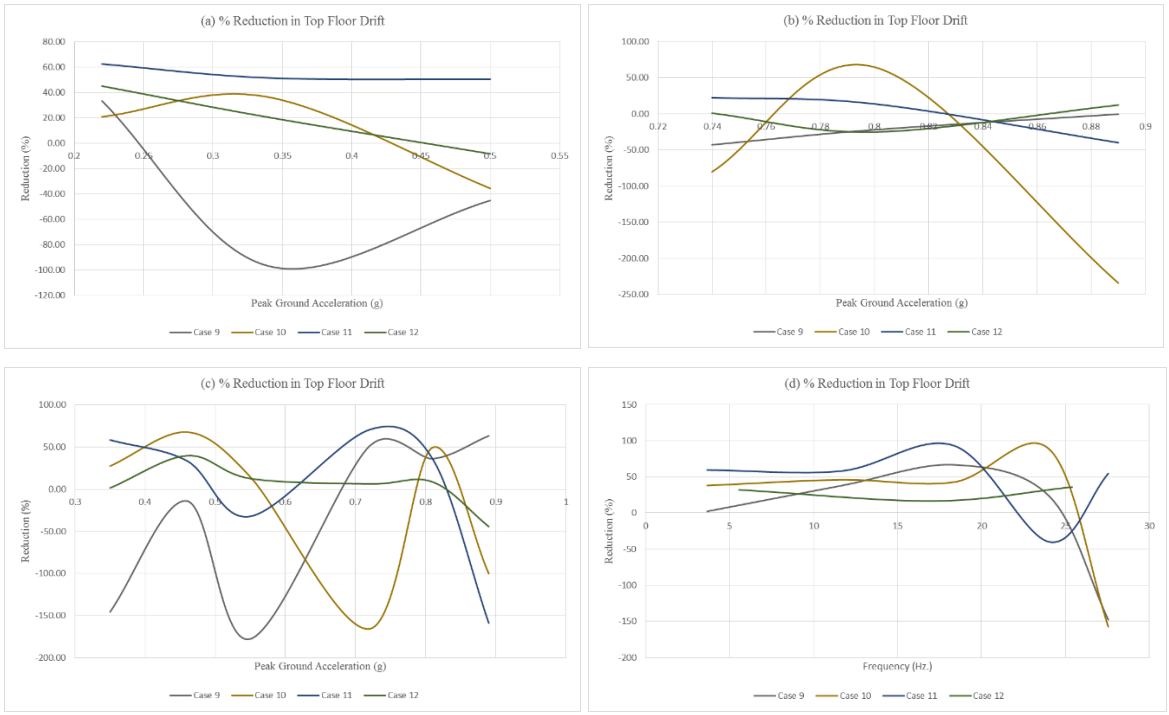

Figure 5.6. Reduction in Top Floor Drift under (a) Kocaeli Earthquake, (b) Kobe Earthquake, (c) El Centro Earthquake, (d) Cyclic Sinusodial Motion for GSI-SL.

5.2.4. Effects of Proposed GSI System on First Floor Drift

More reduction was observed on three story buildings under Kocaeli earthquake as seen in Figure 5.7a. However, three story building showed no reduction under Kobe earthquake as seen in Figure 5.7b. While geosynthetic couple with the configuration type of CL1 provided more reliable results at the lower amplitudes under Kocaeli earthquake, GG

couple with CL2 enhanced the performance of the GSI system under Kobe earthquake. Besides, three story building experienced more reduction than five story building at lower PGA values and about 0.80g. GSI system showed its effectiveness on the five story building in PGA values higher than 0.50g under El Centro earthquake. Besides, GSI 2 provided more reliable results under El Centro earthquake. Also, no specific configuration type was determined under El Centro earthquake. For the five story building, effects of GSI 2 outweighed the efficiency of GSI 1 when looked into overall under cyclic sinusodial motion. In three story building model, Case 8 reacted better between 10 and 17 Hz while Case 7 initiated working in frequency values higher than 15 Hz. It can also be concluded that GG liner with the configuration type of CL1 improved the performance of the GSI system.

Figure 5.7. Reduction in First Floor Drift under (a) Kocaeli Earthquake, (b) Kobe Earthquake, (c) El Centro Earthquake, (d) Cyclic Sinusodial Motion for GSI-CL.

Figure 5.8 indicated the effectiveness of the straight liner on first floor drift. In overall, GSI 3 enhanced the seismic performance of the proposed GSI system better under Kocaeli and Kobe earthquakes as well as cyclic sinusodial motion. Besides, three story building experienced more reduction only under Kocaeli earthquake while five story building underwent more reduction under Kobe and El Centro earthquake as well as cyclic sinusodial motion. GSI 1 and GSI 2 did not work properly under Kobe and Kocaeli earthquakes, respectively. When compared to curved liner, straight liner provided more promising results.

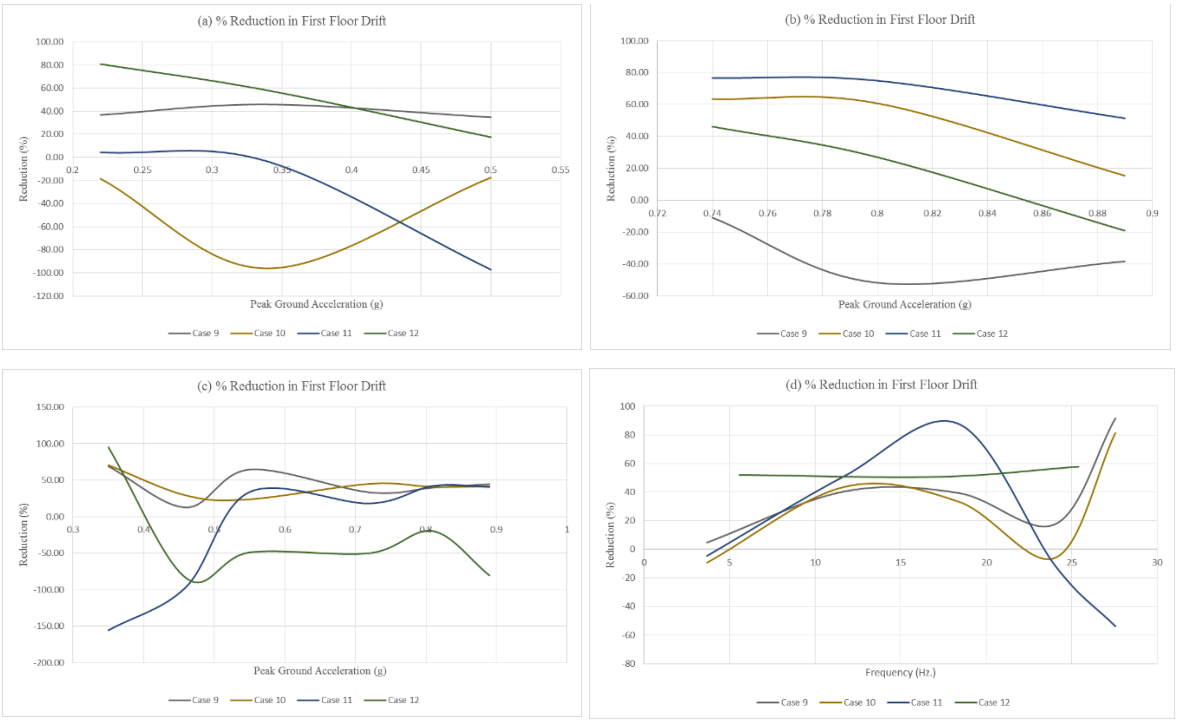

Figure 5.8. Reduction in First Floor Drift under (a) Kocaeli Earthquake, (b) Kobe Earthquake, (c) El Centro Earthquake, (d) Cyclic Sinusodial Motion for GSI-SL.

5.2.5. Effects of Proposed GSI System on Top Floor Arias Intensity

Figure 5.9 illustrates the reduction percentages of top floor Arias intensity with changing PGA values and frequencies. Three story building lost its resistance after 0.27g while the earliest five story building lost its resistance in PGA values higher than 0.35g, except Case 4 that lost its efficiency in PGA values higher than 0.27g under Kocaeli earthquake. GSI 3 provided the best results and CL2 appeared as the most efficient configuration type under Kocaeli earthquake. Moreover, GSI 3 was also the most efficient synthetic liner under the Kobe earthquake, especially for the five story building model because three story building did not show any action against the earthquake. It can be stated that the seismic performance of the system could be enhanced by using CL1 under Kobe earthquake. Additionally, three story building experienced substantial increase in top floor Arias intensity in PGA values higher than 0.50g under El Centro earthquake. Again, GSI 3

was seemed to be the most efficient geosynthetic couple, and no specific efficiency about configuration type was observed under El Centro earthquake. Furthermore, three story building demonstrated more experience in reduction under cyclic sinusodial motion in frequency values higher than 20 Hz as seen in Figure 5.9d. However, top floor Arias intensity was reduced mostly on five story building between 5 and 20 Hz. GSI 2 and GSI 3 were the most efficient GG couple types, and also no specific effective configuratin type was observed under cyclic sinusodial motion.

Figure 5.10 shows the results of foundation isolation using straight liner to evaluate top Arias intensity. When compared to other seismic excitations, it can be stated that GSI 3 worked better among the others under all seismic excitations. However, the efficiency of the Case 12 diminished in PGA values higher than 0.82g under Kobe earthquake. After that, GSI 2 was more efficient. Moreover, three story building was exposed to more reduction under Kocaeli and Kobe earthquakes. On the other hand, five story building experienced more reduction under El Centro earthquake and cyclic sinusodial motions. However, the proposed GSI system reacted better in frequency values higher than 20 Hz for three story building model. Additionally, GSI 2 worked better at lower frequencies. Furthermore, similar behavior was observed between curved and straight liner. However, straight liner enhanced the performance of the proposed GSI system mostly.

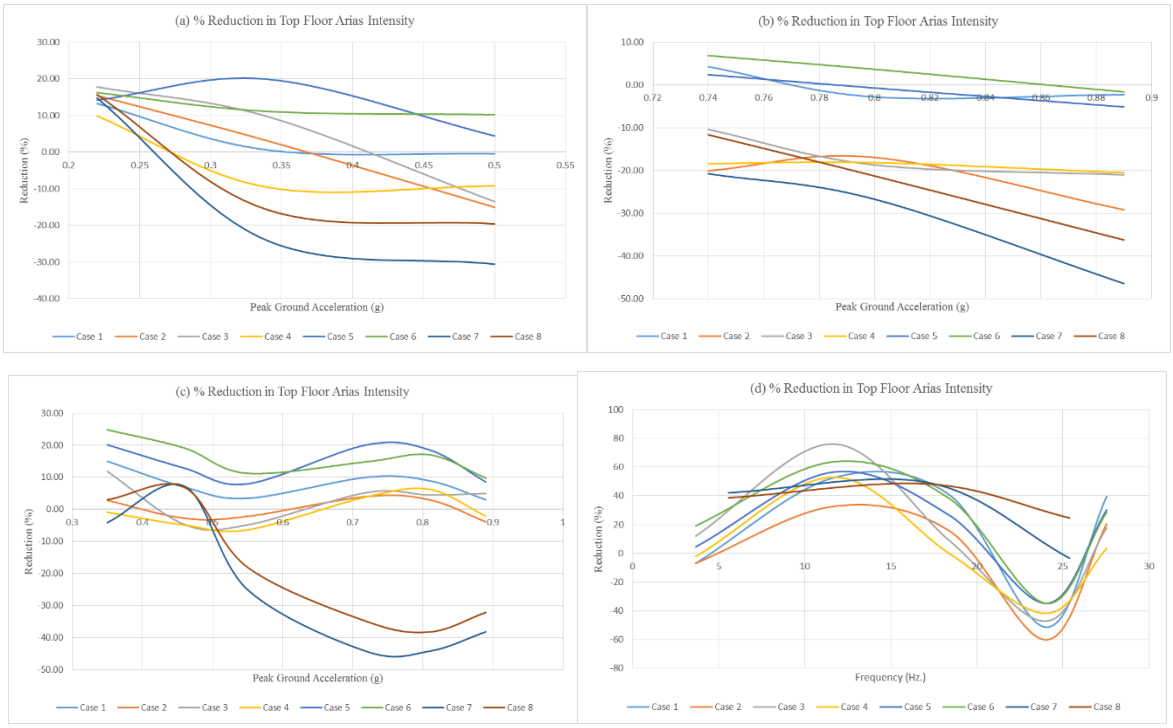

Figure 5.9. Reduction in Top Floor Arias Intensity under (a) Kocaeli Earthquake, (b) Kobe Earthquake, (c) El Centro Earthquake, (d) Cyclic Sinusodial Motion for GSI-CL.

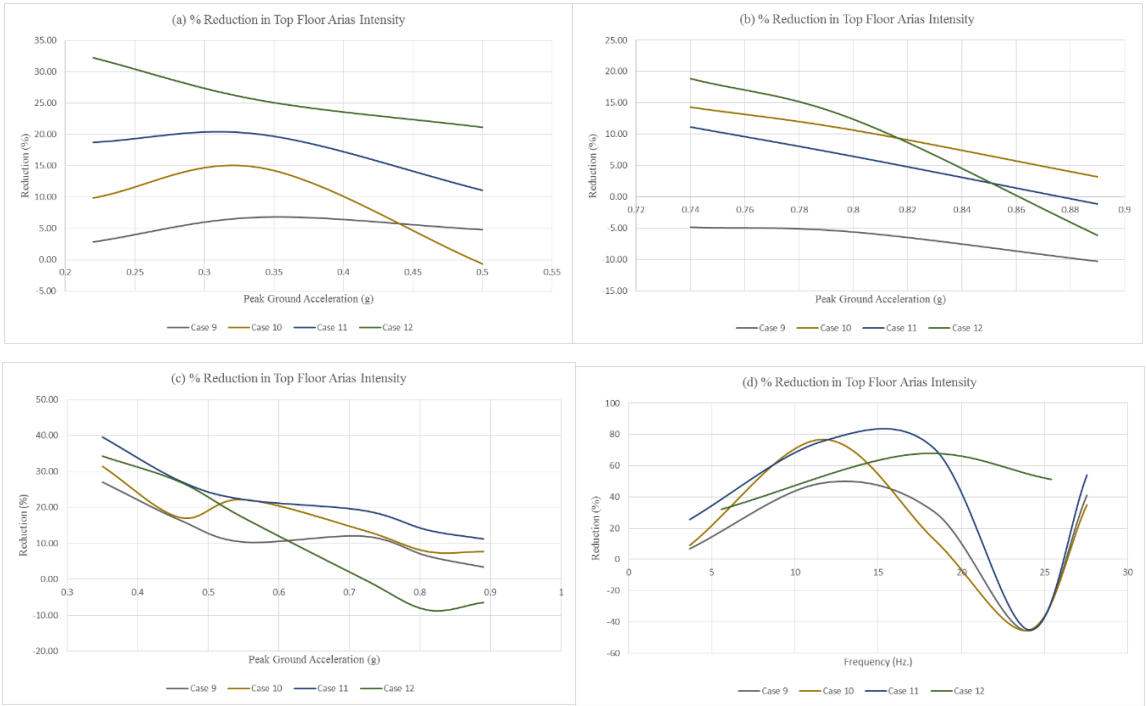

Figure 5.10. Reduction in Top Floor Arias Intensity under (a) Kocaeli Earthquake, (b) Kobe Earthquake, (c) El Centro Earthquake, (d) Cyclic Sinusodial Motion for GSI-SL.

5.2.6. Effects of Proposed GSI System on Foundation Arias Intensity

As seen from Figure 5.11, curved liners beneath three story building model did not functioned properly under Kobe earthquake. However, three story building experienced more reduction than five story building under Kocaeli earthquake. Also, three story building showed more resistance at higher frequencies under cyclic sinusodial motion. Furthermore, three story building functioned worser at 0.50g under El Centro earthquake. Additionally, GSI 3 reacted better under Kocaeli and El Centro earthquakes. However, GSI 2 provided more reduction at lower frequencies under sinusodial motion. Also, GSI 2 worked better for the five story building under Kocaeli and Kobe earthquakes. When looked into overall, GG couple with CL2 improved the performance of proposed GSI system under all applied ground motions.

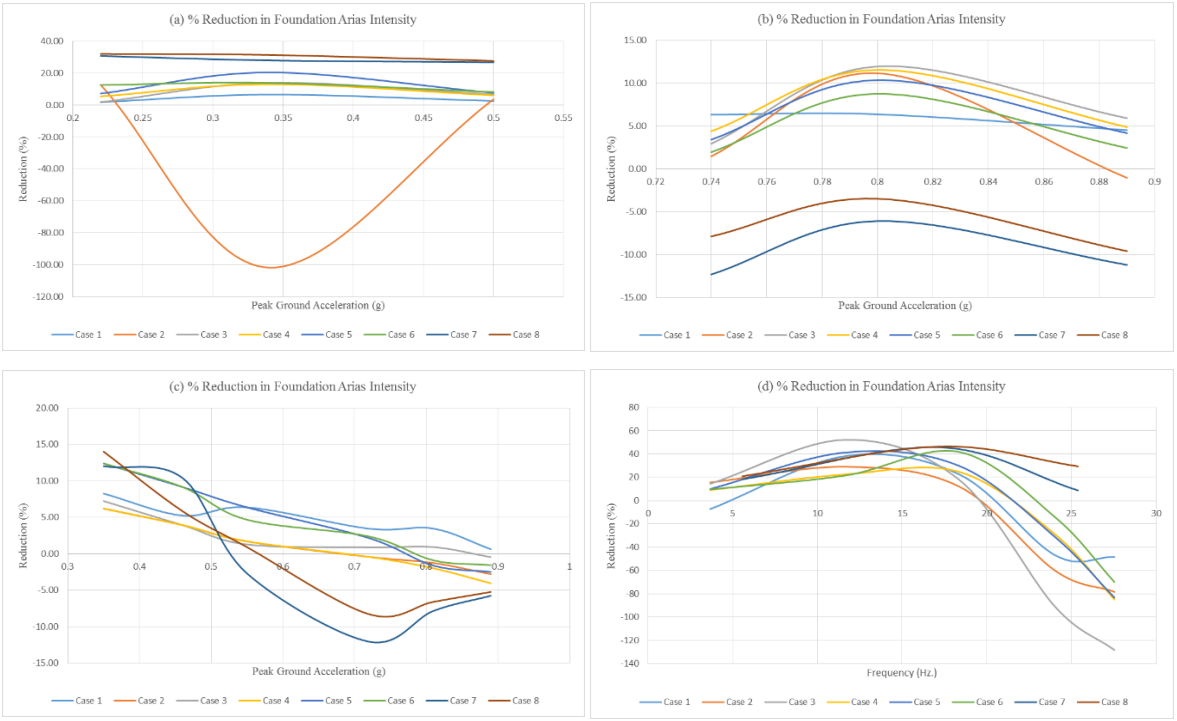

Figure 5.11. Reduction in Foundation Arias Intensity under (a) Kocaeli Earthquake, (b) Kobe Earthquake, (c) El Centro Earthquake, (d) Cyclic Sinusodial Motion for GSI-CL.

Figure 5.11 demonstrates the effect of application of straight line under model building as foundation isolation considering different ground motion. It is clear that three story building experienced more reduction under Kocaeli earthquake and cyclic sinusodial motion. Also, using GSI 3 provided more reduction about 0.50g on three story building under El Centro earthquake. GSI 2 and GSI 3 exhibited similar behavior under El Centro earthquake. Furthermore, GSI 3 improved the performance of the proposed GSI system under cyclic sinusodial motion. When comparison was performed between curve shaped and straight liners, similar behaviors were observed under all seismic excitations. However, Case 2, Case 7 and Case 8 did not work in the presence of curve shaped liner.

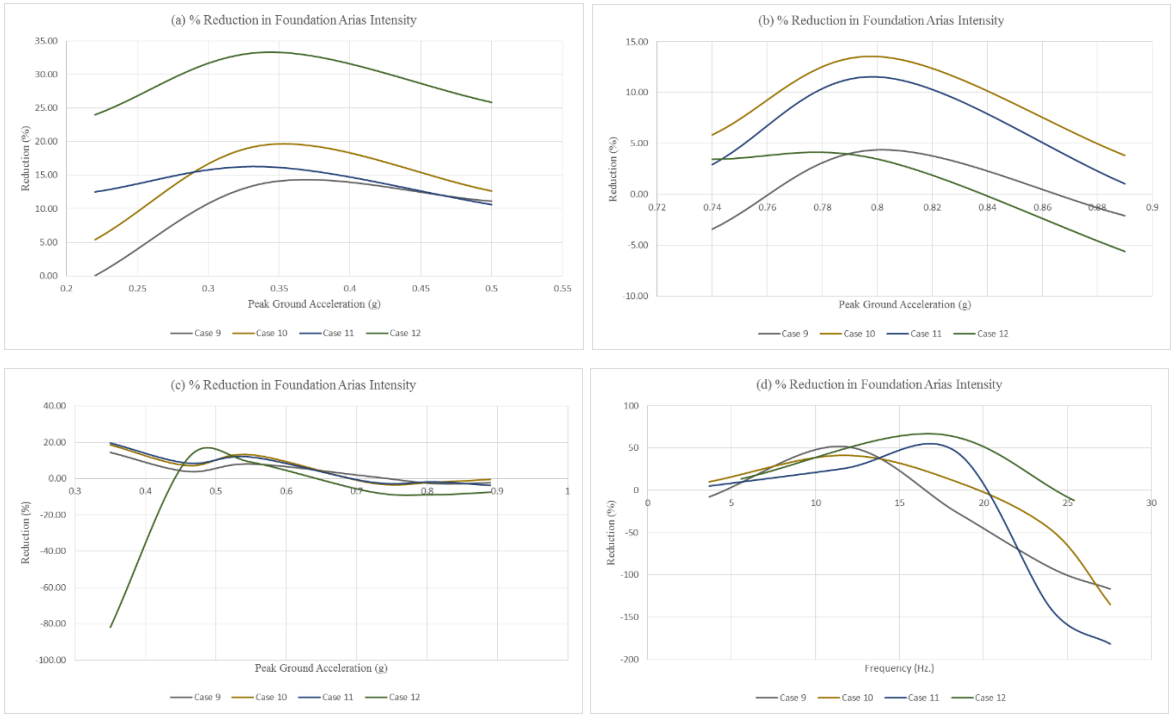

Figure 5.12. Reduction in Foundation Arias Intensity under (a) Kocaeli Earthquake, (b) Kobe Earthquake, (c) El Centro Earthquake, (d) Cyclic Sinusodial Motion for GSI-SL.

5.2.7. Effects of Proposed GSI System on Base Shear

As seen from Figure 5.13, effects of all the ground motions on base shear were reduced mostly in the presence of CL2. Also, three story building model experienced more reduction at higher amplitudes under Kocaeli earthquake and higher frequencies under cyclic sinusodial motion. However, three story building did not work under Kobe earthquake. Additionally, number of stories did not show significant difference in reducing base shear. GSI 2 provided more benefits under Kocaeli earthquake until 0.45g. However, Case 2 did not work between 0.27g and 0.50g. Also, Case 3 exhibited more reduction until 0.78g. Moreover, GSI 2 and GSI 3 contributed to the efficiency of the proposed GSI system under Kobe and El Centro earthquakes as well as cyclic sinusodial motion. It can also be stated that GSI 3 reacted better in frequency values higher than 20 Hz.

Figure 5.13. Reduction in Base Shear under (a) Kocaeli Earthquake, (b) Kobe Earthquake, (c) El Centro Earthquake, (d) Cyclic Sinusodial Motion for GSI-CL.

It can be observed from Figure 5.14, GSI 3 was the most beneficial synthetic liner on three story building model while GSI 2 appeared to be the most efficient application on five story building model under all seismic ground motions. GSI 3 exhibited its effectiveness at higher frequencies. Also, three story building experienced no reduction in PGA values higher than 0.82g. This performance indicator parameter underwent more reduction in the presence of straight liner on three story building. Instead of similarity between the curved liner and straight liner, more reduction was observed when straight liner was used as foundation isolation material.

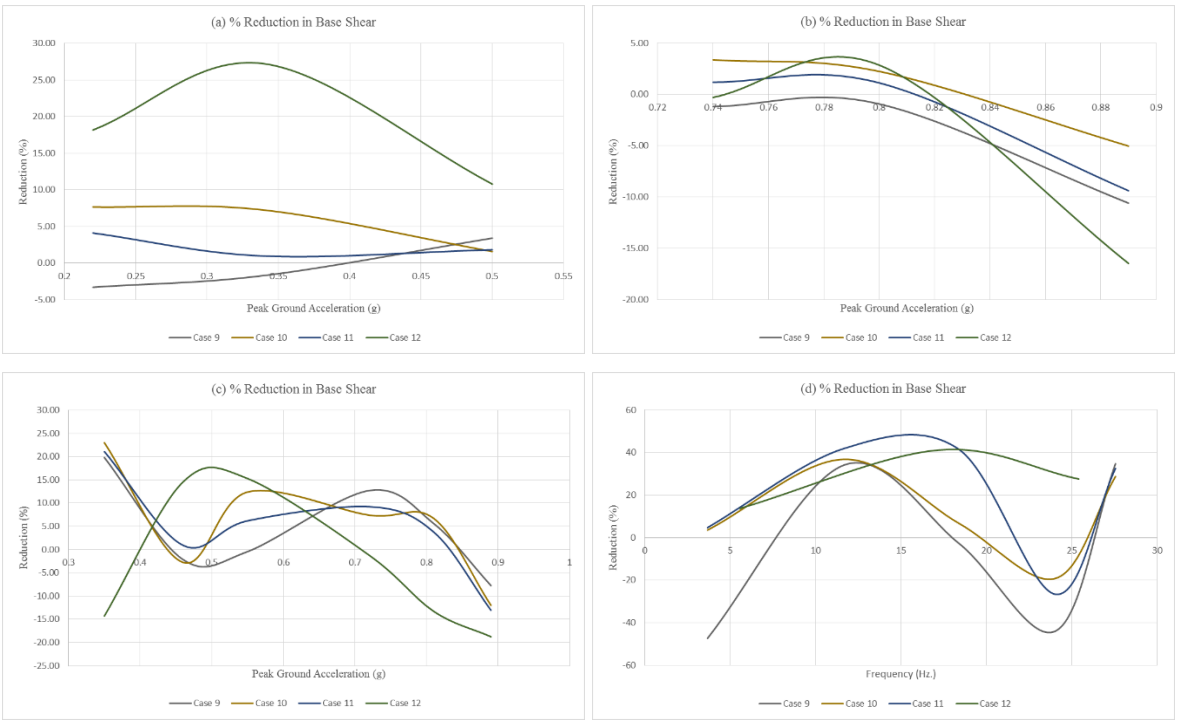

Figure 5.14. Reduction in Base Shear under (a) Kocaeli Earthquake, (b) Kobe Earthquake, (c) El Centro Earthquake, (d) Cyclic Sinusodial Motion GSI-SL.

5.2.8. Effects of Proposed GSI System on Base Moment

The effects of base moment was mostly reduced on three story building at higher PGA values under Kocaeli earthquake as seen in Figure 5.15a. GG couple with the configuration type of CL2 improved the performance of the proposed GSI system under Kocaeli and Kobe earthquake. However, there was no significant difference in the effects of configuration type under El Centro earthquake and cyclic sinusodial motion. Also, GSI 3 provided more promising results under all the ground motions. Three story building experienced more reduction at higher amplitudes and frequencies under Kocaeli and Kobe earthquakes as well as cyclic sinusodial motion. On the other hand, five story building underwent more reduction at lower PGA and frequency values. Moreover, reduction in base moment increased up to 23% under Kocaeli and Kobe earthquakes on three story building. Case 1 and Case 7 underwent sharp decrease in reduction of base moment in PGA values higher than 0.35g under Kocaeli earthquake and in frequency values higher than 17 Hz, respectively. Additionally, effective range of the results was between 0.50 and 0.80g under El Centro earthquake.

Figure 5.15. Reduction in Base Moment under (a) Kocaeli Earthquake, (b) Kobe Earthquake, (c) El Centro Earthquake, (d) Cyclic Sinusodial Motion for GSI-CL.

As it can be seen in Figure 5.16, GSI 3 provided the best results under Kocaeli and Kobe earthquakes as well as cyclic sinusodial motion. However, GSI 1 was more efficient under El Centro earthquake with a large reduction percentage about 78%. Moreover, three story building experienced more reduction under Kocaeli and Kobe earthquakes. On the other hand, GSI 1 and GSI 3 improved the performance of the system mostly under El Centro earthquake and cyclic sinusodial motion, respectively. When comparison was done, more beneficial results were obtained in the presence of straight liner as foundation isolation, especially for three story building, instead of similarities between both configuration type.

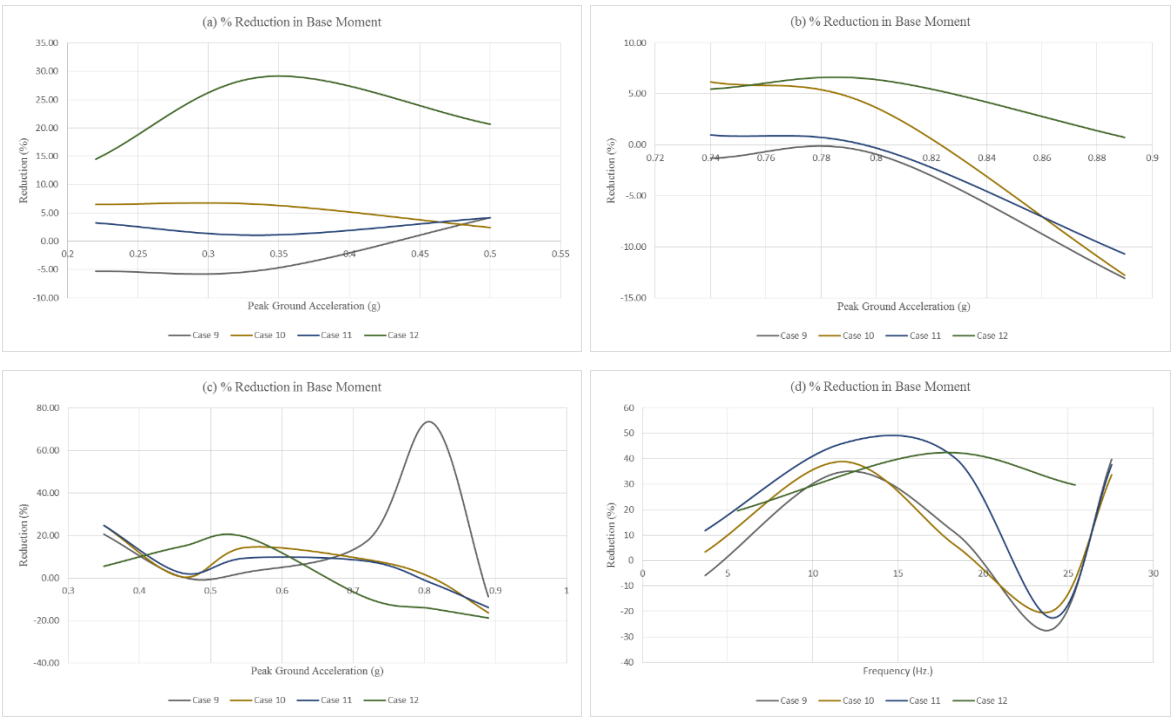

Figure 5.16. Reduction in Base Moment under (a) Kocaeli Earthquake, (b) Kobe Earthquake, (c) El Centro Earthquake, (d) Cyclic Sinusodial Motion GSI-SL.

5.3. Effects of the Proposed GSI System on Spectral Ratios

Spectral ratio is a popular method in the characterization of site amplification, introduced by Borcherdt (1974). Spectral ratio is calculated by taking the ratio of the Fourier Amplitude Spectrum (FAS) of a soil-site record to FAS of a reference-site record (Safak, 2001).

In this study, the effect of the proposed GSI system on spectral ratios of A11 (accelerometer just under the liner) to the top floor was evaluated. The spectral ratios of FAS was observed under real PGA values of Kocaeli, El Centro and Kobe earthquakes. As it was mentioned in previous sections, GSI 3 was the most efficient case for both curved and straight liner under the Kocaeli earthquake. On the other hand, GSI 1 worked better under the El Centro earthquake for both configuration type. Under Kobe earthquake, GSI 1 worked much better for curved liner. However, GSI 3 was the most efficient geosynthetic couple for straight liner under Kobe earthquake as given in the Section 6.2. The most efficient cases are Case 5 and Case 11 for Kocaeli earthquake, Case 1 and Case 11 for Kobe earthquake, and Case 1 and Case 9 for El Centro earthquake.

For the curve shaped liner, GSI 3 with CL2 and GSI 1 with the configuration type of CL1 was used in the comparison.

In the following parts, spectral ratios of Fourier Amplitude Spectrums of the seismic responses under Kocaeli, Kobe and El Centro earthquakes for curved and straight liners were evaluated.

5.3.1. Comparison of Spectral Ratios under Kocaeli earthquake for GSI-CL

As seen in Figure 5.17, spectral ratios of isolated case was a little bit higher than the unisolated case. The result of this comparison indicated that GSI shorter liner with 2B (CL2) showed no efficiency.

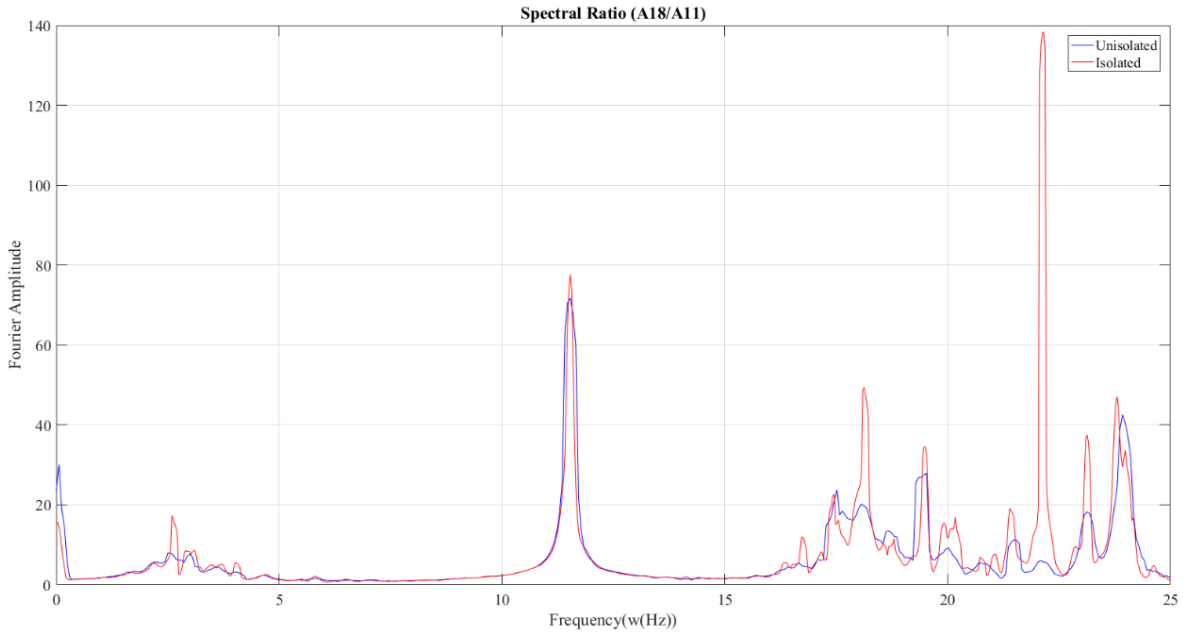

Figure 5.17. Spectral Ratio of Top Floor to A11 level for Case 5.

5.3.2. Comparison of Spectral Ratios under El Centro earthquake for GSI-CL

It can be stated from Figure 5.18 that GSI1-CL1 functioned properly under El Centro earthquake. Small shift in frequency was observed in 1^{st}, 2^{nd} and 3^{rd} modes. Also, substantial decrease in Fourier amplitudes was clearly observed. About 30% decrease in the second mode and 80% reduction in the third mode were observed in spectral ratios.

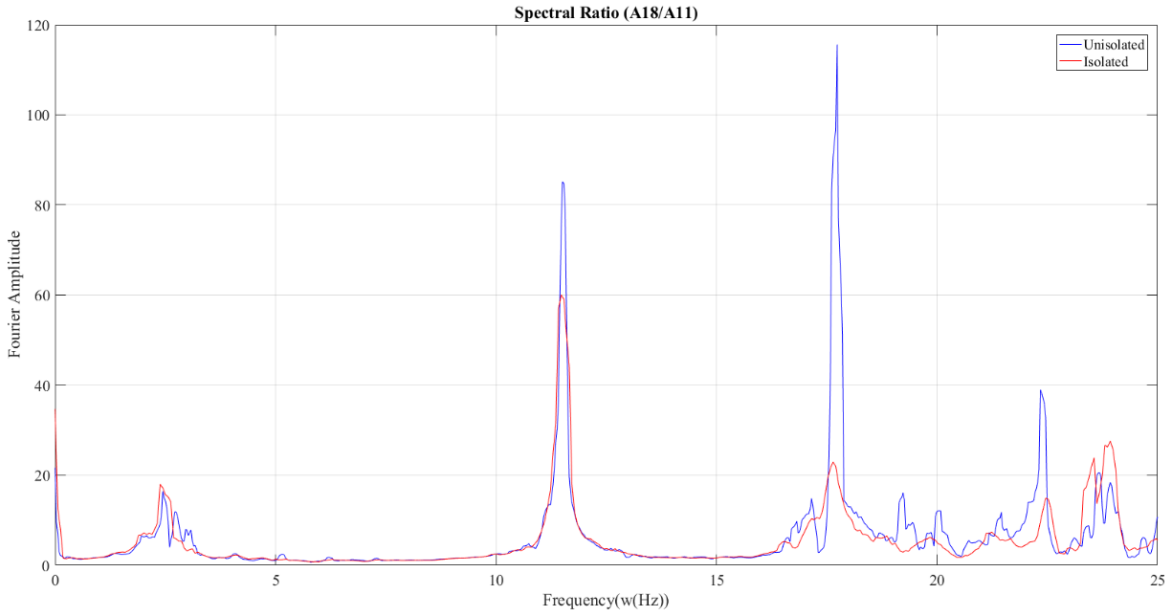

Figure 5.18. Spectral Ratio of Top Floor to A11 level for Case 1.

5.3.3. Comparison of Spectral Ratios under Kobe earthquake for GSI-CL

The comparison between unisolated case and Case 1 was shown in Figure 5.19. In the 2nd mode, Case 1 demonstrated a little bit higher amplitude when compared to the unisolated case. However, frequency shift and large decrease in fourier amplitude was observed in 3rd mode. It means, GSI 1 with CL1 provided beneficial results at 2nd mode of the proposed system.

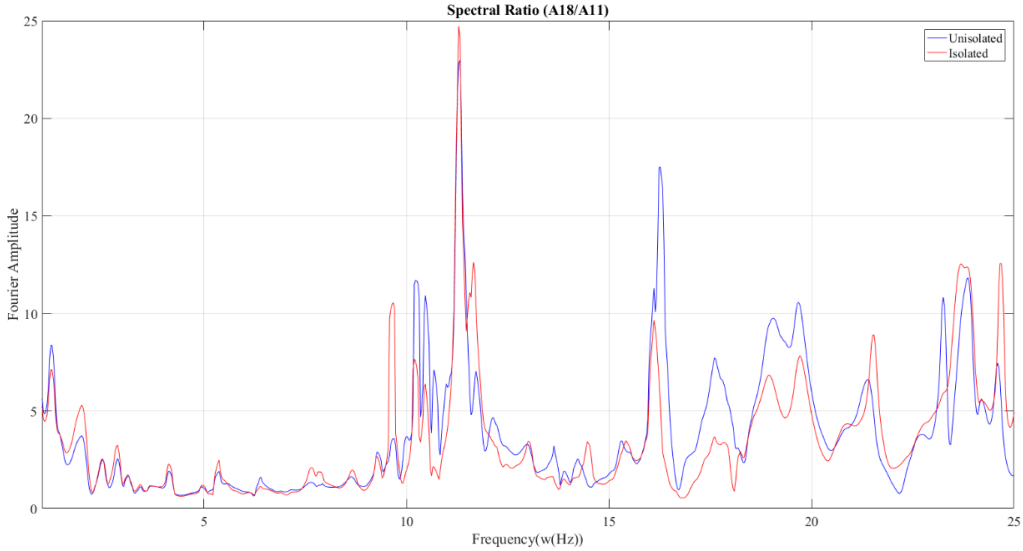

Figure 5.19. Spectral Ratio of Top Floor to A11 level for Case 1.

5.3.4. Comparison of Spectral Ratios under Kocaeli earthquake for GSI-SL

It can obviously be seen that Fourier amplitudes underwent decrease and frequency shifts were observed. GSI 3 functioned properly with straight liner under Kocaeli earthquake. About 24% decrease in spectral ratio was observed in the second mode.

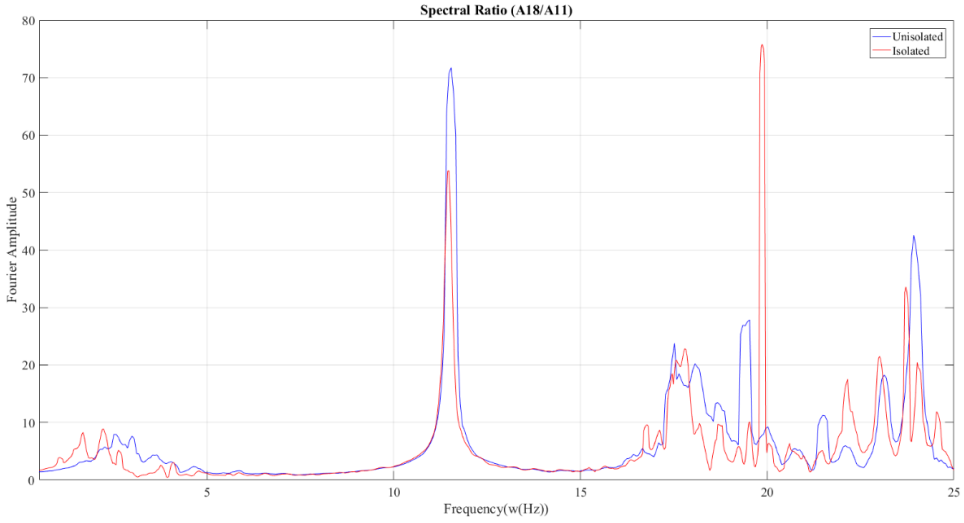

Figure 5.20. Spectral Ratio of Top Floor to A11 level for Case 11.

5.3.5. Comparison of Spectral Ratios under El Centro earthquake for GSI-SL

In Figure 5.21, spectral ratios of top floor to A11 accelerometer in sand was illustrated. Large reduction in Fourier amplitudes was observed in all modes, especially 3rd mode. Also, there was frequency shift in all modes. It means, GSI 1 worked better in mitigation of spectral ratios. The reduction percentage between the spectral ratios was observed about 34% in second mode and 82% in the third mode.

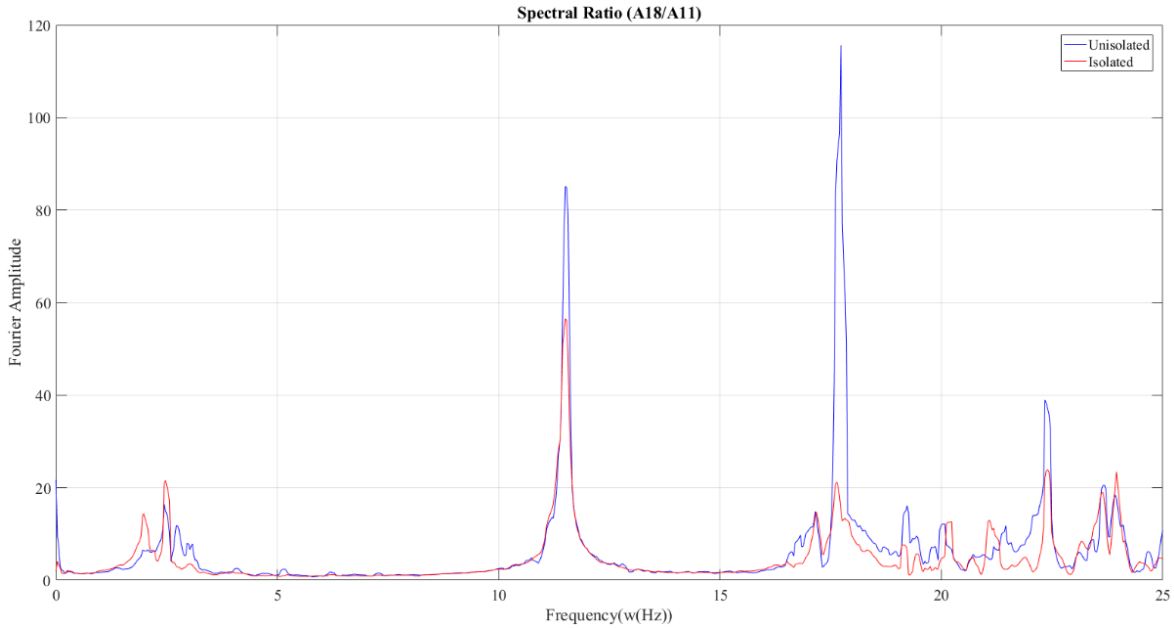

Figure 5.21. Spectral Ratio of Top Floor to A11 level for Case 9.

5.3.6. Comparison of Spectral Ratios under Kobe earthquake for GSI-SL

As it can be seen in Figure 5.22, Fourier amplitudes were alleviated substantially and frequency shift was observed in all modes. The result of this comparison revealed that GSI 3 functioned appropriately under Kobe earthquake.

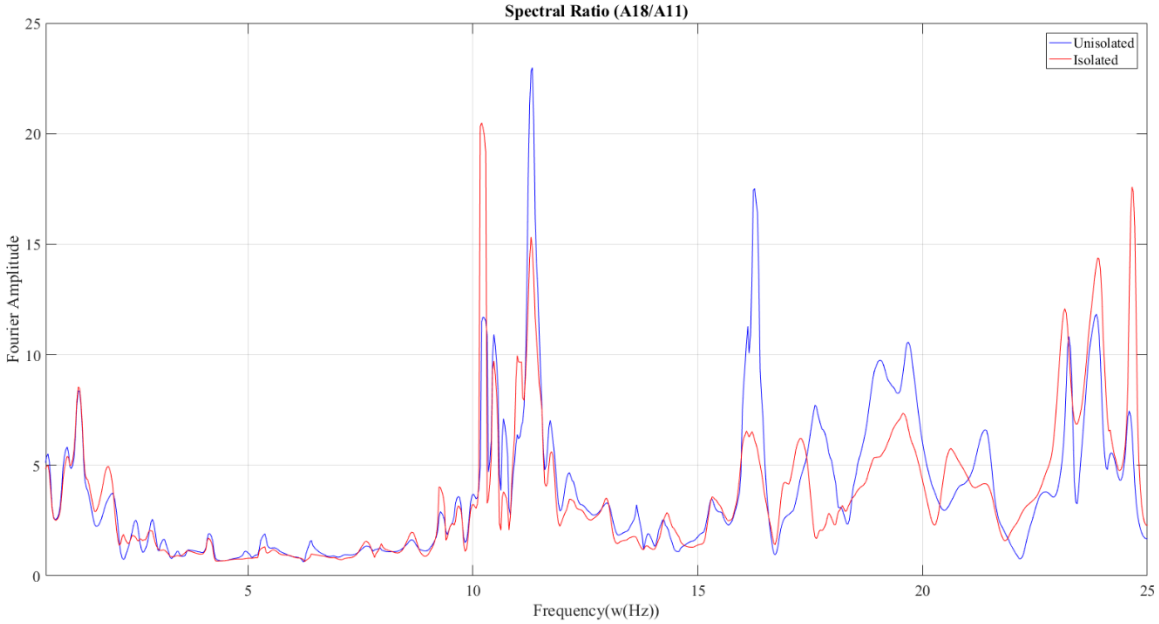

Figure 5.22. Spectral Ratio of Top Floor to A11 level for Case 11.

6. SUMMARY AND CONCLUSION

6.1. Summary

The purpose of this thesis is to investigate the effects of using GSI with geosynthetics as foundation isolation material on seismic performance of low-to-midrise buildings. The reason of this experimental study is to find a more economical and applicable solution to mitigate earthquake hazards for developing countries.

This thesis is composed of six chapters, each of them dealing with distinctive aspects of the study. First chapter is general information on SI and GSI, problem statement and the aim of the thesis. Chapter Two is composed of literature review that is about similar numerical and experimental studies up to now. Development of experimental setup including input ground motion selection, instrumentation and soil sampling process is mentioned in Chapter Three. As input ground motions, Kocaeli, El Centro and Kobe earthquakes were selected. The design of 3-story and 5-story building models were mentioned. Also, the results of the repeated performance checks of the laminar box were given in the same chapter. Experimental results and parametric study to evaluate the results of the experiment were mentioned in Chapter Four and Five. Inferences of the experimental studies were presented in the last chapter.

A special experimental setup considering soil-structure interaction by using GSI with geosynthetics as a foundation isolation material was developed for this study which is the first in the literature. Seismic performances of low-to-mid rise buildings under defined earthquake ground motions and cyclic sinusodial motions were evaluated for unisolated and isolated cases by shaking table tests. Fundamental frequencies of the building models were obtained by using the results of free vibration tests.

Geomembrane and geotextile couples were prepared to simulate GSI with geosynthetics. Three different GSI couples which were determined from the block tests were

used. Junifol HDPE and PTFE geomembranes are used with Typar DuPont SF44 and Typar Dupont SF56 nonwoven geotextiles together. GSI 1 is composed of Junifol HDPE 1 mm geomembrane and Typar DuPont SF44 nonwoven geotextile. Additionally, GSI 2 is made up of PTFE 1 mm geomembrane with Typar DuPont SF44 nonwoven geotextile. Lastly, GSI 3 consists of PTFE 1 mm geomembrane with Typar DuPont SF56 nonwoven geotextile. During the experiments, two different GSI configuration types were studied as curve shaped liners (CL) and straight liner (SL). For each configuration type, GG couples were placed underneath the foundation of 5-storey and 3-storey building models, respectively. Effects of the geosynthetics as foundation isolation material were evaluated considering eight performance parameters which are top and foundation horizontal acceleration, top and first story drift, top and foundation Arias intensity, base shear and base moment. As a result of the parametric study, the effects of the number of story, GSI type, configuration type and ground motion characteristics on the seismic performance of low and medium rise building models were evaluated.

6.2. Conclusion

When the overall results were taken into consideration, it was observed that GSI 3 provided better results under seismic excitations on three story building and five story building models. It means, Typar DuPont SF56 geotextile - PTFE 1 mm geomembrane couple worked properly under selected ground motions. The use of curved liner CL2 exhibited more promising results. Percentages of reduction in selected performance parameters were higher in GSI 3 and the configuration type of CL2. Between the two different configuration type of foundation isolation, most efficient one was observed using straight liner. Most cases revealed similarity, however, straight liner demonstrated a little bit more efficiency in deamplification of seismic ground motions.

Under Kocaeli earthquake, GSI 3 exhibited more efficiency in the most of the parameters on three story building while the most efficiency was obtained by GSI 2 on five story building. It means, different GSI types affects the seismic response of the building models with different number of stories. It shows the importance of the effects of GSI

material on the seismic performance of the low-to-medium rise buildings. The configuration type of CL2 provided the most reliable results under Kocaeli earthquake. Also, straight liner revealed more reduction percentages in most cases than curved liner. This behavior shows the importance of the liner configuration under earthquake excitation.

When the results of El Centro earthquake were evaluated, most effective results were observed in straight liner when compared to curved liner. Considerable results were approached on five story buildings with curve shaped liner. In overall, GSI 1 was the most effective liner couple in both curved and straight liner. Using the configuration type of CL1 provided most positive effect.

Under the Kobe earthquake, most effective geosynthetic couple was observed as GSI 1 for curved shaped liner and GSI 3 for straight liner. However, most efficiency was observed on three story building with straight liner. The use of configuration type of CL1 was the most promising implementation in curve shaped liner.

Under the three destructive earthquake motions, it can be seen that the effects of GSI type and configuration type on the seismic performance may give different results depending on the number of stories and earthquake characteristics as amplitude, time and frequency.

In frequency domain analysis, both configuration types showed similar effects on the both low and medium rise buildings under cyclic sinusodial motions. However, straight liner provided more efficiency compared to curve liner for both models. Also, GSI 2 provided the best results on five story building model. On the other hand, GSI 3 improved the behavior of both three and five story buildings in the presence of straight liner as foundation isolation material. Moreover, frequency content of the seismic motions affects the structural behavior under dynamic motions. If there occurs a coincide between the natural frequencies of the ground and the buildings, the most destructive shaking will be able to occur on the structure. Thus, results indicated that the most efficiency was observed at the natural frequencies of the three and five story buildings. It was also obviously seen that between 20 and 25 Hz, the proposed GSI system did not work. In the frequencies larger than 25 Hz, the system started to improve the seismic behavior again.

When overall results of isolated models compared to unisolated case, great reductions in defined parameters were observed. Transmitted top floor and foundation accelerations underwent reduction up to 46% and 31% with the use of curve shaped liner, respectively. On the other hand, up to 44% and 90% reductions in transmitted horizontal acceleration were observed on top floor and foundation in the presence of straight liner, respectively. Since, soft-story mechanism is the major cause of collapse of many buildings in earthquakes, first floor story drift has been selected as another parameter. Story drifts at top floor and first floor were significantly decreased up to 95% and 96%, respectively. This means, the effects of the earthquake damages due to soft story phenomenon were substantially mitigated. Furthermore, top floor and foundation Arias intensity showed reduction as 80% and 52%, respectively. Additionally, base shear and base moment were alleviated up to 44% and 73%, respectively. Furthermore, spectral acceleration amplitudes of Fourier amplitude spectra of the defined cases were reduced substantially with a reduction percentage up to 82%.

When the results compared under selected earthquake motions, most discrepancy was observed under Kobe earthquake. High spectral acceleration amplitudes deteriorated the performance of proposed GSI system under Kobe earthquake. Efficiency of the proposed GSI system was relatively less during the earthquake. GSI system showed minimal effect on improvement on seismic performance under the most destructive earthquake, Kobe earthquake. When the block test results were considered, slip displacement value obtained from rigid block tests under Kobe earthquake was substantially larger than Kocaeli and El Centro earthquakes. According to the Yegian and Kadakal (2004), the maximum and permanent slip displacements should be small enough to allow functionality. Thus, seismic improvement under Kobe earthquake was slightly less. Differences among the given earthquake motions can be due to the different characteristics of the ground motions such as frequency content, amplitude and time.

As a conclusion, GSI 3 provided the best results under seismic excitations. It may be due to the lower friction coefficient as 0.13 obtained from rigid block tests that causes larger slip displacements. GSI 3 worked better with CL2. Under Kobe and El Centro earthquakes, five story building model was seemed to be more beneficial when compared to three story building model. On the other hand, three story building model experienced more reduction percentages in all defined parameters under Kocaeli earthquake and cyclic sinusodial

motions. Material properties of Typar DuPont SF56 which was used in GSI 3 was more efficient and better than Typar DuPont SF44 such as tensile strength, grab strength and tear strength. Energy absorbtion of the SF56 was higher than the SF44 as given in Appendix A. This also contributed to the seismic improvement with the proposed GSI system under GSI 3. If the dynamic friction angle is low as 7°, the isolation material is more appealing for GSI system (Yegian and Lahlaf, 1992). Thus, GSI 2 and GSI 3 are the more compatible foundation isolation materials due to the fact that they have the lower friction angles which are about 7° as found from rigid block tests. As it was stated in the requirements determined by Yegian and Lahlaf (1992), geosynthetic liner with H/D ratio of 6 was the most efficient foundation isolation material. In this study, H/D ratio of 6 corresponds to the CL2 which was the more efficient liner type.

The defined threshold acceleration values are within limits defined by Yegian and Lahlaf (1992). Similarly, GSI 2 and GSI 3 were observed as the most effective GG couples due to the low threshold acceleration values as 0.11g and 0.13g respectively. However, GSI 1 has higher threshold value as 0.24g. It means, sliding initiated earlier in GSI 2 and GSI 3. This will result in more energy absorption.

As an inference of all the above mentioned results from parametric studies, following conclusions can be drawn.

- GSI 3 provided better results under all seismic excitations.
- GSI 3 improved the seismic performance of the proposed GSI system with the configuration type of CL2.
- Geotextile type SF56 which is the material of GSI 3 provided more energy absorption.
- Top floor acceleration was diminished up to 46% in the presence of curve shaped liner.
- Foundation acceleration was reduced up to 90% with the use of straight liner.
- Destructive earthquake damages caused by soft story phenomenon were mitigated with a large reduction of 95%.
- A great reduction in the amplitudes of Fourier Amplitude Spectra (FAS) was observed up to 82% in GSI with straight liner.
- Base shear and base moment values indicated reduction percentages as 44% and 73%, respectively.

- The effect of the proposed GSI system in Arias intensity can be observed at top and foundation floor with the reduction values of 80% and 52%, respectively.
- In cyclic sinusodial motions, more efficiency was observed at the vicinity of natural frequencies of the proposed GSI system.

As a summary, seismic performance of the system was dependent on the number of stories, utilized material type in foundation isolation, and ground motion characteristics such as amplitude, frequency and time.

As a results of evaluated parameters for the performed experimental studies, the proposed GSI system worked appropriately under seismic excitations. Thus, mitigation of seismic hazards can be achieved on low to mid rise buildings by using GSI with geosynthetics for developing countries.

6.3. Future Recommendation

Further studies on the proposed foundation isolation system with geosynthetics should be performed by using prototype building models. The effects of GSI type, configuration type, number of stories, different soil types and different building widths considering the proposed GSI method on the mitigation of earthquake hazards should be investigated by a series of field experiments, especially by using Mobile Seismic Shaker.

APPENDIX A: PROPERTIES OF THE UTILIZED GEOSYNTHETICS

Table A.1. Properties of the Nonwoven Geotextiles (Sekman, 2016).

Dupont Typar				
Property	Standard	Unit	SF44	SF56
Descriptive properties				
Area weight	EN ISO 9864	g/m^2	150	190
Thickness under 2 kN/m^2	EN ISO 9863-1	mm	0.48	0.57
Thickness under 200 kN/m^2	EN ISO 9863-1	mm	0.4	0.48
Mechanical properties				
Energy Absorbtion	EN ISO 10319	kJ/m^2	4.5	5.8
Tensile Strength	EN ISO 10319	KN/m	10.3	13.1
Elongation	EN ISO 10319	%	52	52
Tensile Strength at %5	EN ISO 10319	kN/m	4.5	5.7
Puncture CBR	EN ISO 12236	N	1575	1850
Dynamic Cone Puncture	EN ISO 13433	mm	27	22
Grab Strength	ASTM D4632	N	900	1100
Tear Strength	ASTM D4533	N	385	460
Hydraulic properties				
opening Size O_{90}	EN ISO 12956	µm	100	80
Permeability V_{IH50}	EN ISO11058	10^{-3} m/s	40	35
Flow Rate at 10 cm WH	BS 6906-3	$I/(m^2.s)$	70	60
Permeability at 20 kN/m2	DIN 60500-4	10^{-4} m/s	2.6	1.9
Permeability at 200 kN/m2	DIN 60500-4	10^{-4} m/s	1.8	1.4

Table A.2. Properties of the Junifol HDPE Geomembrane (Sekman, 2016).

Properties	Test method	Unit	Junifol PEHD
Surface Thickness (min. ave.) lowest individual for 8 out of 10 values lowest individual for an of the 10 values	ASTM D 5994	mm	textured 1.0 (-5 %) -10% -15%
Asperity Height (min. ave.)	GM 12	mm	0.25
Density (min.)	ASTM D 1505	g/cm^3	0.94
Tensile Properties (min. ave.)	ASTM D 6693 typ IV		
Yield strength		kN/m	17
Break strength		kN/m	29
Yield elongation		%	12
Break elongation		%	750
Tear Resistance (min. ave.)	ASTM D 1004	N	130
Puncture Resistance (min. ave.)	ASTM D 4833	N	330
Stress Crack Resistance	ASTM D 5391	hr.	300
Carbon Black Content	ASTM D 1603	%	2 - 3
Carbon Black Dispersion	ASTM D 5596	Category	1 or 2
Oxidative Induction Time (OIT) (min. ave.) Standard OIT	ASTM D 3895	min.	100
Oven Aging at 85 °C Standard OIT (min. ave.) % retained after 90 days	ASTM D 5721 ASTM D 3895	%	55
UV Resistance High Pressure OIT (min. ave.) % retained after 1600 hrs	ASTM D 5885	%	-

Table A.3. Properties of the 1 mm Thick PTFE Geomembrane Sheet (Sekman, 2016).

Properties	Unit	PTFE
General preoperties		
Density	g/cm^3	2.18
Water Absorption	%	0
Mechanical properties		
Tensile Strength	MPa	20
Elongation at Yield	%	25 - 31
Tensile Strength at Break	MPa	9
Elongation at Break	%	> 200
Impact Strength	kJ/m^2	15.5
Notch Impact Strength	kJ/m^2	**
Ball indentation Hardness (Rockwell)	MPa	30
Shore Hardness	**	60 - 65
Flexural Strength ($\sigma_{B3.5\%}$)	MPa	550
Coefficient of Friction	**	0.06
Modulus of Elasticity	MPa	3000
Thermal properties		
Melting Temperature	C^o	**
Permissible Service Temperatures		
Short Term Operating Temperature	C^o	330
Long Term OperatingTemperature	C^o	260
Coefficient of Linear Thermal Expansion	$K^{-1}.10^{-4}$	0.6
Thermal Conductivity at 20 C^o	W/(m.K)	0.24
Electrical properties		
Volume Resistivity	Ω.cm	$> 10^{18}$
Surface Resistivity	Ω	$> 10^{17}$
Dielectric Constant at 1 MHz		- / 2.1
Dielectric Strength	kV/mm	32

REFERENCES

1. Adir, K., *Mitigation of Earthquake Induced Geotechnical Hazards Using Tire Waste-Sand Mixtures*, MSc.Thesis, Bogazici University, 2013.

2. Adams, M.T., and J. Collin, "Large Model Spread Footing Load Tests on Geosynthetic Reinforced Soil Foundations", *Journal of Geotechnical and Geoenvironmental Engineering*, Vol. 123, pp. 66-72, 1997.

3. Alawaji, H.A., "Settlement and Bearing Capacity of Geogrid-Reinforced Sand over Collapsible Soil", *Geotextiles and Geomembranes.* Vol. 19, pp. 75-88, 2001.

4. Arab, M.G., & Jr, E. Kavazanjian, "Time-Domain Analysis of Frictional Base Isolation Using Geosynthetics", *9th International Conference on Geosynthetics*. Vol. 2, pp. 695-698, 2010.

5. Barole, S., "Seismic Base Isolation", Indian Institute of Technology, Kharagpur, 2016.

6. Bayat, E.E., S. Gokyer, M. K. Yegian, E. Ortakci, and A. Alshawabkeh, "Design and Application of Simple Shear Liquefaction Box", *Geotechnical Testing Journal.* Vol. 36, No.3, 2013.

7. Bhattacharya, S., D. Lombardi, L. Dihoru, M.S. Dietz, A.J. Crewe, & C.A. Taylor, "Model Container Design for Soil-Structure Interaction Studies", *Role of Seismic Testing Facilities in Performance- Based Earthquake Engineering*. Vol 5, pp. 135-158, 2012.

8. Borcherdt, R.D., "Effects of Local Geology on Ground Motion Near San Francisco Bay", B*ulletin of the Seismological Society of America*, Vol. 60, pp. 29-61 ,1970.

9. Bozorgnia, Y., and M. Niazi, "Distance Scaling of Vertical and Horizontal Response Spectra of the Loma Prieta Earthquake", *Earthquake Engineering and Structural Dynamics.* Vol. 22, pp. 695-707, 1993.

10. Bozorgnia, Y., and V.V. Bertero, *Earthquake Engineering: From Engineering Seismology to Performance-Based Engineering.* CRC Press, Boca Raton, 2004.

11. Boominathan, A., S. Banerjee, and J.S. Dhanya, "Performance of Soil-Rubber Tyre Scrap Mixture as Seismic Base Isolators for Foundations", *6th International Conference on Earthquake Geotechnical Engineering.* New Zealand, 2015.

12. Bray, J. D., "Geotechnical Earthquake Engineering", *Civil Engineering Handbook.* CRC Press, Chapter 25. 2003.

13. Chang, K.C., Y. B. Yang & J.D. Yau, "Base Isolation", *In Earthquake Engineering Handbook.* CRC Press, 2002.

14. Chen, C. H., T. S. Ueng, and W. C. Lee, "Large Scale Biaxial Shear Box Tests on Shaking Table", *Thirteenth World Conference on Earthquake Engineering.* No. 1778, Canada, 2004.

15. Cheung, W. M., X. Qin, N. Chouw, T. Larkin, and R. Orense, "Experimental and Numerical Study of Soil Response in a Laminar Box", *NZSEE Conference.* 2013.

16. Chunxia, H., Z. Hongru, C. Gouxing, and S. Zhilong, "Design and Performance of a Large-Scale Soil Laminar Shear Box in Shaking Table Test". 2008.

17. Edincliler, A., and M. Sekman, " Investigation of Seismic Performance of the Mid-Rise Buildings with Geosynthetics". *Sixth International Conference on Structural Engineering, Mechanics and Computation.* Cape Town, South Africa, 2016.

18. Edincliler, A., M. Sekman, and B. Goztepe, “Shake Table Tests to Evaluate Seismic Soil Structure Interaction of Low-rise Buildings Under Different Earthquake Motions”, *Sixth European Geosynthetics Congress. EUROGEO 6.* Ljubljana, Slovenia, 2016.

19. Erdik, M., “ Seismic Isolation for Buildings”, *Sixth National Conference on Earthquake Engineering.* Istanbul, Turkey, 2007.

20. Ecemis, N., and I. Kahraman, “Design of Laminar Shear Box for One Dimensional Shaking Table Tests”, *Tenth International Congress on Advances in Civil Engineering.* Ankara, Turkey, 2012.

21. Ecemis, N., H. E. Demirci, and M. Kahraman, “Influence of Consolidation Properties on the Cyclic Re-liquefaction Potential of Sands”, *Bull Earthquake Engineering*. Vol. 13, pp. 1655-1673, 2015.

22. Edil, T. B., and P. J. Bosscher, “Engineering properties of tire chips and soil mixtures”, *Geotechnical Testing Journal.* Vol.17, pp. 453-464, 1994.

23. El-Emam, M. M., and R. J. Bathurst, “Experimental Design, Instrumentation and Interpretation of Reinforced Soil Wall Response using a Shakin Table”, *International Journal of Physical Modelling in Geotechnics.* Vol. 4, pp. 13-32, 2004.

24. Farsakh, M. A., Q. Chen, and J. Gu, “Geosynthetic Reinforced Foundations Laboratory Model Tests and FE Analyses”, Louisiana Transportation Research Center, 2007.

25. Georgarakos, P., M. K. Yegian, and G. Gazetas, “In-ground Isolation using Geosynthetic Liners”, *Ninth World Seminar on Seismic Isolation, Energy Dissipation and Active Vibration Control of Structures.* Kobe, Japan, 2005.

26. Ghazavi M., and A. A. Lavasan, “Interference Effect of Shallow Foundations Constructed on Sand Reinforced with Geosynthetics”, *Geotextiles and Geomembranes.* Vol. 26, pp. 404–415, 2008.

27. Gohil, D. P., C. H. Solanki, and A. K. Desai, "Application of Geosynthetics for Ground Improvement: An Overview", *IGC 2009.* Guntur, India, 2009.

28. Goztepe, B. *Experimental Study on Mitigation of Earthquake Hazards Using Rubber-Soil Mixtures*, MSc. Thesis, Bogazici University, 2016.

29. Hajiani J., "Experimental and Numerical Investigation of the Bearing Capacity of Model Circular and Ring Footings on Reinforced Sand", *Geotextiles and Geomembranes*. Vol.21, pp. 241–256, 2003.

30. Harris, H. G., and G. M. Sabnis, *Structural Modeling and Experimental Techniques*. CRC Press. 1999

31. Hauksson, E., and S. Gross,. "Source Parameters of the 1933 Long Beach Earthquake". *Bull. Seism. Soc. Am.* Vol. 81, pp. 81-98, 1991.

32. Hazarika, H., E. Kohama, and T. Sugano, "Shaking Table Tests on Waterfront Structures Protected with Tire Chips Cushion", *Journal of Geotechnical and Environmental Engineering*. ASCE, USA, 2008.

33. Higashino, M., S. Aizawa, and Y. Hayamizu, "The Study of Base Isolation System for Actual Use", *Proceedings of Ninth World Conference on Earthquake Engineering.* Vol. 5, Tokyo, Japan, 1988.

34. Holtz., R. D., "Geosynthetics", *Civil Engineering Handbook.* CRC Press, Chapter 24. 2003.

35. Humphrey, D. N., "Effectiveness of Design Guidelines for Use of Tire Derived Aggregate as Lightweight Embankment Fill", *In Recycled Materials in Geotechnics.* ASCE, pp. 61-74, Reston, VA, 2005.

36. Hushmand, B., R. F. Scott, and C. B. Crouse, "Centrifuge Liquefaction Tests in a Laminar Box", *Geotechnique.* Vol. 38, No.2, pp. 253-262, 1988.

37. Hussain, M., “Seismic Base Isolation”, Final Seminar, National Institute of Technology, Durgapur, 2014.

38. Iai, S., “Similitude for Shaking Table Tests on Soil-Structure-Fluid Model in 1g Gravitational Field,” *Soils and Foundations,* Vol. 29, pp105-118, 1989.

39. Idriss, I.M., “Response of Soft Soil Sites During Earthquakes”, *In H.B. Seed Memorial Symposium Proceedings.* Bitech Publisher, Vol. 2, Vancouver, BC, 1990.

40. Jafarzadeh, F., “Design and Evaluation Concepts of Laminar Shear Box for 1g Shaking Table Tests”, *Thirteenth World Conference on Earthquake Engineering.* No.1391, Canada, 2004.

41. Kalpakci, V. “Seismic Isolation of Foundations by Composite Liners”, PhD. Thesis, Middle East Technical University, 2013.

42. Kavazanjian, E., B. Hushmand, and G. Martin, “Frictional Base Isolation Using Layered Soilgeosynthetic Liner System”, *Proceedings of the Third U.S. Conference on Lifeline Earthquake Engineering*, Los Angeles, pp.1140–1151, 1991.

43. Kelly, J. M., “Seismic Isolation”, *Earthquake Engineering-From Engineering Seismology to Performance Based Engineering.* CRC Press, Chapter 11. 2004.

44. Kelly, T. E., *Base Isolation Of Structures; Design Guidelines,* S.E. Holmes Consulting Group Ltd, Revision, 2001.

45. Kim, J. M., H. W. Jeon, S. W. Son, G. H. Na, and Y. A. Lee, “Research on Geotechnical Seismic Isolation System”, *2014 International Conference on Geological and Civil Engineering IPCBEE.* Vol. 62, Singapore, 2014.

46. Kumar, S., C. H. Solanki, and B. D. Wabhitkar, “Study on Embedded Square Footing Resting on Geotextile Reinforced Sand”, *International Journal of Civil and Structural Engineering.* Vol. 5, No.3, 2015.

47. Kumar, S., C. H. Solanki, and M. M. Chavda, "Study on Square Footing Resting on Geotextile Reinforced Sand", *Eighth International Conference on Electrical, Electronics and Civil Engineering.* Dubai, 2016.

48. Ling H. I., and Z. Liu, "Performance of Geosynthetic-Reinforced Asphalt Pavements", *Journal of Geotechnical and Geoenvironment Engineering.* Vol. 77, 2001.

49. Ling, H. I., C. Burke, Y. Mohri, and K. Matsushima, "Shear Strength Parameters of Soil Geosynthetic Interfaces Under Low Confining Pressure Using A Tilting Table". *Geosynthetics International*. Vol. 9, pp. 373-380, 2002.

50. Lombardi, D., and S. Bhattacharya, "Shaking Table Tests on Rigid Soil Container with Absorbing Boundaries", *15 WCEE.* Lisboa, 2012.

51. Marto, A., M. Oghabi, and A. Eisazadeh, "The Effect of Geogrid Reinforcement on Bearing Capacity Properties of Soil Under Static Load; A Review", *EJGE.* Vol. 18, 2013.

52. Mashiri, M. S., Sheikh, M. Neaz., Vinod, J. S., and Tsang, H. Ho. Scrap-tyre soil mixture for seismic protection. *Seismic Engineering: Design for Management of Geohazards: Proceeding of the 2010 Symposium.* pp. 157-166, Australia, 2010.

53. Mayes, R. L., A. G. Brown, and D. Pietra, "Using Seismic Isolation and Energy Dissipation to Create Earthquake-Resilient Buildings", *2012 NZSEE Conference.* No. 93, 2012.

54. Papazoglous, A. J., and A. S. Elnashai, "Analytical and Field Evidence of the Damaging Effect of Vertical Earthquake Ground Motion", *Earthquake Engeering and Structural Dynamics*. Vol. 25, pp. 1109-1137, 1996.

55. Perkins, S. W., and E. V. Cuelho, "Soil-geosynthetic Interface Strength and Stiffness Relationships from Pullout Tests", *Geosynthetics International*. Vol. 6, pp. 321-346, 1999.

56. Prasad, S. K., I. Towhata, G. P. Chandradhara, and P. Nanjundaswamy, "Shaking Table Tests in Earthquake Geotechnical Engineering", *Current Science.* Vol. 87, No. 10, 2004.

57. Promputthangkoon, P., and A. F. L. Hyde, "Compressibility and Liquefaction Potential of Rubber Composite Soils". *In International Workshop on Tire Derived GeoMaterials.* PARI, Kurihama, Japan, 2007.

58. Safak, E., "Local Site Effects and Dynamic Soil Behavior", *Soil Dynamics and Earthquake Engineering*, Vol. 21, pp. 453-458, 2001.

59. Schofield, A. N., "Dynamic and Earthquake Geotechnical Centrifuge Modelling", *First International Conference on Recent Advances in Geotechnical Earthquake Engineering and Soil Dynamics.* No.2, 1981.

60. Sekman, M. *Experimental Study on Mitigation of Earthquake Hazards Using Geosynthetics*, MSc. Thesis, Bogazici University, 2016.

61. Sharma R., Q Chen., M. A. Farsakh, and S. Yoon (2009), "Analytical Modelling of Geogrid Reinforced Soil Foundation", *Geotextiles and Geomembranes*. Vol. 27, pp. 63–72, 2009.

62. Son, S. W., and J. M. Kim, "Effect of Geotechnical Seismic Isolation System on Acceleration Reduction", *EJGE.* Vol. 21, 2016.

63. Srivastav, S., "Base Isolation", *CE681, 3rd year, Civil Engineering Seminar.* 2015.

64. Suresh Praveen Kumar, P., Rajendra Kumar, P., and Giridhar, V., "Seismic Base Isolation with Geo-Synthetic Liners – Current Research", *International Journal of Emerging Trends in Engineering and Development.* Vol. 5, 2015.

65. Symans, M. D., " Seismic Protective Systems: Seismic Isolation", *International Material Complementing FEMA 451, Design Examples.* 2013.

66. Thevanayagam, S., and N. Ecemis, "Geotechnical Laminar Box Shaking Facility", UB Users Workshop, University of Buffalo, 2006.

67. Thurston S. J., "Base Isolation of Low-rise Buildings Using Synthetic Liners", *Study Report.* No. 177, 2007.

68. Tsang, H. H., "Geotechnical Seismic Isolation", *In: Earthquake Engineering: New Research.* pp. 55-87, 2008.

69. Tsang, H. H., M. N. Sheikh, S. H. Lo, and N. K. Lam, "Qushion: Earthquake Protection by Rubber-Soil Mixtures", *The Fourteenth World Conference on Earthquake Engineering.* Beijing, China, 2008.

70. Tsang, H. H., N. T. K. Lam, S. Y. Sabegh, M. N. Sheikh, W. Xiong, and S. P. Shang, "Protecting Low-to-medium-rise Buildings by Scrap Tyre-Soil Mixtures", University of Wollongong, Research Online, 2009.

71. Tsang, H. H., N. T. K. Lam, S. Y. Sabegh, M. N. Sheikh, and B. Indraratna, "Geotechnical Seismic Isolation by Scrap Tire-Soil Mixtures", *Fifth International Conference on Recent Advances in Geotechnical Earthquake Engineering and Soil Dynamics and Symposium in Honor of Professor I. M. Idriss".* San Diego, California, 2010.

72. Tsang, H. H., M. N. Sheikh, N. Lam, "Rubber-soil Cushion for Earthquake Protection", University of Wollongong, Research Online, 2007.

73. Tsang, H. H., S. H. Lo, X. Xu, and M. N. Sheikh, "Seismic Isolation for Low-to-medium-rise Buildings using Granulated Rubber-Soil Mixtures: Numerical Study", *Earthquake Engineering and Structural Dynamics,* 2012.

74. Tsatsis, A. K., I. C. Anastasopoulos, F. L. Gelagoti, and R. S. Kourkoulis, "Effectiveness of In-soil Seismic Isolation Taking into Account of Soil-Structure Interaction", *Proceedings of the Eighteenth International Conference on Soil Mechanics and Geotechnical Engineering.* Paris, 2013.

75. Turan, A., S. D. Hinchberger, and H. E. Naggar, "Design and Commissioning of a Laminar Soil Container for Use on Small Shaking Tables", *Soil Dynamics and Earthquake Engineering.* Vol. 29, pp. 404-414, 2009.

76. Tuzun, C., *EQE682 Lecture Notes.* Bogazici University, Kandilli Observatory and Earthquake Research Institute, Turkey.

77. Yang, Y. B., K. C. Chang, and J. D. Yau, "Base Isolation", *Earthquake Engineering Handbook.* CRC Press, Chapter 17, 2003.

78. Yegian, M. K., and A. M. Lahlaf, "Geomembranes as Base Isolation", *Geosynthetic Fabric Report.* 1992.

79. Yegian, M. K., and A. M. Lahlaf, "Dynamic Interface Shear Strength Properties of Geomembranes and Geotextiles", *Journal of Geotechnical Engineering.* Vol. 118, No. 5, 1992.

80. Yegian, M. K., Z. Y. Yee, and J. N. Harb, "Response of Geosynthetics Under Earthquake Excitations", *Geosynthetics'95.* 1995.

81. Yegian, M. K., I. N. Harb, "Slip Displacements of Geosynthetic Systems Under Dynamic Excitations", *Earthquake Design and Performance of Solid Waste Landfills.* San Diego, California, 1995.

82. Yegian, M. K, U. Kadakal, and M. Catan, "Geosynthetics for Earthquake Hazard Mitigation", *Geosynthetics '99: Specifying Geosynthetics and Developing Design Details.* pp. 87-100, Boston, Massachusetts, U.S.A, 1999.

83. Yegian, M. K., and U. Kadakal, “Foundation Isolation for Seismic Protection Using a Smooth Synthetic Liner”, *Journal of Geotechnical and Geoenvironmental Engineering.* 2004.

84. Yegian, M. K., and M. Catan, “Soil Isolation for Seismic Protection Using a Smooth Synthetic Liner”, *Journal of Geotechnical and Geoenvironmental Engineering.* 2004.

85. Yetimoglu, T., J. T. H. Wu, and A. Saglamer, “Bearing Capacity of Rectangular Footings on Geogrid-Reinforced Sand”, *Journal of Geotechnical Engineering.* Vol. 120, pp. 2083-2099, 1994.

86. Yildiz, O. *Investigation on the Mitigation of Earthquake Hazards With Inclusion of Tıre Wastes Into the Sand*, MSc. Thesis, Bogazici University, 2011.

87. Whitman, R.V., and P.C. Lambe, “Effect of Boundary Conditions Upon Centrifuge Experiments Using Ground Motion Simulation", *The American Society for Testing and Materials.* Vol 1, pp. 61-71, 1986.

88. Xiong, W., H.H., Tsang, S. H. Lo, S. Shang, H. Wang, and F. Zhou, “Geotechnical Seismic Isolation System – Experimental Study”, *Advanced Materials Research.* Vols. 163-167, pp. 4449-4453, 2011.